PB-249 016

FORMATION OF NO AND NO2 IN A TURBULENT PROPANE/AIR DIFFUSION FLAME

Nicholas P. Cernansky

California University

Prepared for:

National Science Foundation

November 1974

DISTRIBUTED BY:

NTIS
National Technical Information Service
U. S. DEPARTMENT OF COMMERCE

034156

NSF-RA- N-75-215
PB 249 016

UNIVERSITY OF CALIFORNIA, BERKELEY

COLLEGE OF ENGINEERING

FORMATION OF NO AND NO_2 IN A TURBULENT PROPANE/AIR DIFFUSION FLAME

NICHOLAS P. CERNANSKY

REPORT NO. UCB-ME-74-5
NOVEMBER 1974

RESEARCH SPONSORED BY:
The National Science Foundation
and
The Environmental Protection Agency
NSF/RANN GRANT No. NSF-GI-44379
EPA GRANT No. AP-385

Opinions, findings, conclusions, or recommendations are those of the author and do not necessarily reflect the views of the supporting agencies.

MECHANICAL ENGINEERING

COMBUSTION LABORATORIES
ENGINE COMBUSTION GROUP

Reproduced by
NATIONAL TECHNICAL
INFORMATION SERVICE
US Department of Commerce
Springfield, VA. 22151

RANN DOCUMENT CENTER
NATIONAL SCIENCE FOUNDATION

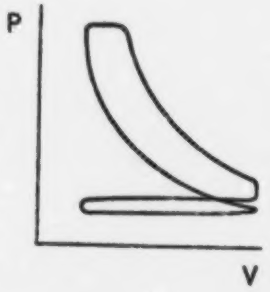

BIBLIOGRAPHIC DATA SHEET

1. Report No. NSF-RA-N-75-215

2.

3. Recipient's Accession No.

4. Title and Subtitle
Formation of NO and NO_2 in a Turbulent Propane/Air Diffusion Flame

5. Report Date
November 1974

6.

7. Author(s)
N.P. Cernansky

8. Performing Organization Rept. No. UCB-ME-74-5

9. Performing Organization Name and Address
University of California, Berkeley
Department of Mechanical Engineering
Berkeley, CA 94720

10. Project/Task/Work Unit No.

11. Contract/Grant No.
AP385
GI44379

12. Sponsoring Organization Name and Address
Research Applied to National Needs (RANN)
National Science Foundation
Washington, D. C. 20550

13. Type of Report & Period Covered

14.

15. Supplementary Notes
Also sponsored by the Environmental Protection Agency.

16. Abstracts

Experimental and theoretical investigations of NO and NO_2 formation and destruction in turbulent hydrocarbon/air diffusion flames have been conducted. Experimental results are presented for turbulent diffusion flames of a round jet of propane in a coflowing mildly swirled, $S = 0.3$, stream of air. Substantial concentrations of nitrogen dioxide were measured and nitrogen dioxide appears to peak slightly on the fuel rich side of the nitric oxide maxima. Several mechanisms for the formation of nitrogen dioxide in combustion systems are examined and the experimental results are discussed with reference to these mechanisms. The governing partial differential equations are solved for the propane/air turbulent diffusion flame. The predicted results from this analytical model are compared with experiment; reasonable agreement is obtained.

17. Key Words and Document Analysis. 17a. Descriptors

Jets
Propane
Fuels
Models

17b. Identifiers/Open-Ended Terms

Combustion Systems

17c. COSATI Field/Group

18. Availability Statement
NTIS

19. Security Class (This Report)
UNCLASSIFIED

20. Security Class (This Page)
UNCLASSIFIED

21. No. of Pages
222

22. Price
7.75

FORM NTIS-35 (REV. 10-73) ENDORSED BY ANSI AND UNESCO. THIS FORM MAY BE REPRODUCED USCOMM-DC 8265-P74

FORMATION OF NO AND NO_2 IN A TURBULENT PROPANE/AIR DIFFUSION FLAME

Nicholas P. Cernansky

Submitted in partial satisfaction of the requirements
for the degree of

Doctor of Philosophy

Approved by Robert F Sawyer
Robert F. Sawyer, Professor
Principal Investigator

Grant Nos. NSF-GI-44379
AP-385

November 1974

1a

ABSTRACT

Experimental and theoretical investigations of NO and NO_2 formation and destruction in turbulent hydrocarbon/air diffusion flames have been conducted. Experimental results are presented for turbulent diffusion flames of a round jet of propane in a coflowing mildly swirled, $S = 0.3$, stream of air. The jet diameter was 8.7 mm and the total flow was confined in a 58 mm diameter combustion tunnel. Buoyancy effects were found to be negligible. Measurements were made at air stream to fuel stream velocity ratios of 45, 61, and 75 to 1 for initial reactant temperatures of 300, 440, and 550°K. Measurements include the spatial distributions of nitric oxide, nitrogen dioxide, and temperature as well as the major stable species: propane, nitrogen, oxygen, water vapor, carbon dioxide, and carbon monoxide.

Substantial concentrations of nitrogen dioxide were measured and nitrogen dioxide appears to peak slightly on the fuel rich side of the nitric oxide maxima. Several mechanisms for the formation of nitrogen dioxide in combustion systems are examined and the experimental results are discussed with reference to these mechanisms. It appears that the formation of nitrogen dioxide occurs through the rapid oxidation of nitric oxide by radicals found in superequilibrium concentrations. In strongly mixed combustion systems where rapid cooling of high temperature eddies occurs, the favored NO_2 formation route involves the build up of hydroperoxy radical, HOO, and subsequent oxidation of NO to NO_2 by the HOO radical.

The governing partial differential equations are solved for the propane/air turbulent diffusion flame. The predicted results from this analytical model are compared with experiment; reasonable agreement is obtained.

ACKNOWLEDGEMENTS

The author wishes to thank Professor Robert F. Sawyer for his support and guidance in this research. His patience and encouragement were most necessary to the success of this effort. Discussions with Professors Ernest S. Starkman and Alexis T. Bell gave perspective to the study and resulted in many suggestions which improved the work. Discussions with several fellow students, especially Bob Schefer, Ron Matthews, and Don Holve, are also appreciated.

The experimental portion of the work was accomplished through the special efforts of Al Shaw, Bill Nelson, Vern Locke, Joe DeCosta, Frank Waymire, and the remainder of the Mechanical Engineering Department technical staff. My thanks to all of them. The pains of data reduction were greatly eased by Ken Daniel, a visiting student from Purdue. The drafting abilities of Gloria Pelatowski proved invaluable to the completion of this effort. The typing and crisis handling of Rebecca Palmer was sincerely appreciated and is gratefully acknowledged.

The research was supported in part by the National Science Foundation (NSF-GI-44379) and the Environmental Protection Agency (AP-385). The author was supported for two years through an NSF traineeship. Computer time was obtained through the University of California Computer Center.

Finally, the author would like to thank his wife, Ellie, for her forbearance and encouragement during the course of this work. Special thanks also go to Rabies and Fred for always being there when I needed them.

TABLE OF CONTENTS

Page

ABSTRACT ii

ACKNOWLEDGEMENTS iv

LIST OF FIGURES ix

LIST OF TABLES xv

NOMENCLATURE xvi

CHAPTER 1 Introduction 1

CHAPTER 2 Background and Literature Review 3

- 2.1 NO and NO_2 in Combustion Systems 3
- 2.2 Importance of NO_2 3
- 2.3 Scope of the Present Study 4
- 2.4 Literature Review 5

CHAPTER 3 Experimental Equipment and Procedures 8

- 3.1 Introduction 8
- 3.2 Combustor Test Facility 8
- 3.3 Sampling and Analytical Equipment . . . 10
  - 3.3.1 Composition Measurements 11
  - 3.3.2 Velocity Measurements 18
  - 3.3.3 Temperature Measurements 18

CHAPTER 4 Experimental Results 24

- 4.1 Introduction 24
- 4.2 Operating Conditions 24
- 4.3 Representative Results and Discussion 25
  - 4.3.1 Initial Velocity Profiles 25
  - 4.3.2 Composition and Temperature . . . 27
  - 4.3.3 Fluctuations 38

TABLE OF CONTENTS (Continued)

Page

4.4 Other Experiments 38

4.4.1 Other Fuels 39
4.4.2 NO Seeding 41

CHAPTER 5 Kinetics of NO and NO_2 Formation 43

5.1 Introduction 43

5.2 NO Kinetics and Mechanisms 43

5.3 NO_2 Formation Mechanisms 44

5.3.1 Past Work 44
5.3.2 Current Study 45
5.3.3 Kinetic Calculations 48
5.3.4 Probe Reactions 55
5.3.5 Summary 55

5.4 NO_2 in Combustion Systems 56

CHAPTER 6 Analytical Model 59

6.1 Introduction 59

6.2 Governing Equations and Their Solution 59

6.3 The Specific Problem - Program Modifications 64

6.3.1 General 64
6.3.2 Thermodynamic Properties 64
6.3.3 Combustion and Pollutant Formation Model 66
6.3.4 The Turbulence Model 67
6.3.5 Pressure Gradient 67

6.4 The Specific Problem - Results 68

6.5 Conclusion 75

CHAPTER 7 Conclusion 76

7.1 Summary of Results 76

7.2 Future Work 77

REFERENCES 79

TABLE OF CONTENTS (Continued)

Page

APPENDIX A Experimental Facility and Equipment 86

A.1 Introduction 86

A.2 Air Supply System 86

A.3 Fuel Supply System 89

A.4 Fuel Injector 90

A.5 Starting Procedure 90

A.6 Air Swirler 91

APPENDIX B Operating Data 92

APPENDIX C Mass Spectrometer and CO Data 98

APPENDIX D NO_x and Temperature Data 113

APPENDIX E Kinetic Calculations 138

E.1 Introduction 138

E.2 Reaction Scheme 138

E.3 Base Cases and Initial Conditions . . . 140

E.4 Results 141

APPENDIX F Sampling Probes and Sampling Difficulties 157

F.1 Introduction 157

F.2 Sampling for NO and NO_2 158

F.2.1 Sampling Probes 158
F.2.2 Transfer System 159

F.3 Analysis of NO and NO_2 160

F.4 Conclusion 161

APPENDIX G Computer Codes 163

G.1 Description of Programs 163

G.2 Operating Data Reduction 164

G.3 Operating Data List 166

TABLE OF CONTENTS (Continued)

Page

G.4 MSDATA 167

G.5 ADDCO 175

G.6 PLOT 176

G.7 GENMIX 4 178

  G.7.1 MAIN 178
  G.7.2 AUX 186
  G.7.3 STRIDE 191
  G.7.4 WF 198

LIST OF FIGURES

Figure Page

3-1. Schematic of combustion test section. 9

3-2. Gas sampling probe. 12

3-3. Schematic of sample flows for gas composition analysis. 13

3-4. Five-hole pitot probe. 19

3-5. Static pressure probe. 20

3-6. Thermocouple probe. 21

4-1. Initial velocity profiles at jet exit plane, 300°K, ○ - $V_A/V_F = 45$; □ - $V_A/V_F = 61$; △ - $V_A/V_F = 75$. 28

4-2. Centerline distributions for propane, oxygen, carbon monoxide, carbon dioxide and water vapor at 300°K initial reactant temperature. —— $V_A/V_F = 45$; ---- $V_A/V_F = 61$; — — — $V_A/V_F = 75$. 29

4-3. Radial distributions for propane, oxygen, carbon monoxide, carbon dioxide, and water vapor at $V_A/V_F = 45$ and 300°K initial reactant temperature. —— $X/D = 1.33$; ---- $X/D = 2.66$; — — — $X/D = 5.33$. 30

4-4. Centerline distributions of nitric oxide, nitrogen dioxide, and temperature at 300°K initial reactant temperature. ○ - $V_A/V_F = 45$; □ - $V_A/V_F = 61$; △ - $V_A/V_F = 75$. 32

4-5. Centerline distributions of nitric oxide, nitrogen dioxide, and temperature for different initial reactant temperatures at $V_A/V_F = 45$. ○ - T = 300°K; □ - T = 440°K; △ - T = 550°K. 33

4-6. Radial distributions of nitric oxide, nitrogen dioxide, and temperature at $V_A/V_F = 45$ and 300°K initial reactant temperature. ◇ - $X/D = 1.33$; ○ - $X/D = 2.66$; □ - $X/D = 5.33$; △ - $X/D = 10.66$; ▽ - $X/D = 21.33$. 34

LIST OF FIGURES (Continued)

Figure Page

4-7. Radial distributions of nitric oxide, nitrogen dioxide, and temperature at axial location X/D = 5.33 and 300°K initial reactant temperature. ○ - $V_A/V_F = 45$; □ - $V_A/V_F = 61$; △ - $V_A/V_F = 75$. 35

4-8. Radial distributions of nitric oxide, nitrogen dioxide, and temperature at axial location X/D = 2.66 and velocity ratio $V_A/V_F = 45$. ○ - T = 300°K; □ - T = 440°K; △ - T = 550°K. 36

4-9. Radial distributions of nitric oxide and nitrogen dioxide using hydrogen fuel at $V_A/V_F = 7.5$ and 300°K initial reactant temperature. ◇ - X/D = 0.67; ◊ - X/D = 1.33; ○ - X/D = 2.66; △ - X/D = 10.66. 40

4-10. Radial distributions of nitric oxide, nitrogen dioxide, and oxides of nitrogen at axial location X/D = 16 and 300°K initial reactant temperature for several concentrations of NO in the reactants ○ - 0 ppm NO; □ - 9.5 ppm NO; △ - 20 ppm NO; ▽ - 32 ppm NO. Solid symbols are equivalent seeding flows of N_2 without NO. 42

5-1. Time history of selected species when equilibrium concentrations of radicals for $\phi = 0.8$ at 2050°K and 50 ppm NO are instantaneously cooled to 900°K. HOO mechanism. 51

5-2. Time history of selected species when equilibrium concentrations of radicals for $\phi = 0.8$ at 2050°K and 50 ppm NO are instantaneously cooled to 900°K. 52

5-3. Time history of selected species when equilibrium concentrations of radicals for $\phi = 0.8$ at 2050°K and 50 ppm NO are instantaneously cooled to 900°K. HOO mechanism + HNO_2, HNO_3, O_3 mechanisms. . . . 53

5-4. Effect of final temperature and reaction scheme on NO conversion. 54

6-1. General arrangement of the flow system for computation. 65

6-2. Comparison of measured C_3H_8 and O_2 centerline profiles with model predictions, $V_A/V_F = 45$, T = 300°K. 69

LIST OF FIGURES (Continued)

Figure Page

6-3. Comparison of measured C_3H_8 and O_2 radial profiles with model predictions, $V_A/V_F = 45$, $T = 300°K$. . 70

6-4. Comparison of measured temperature and nitric oxide centerline profiles with model predictions, $V_A/V_F = 45$, $T = 300°K$. 71

6-5. Comparison of measured temperature and nitric oxide radial profiles with model predictions, $V_A/V_F = 45$, $T = 300°K$. 72

A-1. Schematic of combustor test facility. 87

C-1. Scatter diagram of mass spectrometer and CO data at $V_A/V_F = 45$ and 300°K initial reactant temperature, $X/D = 21.33$. 99

C-2. Scatter diagram of mass spectrometer and CO data at $V_A/V_F = 45$ and 300°K initial reactant temperature, $X/D = 1.33$. 100

D-1. Centerline distributions of temperature and oxides of nitrogen for different initial reactant temperatures at $V_A/V_F = 45$. 114

D-2. Centerline distributions of temperature and oxides of nitrogen for different initial reactant temperatures at $V_A/V_F = 61$. 115

D-3. Centerline distributions of temperature and oxides of nitrogen for different initial reactant temperatures at $V_A/V_F = 75$. 116

D-4. Radial distributions of temperature and oxides of nitrogen at $V_A/V_F = 45$ and 300°K initial reactant temperature. 117

D-5. Radial distributions of temperature and oxides of nitrogen at $V_A/V_F = 61$ and 300°K initial reactant temperature. 118

D-6. Radial distributions of temperature and oxides of nitrogen at $V_A/V_F = 75$ and 300°K initial reactant temperature. 119

D-7. Radial distributions of temperature and oxides of nitrogen at $V_A/V_F = 45$ and 440°K initial reactant temperature. 120

LIST OF FIGURES (Continued)

Figure Page

D-8. Radial distributions of temperature and oxides of nitrogen at $V_A/V_F = 61$ and 440°K initial reactant temperature. 121

D-9 Radial distributions of temperature and oxides of nitrogen at $V_A/V_F = 75$ and 440°K initial reactant temperature. 122

D-10. Radial distributions of temperature and oxides of nitrogen at $V_A/V_F = 45$ and 550°K initial reactant temperature. 123

D-11 Radial distributions of temperature and oxides of nitrogen at $V_A/V_F = 61$ and 550°K initial reactant temperature. 124

D-12. Radial distributions of temperature and oxides of nitrogen at $V_A/V_F = 75$ and 550°K initial reactant temperature. 125

D-13. Centerline distributions of nitric oxide and nitrogen dioxide for different initial reactant temperatures at $V_A/V_F = 45$. 126

D-14. Centerline distributions of nitric oxide and nitrogen dioxide for different initial reactant temperatures at $V_A/V_F = 61$. 127

D-15. Centerline distributions of nitric oxide and nitrogen dioxide for different initial reactant temperatures at $V_A/V_F = 75$. 128

D-16. Radial distributions of nitric oxide and nitrogen dioxide at $V_A/V_F = 45$ and 300°K initial reactant temperature. 129

D-17. Radial distributions of nitric oxide and nitrogen dioxide at $V_A/V_F = 61$ and 300°K initial reactant temperature. 130

D-18. Radial distributions of nitric oxide and nitrogen dioxide at $V_A/V_F = 75$ and 300°K initial reactant temperature. 131

D-19. Radial distributions of nitric oxide and nitrogen dioxide at $V_A/V_F = 45$ and 440°K initial reactant temperature. 132

LIST OF FIGURES (Continued)

Figure — Page

D-20. Radial distributions of nitric oxide and nitrogen dioxide at $V_A/V_F = 61$ and 440°K initial reactant temperature. 133

D-21. Radial distributions of nitric oxide and nitrogen dioxide at $V_A/V_F = 75$ and 440°K initial reactant temperature. 134

D-22. Radial distributions of nitric oxide and nitrogen dioxide at $V_A/V_F = 45$ and 550°K initial reactant temperature. 135

D-23. Radial distributions of nitric oxide and nitrogen dioxide at $V_A/V_F = 61$ and 500°K initial reactant temperature. 136

D-24. Radial distributions of nitric oxide and nitrogen dioxide at $V_A/V_F = 75$ and 550°K initial reactant temperature. 137

E-1. Time history of selected species when equilibrium concentrations of radicals for $\phi = 0.8$ at 2050°K and 50 ppm NO are instantaneously cooled to 1300°K. 144

E-2. Time history of selected species when equilibrium concentrations of radicals for $\phi = 0.8$ at 2050°K and 50 ppm NO are instantaneously cooled to 900°K. 145

E-3. Time history of selected species when equilibrium concentrations of radicals for $\phi = 0.8$ at 2050°K and 50 ppm NO are instantaneously cooled to 500°K. 146

E-4. Time history of selected species when equilibrium concentrations of radicals for $\phi = 0.8$ at 2050°K and 50 ppm NO are instantaneously cooled to 1300°K, including HOO mechanism. 147

E-5. Time history of selected species when equilibrium concentrations of radicals for $\phi = 0.8$ at 2050°K and 50 ppm NO are instantaneously cooled to 900°K, including HOO mechanism. 148

E-6. Time history of selected species when equilibrium concentrations of radicals for $\phi = 0.8$ at 2050°K and 50 ppm NO are instantaneously cooled to 500°K, including HOO mechanism. 149

LIST OF FIGURES (Continued)

Figure | Page

E-7. Time history of selected species when equilibrium concentrations of radicals for $\phi = 0.8$ at 2050°K and 50 ppm NO are instantaneously cooled to 1300°K, including HOO, HNO_2, HNO_3, O_3 mechanisms. 150

E-8. Time history of selected species when equilibrium concentrations of radicals for $\phi = 0.8$ at 2050°K and 50 ppm NO are instantaneously cooled to 900°K, including HOO, HNO_2, HNO_3, O_3 mechanisms. 151

E-9. Time history of selected species when equilibrium concentrations of radicals for $\phi = 0.8$ at 2050°K and 50 ppm NO are instantaneously cooled to 500°K, including HOO, HNO_2, HNO_3, O_3 mechanisms. 152

E-10. Time history of selected species when equilibrium concentrations of radicals for $\phi = 0.8$ at 2050°K, 50 ppm NO and 6 ppm NO_2 are instantaneously cooled to 300°K, 80 torr. 153

E-11. Time history of selected species when equilibrium concentrations of radicals for $\phi = 0.8$ at 2050°K, 50 ppm NO and 10 ppm NO_2 are instantaneously cooled to 300°K, 80 torr including HOO, HNO_2, HNO_3, and O_3 mechanisms. 154

E-12. Time history of selected species when equilibrium concentrations of radicals for $\phi = 0.8$ at 2050°K, 50 ppm NO are instantaenously cooled to 300°K, 80 torr including HOO, HNO_2, HNO_3, and O_3 mechanisms. 155

E-13. Time history of selected species when equilibrium concentrations of radicals for $\phi = 0.8$ at 2050°K, 50 ppm NO and 6 ppm NO_2 are cooled linearly from 2000°K to 300°K in 20 msec, P = 80 torr. 156

LIST OF TABLES

Table		Page
4-1.	Initial conditions at jet exit plane.	26
5-1.	Rate constants for nitrogen dioxide reactions. . .	46
5-2.	Temperature range and evaluation of nitrogen dioxide reactions.	47
B-1.	Calculated fuel and air flows.	94
B-2.	List of raw operating data.	96
C-1.	Mass spectrometer and CO data for 300°K initial reactant temperature.	101
C-2.	Mass spectrometer and CO data for 440°K initial reactant temperature.	105
C-3.	Mass spectrometer and CO data for 550°K initial reactant temperature.	109
E-1.	Initial species concentrations for kinetic calculations.	142

NOMENCLATURE

a = jet nozzle radius

A = preexponential factor in kinetic rate expression

c_p = specific heat at constant pressure

d = diameter

D = jet nozzle diameter

e = electronic charge on a molecule or fragment

e_k = turbulent kinetic energy

E_k = mean flow kinetic energy

E = activation energy

Fr = Froude number (V^2/gL)

g = gravitational acceleration

G_x = axial flux of linear momentum, $G_x = \int_0^R u\rho u 2\pi r dr + \int_0^R p 2\pi r dr$

G_θ = axial flux of angular momentum, $G_\theta = \int_0^R (v_\theta r)\rho u 2\pi r dr$

h = convective heat transfer coefficient

h_i = specific enthalpy of species i

H = total enthalpy

$\Delta H_{R_{298}}$ = standard enthalpy of reaction at 298°K

k = thermal conductivity

ℓ_o = mixing length

L = length

Le = Lewis number ($\mathcal{D}\rho c_p/k$)

Le_{eff} = effective Lewis number for turbulent flow

m = molecular weight of molecule or fragment

m_i = mass fraction of species i

Nu = Nusselt number (hd/k)

P = = pressure

Pr = Prandtl number $(c_p\mu/k)$

Pr_{eff} = effective Prandtl number for turbulent flow

Pr_e = turbulent Prandtl number for turbulent kinetic energy

$Pr_{e_{eff}}$ = effective Prandtl number for turbulent kinetic energy for turbulent flow

r = radius

R = radius of combustion tunnel; universal gas constant

Re = Reynolds number $(\rho ud/\mu)$

S = Swirl number (G_θ/G_xR)

Sc = Schmidt number $(\mu/\rho\mathcal{D})$

Sc_{eff} = effective Schmidt number for turbulent flow

t = time

T = temperature, °K

T_G = actual gas temperature

T_{TC} = measured thermocouple temperature

T_W = average boundry temperature

u = axial component of velocity

v = cross stream component of velocity

V_θ = azimuthal component of velocity

V = velocity

W_i = source term for species i

W_J = generalized source term for quantity J

X = downstream distance from the injector tip

X_i = mole fraction of species i

$X_{i_{MS}}$ = measured mole fraction of species i, wet basis without CO

$X_{CO_{NDIR}}$ = measured mole fraction of carbon monoxide, dry basis

x = downstream coordinate

y = cross-stream coordinate

$[Z]$ = concentration of species Z

$\mathcal{D}$ = mass diffusivity

α = angle made by the x direction with the axis of symmetry; angle of swirling vanes

ε = thermocouple emissivity

ε_M = eddy diffusivity for momentum

μ = dynamic viscosity

μ_{eff} = total viscosity ($\mu+\rho\varepsilon_M$)

ρ = density

σ = Stephen Boltzman constant

σ_{eff} = generalized effective Prandtl number

ϕ = equivalence ratio

ϕ_J = generalized dependent variable indicator

ϕ_{diss} = dissipation of turbulent kinetic energy

ψ = stream function

ψ_E = stream function at external boundary

ψ_I = stream function at internal boundary

ω = dimensionless stream function ($(\psi-\psi_I)/(\psi_E-\psi_I)$)

Subscripts

A = air

F = fuel

i = species i

x = downstream direction

y = cross stream direction

θ = azimuthal direction

CHAPTER 1

Introduction

Combustion plays a vital role in our everyday lives—from heating our homes, and providing electricity, to supplying the energy required to move us around. Combustion also impinges upon us indirectly, providing the power and energy used in virtually all industrial processes for manufacturing the goods we all take so much for granted. Unfortunately, pollution in the form of oxides of sulfur, oxides of nitrogen, unburnt hydrocarbons, carbon monoxide, and other species unnecessarily results from our present knowledge and design of these combustion processes. Because of both the direct and indirect effects of these pollutants on health and the environment, pollutant formation and destruction in combustion processes have become matters of great concern and intensive research.

Much of this research deals with after treatment or add-on devices which remove pollutants from the exhaust gases after they are formed. This practical and applications oriented approach is valuable and necessary and quite often represents the only means at hand for reducing pollutant emissions. A more fundamental approach, although not known a priori to be the best, is to modify the combustion process to avoid production or encourage destruction of the pollutants directly. To this end, some research deals with determining the basic kinetics, mechanisms, and rates of formation and destruction of pollutants. These studies for the most part are carried out on laboratory research devices which may or may not represent the real world. Therefore, other research is carried out on actual in use combustion devices (gas turbines, power plants, etc.) in order to verify the mechanisms developed in the basic studies. Unfortunately, these practical systems have extremely complex interactions of the chemical and physical processes, making analysis difficult and fundamental processes obscure. A middle ground, therefore, lies in laboratory combustion devices which simulate real world conditions but in a well defined and controlled configuration. These studies bridge the gap between research tools (shock tubes, etc.) and practical combustion devices (engines). The present study falls into this category.

The system that was studied was a simple hydrocarbon fueled turbulent diffusion flame. This system may be thought of as being similar to combustion in power plants, gas turbines, diesels, and other devices. While all major species and carbon monoxide were measured, emphasis was placed on the oxides of nitrogen, NO and NO_2. This was done because of the unexpected large concentrations of NO_2 that were measured in preliminary investigations.

Chapter 2 gives more background on the motivation, significance and scope of the study and briefly reviews similar or related work. The experimental apparatus and operating procedures are discussed in Chapter 3 and experimental results are presented in Chapter 4. Chapter 5 discusses the kinetics of NO and NO_2 formation. The analytical investigation is described and comparisons with experiment are made in Chapter 6. Chapter 7 contains the conclusions of the investigation.

CHAPTER 2

Background and Literature Review

2.1 NO and NO_2 in Combustion Systems

Until 1971, it had been generally accepted that nitrogen dioxide constituted at most about five percent of the total oxides of nitrogen from combustion systems (Heywood et al., 1971; Fletcher et al., 1971; Cornelius and Agnew, 1972). At that time, measurements of significant concentrations of nitrogen dioxide in the exhaust of gas turbines (up to 80 percent total NO_x) were reported by AiResearch Manufacturing Corporation (1971). Since that initial study, nitrogen dioxide has also been reported in several laboratory combustion studies: including a model gas turbine combustor (Schefer et al., 1973), a premixed low pressure flame (Merryman and Levy, 1973), a jet stirred combustor (Malte and Pratt, 1973) (although attributed to sampling difficulties in this latter case) and others. Also recently, significant concentrations of NO_2 (again up to 80 percent total NO_x) were reported in the stack gases of gas turbine power plant peaking units (Coppersmith et al., 1974). The present work presents results for a simple turbulent diffusion flame.

2.2 Importance of NO_2

The explanation of the formation and existence of this NO_2 is important to the basic understanding and modeling of the combustion and pollutant formation processes. Also, the form of the oxides of nitrogen is critical to the design and operation of exhaust gas treatment devices, to the nature of the atmospheric reactions of the pollutants and to the visibility of the exhaust. Thus there is great impetus for understanding and explaining NO_2 in combustion systems. The present work moves toward this understanding in that it presents comprehensive measurements for a simple combustion system, thereby providing data against which theories can be tested.

2.3 Scope of the Present Study

Experimental results are presented for turbulent diffusion flames of a round jet of propane issuing into a coflowing stream of air. Temperature and stable chemical species including NO_2 were measured and are reported for a range of fuel/oxidizer velocity ratios and over a range of inlet air temperatures. The effects of the air preheat are of special interest because of the preheat conditions achieved in many practical combustion systems. Also of particular importance, as was pointed out earlier, are the nitric oxide and nitrogen dioxide measurements, since the latter species is not usually measured and is not predicted by conventional theories.

Several mechanisms for the formation of NO_2 in combustion systems are examined and the experimental results are discussed with reference to these mechanisms.

The governing partial differential equations are solved for a propane/air turbulent diffusion flame. Predicted results are compared with experiment and suggestions for refining the model are made.

2.4 Literature Review

Work on turbulent diffusion flames is reviewed here while the review of NO and NO_2 formation is deferred to Chapter 5.

The study of turbulent diffusion flames extends over a wide range of topics. Work has been done on calculating radiation from diffusion flames (Masliryah and Steward, 1969), the effects of swirl (Rubel, 1972; Beer and Chigier, 1972), the cold modeling of diffusion flames (Beer et al., 1963), and stability aspects (Gunther, 1970). A particularly good review of studies dealing with the measurement and prediction of the thermo fluid mechanics of axisymmetric turbulent jet diffusion flames has been made by Kent (1972). The review shows the evolution of the theoretical analyses from a state of dimensional analysis, to the solution of all relevant conservation equations together with predictions of turbulence quantities in the flow. Also the review discusses experimental measurements that have been performed on flows ranging from simple jets in still air to complex supersonic configurations. In view of this work by Kent, a complete review will not be given here. Instead, only recent and relevant work will be noted.

Previous work on subsonic turbulent diffusion flames has concentrated mostly on the case of a fuel jet issuing into still air. The work of Bilger and Beck (1974), Lockwood and Odidi (1974), Elghobashi and Pun (1974), Magnussen (1973), Becker (1974), and others continue to deal with these type systems. They concentrate primarily on providing experimental data and developing better models for the turbulent diffusivities and for the fluctuating properties.

Kent (1972), Kent and Bilger (1973) and Bilger and Beck (1974) reported results for a horizontal hydrogen jet in a coflowing air stream over a variety of velocity ratios (5:1 to .5:1). Kent reported what is believed to be the first measurements of NO in such systems, however, the primary emphasis was on developing fluctuating property data for refining the turbulent transport models. The current study extends this work to a hydrocarbon fueled system and also to high air/fuel velocity ratios (45-75:1), giving special attention to NO and NO_2. Swirl in the air stream is also added.

Nitric oxide formation in turbulent jet diffusion flames has been treated analytically by Quan *et al*. (1973, 1974) and Quan (1974). They demonstrate the importance of mixing processes and the lifetime of burning eddies in the NO formation process. Bilger and Beck (1974) show that the important time scale for NO formation is the Kolmogoroff time scale which represents the dissipation time of a burning eddie and scales as $D^{1/2}/V^{3/2}$. Lavoie and Schlader (1974) also studied the scaling of NO formation in turbulent hydrocarbon/air diffusion flames. Takagi *et al*. (1974) presented measurements and calculations of NO production in turbulent propane/air and hydrogen/air diffusion flames. This study was, however, at very low air/fuel velocity ratios.

Swirl in the coflowing turbulent diffusion flame configuration has been treated by Rubel (1972, 1973), Beer and Chigier (1972), and others. Beer and Chigier review the relevant work on swirling combustion and therefore it will not be repeated here. They discuss both swirling jets and bouyant jets in a rotating flow field (low velocity and low A/F velocity ratio). Rubel presents a model and computations for the case of a swirling jet into a coflowing air stream; NO production is also followed. The present study uses swirl in the external air flow at high air/fuel velocity ratios and therefore past analyses are not directly applicable.

It is noted that United Aircraft Corporation (Bowman, 1974) is currently performing studies on a combustor of similar design to the one used in this study and they will also encompass the fuels, swirl levels, velocity ratios, and levels of reactant preheat that were used. No data are yet available from this study.

CHAPTER 3

Experimental Equipment and Procedures

3.1 Introduction

As was stated, the current study deals with simple turbulent propane/air diffusion flames operated over a range of fuel/oxidizer velocity ratios and over a range of inlet reactant temperatures. Details of the experimental equipment and description of special operating procedures are presented in the remainder of this chapter. The combustion facility is described briefly in section 3.2 and in more detail in Appendix A. Section 3.3 gives the details of the sampling and analytical system and includes, where appropriate, description of special procedures and corrections that were required. Discussion of experimental design and presentation of the actual operating conditions are deferred until Chapter 4.

3.2 Combustor Test Facility

A schematic of the combustion test section is shown in Fig. 3-1. Closely metered fuel and air flows are preheated and supplied to the 58 mm inside diameter X 356 mm Vycor combustion section. Propane is injected axially through an 8.7 mm inside diameter X 0.4 mm wall tube located 152 mm into the horizontal combustion tunnel and is mixed and burned with a slightly swirled coaxial air flow. The one atmosphere flames are attached to the injector tip and are contained within the combustion tunnel where flame structure measurements are made.

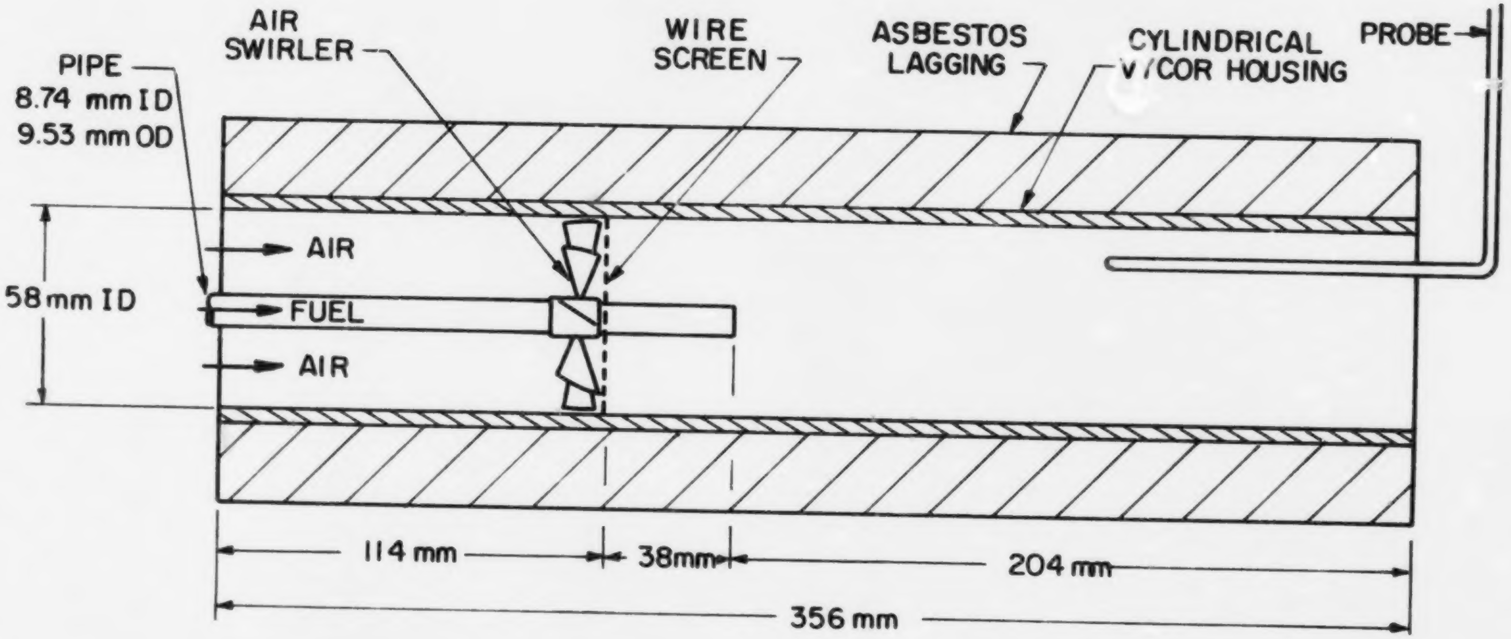
AIR
SWIRLER
WIRE
SCREEN
ASBESTOS
LAGGING
CYLINDRICAL
VYCOR HOUSING
PROBE
PIPE
8.74 mm ID
9.53 mm OD
AIR
FUEL
AIR
58 mm ID
114 mm
38 mm
204 mm
356 mm

Figure 3-1. Schematic of combustion test section.

The swirl, $S \approx 0.3$, was used to enhance the stability of the flame but was maintained at a sufficiently low level to avoid recirculation. The absence of recirculation is supported by static pressure measurements and measurements using a directional velocity probe. Buoyancy effects were also found to be negligible.

Details of the air and fuel supply systems, fuel injector design, air swirler design, and starting procedures are presented in Appendix A.

3.3 Sampling and Analytical Equipment

Horizontal and axial traverses of the flame were made using probes inserted through the downstream end of the combustion tunnel. Vertical traverses were also made to establish the precise location of the jet center and to test for symmetry. The movement of the probes is controlled by a specially designed traverse with three degrees of freedom. The probes can be positioned axially using a slide allowing any axial location from upstream of the fuel injector to downstream of the combustor exit. Once located axially, the probe is moved horizontally and vertically using a worm drive milling mount capable of 0.001 inch positioning accuracy. Typically, the vertical position would be set and the probe traversed horizontally to obtain radial profiles. The usual data point spacing was 0.100 inches with 0.050 inch spacing or less in regions of strong gradients. All probes were protected with a sheet metal heat shielding near the base of the probe.

3.3.1 Composition Measurements

Gas samples were removed from the flame using a 3/16 inch outside diameter water cooled stainless steel probe with a tip designed to provide aerodynamic quenching (Schefer et al.,1973). A schematic of the probe is shown in Fig. 3-2. With a vacuum (~ 30 torr) maintained on the sample line, the sample is drawn into the probe through the small converging-diverging nozzle. This has the effect of rapidly quenching the reactions by aerodynamic cooling. The sample is maintained cool and the probe itself protected by circulation of cooling water through concentric inner tubes. The 30 torr pressure in the probe and sample line is sufficiently low to prevent condensation of water.

After leaving the probe the sample is passed through an 11 cm diameter glass fiber filter particulate trap and then passed on to the gas analysis equipment. A schematic of the sample gas flow is shown in Fig. 3-3. All transfer lines were 1/4 inch diameter teflon lines. Carbon monoxide was measured using a Beckman model 315A nondispersive infrared analyzer. For these measurements, the samples were passed through about ten feet of sample line and an ice bath water condensation trap before entering the analyzer. All other composition measurements were taken on a wet basis and required about 40 ft. of sample line before the analyzers.

Nitric oxide and nitrogen dioxide were measured using a laboratory built chemiluminiscent NO analyzer modified for the measurement of total NO_x (Patterson et al., 1970; Matthews, 1973; Schefer et al., 1973). Nitrogen dioxide was determined by difference. One concern with the NO and NO_2 measurements was the possibility of

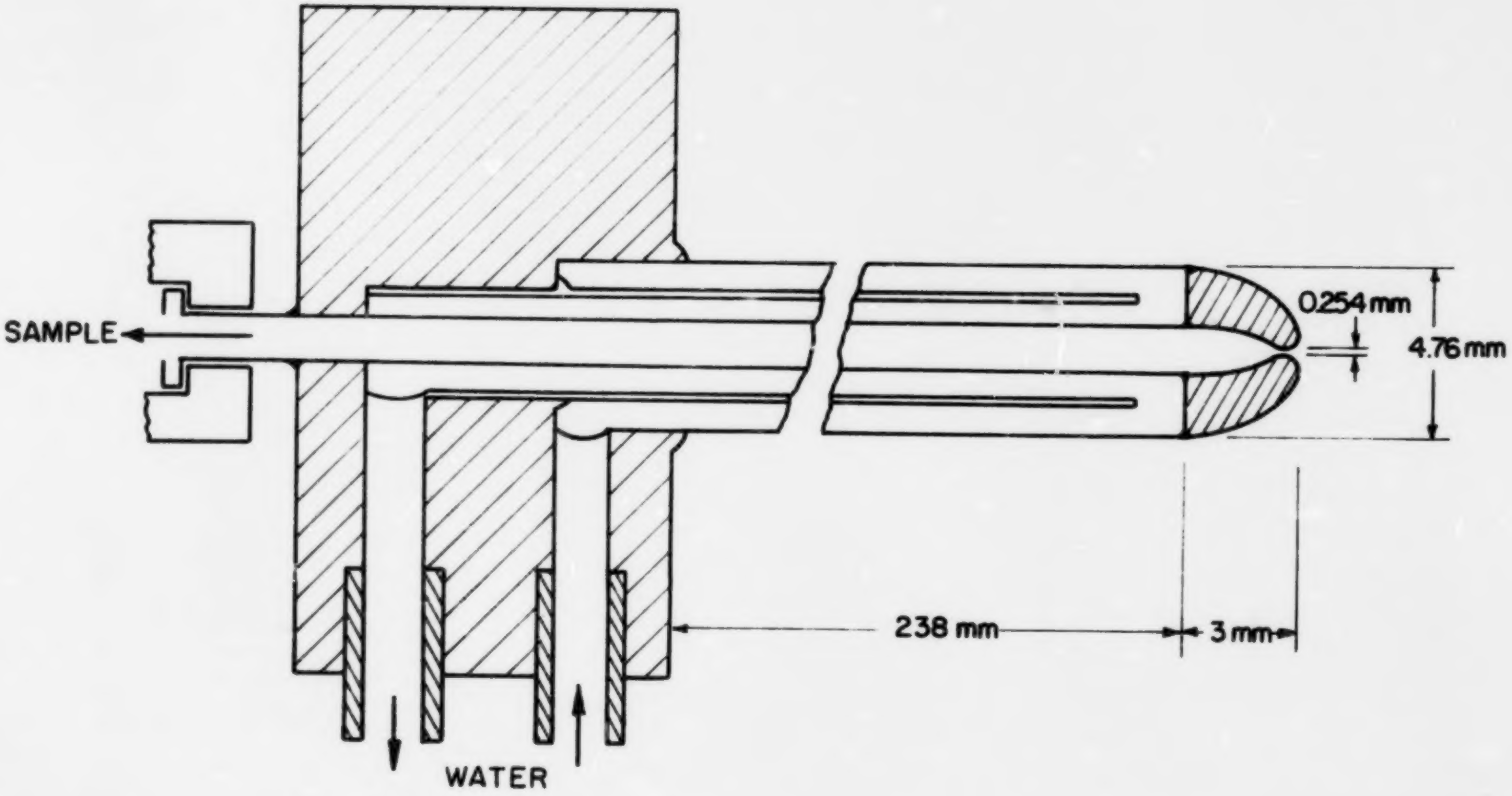
SAMPLE
0.254 mm
4.76 mm
238 mm
3 mm
WATER

Figure 3-2. Gas sampling probe.

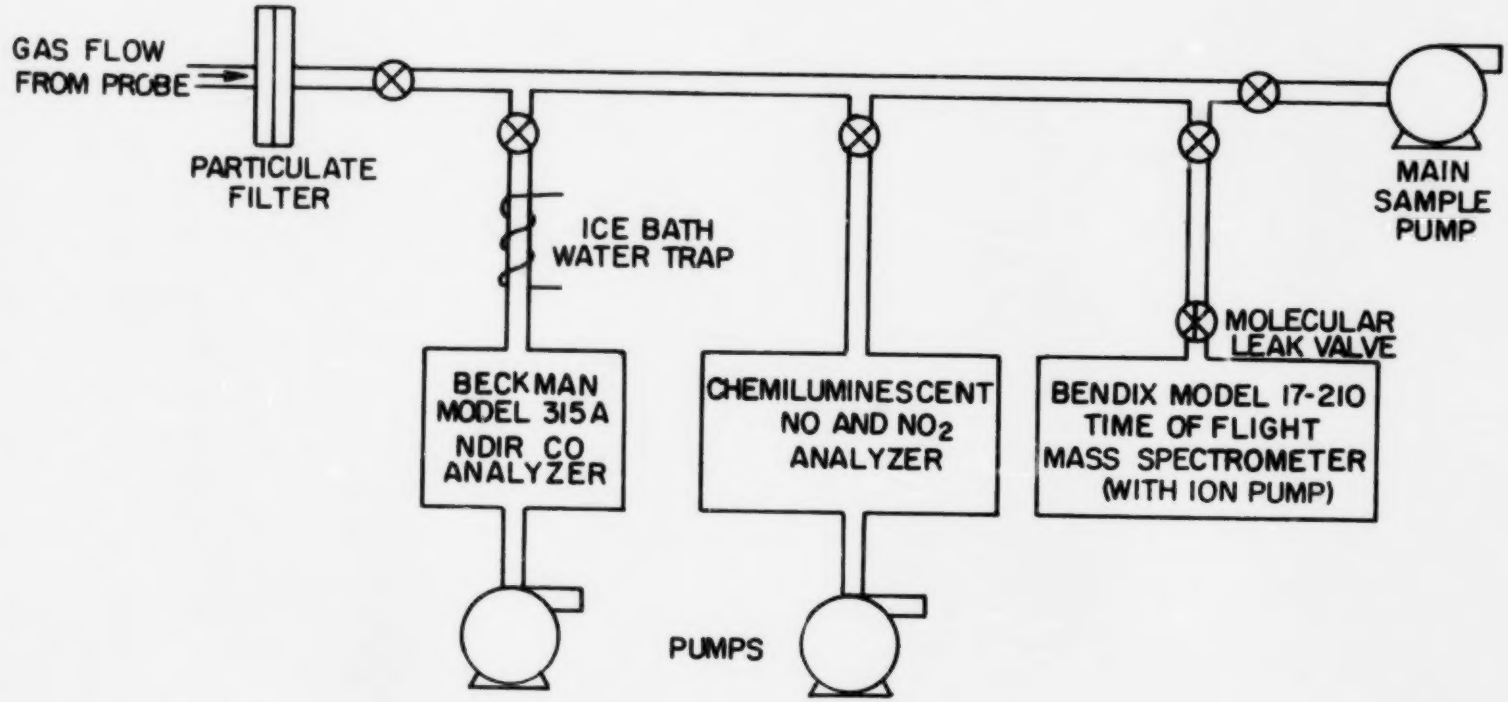
GAS FLOW
FROM PROBE
PARTICULATE
FILTER
ICE BATH
WATER TRAP
BECKMAN
MODEL 315A
NDIR CO
ANALYZER
CHEMILUMINESCENT
NO AND NO_2
ANALYZER
BENDIX MODEL 17-210
TIME OF FLIGHT
MASS SPECTROMETER
(WITH ION PUMP)
MOLECULAR
LEAK VALVE
MAIN
SAMPLE
PUMP
PUMPS

Figure 3-3. Schematic of sample flows for gas composition analysis.

oxidizing NO to NO_2 by molecular oxygen in the rather long sample line. To resolve this question, mixtures of NO in N_2 and O_2 were supplied to the probe and conversion to NO_2 was measured. In the case of 40 ppm NO in 10% N_2 and 90% O_2, less than 1% of the NO was converted to NO_2 in over 80 feet of sample line (more than double the normal length). Hence we conclude that under normal operating conditions, NO $\approx$ 50 ppm and $O_2 \leq 21\%$, conversion of NO to NO_2 by molecular oxygen will be negligible.

Another problem encountered in the collection of NO and NO_2 data involved accumulation of soot in the sampling system. In any hydrocarbon diffusion flame there is a considerable amount of soot in the flame interior region making sampling from these regions difficult. As carbon particulate built up in the sampling system, it would reduce NO_2 to NO as well as adsorbing NO_2 and to a much lesser extent reduce NO to N_2, thus making quantitative measurements difficult. (The carbon particulate did not affect any of the other gaseous species.) The problem was solved by placing the glass fiber filter close to the probe and changing the filter after every few data points, thereby preventing buildup of carbon and conversion of NO_2 to NO. These and other sampling system and probe effects are discussed in more detail in Chapter 5 and Appendix F.

Still, another problem associated with chemilumenescent NO measurements is that the NO measurement can be affected by the composition of the sample gas. Once excited nitrogen dioxide, NO_2^*, is formed by the oxidation of nitric oxide by ozone

$$NO + O_3 \rightarrow NO_2^* + O_2 \quad , \qquad (3\text{-}1)$$

the chemiluminescent decay reaction

$$NO_2^* \rightarrow NO_2 + h\nu \qquad (3\text{-}2)$$

is in competition with the third body decay reaction

$$NO_2^* + M \rightarrow NO_2 + M . \qquad (3\text{-}3)$$

Since different species have different third body efficiencies (Mellor, 1974; Schefer, 1974), the signal from the chemiluminescence detector will be affected by sample gas composition. This effect was observed and quantized for our instrument. The primary interference in typical combustion gases was associated with water vapor; at 15 mole percent water, the NO measurements read 25% too low at a 2.5 torr reactor pressure. Ideally, the NO_x data should be corrected to account for this effect; however, corrections were not attempted in the current study. Since the present measurements were made in a highly turbulent and fluctuating environment, conditions in the sampling and analytical system were changing in time. To accurately correct the readings would require knowledge of the instantaneous composition of the sample gas. This information is not known and all that is available is the time mean average composition. It was felt that in such a circumstance it was better not to attempt correction but merely to be aware that the NO_x levels may be as much as 20% too low in regions with large water concentrations. These fluctuations in the sampling system are discussed in more detail in Chapter 4.

Oxygen, nitrogen, carbon dioxide, water, and unburnt fuel were measured using a Bendix model 17-210 time of flight mass spectrometer. Analysis of the mass spectrometer data was performed using a least mean squares computer program developed by McLean and Sawyer (1967). Where unambiguous mass spectra peaks exist the concentration of the defined species is determined directly. Otherwise (and also) the LMS program computes the most likely composition for the observed spectra. In the present study oxygen and water vapor could be determined directly while nitrogen, carbon dioxide and unburnt fuel had ambiguous peaks and were determined by LMS analysis. Because of interference from carbon monoxide, the primary or base peak for nitrogen (mass number m/e = 28) could not be used and nitrogen had to be determined from its secondary peak (m/e = 14), resulting in N_2 measurements somewhat less accurate than would normally be expected. While the N_2 data exhibit more scatter than other species, the general trends are as one would expect.

The measurements of unburnt fuel are reported as propane. These are, however, more nearly total hydrocarbon measurements than simply propane. The cracking pattern for propane includes mass numbers (m/e) in order of relative magnitude: 29, 28, 27, 44, 43, 39, 41, 42, 26, 15, 16 and others. Several of these peaks can be associated with particular hydrocarbon species and their cracking patterns (Cornu and Massot, 1966): CH_4-16, 15; C_2H_2-26; C_2H_4-28, 27, 26; C_2H_6-28, 27, 30, 26, 29; C_3H_6-41, 42, 39, 27, 40. All of these hydrocarbon species have been observed in a propane/air turbulent diffusion flame by Takagi et al. (1974) and along with propane constituted the predominate portion of total hydrocarbons. Thus consideration of the above mentioned mass numbers includes contributions from all of these hydrocarbon species and the results presented as propane more nearly represent total hydrocarbons. Ideally calibrations for all of the hydrocarbons should have been obtained and the distribution among species predicted. These calibrations were not made, however, and all data were assumed to be for propane only. There is some error involved in this procedure in that only in the case where the hydrocarbon species are present in the same proportions as in the propane cracking pattern will the results be completely correct. The results therefore, while reasonably representing the data, are actually only best estimates of the total hydrocarbon concentrations.

To get all of the composition data on a common basis certain corrections had to be applied. The mass spectrometer data were taken on a wet basis ignoring carbon monoxide while the carbon monoxide data were taken on a dry basis. Thus carbon monoxide data had to be corrected to a wet basis and the mass spectrometer data had to be corrected to allow for the presence of carbon monoxide. It can be shown that the appropriate corrections to the data are:

$$X_i = X_{i_{MS}} * \left\{ 1 - X_{CO_{NDIR}} \left[1 - \left(\frac{X_{H_2O_{MS}} - X_{CO_{NDIR}} X_{H_2O_{MS}}}{1 - X_{H_2O_{MS}} X_{CO_{NDIR}}} \right) \right] \right\} \quad (3\text{-}4)$$

$$X_{CO} = X_{CO_{NDIR}} * \left\{ 1 - \left(\frac{X_{H_2O_{MS}} - X_{CO_{NDIR}} X_{H_2O_{MS}}}{1 - X_{H_2O_{MS}} X_{CO_{NDIR}}} \right) \right\} \quad (3\text{-}5)$$

where:

X_i - mole fraction of species i

X_{CO} - mole fraction of species CO

$X_{i_{MS}}$ - measured mole fraction of species i, wet basis without CO

$X_{CO_{NDIR}}$ - measured mole fraction of carbon monoxide, dry basis.

These corrections were applied to all data and hence all data are presented as actual mole fractions on a wet basis.

3.3.2 Velocity Measurements

Velocity measurements were made with a specially fabricated five-hole pitot type directional velocity probe shown in Fig. 3-4. A directional type probe was required because of the swirling air flow in the combustor. By taking two separate pressure differentials (top-bottom, and dynamic-static) both the magnitude and direction of the velocity can be determined. In order to obtain more accurate static pressure measurements as well as to obtain them at the same physical location as the other pressure measurements, separate static pressure traverses were made using a static pressure probe, Fig. 3-5. Pressure measurements from these probes were made using a Meriam Model 34MBZTM micromanometer capable of reading to 0.01 mm of water accuracy.

3.3.3 Temperature Measurements

The temperature in the combustor was measured with a Pt/Pt-13% Rh fine wire thermocouple mounted on a 3/32 inch diameter ceramic probe, Fig. 3-6. Relatively heavy thermocouple wires (0.010 inch) are fed through the ceramic probe and act as support wires for the finer thermocouple wire (0.003 inch) used to form the junction. The wires are butt welded together using the techniques of Fristrom and Westenberg (1965); thereby forming a junction only slightly larger than the thermocouple wires (approximately a 0.0045 inch diameter bead). The thermocouple is coated with a Y/Be noncatalytic

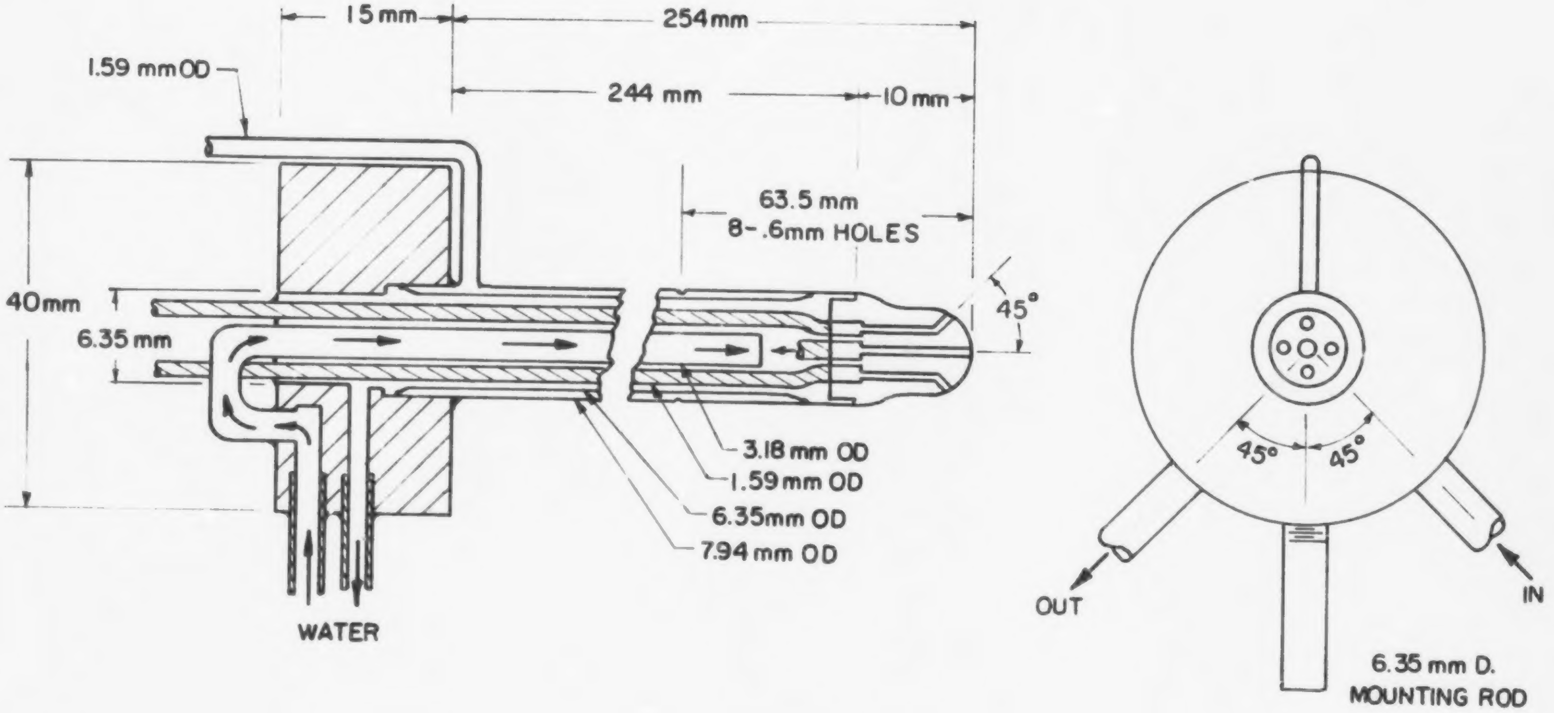
15 mm
254mm
1.59 mm OD
244 mm
10 mm
63.5 mm
8-.6mm HOLES
45°
40mm
6.35 mm
3.18 mm OD
1.59 mm OD
6.35mm OD
7.94 mm OD
WATER
45°
45°
OUT
IN
6.35 mm D.
MOUNTING ROD

Figure 3-4. Five-hole pitot probe.

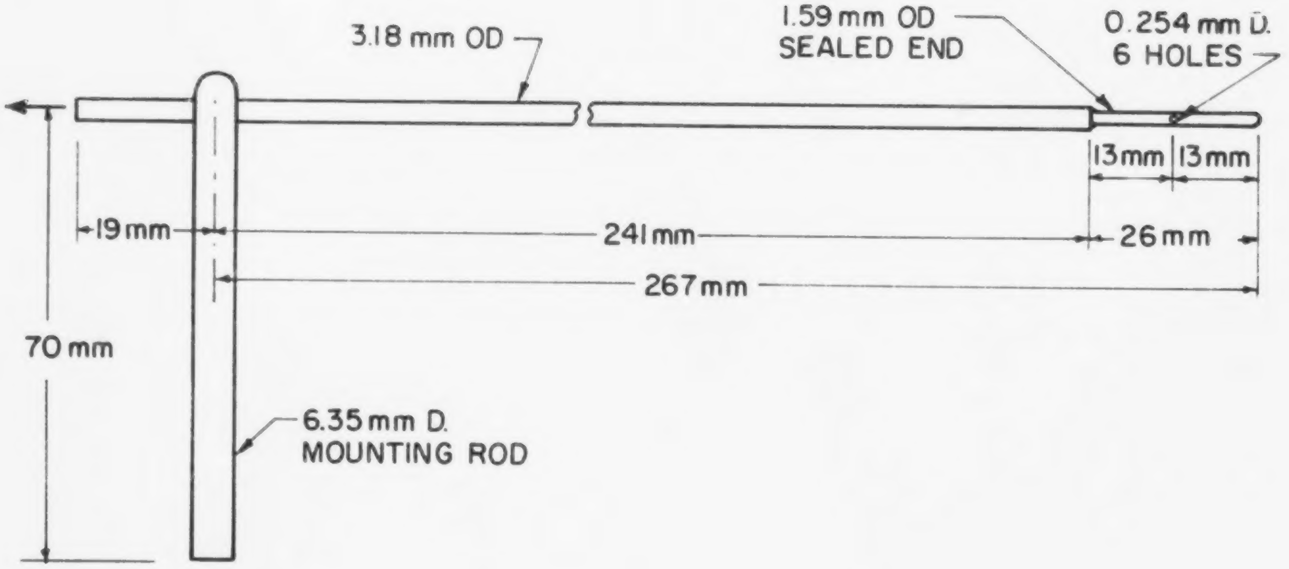
3.18 mm OD
1.59 mm OD
SEALED END
0.254 mm D.
6 HOLES
13 mm
13 mm
19 mm
241 mm
26 mm
267 mm
70 mm
6.35 mm D.
MOUNTING ROD

Figure 3-5. Static pressure probe.

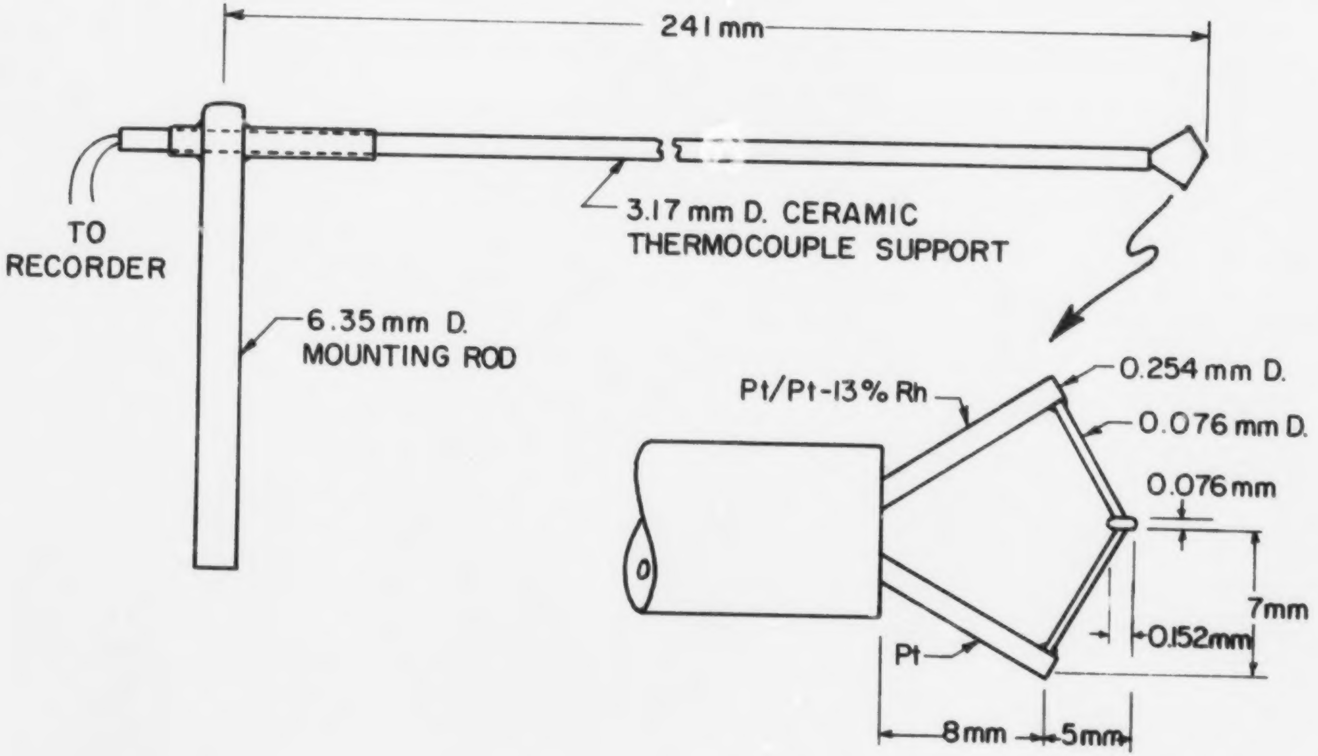
241 mm
TO
RECORDER
6.35 mm D.
MOUNTING ROD
3.17 mm D. CERAMIC
THERMOCOUPLE SUPPORT
Pt/Pt-13% Rh
0.254 mm D.
0.076 mm D.
0.076 mm
7mm
0.152mm
Pt
8mm
5mm

Figure 3-6. Thermocouple probe.

coating developed by Kent (1974). The thermocouple was connected directly to a Varian Model A4023 strip chart recorder and the output EMF recorded. The recorder was biased to reflect the ambient temperature even though this represented a negligible contribution to the total EMF throughout most of the combustion region.

There are three major sources of error in using fine wire thermocouples for temperature measurements — radiation losses from the probe, heat conduction losses along the thermocouple lead wires, and catalytic promotion of reaction on the thermocouple surface (Bradley and Matthews, 1968). The latter effect was minimized by using the noncatalytic coating described above. Conduction losses can be shown to be negligible for the present system with 0.003 inch lead wires 0.5 inch long. The remaining and most important source of error, therefore, is radiation from the junction of the probe. Usual radiation corrections take the form

$$T_G = T_{TC} + \frac{\sigma\varepsilon}{h}[T_{TC}^4 - T_W^4] \tag{3-6}$$

where

T_G = actual gas temperature
T_{TC} = measured thermocouple temperature
T_W = average boundary temperature
σ = Stefan-Boltzman constant
ε = emissivity of the thermocouple junction
h = heat transfer coefficient

The heat transfer coefficient, h, can be related to the properties of the flow through the junction diameter, d, and the thermal conductivity of the gas, k, by way of the Nusselt number,

$$Nu = \frac{hd}{k} . \qquad (3\text{-}7)$$

The Nusselt number is usually expressed as (Kays, 1966; Bradley and Matthews, 1968)

$$Nu \approx 0.42\ Pr^{0.2} + 0.57\ Pr^{0.33}\ Re^{0.5}, \qquad (3\text{-}8)$$

which is valid for $0.01 < Re_{TC} < 10{,}000$. Thus the radiation corrections can be expressed in terms of the properties of the flow and physical constants. Unfortunately all of this required information is not generally known. The thermocouple emissivity, 0.2-0.3 for an uncoated junction, is altered by the addition of the non-catalytic coating, 0.7 reported by Kent, and deposition and subsequent burn off of soot on the probe will cause further alterations in the emissivity. Also, the highly turbulent and fluctuating nature of the flow causes large variations in the fluid properties at the thermocouple junction, making evaluation of the Nusselt number and heat transfer coefficient difficult if not impossible. Because of these difficulties introduced by variations in the Nusselt number and difficulties in computing the properties and conditions of the high temperature gases, as well as uncertainty in the emissivity of the thermocouple, radiation corrections were not attempted and all temperature results are reported as measured. It is estimated that such corrections could amount to greater than 200°K at a measured temperature of 1800°K.

CHAPTER 4

Experimental Results

4.1 Introduction

As was stated in Chapter 3, the experimental apparatus used consisted of a horizontal 58 mm inside diameter X 356 mm Vycor combustion tunnel which contained the flame. Propane was injected axially through an 8.7 mm inside diameter X 0.4 mm wall type 304 stainless steel tube located 152 mm into the combustor and mixed with a slightly swirled coaxial air flow. A complete description of the experimental apparatus is given in Chapter 3 and Appendix A.

The actual operating conditions studied are described in the next section, section 4-2. Initial velocity profiles and results of composition and temperature measurements are presented in section 4-3. Section 4-4 describes additional experiments that were performed and presents representative data from these experiments.

4.2 Operating Conditions

Fuel and air flows for the experiments were chosen such that the flame was contained within the combustion tunnel over the full range of operating conditions, thereby allowing traverses downstream of the flame but yet within the tunnel. In addition, a single fuel flow rate was used for all test conditions in order to maintain a constant enthalpy release rate within the combustor. Experiments were carried out at nominal external stream to jet velocity ratios of 45, 61, and 75:1 and for initial reactant temperatures of 300, 440, and 550°K. All experiments were carried out at one atmosphere pressure. The nominal velocities, temperatures, and mass flows for the nine experimental conditions are shown in Table 4-1. The actual velocities and mass flows for the experimental runs are listed in Appendix B.

Although the combustor was operated at relatively low Froude numbers, $Fr \approx 10$, buoyancy effects were considered negligible as no significant asymmetries were found between the upper and lower portions of the flame.

4.3 Representative Results and Discussion

4.3.1 Initial Velocity Profiles

Velocity measurements were attempted but were difficult due to the swirling air flow and the sooty nature of the flame. The swirled air flow necessitated using a directional type of probe described in Chapter 3. Unfortunately, any deposition of soot on the probe tip changes the instrument calibration making velocity measurements unreliable. It was assumed that the swirl and velocity distribution would be given by the analytical relation (Beer and Chigier, 1972):

$$S = \frac{G_\theta}{G_x R} = \frac{2}{3}\ \frac{1-(a/R)^3}{1-(a/R)^2}\ \tan\alpha \qquad (4\text{-}1)$$

where

α - angle of the swirling vanes

a - radius of fuel injector

R - radius of Vycor housing

TABLE 4-1. Initial conditions at jet exit plane

Nominal velocity (V_A/V_F)	Fuel flow (g/sec)	Air flow (g/sec)	Initial reactant temperature (°K)	Fuel jet velocity (cm/sec)	Air velocity (cm/sec)
45	0.0074	7.4	300	5.70	254
			440	8.61	384
			550	10.5	467
61	0.0074	10.2	300	5.70	348
			440	8.61	529
			550	10.5	652
75	0.0074	12.5	300	5.70	440
			440	8.61	646
			550	10.5	804

G_θ - axial flux of angular momentum

G_x - axial flux of linear momentum

For $\alpha = 25°$, this expression yields a swirl number $S = 0.31$. The adequacy of this relation was checked by measurements made at the jet exit plane where soot is not a problem. (This is also the initial condition station for computational purposes). The results for all three velocity ratios are shown in Fig. 4-1. Agreement between theory and experiment is very good. Hence, no further velocity data are reported.

4.3.2 Composition and Temperature

Only selected results are presented for the major species, while results for NO and NO_2 are treated more comprehensively. Data for all species over the complete set of operating variables can be found in Appendix C and D. Where clarity is enhanced, data points are sometimes omitted from the figures.

Figure 4-2 shows centerline concentration profiles of propane, oxygen, carbon monoxide, carbon dioxide and water for the three velocity ratios at 300°K. The effect upon these species of increasing reactant temperature is similar to that of increasing the velocity ratio; hence, no new data are presented. Typical radial profiles for these same species are shown in Fig. 4-3. The trends shown by these species are as one would expect and vary rather smoothly from the free stream to the jet centerline and over the full range of operating conditions. Nitrogen data also followed the expected trends; they are not presented here but can be found in Appendix C.

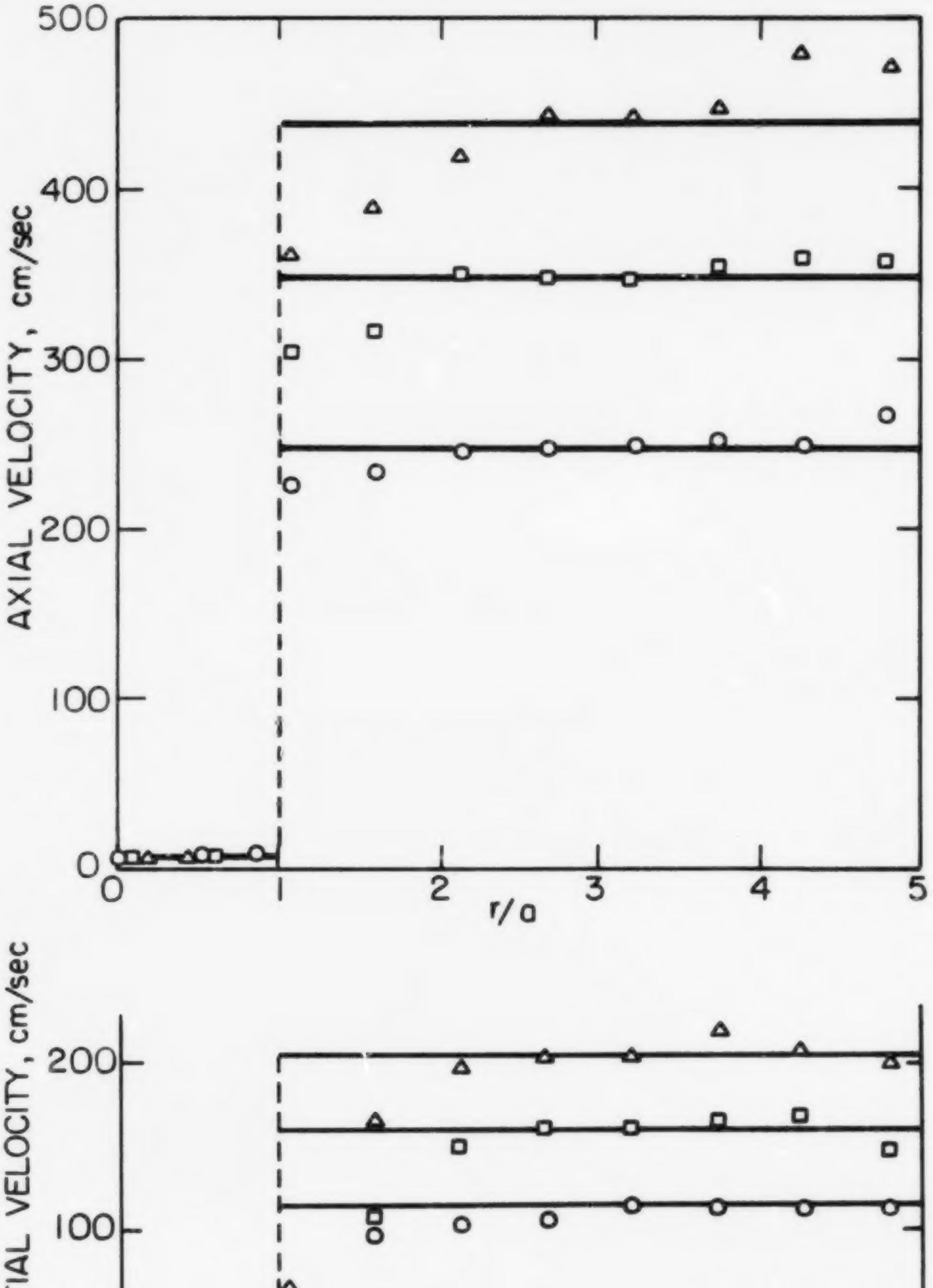

Figure 4-1. Initial velocity profiles at jet exit plane, 300°K, ○ = V_A/V_F = 45; □ - V_A/V_F = 61; Δ - V_A/V_F = 75.

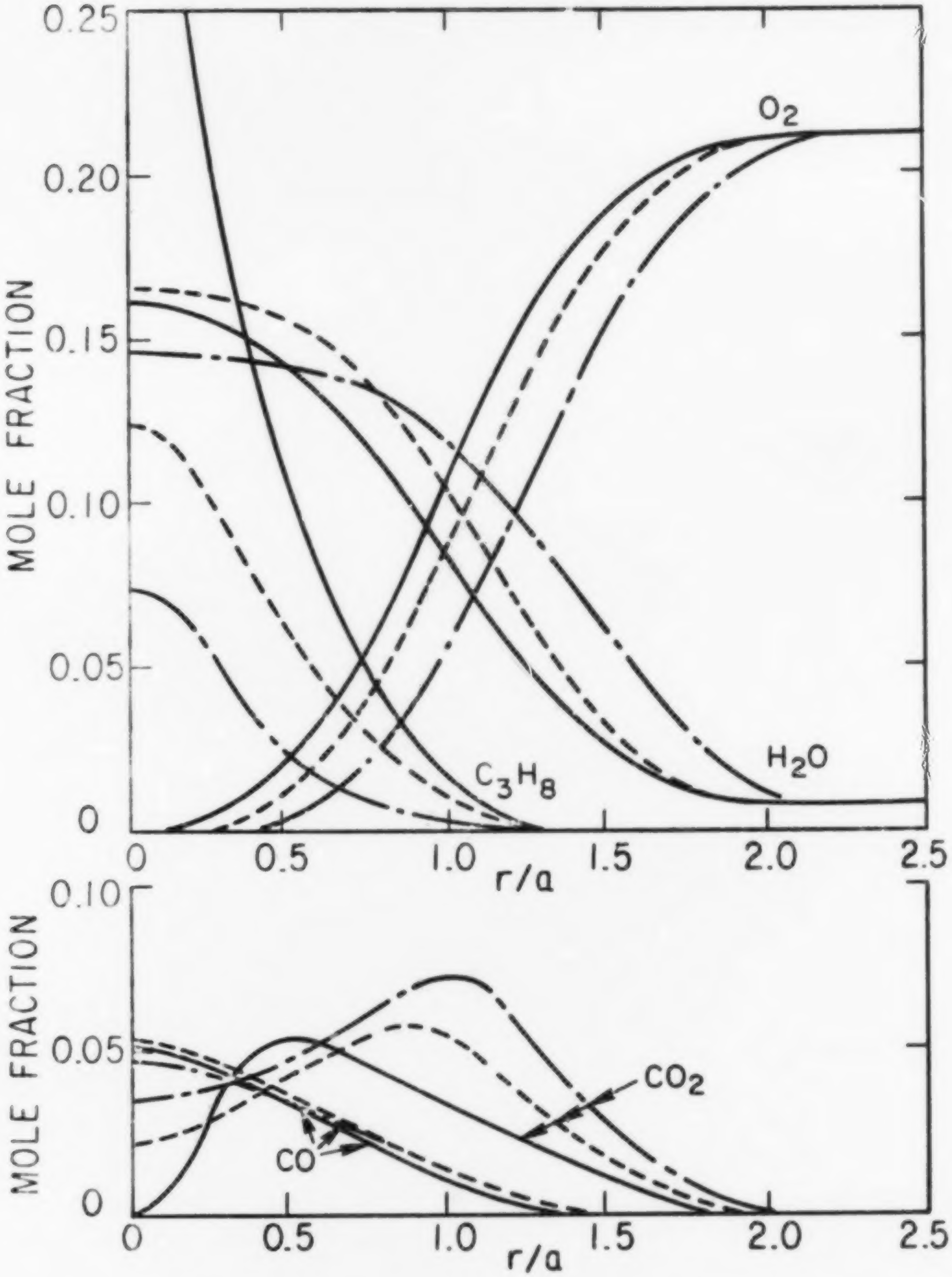

Figure 4-3. Radial distributions for propane, oxygen, carbon monoxide, carbon dioxide, and water vapor at $V_A/V_F = 45$, and 300°K initial reactant temperature. —— X/D = 1.33; ---- X/D = 2.66; — - — X/D = 5.33.

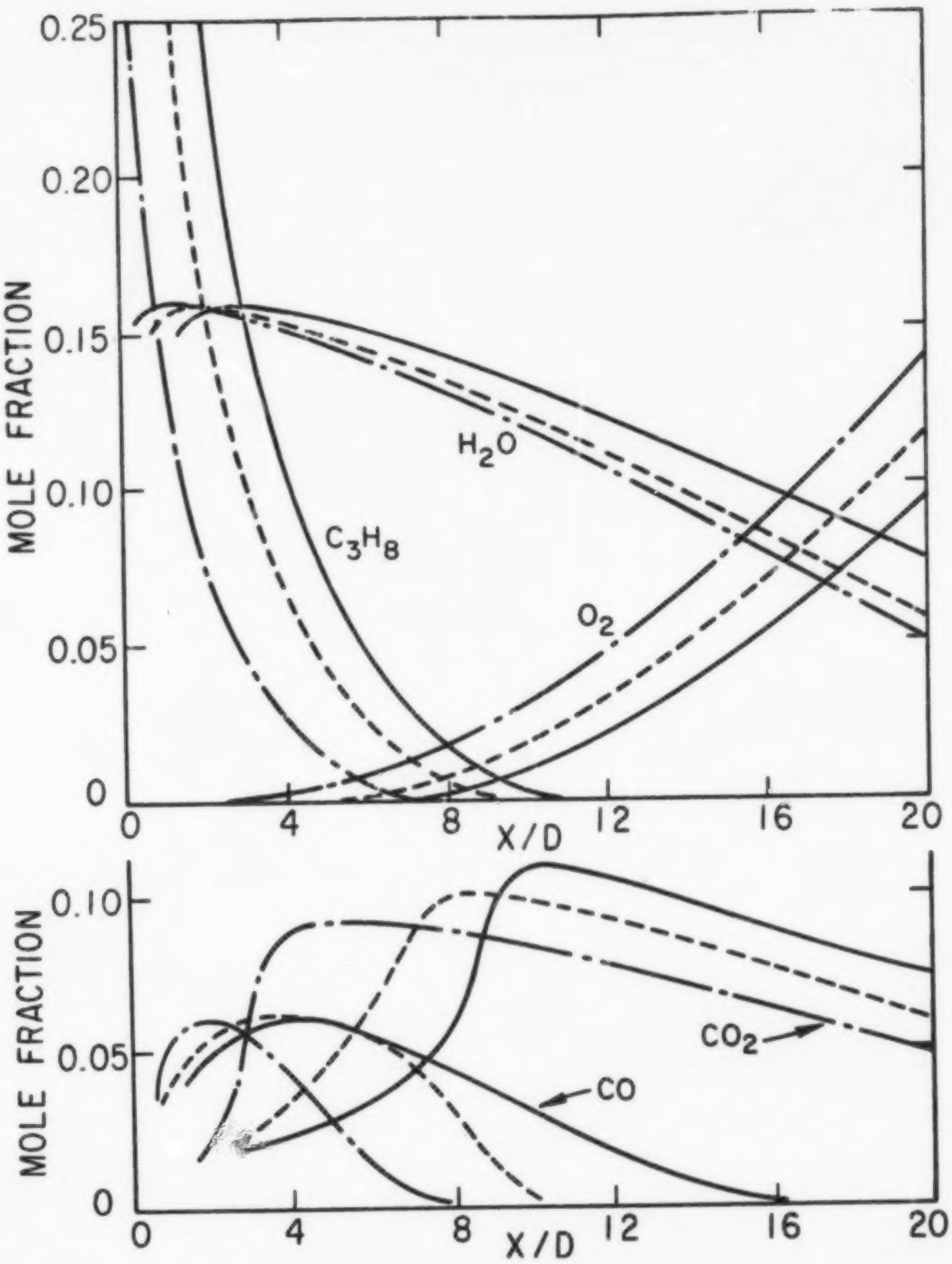

Figure 4-2. Centerline distributions for propane, oxygen, carbon monoxide, carbon dioxide and water vapor at 300°K initial reactant temperature. —— $V_A/V_F = 45$; ---- $V_A/V_F = 61$; — - — $V_A/V_F = 75$.

A significant point illustrated in these two figures is the overlapping of the propane and oxygen profiles, indicative of the strong mixing processes that are occurring. Since these are time mean average profiles, they merely indicate the average state of fuel rich and fuel lean conditions varying in time. We cannot quantify the extent to which the propane and oxygen actually coexist without time resolved measurements. It seems likely however, that in such a strongly mixed and turbulent situation overlapping can be substantial, providing a mechanism for supplying oxygen to the flame interior region.

The data for NO, NO_2 and temperature are of interest and are presented in more detail. Figures 4-4 and 4-5 show centerline profiles parameterized in velocity ratio and inlet reactant temperature respectively, while Figs. 4-6, 4-7, and 4-8 show radial profiles parameterized in axial distance, velocity ratio, and inlet reactant temperature.

The data for NO are qualitatively as we would expect: along the centerline NO increases downstream from the injector tip, reaches a maximum in the hot region near the flame tip, and then decreases as mixing causes dilution and cooling; radially NO is symmetric about the centerline, with a maximum at the flame surface. The effect of air preheat is to increase the flow velocities and reaction rate thus shortening the flame and decreasing the residence time. However, since NO formation is linear in time but exponential in temperature, the peak NO is increased accordingly. The effect of increased velocity ratio is to shorten the flame due to increased mixing with no significant effect on peak NO. This result is some-

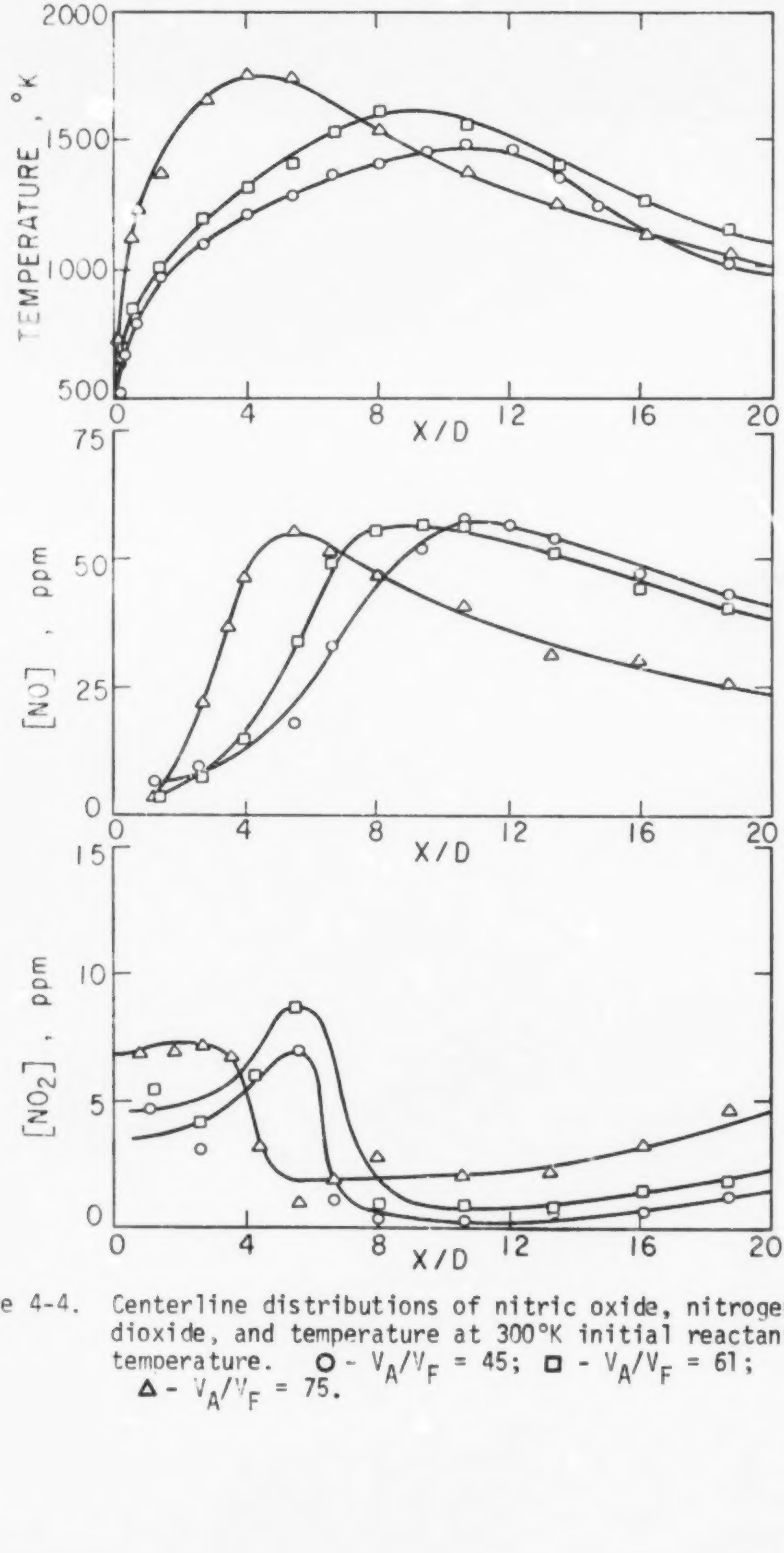

Figure 4-4. Centerline distributions of nitric oxide, nitrogen dioxide, and temperature at 300°K initial reactant temperature. ○ - $V_A/V_F = 45$; □ - $V_A/V_F = 61$; △ - $V_A/V_F = 75$.

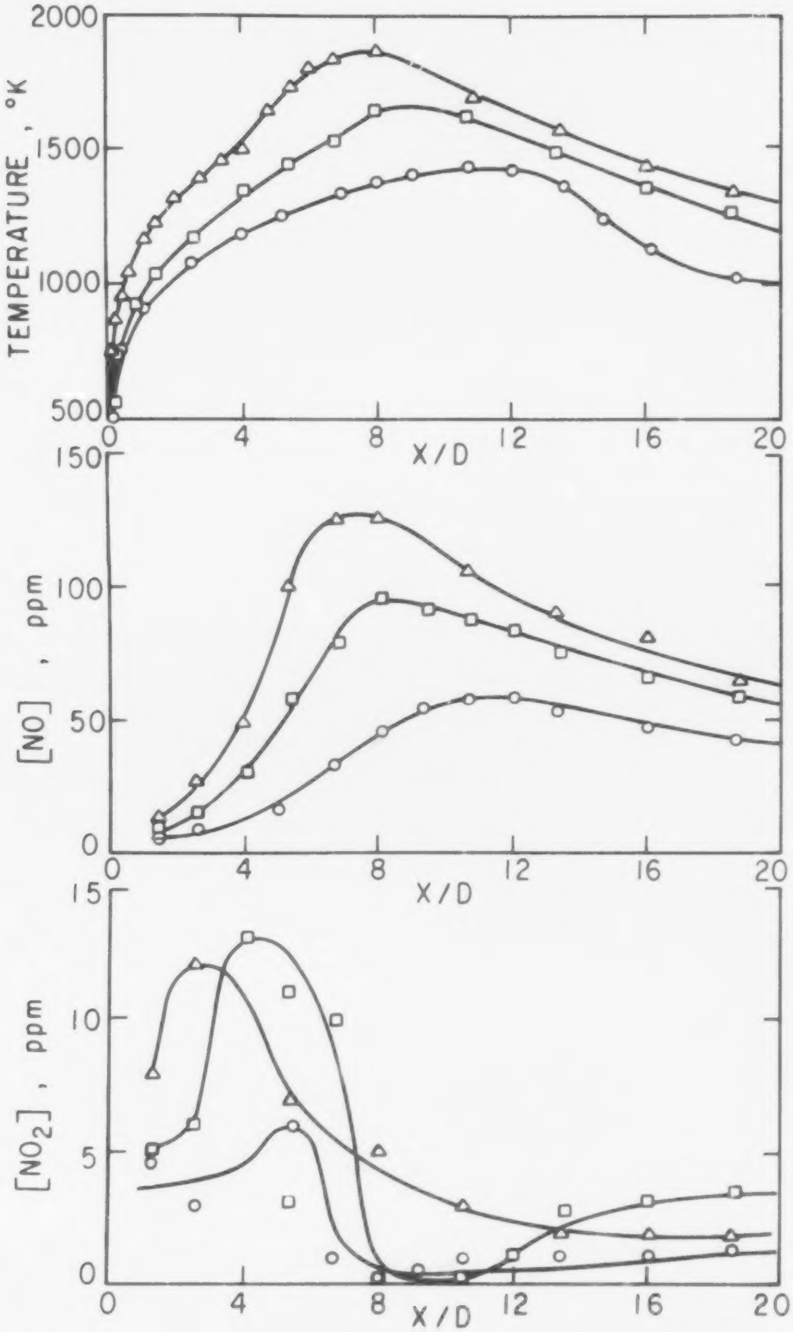

Figure 4-5. Centerline distributions of nitric oxide, nitrogen dioxide, and temperature for different initial reactant temperatures at $V_A/V_F = 45$. ○ - T = 300°K; □ - T = 440°K; △ - T = 550°K.

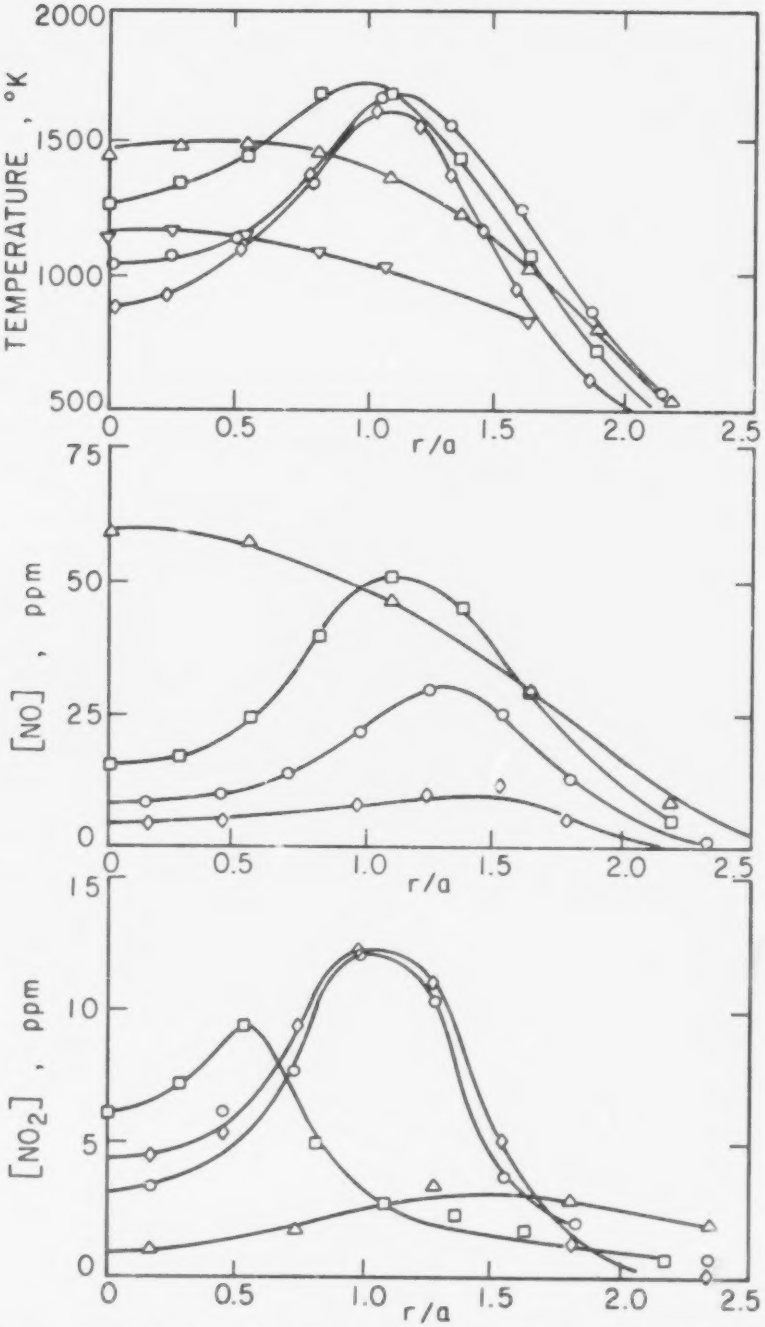

Figure 4-6. Radial distributions of nitric oxide, nitrogen dioxide, and temperature at V_A/V_F = 45 and 300° initial reactant temperature. ◇ - X/D = 1.33; ○ - X/D = 2.66; □ - X/D = 5.33; △ - X/D = 10.66; ▽ - X/D = 21.33.

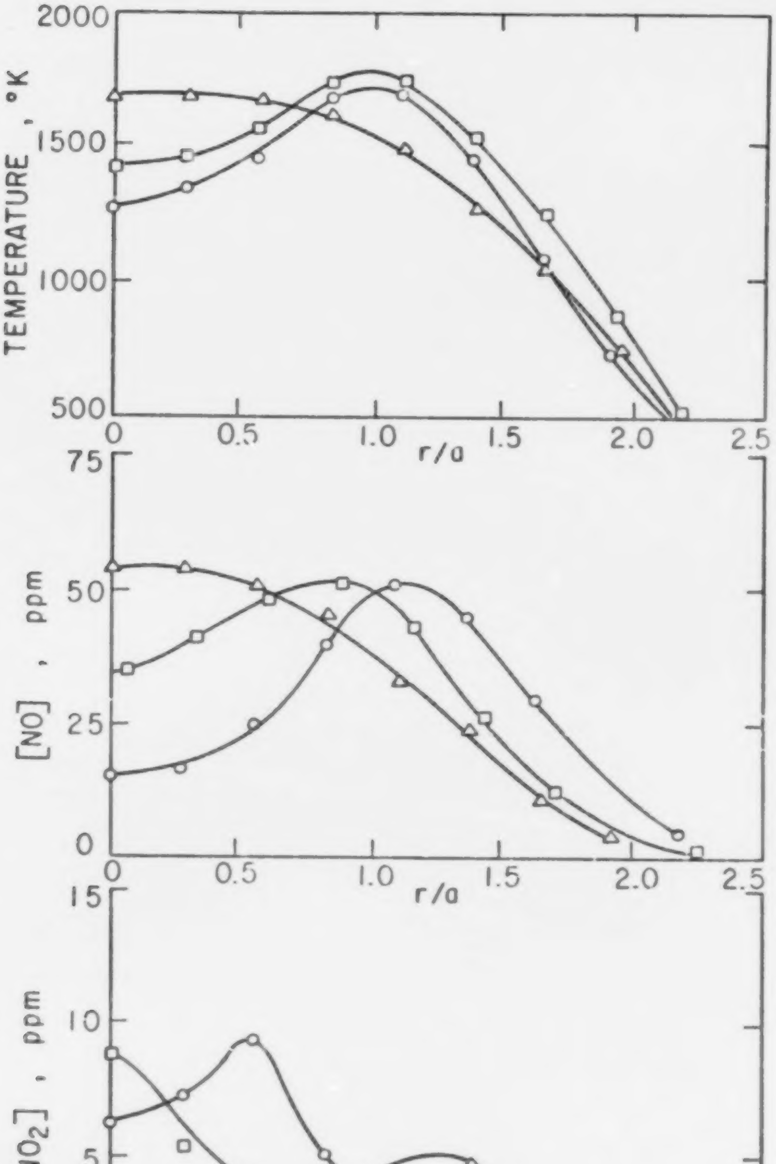

Figure 4-7. Radial distributions of nitric oxide, nitrogen dioxide, and temperature at axial location X/D = 5.33 and 300°K initial reactant temperature. ○ - V_A/V_F = 45; □ - V_A/V_F = 61; △ - V_A/V_F = 75.

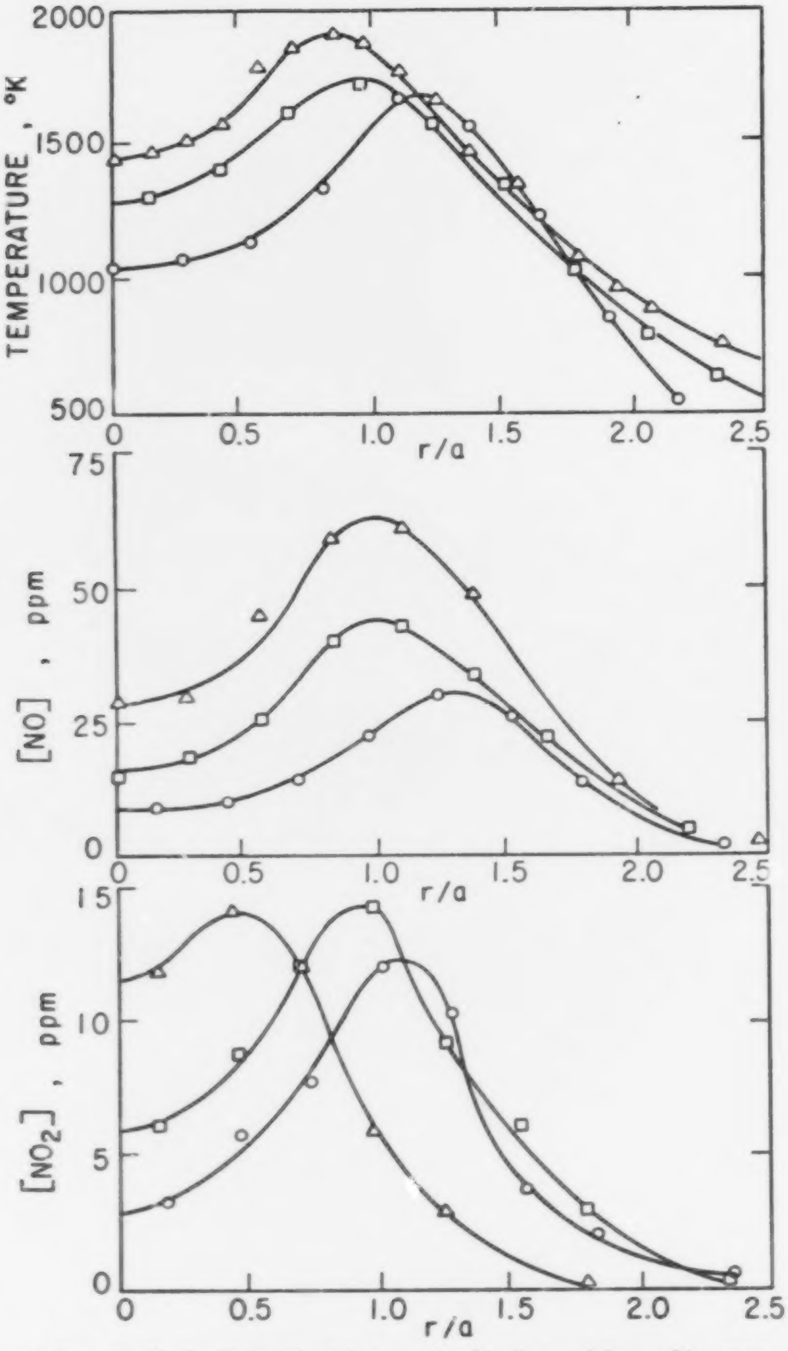

Figure 4-8. Radial distributions of nitric oxide, nitrogen dioxide, and temperature at axial location X/D = 2.66 and velocity ratio V_A/V_F = 45. ○ - T = 300°K; □ - T = 440°K; △ - T = 550°K.

what surprising in that increased mixing would be expected to result in both shorter eddy lifetimes and shorter total residence times, thereby reducing the time available for NO formation. A detailed explanation of the results lies in understanding the complex fluid mechanical, kinetic, radiative and other processes that are occurring. Complete elucidation of this problem, therefore, would require time resolved measurements to identify the details of the combustion zone processes and, in their absence all that can be said with certainty is that peak NO does not scale with flame length. Bilger and Beck (1974), Lavoie and Schlader (1974), Quan (1974) and Quan et al. (1973, 1974) discuss the scaling of NO in turbulent diffusion flames in more detail.

The measured NO_2 concentrations, determined by the difference of NO and total NO_x essentially follow the same trends as the NO curves. However, the NO_2 appears to peak slightly on the fuel rich side of the NO maxima for both radial and axial profiles. Also, in the fuel rich flame interior region, NO_2 constitutes a larger percentage of total NO_x than near the flame surface. The presence of O_2 in the flame interior provides a plausible mechanism for explaining these phenomena, however, no completely satisfactory explanation was found. NO_2 formation mechanisms are discussed in Chapter 5.

As was pointed out in Chapter 3, considerable effort was required to obtain acceptable NO_2 data, the main problem being the accumulation of soot in the sample system. Even with all of the precautions that were taken, the NO_2 data do not have the same smooth trends exhibited by the NO data. Part of this scatter is due to the low levels being measured as well as the inherent difficulties of a subtractive analytical procedure. Results were generally reproducible to within ± 1 ppm.

The temperature measurements also follow expected patterns and correspond fairly closely with the NO_x profiles, indicating the strong coupling of temperature and NO_x production. The temperature profiles are reported as measured.

4.3.3 Fluctuations

It should be emphasized that the measurements reported here are time mean averages of the concentrations and temperatures at each physical location in the combustor. Hence, the instantaneous peak values will be higher, and in some regions substantially higher, than the mean. For example, along the mean flame surface, any particular physical location will be alternately fuel rich and fuel lean as the actual flame front passes back and forth across the point causing large fluctuations in species concentrations and temperature. These fluctuations are averaged out in the sampling and analytical system and results are reported as measured. Bilger and Kent (1972) discuss these fluctuations in more detail.

4.4 Other Experiments

As was pointed out in Chapter 2, the measurement of NO_2 in combustion systems is somewhat surprising. In an attempt to isolate some of the possible effects contributing to NO_2 formation, a number of additional experiments were performed. These included experiments using hydrogen and carbon monoxide as the fuel and also experiments where the fuel and air streams were seeded with NO. These results are presented next.

4.4.1 Other Fuels

The discussion of NO_2 formation mechanisms in Chapter 5 points out a number of possible NO_2 formation routes. These include hydrocarbon species and fragments (ROO), hydrogen and its radicals (OH, HOO), and carbon dioxide (CO_2). By using carbon monoxide and hydrogen in addition to propane as the fuel, the importance of these various reactions can be explored.

Results for one run using hydrogen as the fuel are shown in Fig. 4-9. Since in this configuration there are no hydrocarbon species present and since NO_2 was measured, postulated reactions involving ROO are probably not important in this system.

Similarly, if NO_2 could be measured in carbon monoxide flames in the absence of hydrogen species, the effect of OH and HOO could be isolated. Runs using carbon monoxide as the fuel did result in NO_2 observations, however, there was sufficient water vapor in the air stream (3-5% relative humidity) to provide an ample source of the hydrogen related radical species. Thus no definite conclusions could be drawn from this experiment about the importance of the HOO and OH species in NO_2 formation and no data are included. (A particular problem that showed up in the carbon monoxide experiments was related to conditioning the probe and sampling and analytical equipment in a reducing atmosphere. This and other sampling difficulties are discussed in detail in Appendix F.)

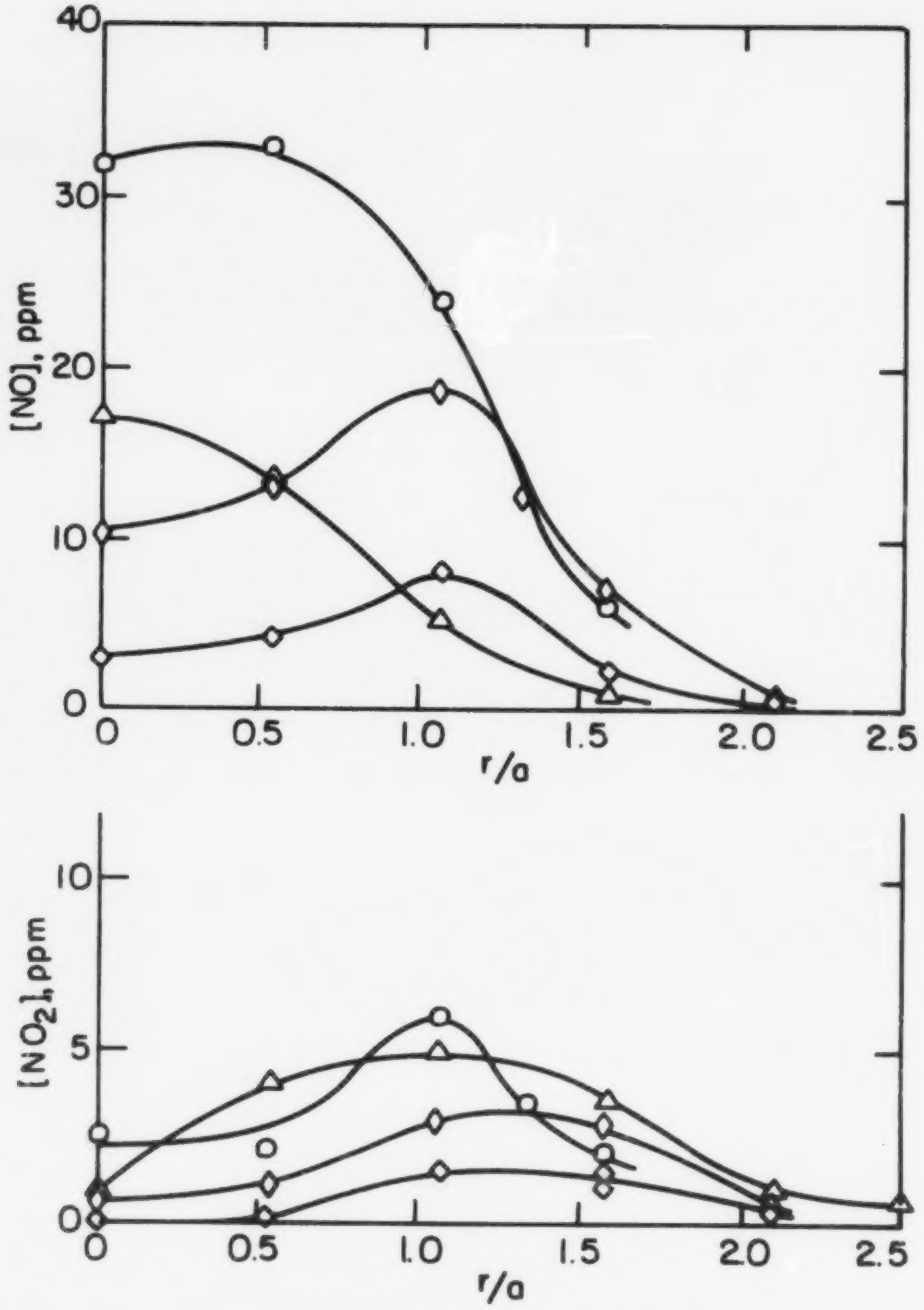

Figure 4-9. Radial distributions of nitric oxide and nitrogen dioxide using hydrogen fuel at V_A/V_F = 7.5 and 300°K initial reactant temperature. ◇ - X/D = 0.67; ◊ - X/D = 1.33; ○ - X/D = 2.66; △ - X/D = 10.66.

4.4.2 NO Seeding

Another problem discussed in Chapter 5 deals with the possibility of probe reactions and probe effects. To explore this problem and also to obtain information on the formation route of NO_2, experiments were carried out where various concentrations of NO were seeded in both the fuel and air streams. This experiment is designed to show if NO_2 goes through an NO step and also, to elucidate sampling difficulties.

Four levels of NO seeding were used (0, 9.5, 20, and 32 ppm) and both the fuel and air stream were seeded to the same level. Equivalent seeding flows of pure N_2 were also used to account for dilution effects. The results are shown in Fig. 4-10. The level of seeding can be observed out in the freestream where the flow is undisturbed (large r/a). Also, a conversion of this NO to NO_2 can be observed, apparently in the strongly mixed layer near the flame surface. Since these measurements were made in a relatively cool downstream region where sampling effects would be expected to be negligible (see Chapter 5), we conclude that NO_2 can actually be formed in this combustion system. An in situ measurement would of course be desirable in confirming this conclusion. Also, it appears that NO_2 formation probably proceeds through a NO step. This is not completely certain, however, because it is possible that the seeded NO is first converted to some other form before being converted to NO_2.

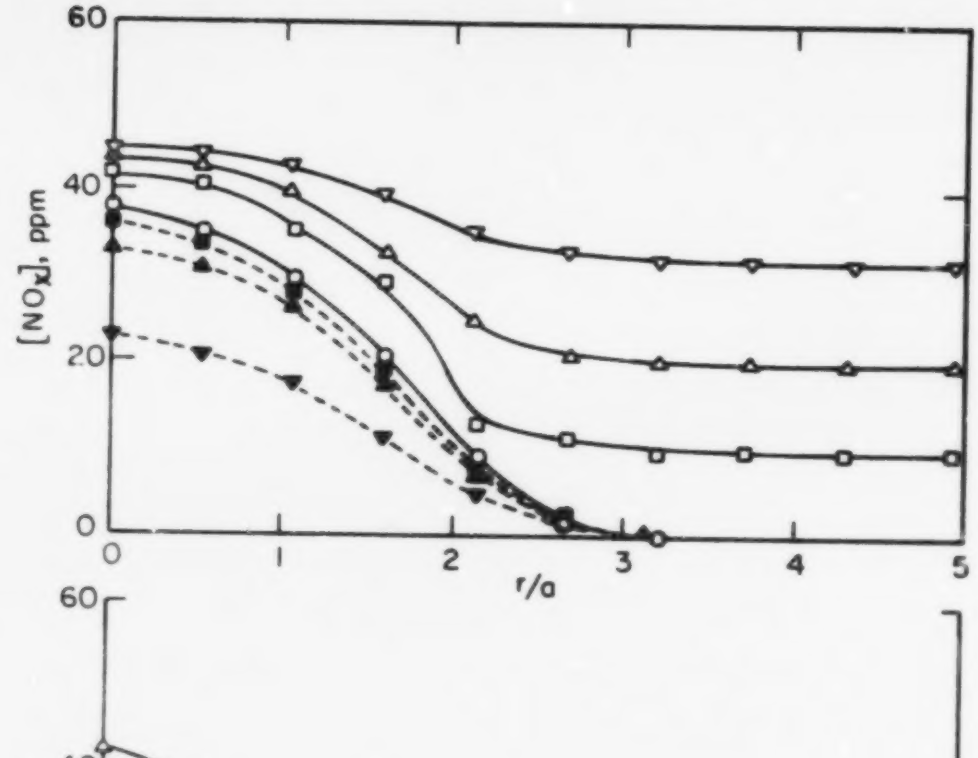

Figure 4-10. Radial distributions of nitric oxide, nitrogen dioxide, and oxides of nitrogen at axial location X/D = 16 and 300°K initial reactant temperature for several concentrations of NO in the reactants ○ - 0 ppm NO; □ - 9.5 ppm NO; △ - 20 ppm NO; ▽ - 32 ppm NO. Solid symbols are equivalent seeding flows of N_2 without NO.

CHAPTER 5

Kinetics of NO and NO_2 Formation

5.1 Introduction

As was pointed out, the existence of NO_2 in combustion systems is not generally predicted by conventional theories. Thus the NO_2 measurements are of considerable interest and provide motivation for one to examine possible NO_2 formation routes in combustion systems. The remainder of this chapter is devoted to this end.

First, NO and NO_2 formation routes that have been used previously are discussed. Attention is then given to new NO_2 formation routes that are not traditionally considered and a new mechanism is proposed. Results of kinetic calculations verifying the plausibility of this mechanism are presented. Finally, NO_2 in combustion systems and in particular NO_2 in the present experiment are discussed with reference to this mechanism.

5.2 NO Kinetics and Mechanisms

The mechanisms of NO formation for many different combustion configurations over a wide range of operating parameters are known and well documented (Cornelius and Agnew, 1972; Malte and Pratt, 1973; Edelman and Economos, 1971; Marteney, 1970). Therefore, these mechanisms will not be repeated here. Instead, emphasis will be placed on possible NO_2 mechanisms.

5.3 NO_2 Formation Mechanisms

5.3.1 Past Work

Some NO_2 reactions that have been suggested are the following:

	$\Delta H_{R_{298}}$	
$NO + NO + O_2 = NO_2 + NO_2$	- 27 kcal/mole	(5-1)
$N_2 + O_2 = NO_2 + N$	+ 121 kcal/mole	(5-2)
$NO + NO = NO_2 + N$	+ 78 kcal/mole	(5-3)
$NO + O + M = NO_2 + M$	- 73 kcal/mole	(5-4)
$O_2 + N + M = NO_2 + M$	- 105 kcal/mole	(5-5)
$NO + O_2 = NO_2 + O$	+ 46 kcal/mole	(5-6)
$NO + OH = NO_2 + H$	+ 29 kcal/mole	(5-7)
$NO + HOO = NO_2 + OH$	- 9 kcal/mole	(5-8)
$NO + CO_2 = NO_2 + CO$	+ 54 kcal/mole	(5-9)
$R \cdot OO + NO = NO_2 + R \cdot O$	-	(5-10)
$HNO_2 + O = NO_2 + OH$	- 24 kcal/mole	(5-11)
$HNO_2 + OH = NO_2 + H_2O$	- 41 kcal/mole	(5-12)
$NO + O_3 = NO_2 + O_2$	- 48 kcal/mole	(5-13)

Steric considerations indicate that reactions (5-2) and (5-5) are impossible; they are listed nune the less because of their inclusion in the work of other investigators.

Several schemes for NO_2 formation have been examined by other investigators. Cornelius and Wade (1970) and MacKinnon and Ingraham (1972) attempted to use reaction (5-1) and concluded that no significant amounts of NO_2 could be formed in practical combustion systems. Edelman and Economos (1971), Edelman et al. (1972), and Marteney (1970) performed analyses involving reactions (5-2) through (5-6) and all found that NO_2 formation was negligible even when super-equilibrium radical concentrations were considered. The results of these and other studies are discussed in more detail by Tuttle, et al. (1973) and Mellor (1972).

The mechanism preferred by Tuttle, et al. for NO_2 formation involved the following reaction scheme:

$$O_2 + M = O + O + M \qquad (5\text{-}14)$$

$$O + NO + M = NO_2 + M \qquad (5\text{-}4)$$

$$NO + O_2 = NO_2 + O \qquad (5\text{-}6)$$

The scheme depends on convection of oxygen atoms from a hot reaction zone into a cooler region, where they oxidize NO to NO_2. The scheme is adequate for high pressure systems at low local temperatures (e.g., 5 atm., < 900°K) and for low pressure systems at lower local temperatures (e.g., 1 atm., < 500°K). At temperatures higher than these however, NO_2 destruction via reaction (5-6) is comparable to production from reaction (5-4) and significant amounts of NO_2 are not predicted.

Also, whenever there is transport into cooler regions, conversion of NO to NO_2 through direct low temperature oxidation by O_2 is possible. However, this mechanism, reactions (5-1) and (5-6), is not rapid enough to be of importance in most practical combustion systems; this is the case with the current work.

5.3.2 Current Study

Examination and evaluation of the rate data for reactions (5-1) through (5-13) as wel [illegible] consideration of steric factors shows that reactions (5-1), (5-[illegible] (5-3) and (5-5) contribute negligibly to the NO_2 formation and destruction in virtually all practical combustion systems. The remaining reactions are considered to be of possible importance. These reactions are summarized along with reaction rate data in Table 5-1. Table 5-2 shows the temperature range over which the rate data have been demonstrated to be valid and also contains

TABLE 5-1. Rate constants for nitrogen dioxide reactions*

Reaction		Forward Rate Constant	Backward Rate Constant	Reference
(5-4)	$O + NO + M = NO_2 + M$	$10^{15.037}$ exp(1.87/RT)	$10^{16.035}$ exp(-65.54/RT)	Garvin(1974)
(5-6)	$NO + O_2 = NO_2 + O$	$10^{12.484}$ exp(-47.40/RT)	$10^{13.000}$ exp(-0.60/RT)	Laurendeau(1972)
(5-7)	$NO + OH = NO_2 + H$	$10^{12.496}$ exp(-29.99/RT)	$10^{14.543}$ exp(-1.50/RT)	Garvin(1974)
(5-8)	$NO + HOO = NO_2 + OH$	$10^{12.48}$ $T^{0.5}$ exp(-2.4/RT)	$10^{12.19}$ $T^{0.5}$ exp(-6.56/RT)**	Kondratiev(1972)
(5-9)	$NO + CO_2 = NO_2 + CO$	$10^{12.3}$ exp(-81.6/RT)	$10^{12.28}$ exp(-29.26/RT)	Kondratiev(1972)
(5-10)	$R{\cdot}OO + NO = NO_2 + R{\cdot}O$	$<10^{10.60}$exp(-0.99/RT)	-	Garvin(1974)
(5-11)	$HNO_2 + O = NO_2 + OH$	$10^{12.780}$ exp(-0.80/RT)	$10^{12.33}$ exp(-25.0/RT)**	Anderson and Meyer (1973)
(5-12)	$HNO_2 + OH = NO_2 + H_2O$	$10^{11.930}$ exp(-2.00/RT)	$10^{12.50}$ exp(-43.7/RT)**	Anderson and Meyer (1973)
(5-13)	$NO + O_3 = NO_2 + O_2$	$10^{11.734}$ exp(-2.380/RT)	$10^{12.226}$ exp(-50.4/RT)	Garvin(1974)

---

*All rates in unites of moles/cc, sec; R = 0.001986 kcal/gm mole/°K.

**Calculated from equilibrium constant and forward reaction rate.

TABLE 5-2. Temperature range and evaluation of nitrogen dioxide reactions*

Reaction	Temperature Range of Rate Data		Evaluation of Reaction Rates**		
	Forward	Reverse	T < 700	700 < T < 1300	T > 1300
(5-4) $O + NO + M = NO_2 + M$	200-500	1400-2400	F	F	F B
(5-6) $NO + O_2 = NO_2 + O$	280-550	280-550	B	B	F B
(5-7) $NO + OH = NO_2 + H$	300-600	300-600	B	F B	F B
(5-8) $NO + HOO = NO_2 + HO$	-	-	F B	F B	F B
(5-9) $NO + CO_2 = NO_2 + CO$	500-800	500-800			B
(5-10) $NO + R{\cdot}OO = NO_2 + R{\cdot}O$	-	-	F	F	F
(5-11) $HNO_2 + O = NO_2 + OH$	-	-	F	F	
(5-12) $HNO_2 + OH = NO_2 + H_2O$	-	-	F	F	
(5-13) $NO + O_3 = NO_2 + O_2$	200-350	200-350	F	F	

---

*T = °K, F = forward rate important, B = backward rate important.

**based on expected concentrations of reactants, including superequilibrium radical species.

a qualitative evaluation of the temperature regions in which the reactions can be considered important.

The NO_2 formation reaction involving oxidation of NO by ROO radicals is very hard to quantify due to the largely unknown hydrocarbon oxidation mechanisms which form ROO. It is generally assumed that the formation of NO_2 by this mechanism will be small. Experiments using hydrogen as a fuel where NO_2 has been measured (see Figure 4-9) support this assumption.

The nitrous acid reactions, (5-11) and (5-12), and the ozone reaction, (5-13), should contribute negligibly to NO_2 production at temperatures greater than 900°K. At lower temperatures, however, their contribution can become significant and they should be included in any analysis.

The possibility for heterogeneous reactions for production of NO_2 exists in hydrocarbon fueled combustion systems. Chang and Novakov (1974) discuss NO-soot and NO_2-soot reactions in some detail. Mechanisms and their importance are for the most part unknown and need to be explored.

Reactions of NO and NO_2 with hydrocarbon species has also been reported (Tuttle et al., 1973; Myerson, 1974). The reactions and rates are not well known; additional work is required in this area.

5.3.1 Kinetic Calculations

Recognizing the limitations on the rate data, we can proceed to examine the process of NO_2 formation using detailed kinetic calculations. (See Appendix E for details of the calculation procedure.) We shall ignore the carbon dioxide and peroxy radical reactions (Eqs. (5-9)-(5-10)) as well as heterogeneous mechanisms. Near flame temperatures with equilibrium or normal superequilibrium concentrations of radicals, NO_2 is not predicted in significant amounts. The major radical species, H, O, and OH, at these high temperatures all favor maintenance of NO_2 concentrations several orders of magnitude below NO. If a burning eddy is cooled slowly, allowing the radical species to maintain equilibrium as the temperature is decreased, eventually NO_2 production will be favored (< 500°K at 1 atm.), but the radical concentrations will be so low that the time scale will be much too long to be of practical concern. If the temperature of a burning eddy is decreased rapidly and/or large concentrations of radicals are transported into cool regions as might be the case in turbulent, strongly mixed combustion systems, significant production of NO_2 can be predicted. In this case, the relaxation of the superequilibrium radical concentrations can result in the buildup and maintenance of large superequilibrium concentrations of HOO, favoring production of NO_2. It is expected that this is the important mechanism for formation of NO_2 in combustion systems.

Once formed in a cool eddy, HOO can persist until the concentrations of H, O, and OH, which favor destruction of NO_2, fall to levels consistent with NO_2 formation. The concentrations of radicals that occur in such a case depend on the cooling rate, the oxygen concentration, and the initial radical concentrations. In general, fuel lean mixtures can satisfy the conditions necessary for NO_2 formation, while fuel rich mixtures almost always favor NO_2 destruction.

Using equilibrium concentrations of radicals for $\phi = 0.8$ at 2050°K and 50 ppm NO, kinetic calculations including HOO reactions predict that instantaneous cooling to 900°K results in ten percent conversion to NO_2 in 1 msec., Fig. 5-1. Calculations with only the usual radical species result in no predicted conversion of NO to NO_2, Fig. 5-2. Inclusion of the nitrous acid, nitric acid, and ozone reactions in addition to the HOO mechanism results in additional conversion of NO, Fig. 5-3. In this case some of the converted NO appears as nitrous and nitric acid rather than solely as NO_2. It is felt that in the chemiluminescent analyzer these compounds will be measured as NO_2 so that their effect on NO will not be missed. Fig. 5-4 shows conversion of NO versus time for different final temperatures and reaction schemes. When only the "usual" reactions and radicals species are considered, no appreciable conversion of NO is predicted down to a temperature of 500°K. If the hydroperoxy radical reactions are included (solid lines), substantial NO conversion is predicted in very short times, with more conversion as the final temperature is lowered. Including the nitrous and nitric acid and ozone reactions accentuates this NO conversion at lower temperatures (the dashed lines).

We have then a plausible mechanism for NO_2 formation. It requires strong mixing processes to rapidly quench high temperature eddies and/or to transport large radical concentrations into cooler regions. Such strong mixing processes occur in many combustion systems - gas turbine combustors, power plant boilers, as well as the current system. The mechanism can apply for situations in which oxygen, low temperature, and superequilibrium radicals

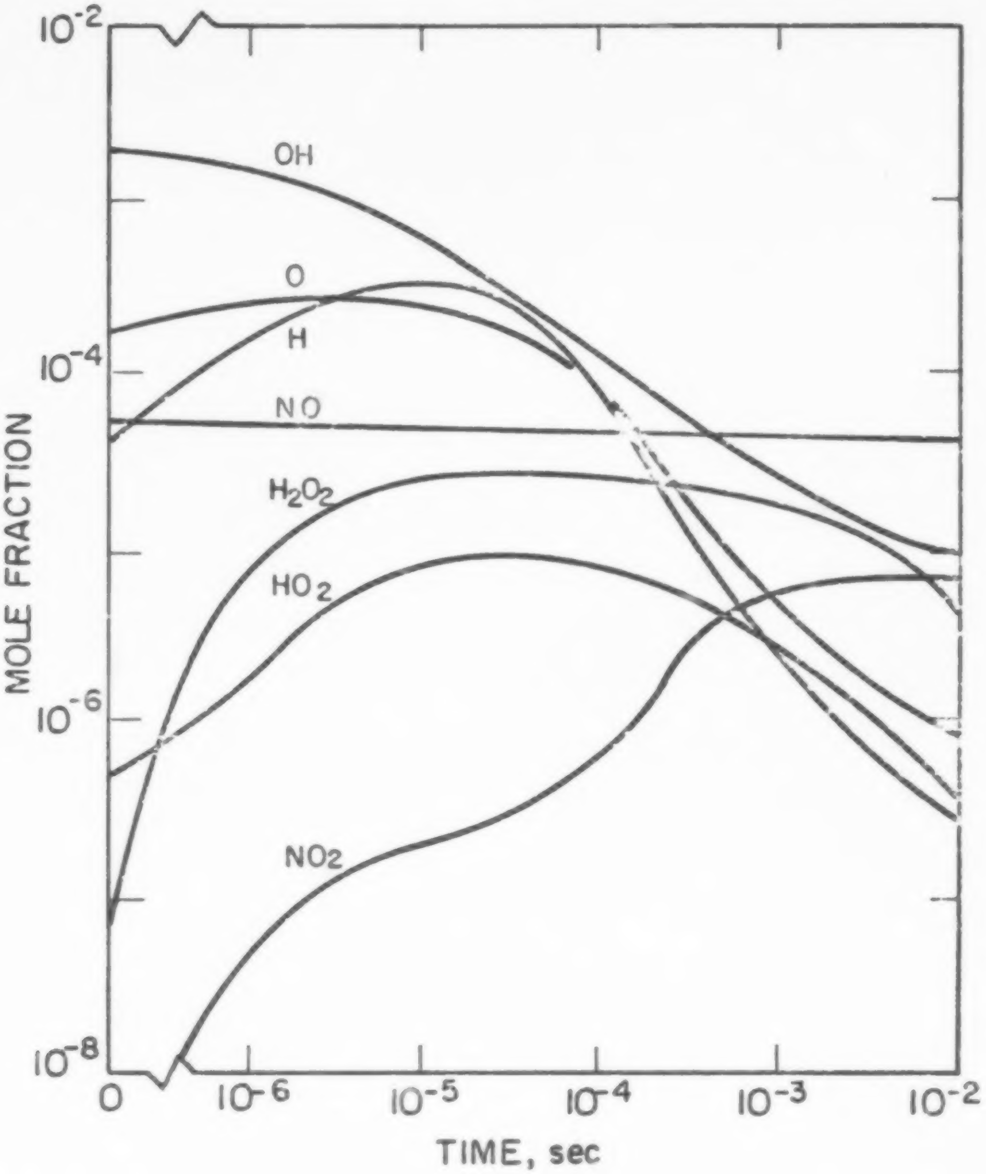

Figure 5-1. Time history of selected species when equilibrium concentrations of radicals for ϕ = 0.8 at 2050°K and 50 ppm NO are instantaneously cooled to 900°K. HOO mechanism.

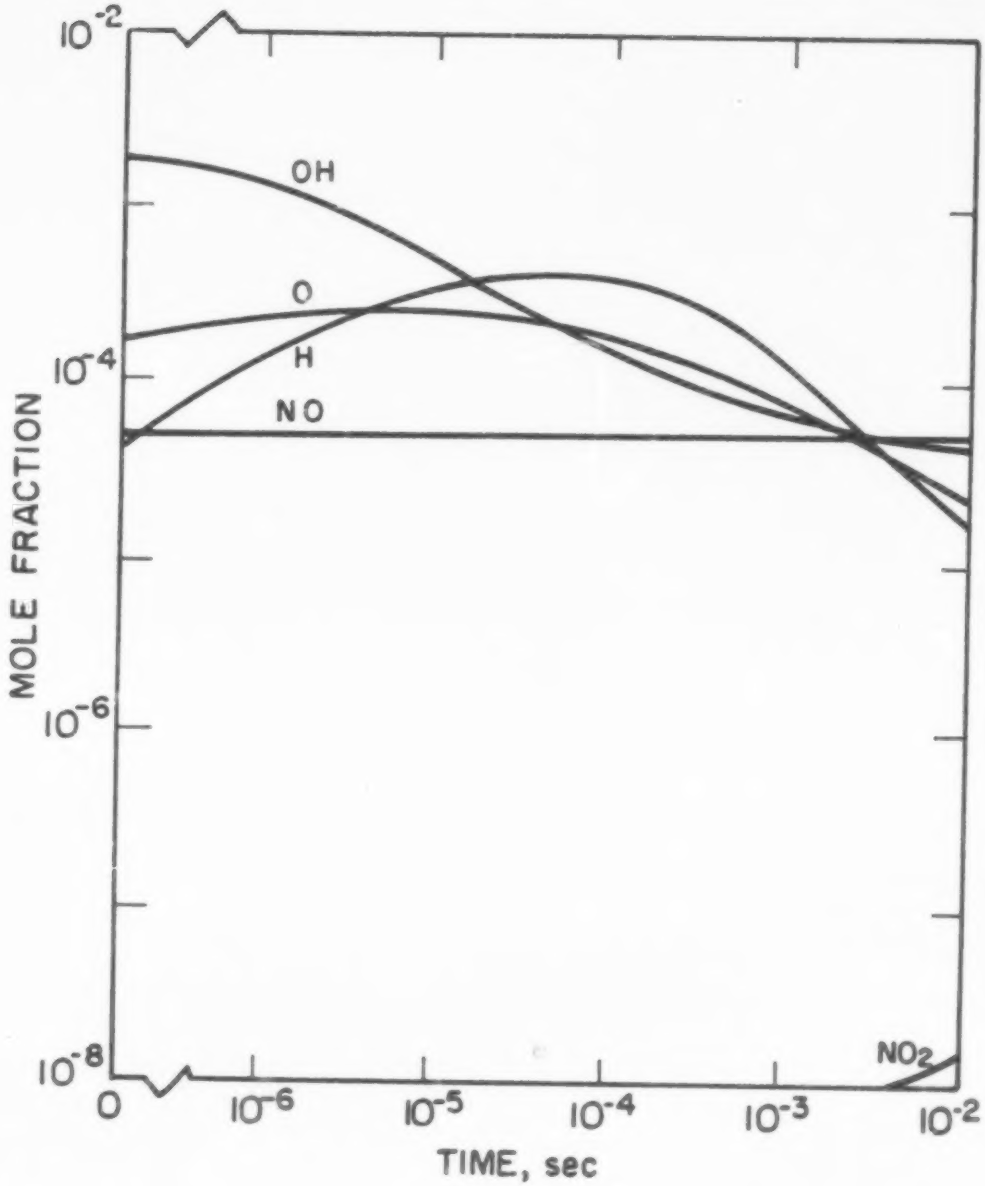

Figure 5-2. Time history of selected species when equilibrium concentrations of radicals for $\phi = 0.8$ at 2050°K and 50 ppm NO are instantaneously cooled to 900°K.

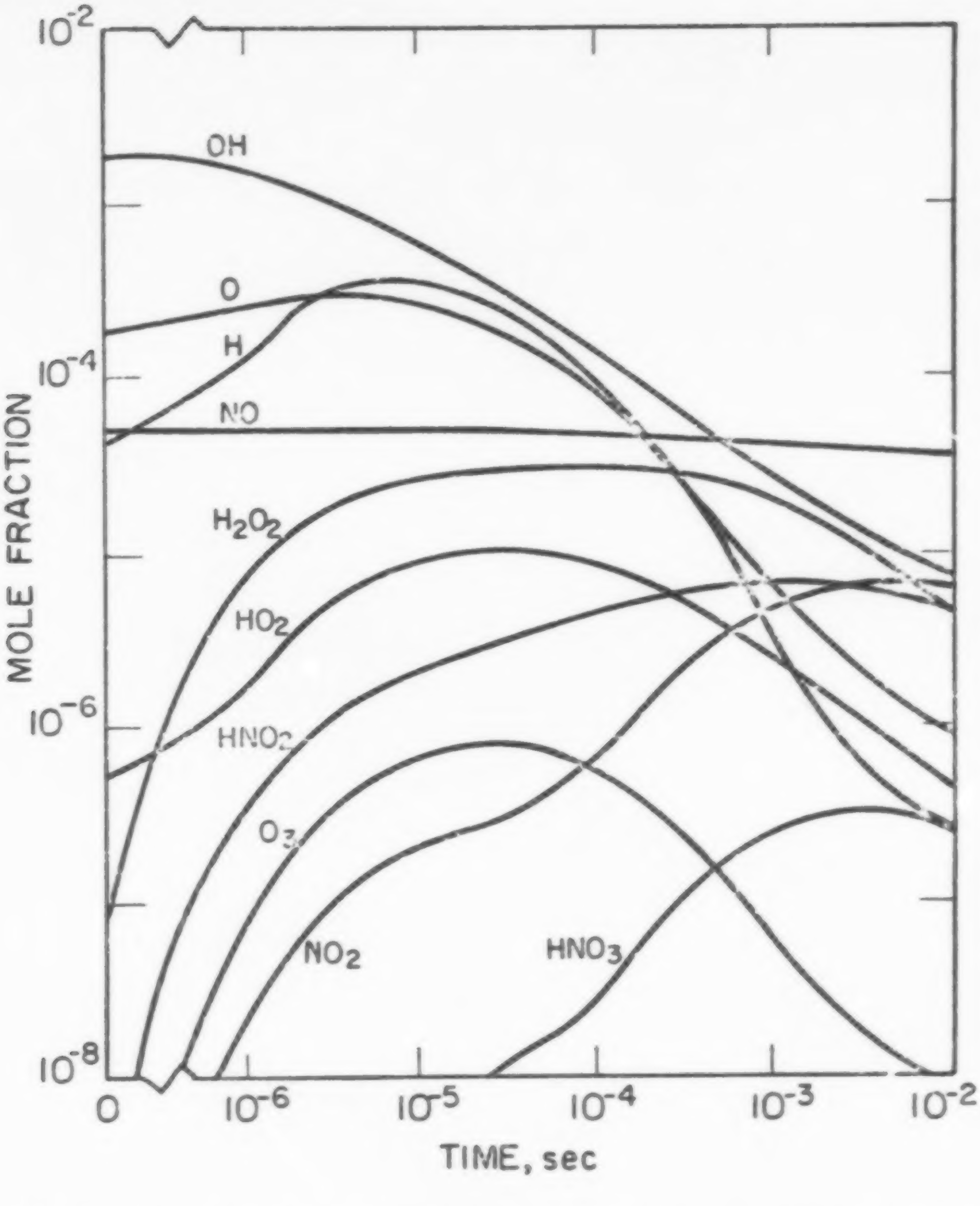

Figure 5-3. Time history of selected species when equilibrium concentrations of radicals for ϕ = 0.8 at 2050°K and 50 ppm NO are instantaneously cooled to 900°K. HOO mechanism + HNO_2, HNO_3, O_3 mechanisms.

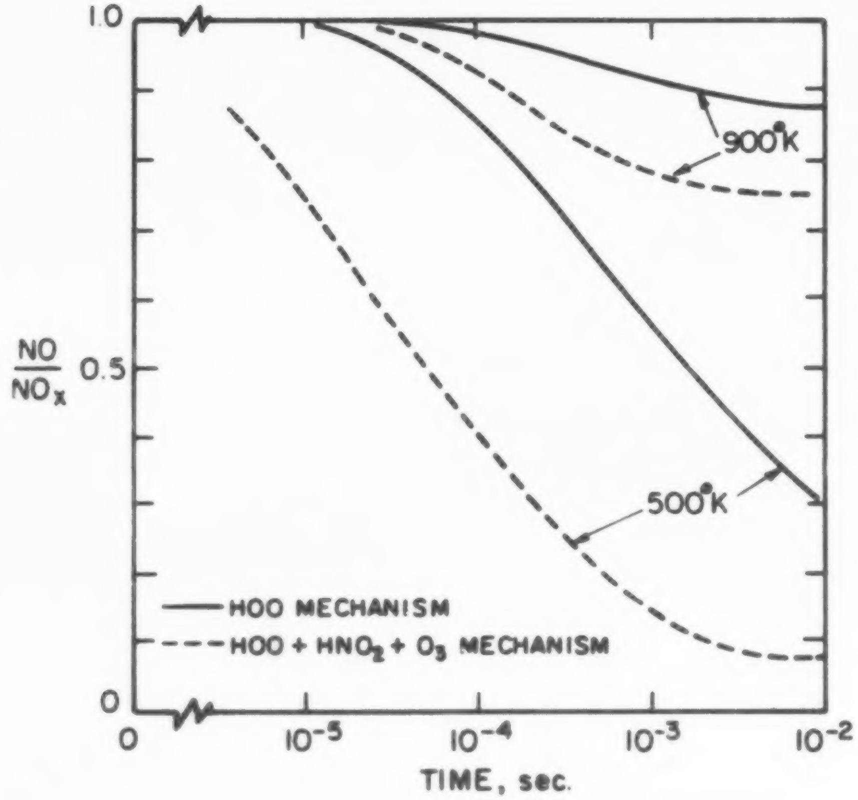

Figure 5-4. Effect of final temperature and reaction scheme on NO conversion.

coexist. These conditions can occur by simple quenching, by transport of fuel lean or fuel rich eddies into fuel lean regions, and so on. It is important to note the strong dependence and interaction of the kinetics with the turbulent mixing processes. This complex coupling of the physical-chemical processes is the heart of the combustion and pollutant formation and destruction processes.

5.3.4 Probe Reactions

The strong dependence of HOO and NO_2 on cooling rate suggests that NO_2 formation is possible in aerodynamic or other cooled probes where rapid quenching is obtained. Kinetic calculations using equilibrium radicals at 2050°K and including nitrous acid and ozone reactions indicate that NO_2 reactions in an idealized sample probe are possible. Formation of NO_2 is possible when sampling from fuel lean high temperature regions and destruction of NO_2 is possible in fuel rich high temperature regions. Sampling from moderate and low temperature regions, where initial radical concentrations are considerably lower but still possibly in superequilibrium concentrations, has no effect on NO_2. One concludes then that sampling from high temperature regions can result in considerable sampling system errors and one cannot reliably measure NO_2.

5.3.5 Summary

In summary then, it appears that one cannot predict NO_2 formation in combustion systems using conventional formation routes. A possible mechanism for NO_2 formation involves rapidly quenching burning eddies or transporting radicals into cooler regions by strong mixing processes. If the cooler region is still at high temperature (> 1300°K), significant concentrations of NO_2 are not predicted. At moderate temperatures in the cool region ($900 < T < 1300$°K), NO_2 is predicted for fuel lean conditions through the buildup of HOO and subsequent oxidation of NO to NO_2. Fuel rich conditions cause no such buildup of HOO and no NO_2 is predicted; in fact NO_2 destruction is favored by the large concentrations of H and OH. As the cool region temperature is reduced further, nitrous and nitric acid, ozone, and O atom mechanisms become more important but still with the constraint of requiring fuel lean mixtures to oxidize NO to NO_2. These same mechanisms can occur in sampling probes and care must be taken to allow for sampling and analytical system effects.

5.4 NO_2 in Combustion Systems

The NO_2 measured for the turbulent diffusion flame can be examined with reference to the preceding discussion. The explanation of the observed NO_2 would seem to lie in the strong mixing processes occurring in this system due to the large velocity gradients which control the mixing. Very strong mixing and cooling occurs allowing formation of NO_2 as NO and radicals are convected and diffused towards the center of the flame. Comparison of Figs. 4-2 and 4-4 and Figs. 4-3 and 4-6 show that on the fuel rich side of the mean flame surface, substantial concentrations of oxygen are found, providing a possible explanation for the peaking of the NO_2 profiles on the fuel rich side of the NO maxima. While the overall stoichiometry is fuel rich, the penetration of oxygen into the flame interior region provides the local oxygen rich conditions required by the proposed HOO mechanism. Also, since this region has the maximum H atom concentrations and since the primary HOO formation route is combination of H with O_2, HOO and subsequent NO_2 production would be favored on the fuel rich side of the NO maxima and flame surface. Unfortunately, these same favorable conditions are supplied to the sampling probe. Consequently along the flame surface and to some extent in the flame interior region a direct chemical kinetic interpretation is not possible at this time. The intermittency of fuel rich and fuel lean high temperature reaction zones at these sampling points can result in NO_2 reactions in the probe.

Of concern is the possibility that NO_2 is solely a sampling phenomenon and does not exist in the flame at all. As long as there is rapid quenching of burning eddies, however, the postulated NO_2 reactions would be expected to occur in the combustion system. The existence of NO_2 in the flame is supported by the measurement of NO_2 in the cool fuel rich flame interior region. In this region radical concentrations are low and NO_2 should be unaffected by the sampling system. Even if radicals were present in large superequilibrium concentrations, H and OH radicals should be abundant, favoring destruction of NO_2. Futher evidence for the existence of NO_2 in combustion systems comes from studies where measurements are taken well downstream of the combustor where sampling effects should be negligible (e.g., Coppersmith et al., 1974). An important experiment in this problem was the one where both the fuel and air streams of the combustor were seeded with NO and measurements taken near the combustor exit, Fig. 4-10. A substantial portion of this NO was converted to NO_2, apparently in the strongly mixed layer near the flame surface. Since these measurements were made in a relatively cool downstream region, sampling system effects would be expected to be negligible. A conclusion then is that NO_2 is actually present in the flame. An in situ measurement would of course be highly desirable in confirming this conclusion.

The complex fluid mechanics and kinetics of the turbulent diffusion flame make a detailed analysis difficult. A more precisely defined system should be used to explore the problem further. Experiments performed by Merryman and Levy (1973) on a premixed burner and experiments on a premixed opposed reacting jet in our own laboratory indicate substantial NO_2 in measurements from fuel lean regions decreasing to near zero as one approaches stoichiometric and fuel rich combustion. Since strong mixing and rapid cooling are not present in these cases, NO_2 is not predicted in the flame, but these results are consistent with the proposed mechanism of formation in the sampling probe. However, probe calculations for the latter case failed to fully explain the observed NO_2 concentrations. Reasons for the discrepancy may be attributable to neglected mechanisms and to the poor quality of much of the reaction rate data. Additional work to attempt to elucidate the NO_2 formation problem and to isolate sampling system effects is required.

CHAPTER 6

Analytical Model

6.1 Introduction

An analytical model for computing the flow properties and nitric oxide production in the current experiment has been developed. The model is based on the solution of the governing conservation equations along with the appropriate auxilliary relations and initial and boundary conditions following the treatment of Patankar and Spalding (1970). The flow is a boundary layer type flow without recirculation and therefore the equations are cast in parabolic form.

In section 6.2 of this chapter the form and solution of these equations are discussed. Section 6.3 discusses the physical models that were used and indicates modifications to the basic computer program. Results of computations are presented in section 6.4 and are compared with experiment. Improvements to the model are also suggested.

6.2 Governing Equations and Their Solution

The parabolic conservation equations for axisymmetric rotating flow are given below. Their development is treated at length by Mason (1971) and details will not be given here.

Conservation of mass:

$$\frac{\partial}{\partial x}(\rho u r) + \frac{\partial}{\partial y}(\rho v r) = 0 \tag{6-1}$$

Conservation of axial momentum:

$$\rho u \frac{\partial u}{\partial x} + \rho v \frac{\partial u}{\partial y} = \frac{1}{r}\frac{\partial}{\partial y}\left(r\mu_{eff}\frac{\partial u}{\partial y}\right) + \rho\frac{V_\theta^2}{r}\sin\alpha - \left(\frac{\partial P}{\partial x}\right)_y \tag{6-2}$$

Conservation of cross-stream momentum:

$$\frac{\partial P}{\partial y} = \frac{\rho V_\theta^2}{r}\cos\alpha \tag{6-3}$$

Conservation of azimuthal momentum:

$$\rho u \frac{\partial(V_\theta r)}{\partial x} + \rho v \frac{\partial(V_\theta r)}{\partial y} = \frac{1}{r}\frac{\partial}{\partial y}\left[r^3\mu_{eff}\frac{\partial}{\partial y}\left(\frac{V_\theta r}{r^2}\right)\right] \tag{6-4}$$

Conservation of thermal energy:

$$\rho u \frac{\partial H}{\partial x} + \rho v \frac{\partial H}{\partial y} = \frac{1}{r}\frac{\partial}{\partial y}\left\{ r\frac{\mu_{eff}}{Pr_{eff}}\left[\frac{\partial H}{\partial y} + \Sigma(Le_{eff}-1)h_i\frac{\partial m_i}{\partial y}\right.\right. \tag{6-5}$$

$$\left.\left. + (Pr_{eff}-1)\frac{\partial E_k}{\partial y} + \left(\frac{Pr_{eff}}{(Pr_e)_{eff}} - 1\right)\frac{\partial e_k}{\partial y}\right] - \mu_{eff}V_\theta^2\cos\alpha\right\}$$

Conservation of chemical species i :

$$\rho u \frac{\partial m_i}{\partial x} + \rho v \frac{\partial m_i}{\partial y} = \frac{1}{r}\frac{\partial}{\partial y}\left(r\frac{\mu_{eff}}{Sc_{eff}}\frac{\partial m_i}{\partial y}\right) + W_i \tag{6-6}$$

Conservation of turbulent kinetic energy:

$$\rho u \frac{\partial e_k}{\partial x} + \rho v \frac{\partial e_k}{\partial y} = \frac{1}{r} \frac{\partial}{\partial y} \left[r \frac{\mu_{eff}}{(Pr_e)_{eff}} \frac{\partial e_k}{\partial y} \right] + \rho \varepsilon_M \left[\left(\frac{\partial u}{\partial y}\right)^2 + \left(r \frac{\partial (v_\theta / r)}{\partial y} \right)^2 \right] - \mu \phi_{diss} \tag{6-7}$$

It is noted that equations (6-2) and (6-5) - (6-7) may be written in a common form equating convection to diffusion and sources:

$$\rho u \frac{\partial \phi_J}{\partial x} + \rho v \frac{\partial \phi_J}{\partial y} = \frac{1}{r} \frac{\partial}{\partial y} \left(\frac{\mu_{eff}}{\sigma_{eff}} \frac{\partial \phi_J}{\partial y} \right) + W_J \tag{6-8}$$

where ϕ_J is u, H, m_i or any variable which can be expressed in similar form. W_J represents the source terms unique to each equation and σ_{eff} is the generalized effective Prandtl number. Equation (6-4) for the azimuthal momentum is also parabolic, but has a diffusion term different from the common form of Eq. (6-8) and requires separate treatment.

For the present analysis, conservation of mass is identically satisfied by introduction of the stream function ψ :

$$\frac{\partial \psi}{\partial x} = -\rho v r, \quad \frac{\partial \psi}{\partial y} = \rho u r \tag{6-9}$$

The dimensionless stream function, ω , is also introduced:

$$\omega = \frac{\psi - \psi_I}{\psi_E - \psi_I} \tag{6-10}$$

where

ψ_E - stream function at external boundary of grid

ψ_I - stream function at internal boundary of grid.

Further simplifications occur with the assumption of $Le_{eff} = 1$ and with the dropping of the turbulent kinetic energy equation, thereby eliminating Eq. (6-7) and several terms in the energy equation, Eq. (6-5).

Yet to be specified are the values of the turbulent exchange coefficients for effective viscosity, μ_{eff}, effective Prandtl number, Pr_{eff}, and the effective Schmidt number, Sc_{eff}. Keston and Richardson (1963) reviewed experimental determinations of Pr_{eff} and suggested a value of 0.8 for turbulent pipe flows. Values of Pr_{eff} and Sc_{eff} for free turbulent flows seem to be lower; for axysmmetric jets Forstall and Shapiro (1950) and Hinze and Hegge Zijnen(1949) report a value of 0.7. Since the region of interest in the present study can be approximated by an unbounded jet, the value 0.7 was used in all calculations.

The effective viscosity was determined from a simple Prandtl mixing length hypothesis. For axisymmetric rotating flows the appropriate expression is:

$$\mu_{eff} = \rho \ell_o^2 \left[\left(\frac{\partial u}{\partial y} \right)^2 + \left(r \frac{\partial (V_\theta / r)}{\partial y} \right)^2 \right]^{1/2} \qquad (6\text{-}11)$$

where ℓ_o is the mixing length. For flows remote from the wall the mixing length is generally taken to be proportional to the thickness of the shear layer and constant across the layer. In the vicinity of the wall ℓ_0 is usually taken to be proportional to the distance from the wall. The mixing length model is discussed later.

The only terms remaining to be specified are the source terms. The only one of these terms that is not determined a priori from known or calculated quantities, and therefore requiring a model, is the rate of production of chemical species i. These are determined from Arrhenius type expressions of the general form:

$$W_i = m_i m_j \rho^x T^y A \exp(-E/RT). \tag{6-12}$$

where E is the activation energy and A is the prexponential factor. The details of the expressions that were used are discussed later.

The complete statement of the problem to be solved requires initial and boundary conditions. For the parabolic equations governing the boundary layer flow specification of initial properties across the radius of flow and conditions along the wall are necessary. The wall conditions for each fluid property may be specified as either a constant value or as a prescribed flux.

The calculational procedure of Patankar and Spalding (1970) was the basis for the numerical solution of the complete set of governing equations together with auxilliary relations and boundary and initial conditions. Since the basic solution method is given by Patankar and Spalding a complete derivation of the numerical solution is not given here. Only the significant modifications and extensions of the program will be listed and where appropriate discussed. Modifications to the basic GENMIX 4 rogram include:

i) addition of equations for the calculation of rotational velocity and the production of nitric oxide.

ii) modification of the turbulence model to include the effects of rotation and free stream turbulence.

iii) a number of small changes including: grid structure, fluid properties, radiation, inputting and printing of variables, etc.

6.3 The Specific Problem - Program Modifications

6.3.1 General

The general arrangment of the flow system considered for these computations is shown in Fig. 6-1. The formulation of the problem follows closely the sample problem in Chapter 8 of Patankar and Spalding (1970) and therefore only the important differences will be detailed.

6.3.2 Thermodynamic Properties

The molecular weights of fuel, oxygen, nitrogen, and combustion product are taken as 44, 32, 28 and 28 respectively. These changes reflect the difference in fuels - propane versus methane.

Rather than using constant specific heats, the specific heats were assumed to be linear functions of temperature to allow for the known temperature dependence of C_p. This also modifies the calculation of temperature from enthalpy.

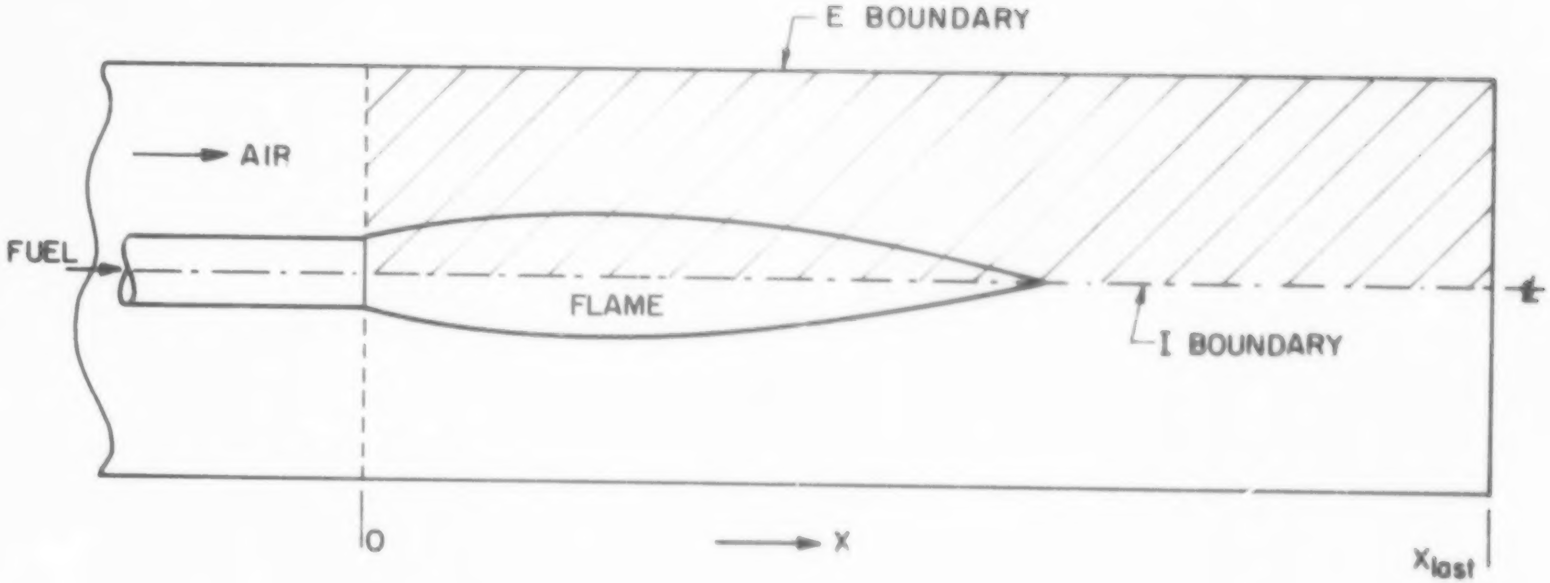
E BOUNDARY
AIR
FUEL
FLAME
I BOUNDARY
℄
O
X
X_{last}

Figure 6-1. General arrangement of the flow system for computation.
Shading indicates the region over which the computation is conducted.

6.3.3 Combustion and Pollutant Formation Model

A one step combustion reaction of fuel + oxidizer going to products was used following the treatment in the sample problem. The reaction rate parameters, heat of combustion, and oxidant to fuel ratio were modified to represent propane as the fuel. It should be noted that this treatment precludes following any of the pollutant species with the exception of NO, which is independent and does not affect the other chemistry. This is unfortunate, but the formulation does represent a first attempt at modeling the system and an obvious refinement is to include finite reaction kinetics.

The production and distribution of nitric oxide was also followed. Since NO is present in such small quantities, it has a negligible effect on any of the properties of the system. This means that NO can be effectively uncoupled from the other governing equations and followed independently. The NO formation model that was used was developed using the Zeldovich mechanism and the assumption of O-atom partial equilibrium following Laurendeau (1972) and Sawyer *et al*. (1973). The governing expression reduces to:

$$\frac{dX_{NO}}{dt} = 10^{15.563}\, T^{-1} \exp\left(-\frac{68222}{T}\right) X_{N_2} X_{O_2}^{\frac{1}{2}} \qquad (6\text{-}13)$$

The effect of O-atom superequilibrium in the reaction zone is discussed later.

6.3.4 The Turbulence Model

A Prandtl mixing length formulation was used as was indicated in section 6.2. The mixing length was determined in the same manner as in the sample problem with the exception that the provision for a small additive constant to the mixing length was provided. This allows for inclusion of free stream turbulence and large scale effects introduced by screens and other turbulence inducing devices. Values used for this constant were on the order of 20 percent or less of the turbulence screen wire diameter.

6.3.5 Pressure Gradient

As was necessary for calculation of a swirling flow, the governing differential equations were modified to include the effects of rotating flow. Inclusion of conservation of angular momentum was accomplished following the procedures outlined by Patankar and Spalding. Inclusion of this equation also results in the introduction of a cross stream pressure gradient to balance the centrifugal force set up by the rotation. Attempts were made to include this effect but flow and computational instabilities always resulted. This resulted because of the coupling of the lateral and longitudinal pressure gradient to the calculation and correction of an artificial combustor radius about the specified radius. Correction of this defect would have required substantial modification to the basic computation scheme and therefore was not attempted. In other words, constant pressure across the radius was assumed and the Y momentum equation was not satisfied. This should have a minimal effect because the air flow is only mildly swirled and the actual radial pressure gradients are very small (a few mm. of water).

6.4 The Specific Problem - Results

Computations were carried out for the different experimental conditions. Results will be presented for one case, i.e., $V_A/V_F = 45$, $T = 300°K$. The initial and boundary conditions as well as the values specified for other variables and parameters can be found in the program listing in Appendix G and are not repeated here.

Comparisons of predicted and measured propane and oxygen centerline profiles are shown in Fig. 6-2. Agreement is very good indicating a reasonable mixing model. However, the slower than measured prediction of oxygen build up on the centerline indicates that the mixing model is slightly underpredicting the mixing. Radial profiles are shown in Fig. 6-3. The predictions follow the general trends of the data and once again prediction of too little mixing is indicated. The sharp drop in the O_2 curve results because of the artificial constraints placed on the mixing and combustion models. Inclusion of a better turbulence model taking concentration fluctuations into account as well as inclusion of more accurate kinetics would improve the fit. All in all, the predictions are reasonable and the deviations explainable.

Centerline and radial profiles of measured and predicted temperature and nitric oxide are presented in Figs. 6-4 and 6-5, respectively. In both cases, the predicted temperature profiles

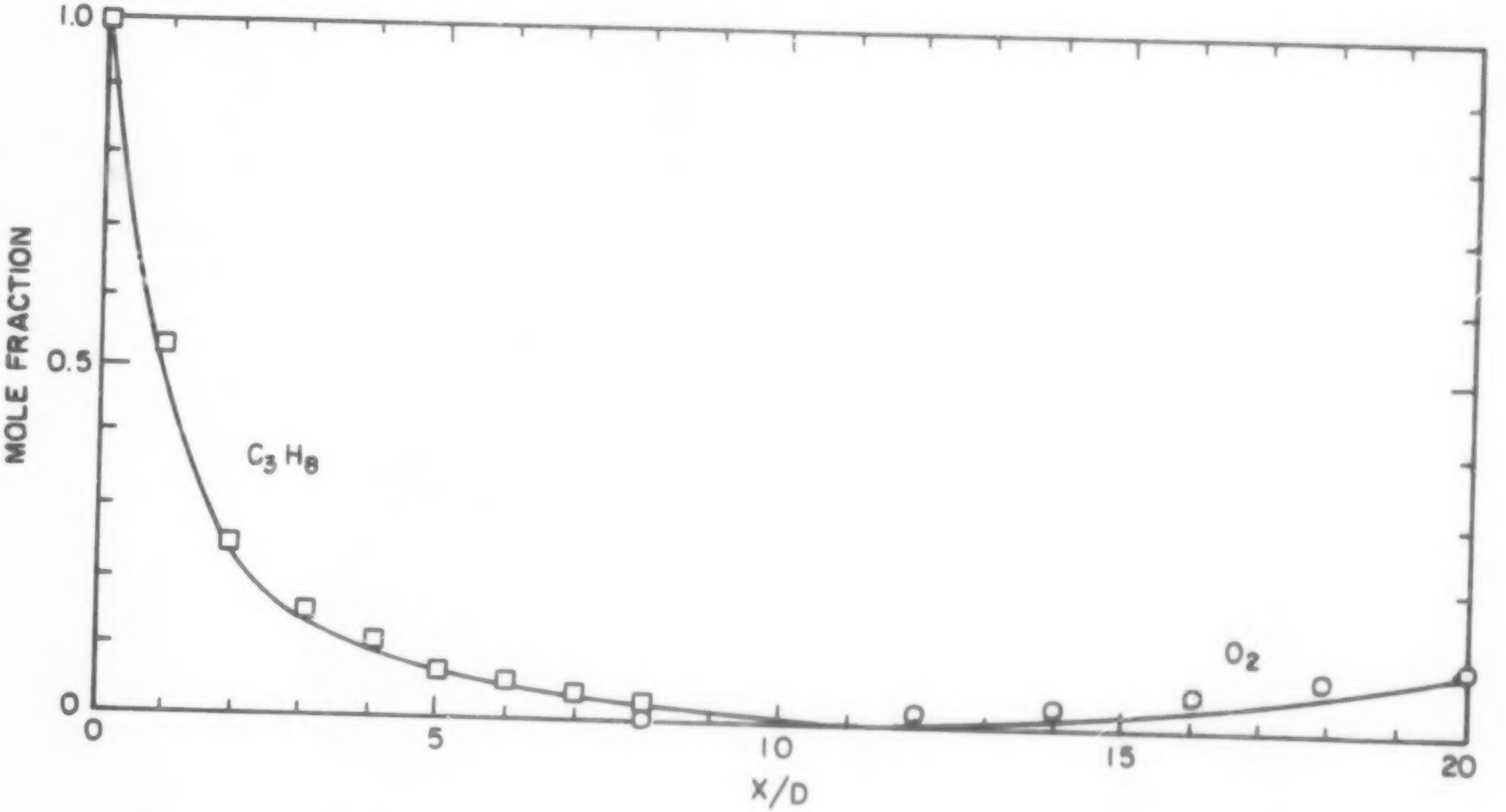

Figure 6-2. Comparison of measured C_3H_8 and O_2 centerline profiles with model predictions, $V_A/V_F = 45$, T = 300°K.

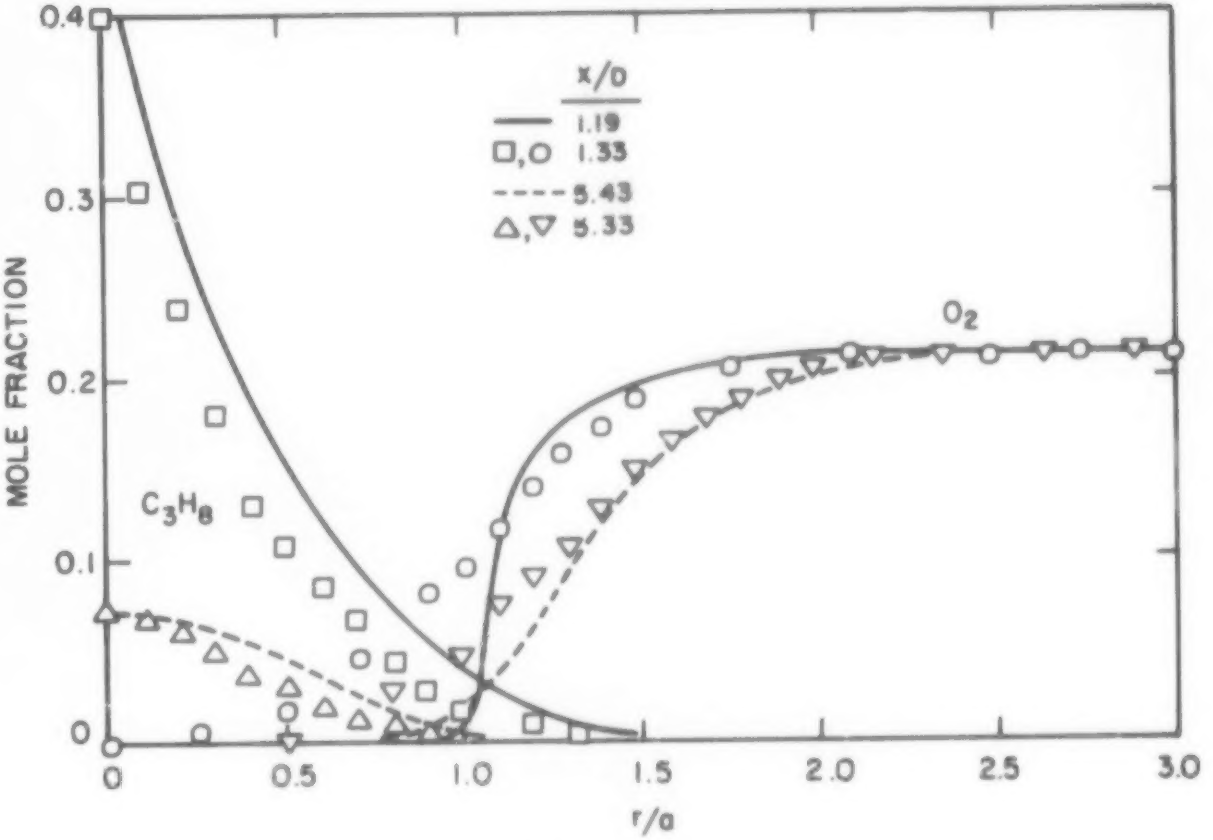

Figure 6-3. Comparison of measured C_3H_8 and O_2 radial profiles with model predictions. $V_A/V_F = 45$, $T = 300°K$.

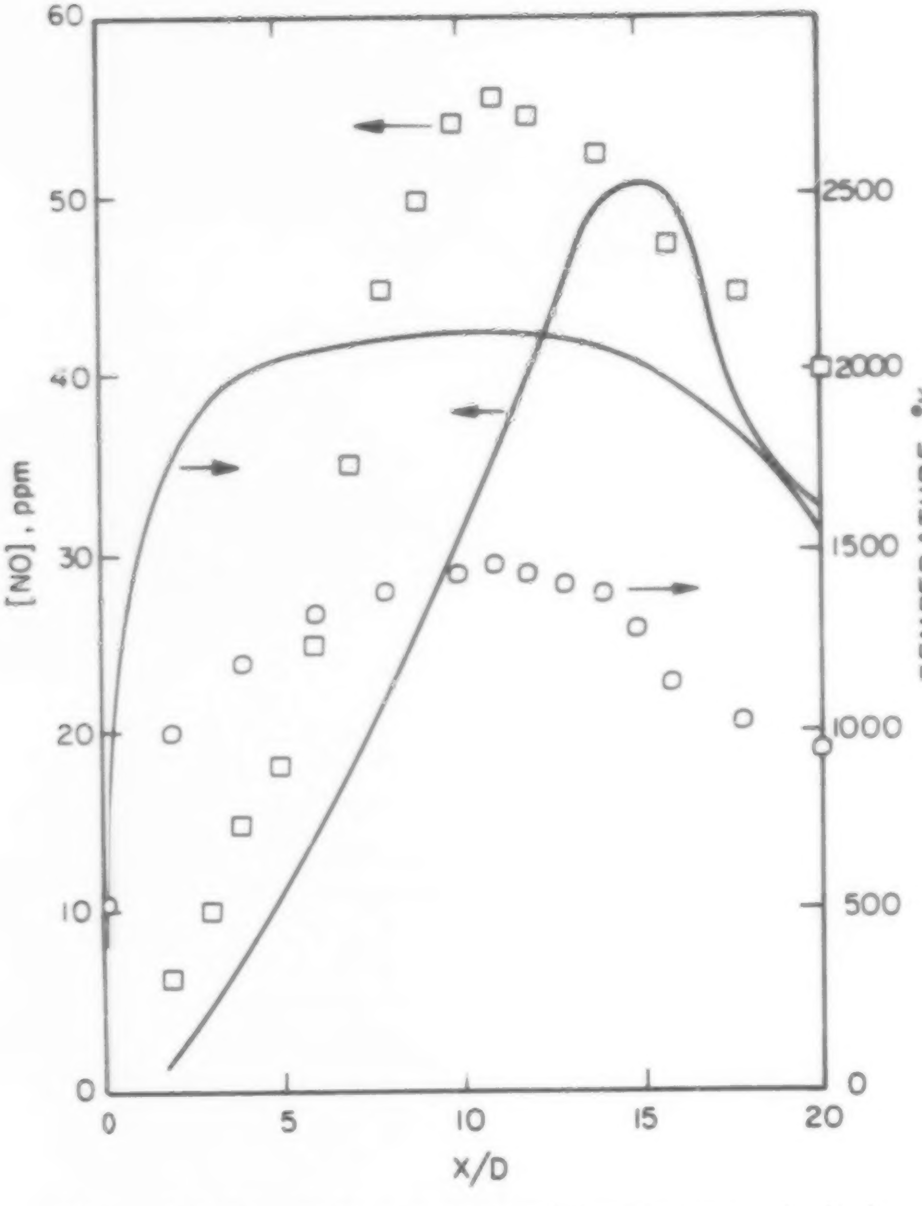

Figure 6-4. Comparison of measured temperature and nitric oxide centerline profiles with model predictions, $V_A/V_F = 45$, T = 300°K.

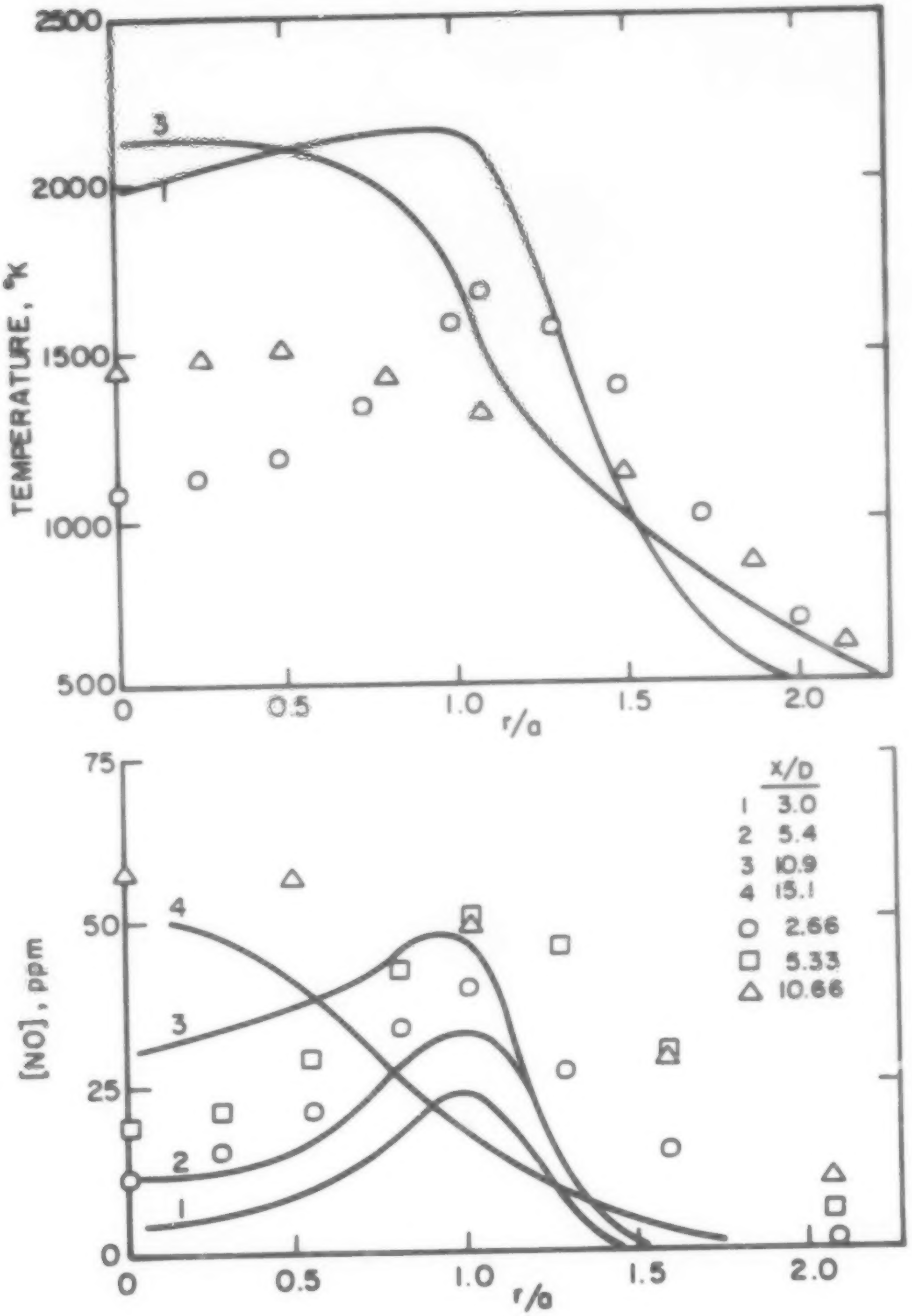

Figure 6-5. Comparison of measured temperature and nitric oxide radial profiles with model predictions, V_A/V_F = 45, T = 300°K.

are substantially higher than the measured data, although they have the same general shape. There are a number of reasons for this behavior. First, the measured values are "as measured" and thermocouple radiation corrections have not been applied; it is estimated that such corrections could be about 200°K at the peak temperatures bringing the curves somewhat closer together. Second, the effects of soot formation and destruction have not been included. This means that an effective thermal capacitance in the flame interior region has been excluded. Inclusion of this effect would give better shaping to the predicted curves. Third, the effects of fluctuations are ignored. The measured values are mean values and the actual peak values are substantially higher. Inclusion of this effect would also raise the measured values substantially. Also, radiation effects from the flame have been ignored. These flame radiation effects would be particularly important in the sooty flame interior region and would lower the predicted temperature and give better shape to the curve. Once again, the deviations between model and measurement are apparently explainable.

The NO data in Figs. 6-4 and 6-5 also look reasonably good. The shift in the peak along the centerline is explainable in terms of the mixing model giving to little mixing. This also accounts for slower movement of the NO maximum to the centerline in the radial profiles. The lack of agreement at large r/a cannot be explained solely by too little mixing and is very likely due to the simplistic turbulence and mixing model. Using a concentration fluctuation model with high temperature burning eddies moving out into the free stream should give the desired result.

Since the NO formation kinetics are exponentially dependent upon temperature, a valid concern is how much reliance can be placed in the NO comparisons when the predicted temperature differs so much from the measured temperature. In the flame, it is the peak temperature which dominates NO production and these occur at the flame surface. Along the flame surface the actual temperatures are probably quite close to the predicted temperature. The soot and flame radiation should have minimal effect on predicted temperature in this region, while consideration of thermocouple radiation and temperature fluctuations should raise the observed readings by several hundred degrees. Thus in the primary region for NO formation, the flame zone, the predicted temperature data would be expected to be nearly correct giving reasonable NO predictions. In the flame interior region, while the predicted temperature is still high, the O_2 available for NO formation is too small and the NO production is limited to the flame zone. One additional factor in NO formation predictions that should be mentioned is that radical overshoot or superequilibrium radical concentrations and inclusion of reactions involving OH would be expected to increase the predictions of NO production.

No attempts were made at trying to compute NO_2 production. In its present state, the model is too crude to allow such calculations. Inclusion of NO_2 must await incorporation of finite reaction kinetics so that radical species can be followed and also incorporation of advanced turbulence models allowing concentration and temperature fluctuations.

6.5 Conclusion

A preliminary analytical model has been presented which reasonably predicts the experimental data. Discrepancies between theory and experiment have been rationalized and directions for further improvements have been indicated. The major improvements suggested involve incorporation of higher order turbulence and mixing models and also inclusion of detailed finite rate reaction kinetics (see for example: Launder and Spalding (1972); Pratt (1973); Cornelius and Agnew (1972)). With these improvements the analytical model should be a useful and successful tool for predicting swirling turbulent diffusion flames.

CHAPTER 7

Conclusion

7.1 Summary of Results

Experimental and theoretical investigations of nitric oxide and nitrogen dioxide formation and destruction in turbulent propane/air diffusion flames have been conducted. Comprehensive flame structure measurements (composition and temperature) have been presented for round jets of propane in coflowing mildly swirled air streams over several velocity ratios and over several levels of reactant preheat.

Significant concentrations of nitrogen dioxide have been measured and nitrogen dioxide appears to peak slightly on the fuel rich side of the nitric oxide maxima. These samples, however, still contained substantial concentrations of molecular oxygen. This is indicative of the strong mixing processes that are occurring in the system and also indicates that the oxygen necessary for nitrogen dioxide formation is present on the fuel rich side of the flame surface and nitric oxide maxima. Strong mixing phenomena and rapid cooling appear to be associated with appreciable nitrogen dioxide levels. Some but not all of the measured nitrogen dioxide can be attributed to sampling difficulties.

Mechanisms for nitrogen dioxide formation were discussed. The most likely source of nitrogen dioxide in the combustion region is through the rapid oxidation of nitric oxide by radicals found in superequilibrium concentrations. In strongly mixed combustion systems where there is rapid cooling of high temperature eddies, the favored nitrogen dioxide formation route involves the buildup of superequilibrium concentrations of hydroperoxy radical, HOO, and subsequent oxidation of nitric oxide to nitrogen dioxide by the HOO radical. The plausibility of this proposed mechanism has been verified by detailed kinetic calculations. The proposed mechanism is consistent with the present experimental observations and with the observations of other investigators.

Sampling effects can be significant when sampling from high temperature regions and care must be taken when attempting to distinguish between NO and NO_2. However, experiments and measurements that were made where sampling effects should be negligible indicate that nitrogen dioxide is actually present in the flame.

An analytical model was presented which reasonably predicts the experimental data. Discrepancies between theory and experiment were rationalized and directions for further improvements were indicated.

7.2 Future Work

The study of nitric oxide and nitrogen dioxide in combustion systems remains clouded due to uncertainties and difficulties in the sampling and analytical system. Additional work needs to be done to isolate sampling system effects in order that quantitative measurements of NO and NO_2 in high temperature regions can be made. Such work will enable future studies to further elucidate the NO_2 formation and destruction processes. An important advance towards achieving these objectives would be development of optical measurement techniques for NO and NO_2. A particularly promising approach at this time is laser excited resonance flouresence spectrosocopy; in situ NO_2 measurements may be possible using this technique.

Further work on analytical modeling and on the kinetics of NO_2 formation and destruction in combustion processes is required. Improved rate data represents a particularly acute need for refining the kinetic modeling and improved turbulence models must be developed for the overall modeling work.

REFERENCES

AiResearch Company
1971, "Exhaust Emissions Test, AiResearch Aircraft Propulsion and Auxiliary Power Gas Turbine Engines," Report No. GT-8747-R.

Anderson, L.B. and J.W. Meyer
1973, "High Altitude Jet Plume Chemistry," Lockheed Palo Alto Research Laboratory, presented at the Fourth International Colloquium of Explosions and Reactive Systems, La Jolla, California.

ASME
1961, "Flowmeter Computation Handbook," American Society of Mechanical Engineers, New York.

Becker, H.A.
1974, "Effects of Concentration Fluctuations in Turbulent Diffusion Flames," presented at the Fifteenth Symposium (International) on Combustion, Tokyo, Japan, August 25-31.

Beer, J.M., N.A. Chigier, and K.B. Lee
1963, "Modeling of Double Concentric Burning Jets," Ninth Symposium (International) on Combustion, p.892, Academic Press.

Beer, J.M. and N.A. Chigier
1972, Combustion Aerodynamics, Applied Science Publishers, Ltd., London.

Bilger, R.W. and J.H. Kent
1972, "Concentration Fluctuations in Turbulent Jet Diffusion Flames," Report No. T.N.F-46, Department of Mechanical Engineering, University of Sidney, Australia.

Bilger, R.W. and R.E. Beck
1974, "Further Experiments on Turbulent Jet Diffusion Flames," presented at the Fifteenth Symposium (International) on Combustion, Tokyo, Japan, August 25-31.

Bowman, C.T.
1974, Private Communication
United Aircraft Research Laboratories, Hartford, Connecticut.

Bradley, D. and K.J. Matthews
1968, "Measurement of High Gas Temperatures with Fine Wire Thermocouples
J. Mech. Engr. Sci. 10, 4, 299-305.

Breitenbach, L.P. and M. Shelef
1973, "Development of a Method for the Analysis of NO_2 and NH_3 by
NO-Measuring Instruments,"
J APCA 23, 2, 128-131.

Cernansky, N.P.
1974, "Evaluation and Selection of Rate Data for Pollutant Formation
and Distruction Calculations in Hydrocarbon/Air Combustion
Systems,"
Department of Mechanical Engineering, University of California,
Berkeley.

Chang, S.G. and T. Novakov
1974, "Formation of Pollution Particulate Nitrogen Compounds by
Soot-NO and Soot-NH_3 Surface Reactions,"
Report No. LBL-3068, Lawrence Berkeley Laboratory,
University of California, Berkeley.

Coppersmith, F.M., R.F. Jastrozebski, D.V. Giovanni, and S. Hersh
1974, "Con Edison's Gas Turbine Test Program: a Comprehensive
Evaluation of Stationary Gas Turbine Emissions Levels,"
APCA Paper No. 74-12.

Cornelius, W. and W.G. Agnew (eds.)
1972, *Emissions from Continuous Combustion Systems*
Plenum Press, New York.

Cornelius, W. and W.R. Wade
1970, "The Formation and Control of Nitric Oxide in a Regenerative
Gas Turbine Burner,"
SAE Paper No. 700708.

Cornu, A. and R. Massot
1966, "Compilation of Mass Spectral Data: Index De Spectres de
Masse,"
Heydon and Son, Ltd., London

Cunnigham, R.G.
1951, "Orifice Meters with Supercritical Compressible Flow,"
Trans. Am. Soc. Mech. Engr., *73*, 625-638.

Edelman, R. and C. Economos
1971, "A Mathematical Model for Jet Engine Combustor Pollutant
Emissions,"
AIAA Paper No. 71-714.

Edelman, R., *et al*.
1972, "Some Observations on Flows Described by Coupled Mixing and
Kinetics,"
Emissions from Continuous Combustion Systems, p. 55, Plenum
Press, New York.

Elghobashi, S.E. and W.M. Pun
1974, "A Theoretical and Experimental Study of Turbulent Diffusion Flames in Cylindrical Furnaces,"
presented at the Fifteenth Symposium (International) on Combustion, Tokyo, Japan, August 25-31.

Fletcher, R.S., *et al.*
1971, "The Control of Oxides of Nitrogen Emissions from Aircraft Gas Turbine Engines," Vol. 1: Program Descriptions and Results - Report No. 1162-1, Vol. 2: The NO_x Formation Process - Report No. 1162-2, Vol. 3: The Flow Model - Report No. 1162-3, Northern Research and Engineering Corporation, Cambridge, Massachusetts.

Forstall, W. and A.H. Shapiro
1950, "Momentum and Mass Transfer in Coaxial Gas Jets,"
J. Applied Mechanics, *17*, 399.

Fristrom, R.M. and A.A. Westenberg
1965, *Flame Structure*
McGraw-Hill, New York.

Garvin, D. and R.F. Hampson (eds.)
1974, "Chemical Kinetics Data Survey VII. Tables of Rate and Photochemical Data for Modeling of the Stratosphere (revised)",
Report No. NBSIR-74-430, National Bureau of Standards, Washington, D.C.

Gordon, S. and B.J. McBride
1971, "Computer Program for Calculation of Complex Chemical Equilibrium Compositions, Rocket Performance, Incident and Reflected Shocks, and Chapman-Jouget Detonations,"
NASA Report SP-273.

Günther, R.
1970, *Chemie Ingenieur Technik*, *42*, 105.

Heywood, J.B., *et al.*
1971, "Jet Aircraft Air Pollutant Production and Dispersion,"
AIAA J. *9*, 5, 841-850.

Hinze, J.O. and B.G. Von der Hegge Zijnen
1949, "Transfer of Heat and Matter in the Turbulent Mixing Zone of an Axially Symmetric Jet,"
Appl. Sci. Res., sec. AA1, 435-61.

Kays, W.M.
1966, *Convective Heat and Mass Transfer*
McGraw-Hill, New York.

Kent, J.A.
1970, "A Noncatalytic Coating for Platinum-Rhodium Thermocouples,"
Combustion and Flame, *14*, 279-282.

Kent, J.H.
1972, "Turbulent Jet Diffusion Flames,"
Ph.D. Thesis, Department of Mechanical Engineering, University of Sidney, Australia.

Kent, J.H. and R.W. Bilger
1973a, "Measurement Techniques in Turbulent Diffusion Flames," presented at the First Australasian Conference on Heat and Mass Transfer, Melbourne, Australia.

Kent, J.H. and R.W. Bilger
1973b, "Turbulent Diffusion Flames,"
Fourteenth Symposium (International) on Combustion, p.615, The Combustion Institute, Pittsburgh, Pa.

Kestin, J. and P.D. Richardson
1963, "Heat Transfer Across Turbulent, Incompressible Boundary Layers,"
Int. J. Heat Mass Transfer, 6, 147-189.

Kondratiev, V.N.
1972, "Rate Constants of Gas Phase Reactions,"
National Technical Information Service No. COM-72-10014.

Launder, B.E. and D.B. Spalding
1972, Mathematical Models of Turbulence
Academic Press, New York.

Laurendeau, N.M.
1972, "The Thermal Decomposition of Nitric Oxide and Nitrogen Dioxide," Ph.D. Thesis, also Report No. TS-72-4, Department of Mechanical Engineering, University of California, Berkeley.

Lavoie, G.A. and A.F. Schlader
1974, "A Scaling Study of NO Formation in Turbulent Diffusion Flames of Hydrogen Burning in Air,"
Combustion Science and Technology, 8, 215-224.

Lockwood, F.C. and A.O. Odidi
1974, "Measurement of Mean and Fluctuating Temperature and of Ion Concentration in Round Free Jet Turbulent Diffusion and Premixed Flames," presented at Fifteenth Symposium (International) on Combustion, Tokyo, Japan, August 25-31.

MacKinnon, D.J. and T.R. Ingraham
1972, "Minimizing NO_x Pollutants from Steam Boilers,"
APCA J, 22, 471.

Magnussen, B.F.
1973, "Prediction of Characteristics of Enclosed Turbulent Jet Flames,"
Fourteenth Symposium (International) on Combustion, the Combustion Institute, Pittsburgh, Pa.

Malte, P.C. and D.T. Pratt
1973, "Oxides of Nitrogen Formation for Fuel-Lean, Jet Stirred Carbon Monoxide Combustion," Paper No. WSCI 73-37, presented at the Western States Section/Combustion Institute, El Segundo, California.

Marteney, P.J.
1970, "Analytical Study of the Kinetics of Formation of Nitrogen Oxide in Hydrocarbon-Air Combustion," Combustion Science and Technology 1, 461.

Masliyah, J.H. and F.R. Steward
1969, "Radiative Heat Transfer from a Turbulent Diffusion Buoyant Flame with Mixing Controlled Combustion," Combustion and Flame 13, 6, 613-625.

Mason, H.B.
1971, "Numerical Computation of Steady Natural Convective Flows with Rotation and Stratification," Ph.D. Thesis, Department of Mechanical Engineering, University of California, Berkeley.

Matthews, R.D.
1973, "Distributions of NO, NO_2, and NO_x in a Model Gas Turbine Combustor,"
M.S. Thesis, Department of Mechanical Engineering, University of California, Berkeley.

McLean, W.J. and R.F. Sawyer
1967, "Mass Spectrometer Data Reduction and Error Analysis," Report No. TS-67-4, Department of Mechanical Engineering, University of California, Berkeley.

Mellor, A.M.
1972, "Current Kinetic Modeling Techniques for Continuous Flow Combustors," Emissions from Continuous Combustion Systems, Plenum Press, New York, p. 23.

Mellor, A.M.
1974, "Private Communication,"
Purdue University, West Lafayette, INdiana.

Merryman, E.L. and A. Levy
1973, "NO_x Formation in Combustion: Anomalous-early NO_2 Formation," Proceedings of the Third International Clean Air Congress, Dusseldorf, West Germany.

Myerson, A.L.
1974, "The Reduction of Nitric Oxide in Simulated Combustion Effluents by Hydrocarbon-Oxygen Mixtures,"
presented at the Fifteenth Symposium (International) on Combustion, Tokyo, Japan, August 25-31.

Nickerson, G.R. and H.M. Frey
1971, "GKAP-Generalized Kinetic Analysis Program," Ultrasystems, Irvine, California.

Patankar, S.V. and D.B. Spalding
1970, Heat and Mass Transfer in Boundary Layers, 2nd Ed., Intertext, London.

Patterson, J.A., M.W. McElroy, R.F. Sawyer, T. Singh
1970, "A Prototype Chemiluminescent NO Analyzer," Report No. TS-70-9, Department of Mechanical Engineering, University of California, Berkeley.

Pratt, D.T.
1973, "Improved Turbulence Models in Symjet and Related Computer Codes: Literature Review, Evaluation, and Recommendations for Implementation," Report No. BNWL-B-311, Battelle Pacific Northwest Laboratories, Richland, Washington.

Quan, V., F.E. Marble and J.R. Kliegel
1973, "Nitric Oxide Formation in Turbulent Diffusion Flames," Fourteenth Symposium (International) on Combustion, p. 851, The Combustion Institute, Pittsburgh, Pa.

Quan, V.
1974, "Nitric Oxide Formation in Turbulent Jet Diffusion Flames," Acta Astronautica 1, 505-521.

Quan, V., J.R. Kliegel, N. Bayard de Volo, D.P. Teixeira,
1974, "Analytic Scaling of Flowfield and Nitric Oxide in Combustors," Combustion Science and Technology, in press.

Rubel, A.
1972, "Some Effects of Swirl on Turbulent Mixing and Combustion," NASA Report No. CR-1956.

Rubel, A.
1973, "Swirling Jet Turbulent Mixing and Combustion Computations," NASA Report No. CR-2231.

Samuelsen, G.S.
1970, "Analytical and Experimental Investigation of an Ammonia/Air Opposed Reacting Jet," Report No. TS-70-10, Department of Mechanical Engineering, University of California, Berkeley.

Sawyer, R.F., N.P. Cernansky, and A.K. Oppenheim
1973, "Factors Controlling Pollutant Emissions from Gas Turbine Engines," in AGARD CP-125 on Atmospheric Pollution by Aircraft Engines, NATO.

Schefer, R.W., R.D. Matthews, N.P. Cernansky, R.F. Sawyer
1973, "Measurement of NO and NO_2 in Combustion Systems,"
Paper No. WSCI 73-31, presented at the 1973 Fall meeting, Western States Section of the Combustion Institute, El Segundo, California.

Schefer, R.W.
1974, "Private Communication,"
Department of Mechanical Engineering, University of California, Berkeley.

Takagi, T. and M. Ogasawara, K. Fujii, M. Daizo
1974, "A Study of Nitric Oxide Formation in Turbulent Diffusion Flames,"
presented at the Fifteenth Symposium (International) on Combustion, Tokyo, Japan, August 25-31.

Tuttle, J.H., R.A. Shisler, and A.M. Mellor
1973, "Nitrogen Dioxide Formation in Gas Turbine Engines: Measurement Methods,"
Report No. PURDU-CL-73-06, The Combustion Laboratory, Purdue University.

APPENDIX A

Experimental Facility and Equipment

A.1 Introduction

A brief description of the combustor and combustion test section was given in Chapter 3. This appendix gives details of the combustion facility and its related support equipment and includes descriptions of the air and fuel metering system, fuel injector design, air swirler design and starting procedures.

A schematic of the experimental facility is shown in Fig. A-1. Fuel and air flows are metered, preheated, and supplied to the combustion section (Fig. 3-1). Propane is injected axially into the horizontal Vycor combustion tunnel and is mixed and burned with a slightly swirled, $S \approx 0.3$, coaxial air flow. The one atmosphere flames are attached to the injector tip and are contained within the combustion tunnel.

All thermocouples shown in Fig. A-1 are chromel/alumel and the emf is read using a Leeds and Northrup Potentiometer (Model 8690) using an ice bath for a reference junction.

A.2 Air Supply System

The main air is supplied from the house compressed air system which is maintained at a nominal pressure of 200 psig. A two inch line is used to supply the experimental facility and the pressure is reduced to 80 psig prior to metering. The main air is metered by an Emco positive displacement meter and by a standard ASME orifice

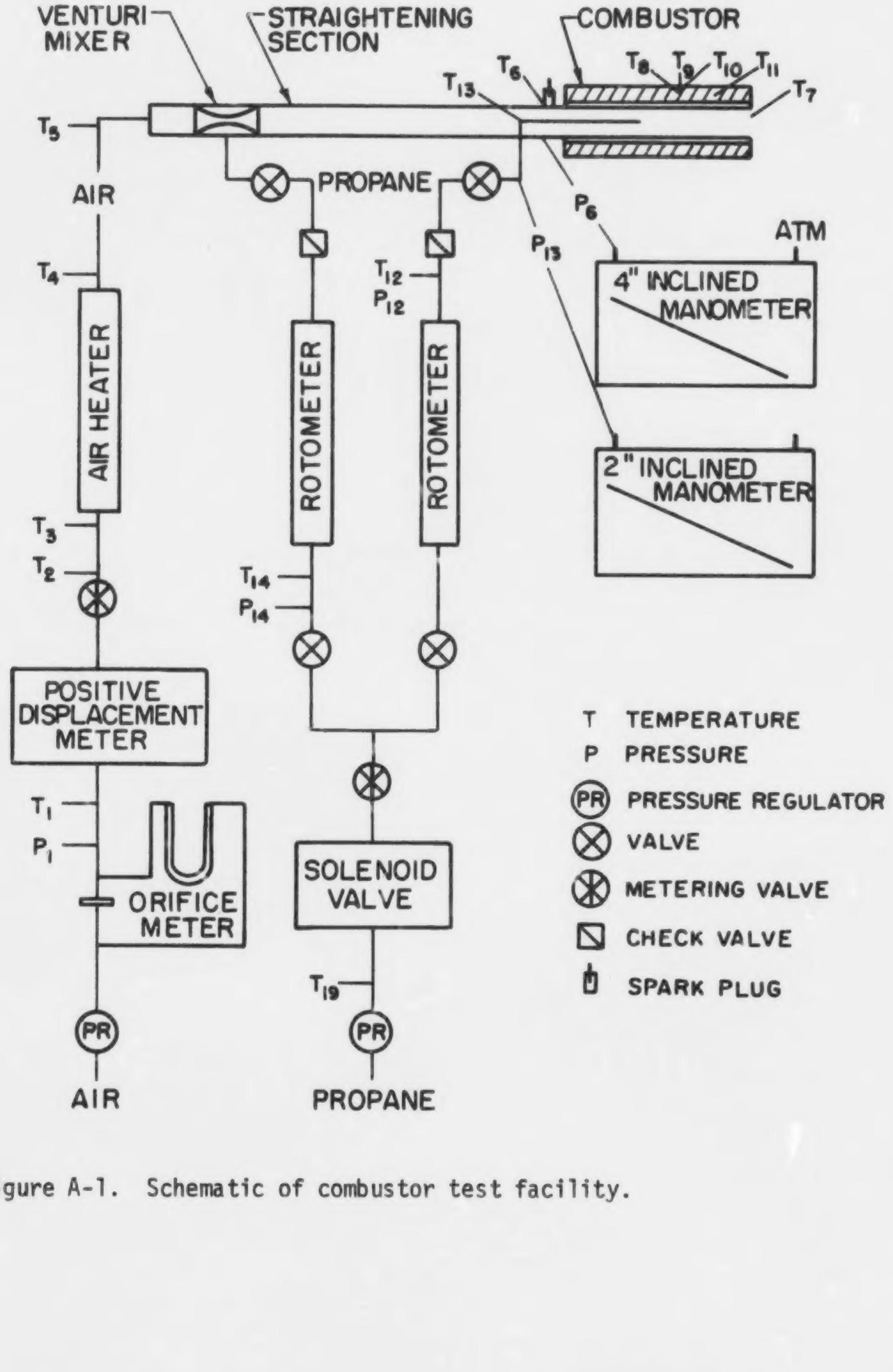
VENTURI MIXER
STRAIGHTENING SECTION
COMBUSTOR
T5
T6
T7
T8
T9
T10
T11
T13
AIR
PROPANE
P6
P13
ATM
4" INCLINED MANOMETER
2" INCLINED MANOMETER
T4
AIR HEATER
T12
P12
ROTOMETER
ROTOMETER
T3
T2
T14
P14
POSITIVE DISPLACEMENT METER
T1
P1
ORIFICE METER
SOLENOID VALVE
T19
PR
PR
AIR
PROPANE
T TEMPERATURE
P PRESSURE
PR PRESSURE REGULATOR
VALVE
METERING VALVE
CHECK VALVE
SPARK PLUG

Figure A-1. Schematic of combustor test facility.

(flange pressure taps) in accordance with ASME codes (ASME, 1961; Cunningham, 1951). The orifice diameter is 0.600 inch and the pressure ratio across the orifice is read in inches of water on a manometer. The static pressure is measured by a Bourdon gauge and the temperature of the flow is measured by thermocouple. Air mass flows were measured primarily using the positive displacement meter but cross checks were made with the orifice meter.

Control of the main air flow is maintained by a 1/2 inch needle metering valve. The two-inch line is reduced to a 1/2 inch line downstream of the metering section to accomodate the valve. After the control valve the air is fed into a General Electric air circulation heater, with six 6-KW stages one of which has a Chromalox (Model CIPD73-6C) solid state proportional temperature controller. The controller senses the heater outflow temperature and proportions the power to obtain a preset temperature. By matching the number of stages to the heating requirements for the desired air flow and temperature conditions any degree of preheat up to a maximum of 1000°F can be maintained. The air is then supplied to a venturi mixing section through a two-inch line. The venturi section is used to enhance the mixing of fuel and air where premixing is desired (used primarily for ignition purposes in the current study). The operation and design of the venturi section is discussed in detail by Samuelsen (1970). After a three-foot 2 1/4 inch diameter straightening section, a 14 inch (356 mm) long Vycor combustion chamber is attached. The chamber has a 2 1/4 inch (58 mm) inside diameter and a 2 1/2 inch (63.5 mm) outside diameter. Just prior to the entrance of the Vycor combustion tunnel, the pressure and temperature of the air stream are measured through taps in the straightening section.

A.3 Fuel Supply System

Propane fuel is supplied from Matheson commercial grade bottles (typical analysis: 99.4% propane, 0.05% ethane, 0.50% iso butane, 0.05% propylene, with a minimum purity of 99.0 mole percent). There is a fast-response solenoid shut-off valve in the propane supply line for positive and rapid shut off of the fuel. The fuel is metered in a Matheson ball rotometer (tube 602), which was calibrated with a wet test meter. Pressure and temperature of the fuel is measured at the rotometer to enable calculation of the mass flow rate of fuel.

The fuel is fed into a 3/8 inch (9.53 mm) type 304 stainless steel fuel injector tube positioned coaxially with the straightening and combustion section. An upstream location, eight inches before the end of the straightening section, was selected to allow adequate time to heat the previously unheated fuel stream to the same temperature as the air stream. Screens are provided to enhance this process as well as to smooth out any macro effects at the location where the fuel tube enters the straightening section. Pressure is again measured at the entrance point and fuel temperature is measured about two inches after this entrance point. The adequacy of this system for preheating the fuel stream is verified by temperature measurements in the fuel tube as well as by temperature traverses at the fuel injector exit.

A.4 Fuel Injector

The 3/8 inch (9.53 mm) outside diameter injector tube is coaxial with the 2 1/4 inch straightening section and continues coaxially for six inches (152 mm) into the combustion section where it terminates. The end of the fuel tube is honed to a 8.74 mm inside diameter and has a stainless steel screen placed 3/16 inch (4.76 mm) before the exit to smooth the flow and act as a turbulence inducer. The flame is attached to the fuel injector and is positioned horizontally downstream in the air flow. The combustion section is shown schematically in Fig. 3.1.

Several different sizes and end configurations for the fuel injector tube were attempted. The size used was chosen after consideration of many factors including: stability, maintenance of a flame confined within the combustion tunnel at a reasonable fuel flow rate, sufficient dimension to make reasonable radial structure measurements, and others. The honed exit was used to minimize end effects of the injection tube.

A.5 Starting Procedure

For the purpose of starting the combustor the fuel line is tapped and propane is fed into the venturi mixing section. This premixed fuel and air is ignited by a spark plug (Champion H-14Y) located diametrically opposite the pressure and temperature taps at the end of the straightening section. The flame from this ignited mixture carries downstream and ignites the fuel leaving the injector. After ignition, the premix fuel is shut off, returning the system to the coflowing fuel and air configuration.

The spark is energized by a 120/120,000 volt AC transformer.

A.6 Air Swirler

Running this configuration at higher air flows resulted in occasional spontaneous blow out especially at conditions without air preheat. To avoid this problem, the stability of the combustion system was enhanced by slightly swirling the air flow. The swirl was induced using a 16 blade vane type swirl generator. The swirler has a constant 28° blade angle and extends from the injector tube to within 1/16 inch (1.59 mm) of the Vycor housing. Immediately downstream of the swirler a stainless steel screen (0.015 inch wire; 14 grids per inch) was positioned to smooth out the flow and eliminate macro effects from the swirl vanes. The distance from the face of the screen to the tip of the fuel injector was 1 1/2 inches (38 mm). The swirler produced initial swirl levels of about $S = 0.3$ and stabilized the combustion process over the full range of operating conditions. The swirl levels were low enough, however, to avoid recirculation. Static pressure measurements and directional velocity probe measurements support this conclusion.

APPENDIX B

Operating Data

Appendix B consists of two tables. Table B-1 shows the calculated fuel and air flows and their ratio for each of the experimental data runs. Table B-2 shows the actual operating data as collected. The data reduction program is listed in Appendix G.

The variables and parameters that are not self explanatory are:

DATE - case number, date and run number on that day

HW - V_A/V_F; 1 ≈ 45:1, 2 ≈ 61:1, 3 ≈ 75:1

TIME - minutes and seconds for air flow measurements

T_1 - air temperature at positive displacement meter, °C

P_1 - air pressure at positive displacement meter, PSIG

PYREX - fuel rotometer reading, pyrex ball, mm

SS - fuel rotometer reading, stainless steel ball, mm

T12 - fuel temperature at rotometer, °C

P12 - fuel pressure at rotometer, always very close to 1 atm.

P13 - fuel pressure at beginning of injector, in. meriam red fluid (S.G = 0.827)

T13 - fuel temperature two inches downstream from beginning of injector, °C

T6 - air temperature at wall at end of straightening section, °C

P6 - air pressure at end of straightening section, inches of water

T7 - air temperature at X/D = 22, r/a = 4.2, °C

T8, T9, T10, T11 - temperatures of thermocouples implanted in the lagging of the Vycor housing (see Samuelsen (1970) for locations)

T18 - sample temperature just after the probe, °C

BP - Barometric pressure, inches of mercury

TABLE B-1. Calculated fuel and air flows

		AIR		FUEL		AIR/FUEL	
DATE	HW	G/SEC	CM/SEC	G/SEC	CM/SEC	MASS	VELOCITY
27JUL731	1	7.319E+00	2.533E+02	7.404E-03	5.707E+00	9.885E+02	4.438E+01
30JUL731	1	7.394E+00	2.540E+02	7.417E-03	5.693E+00	9.969E+02	4.476E+01
31JUL731	1	7.630E+00	2.640E+02	7.402E-03	5.705E+00	1.031E+03	4.628E+01
1AUG731	1	7.510E+00	2.587E+02	7.428E-03	5.699E+00	1.011E+03	4.539E+01
2AUG732	2	1.023E+01	3.522E+02	7.407E-03	5.680E+00	1.381E+03	6.201E+01
3AUG731	1	7.507E+00	3.899E+02	7.331E-03	8.481E+00	1.024E+03	4.597E+01
6AUG731	1	7.470E+00	2.563E+02	7.380E-03	5.640E+00	1.012E+03	4.545E+01
7AUG731	3	1.239E+01	4.243E+02	7.441E-03	5.677E+00	1.665E+03	7.474E+01
7AUG732	5	1.564E+01	5.357E+02	7.441E-03	5.677E+00	2.102E+03	9.436E+01
8AUG731	3	1.248E+01	6.488E+02	7.413E-03	8.581E+00	1.684E+03	7.561E+01
9AUG731	2	1.020E+01	5.326E+02	7.407E-03	8.611E+00	1.378E+03	6.185E+01
10AUG731	1	7.484E+00	4.770E+02	7.364E-03	1.045E+01	1.016E+03	4.562E+01
10AUG732	2	1.038E+01	6.677E+02	7.334E-03	1.050E+01	1.416E+03	6.358E+01
10AUG733	3	1.262E+01	8.111E+02	7.371E-03	1.055E+01	1.712E+03	7.687E+01
13AUG731	1	7.444E+00	2.563E+02	7.487E-03	5.741E+00	9.943E+02	4.464E+01
13AUG732	2	1.033E+01	3.575E+02	7.367E-03	5.678E+00	1.402E+03	6.296E+01
13AUG733	3	1.241E+01	4.279E+02	7.379E-03	5.669E+00	1.681E+03	7.548E+01
14AUG732	2	1.021E+01	6.492E+02	7.364E-03	1.043E+01	1.387E+03	6.225E+01
14AUG733	3	1.233E+01	7.985E+02	7.334E-03	1.058E+01	1.682E+03	7.550E+01
15AUG732	2	1.011E+01	5.273E+02	7.398E-03	8.597E+00	1.366E+03	6.133E+01
15AUG733	3	1.235E+01	6.450E+02	7.379E-03	8.585E+00	1.673E+03	7.513E+01
15AUG731	1	7.484E+00	3.894E+02	7.367E-03	8.537E+00	1.016E+03	4.561E+01
15AUG734	1	7.433E+00	4.774E+02	7.242E-03	1.036E+01	1.026E+03	4.608E+01
15AUG735	3	1.253E+01	8.159E+02	7.236E-03	1.049E+01	1.732E+03	7.776E+01
16AUG731	1	7.490E+00	2.487E+02	7.438E-03	5.500E+00	1.007E+03	4.521E+01
16AUG733	3	1.234E+01	4.249E+02	7.438E-03	5.704E+00	1.659E+03	7.449E+01
26AUG731	1	7.627E+00	2.626E+02	7.400E-03	5.675E+00	1.031E+03	4.627E+01
26AUG732	1	7.613E+00	2.621E+02	7.400E-03	5.675E+00	1.029E+03	4.619E+01
28AUG731	1	7.391E+00	2.558E+02	7.329E-03	5.649E+00	1.008E+03	4.528E+01
28AUG732	1	7.432E+00	2.576E+02	7.298E-03	5.635E+00	1.018E+03	4.572E+01
6DEC731	1	7.480E+00	2.545E+02	7.495E-03	5.679E+00	9.979E+02	4.481E+01
7DEC731	1	7.524E+00	2.557E+02	7.525E-03	5.697E+00	9.998E+02	4.489E+01
7DEC732	2	1.023E+01	3.479E+02	7.616E-03	5.771E+00	1.343E+03	6.028E+01
8DEC733	3	1.243E+01	4.235E+02	7.482E-03	5.677E+00	1.661E+03	7.460E+01
10DEC731	1	7.328E+00	3.819E+02	7.502E-03	8.708E+00	9.768E+02	4.386E+01
10DEC732	2	1.045E+01	5.400E+02	7.489E-03	8.634E+00	1.395E+03	6.264E+01
14DEC731	1	7.279E+00	4.589E+02	7.321E-03	1.028E+01	9.943E+02	4.464E+01
14DEC732	2	1.024E+01	6.509E+02	7.308E-03	1.035E+01	1.401E+03	6.290E+01
14DEC733	3	1.227E+01	7.906E+02	7.308E-03	1.049E+01	1.678E+03	7.535E+01
17DEC733	3	1.235E+01	6.460E+02	7.337E-03	8.546E+00	1.684E+03	7.559E+01
17DEC732	2	1.025E+01	5.384E+02	7.450E-03	8.716E+00	1.376E+03	6.178E+01
9JAN741	1	7.537E+00	2.524E+02	7.524E-03	5.612E+00	1.002E+03	4.498E+01
11JAN741	1	7.322E+00	2.459E+02	7.469E-03	5.586E+00	9.803E+02	4.402E+01
14JAN741	1	7.347E+00	2.521E+02	7.456E-03	5.698E+00	9.854E+02	4.424E+01
15JAN741	2	1.010E+01	3.480E+02	7.414E-03	5.691E+00	1.362E+03	6.115E+01
15JAN742	3	1.244E+01	4.299E+02	7.414E-03	5.705E+00	1.678E+03	7.534E+01
22JAN741	1	7.354E+00	3.819E+02	7.464E-03	8.635E+00	9.852E+02	4.423E+01
22JAN742	2	1.010E+01	5.238E+02	7.430E-03	8.527E+00	1.368E+03	6.143E+01
22JAN743	3	1.247E+01	6.508E+02	7.458E-03	8.667E+00	1.673E+03	7.510E+01
23JAN743	3	1.248E+01	8.[illegible]45E+02	7.554E-03	1.098E+01	1.652E+03	7.417E+01
23JAN742	2	1.020E+01	6.571E+02	7.503E-03	1.077E+01	1.359E+03	6.101E+01
23JAN741	1	7.430E+00	4.575E+02	7.490E-03	1.027E+01	9.920E+02	4.454E+01

TABLE B-1 (Continued). Calculated fuel and air flows

```
24JAN741 1 7.439E+00 2.526E+02 7.550E-03 5.711E+00 9.853E+02 4.424E+01
24JAN742 2 1.014E+01 3.458E+02 7.575E-03 5.754E+00 1.339E+03 6.010E+01
24JAN743 3 1.239E+01 4.261E+02 7.543E-03 5.779E+00 1.642E+03 7.373E+01
25JAN741 1 7.337E+00 3.789E+02 7.573E-03 8.711E+00 9.689E+02 4.350E+01
25JAN742 2 9.947E+00 5.111E+02 7.470E-03 8.691E+00 1.318E+03 5.919E+01
25JAN743 3 1.229E+01 6.382E+02 7.457E-03 8.656E+00 1.642E+03 7.373E+01
25JAN744 3 1.231E+01 7.950E+02 7.489E-03 1.077E+01 1.644E+03 7.391E+01
25JAN745 2 9.958E+00 6.354E+02 7.476E-03 1.063E+01 1.332E+03 5.960E+01
25JAN746 1 7.296E+00 4.639E+02 7.470E-03 1.058E+01 9.768E+02 4.385E+01
26JAN741 1 7.163E+00 2.435E+02 7.494E-03 5.674E+00 9.558E+02 4.291E+01
27JAN741 1 7.155E+00 2.443E+02 7.493E-03 5.697E+00 9.550E+02 4.288E+01
27JAN742 2 9.935E+00 3.403E+02 7.486E-03 5.712E+00 1.327E+03 5.958E+01
27JAN743 3 1.235E+01 4.253E+02 7.486E-03 5.741E+00 1.650E+03 7.400E+01
AVERAGES
  NUM INDEX
   19    1 7.436E+00 2.543E+02 7.442E-03 5.667E+00 9.994E+02 4.487E+01
    5    2 7.402E+00 3.844E+02 7.447E-03 8.614E+00 9.941E+02 4.464E+01
    5    3 7.384E+00 4.669E+02 7.378E-03 1.039E+01 1.001E+03 4.495E+01
    6    4 1.016E+01 3.486E+02 7.470E-03 5.714E+00 1.359E+03 6.101E+01
    6    5 1.017E+01 5.296E+02 7.442E-03 8.629E+00 1.367E+03 6.137E+01
    5    6 1.020E+01 6.521E+02 7.397E-03 1.054E+01 1.379E+03 6.191E+01
    8    7 1.280E+01 4.397E+02 7.453E-03 5.704E+00 1.717E+03 7.711E+01
    5    8 1.238E+01 6.458E+02 7.409E-03 8.607E+00 1.671E+03 7.503E+01
    6    9 1.242E+01 8.043E+02 7.382E-03 1.064E+01 1.683E+03 7.558E+01
```

TABLE B-2. List of raw operating data

DATE	HW	MIN	SEC	T1	P1	PYREX	SS	T12	P13	T13	T6	P6	T7	T8	T9	T10	T11	T18	BP
27JUL731	1	4.	58.	21.5	80.0	85.0	45.0	21.5	-.	21.5	21.5	-0.	-0.	55.4	44.3	32.8	37.1	27.3	29.58
30JUL731	1	4.	57.	19.5	80.0	85.0	45.0	20.5	-.	20.0	20.5	-0.	-0.	55.6	44.2	34.5	37.8	27.5	29.58
31JUL731	1	4.	48.	21.0	80.5	85.0	45.0	22.5	-.	21.5	21.5	-0.	-0.	55.0	44.2	34.5	38.0	26.5	29.66
1AUG731	1	4.	52.	20.0	80.0	85.0	45.0	20.0	-.	20.0	20.3	-0.	-0.	54.6	44.2	33.0	36.5	27.0	29.62
2AUG732	2	3.	35.	19.0	90.0	85.0	45.0	21.0	-.	19.0	21.0	-0.	-0.	37.0	31.5	25.0	27.0	24.0	29.55
3AUG731	1	4.	57.	20.0	80.0	84.5	45.0	23.5	-.	180.0	150.0	-0.	164.0	144.0	104.0	58.0	89.0	31.0	29.55
6AUG731	1	4.	55.	18.5	80.0	84.5	45.0	20.0	-.	19.0	19.0	-0.	29.0	53.0	42.0	30.5	35.0	24.5	29.59
7AUG731	3	2.	56.	18.6	79.0	85.0	45.0	19.0	-.	19.0	18.0	-0.	21.5	26.0	23.5	21.5	22.0	23.5	29.62
7AUG732	5	2.	20.	18.9	79.5	85.0	45.0	19.0	-.	19.0	18.0	-0.	21.5	26.0	23.5	21.5	22.0	23.5	29.62
8AUG731	3	2.	55.	19.5	79.5	85.0	45.0	21.0	.03	178.2	160.3	-0.	159.0	128.0	87.0	53.0	60.0	30.0	29.60
9AUG731	2	3.	35.	20.0	80.0	85.0	45.0	22.5	.02	181.4	161.0	.1	165.0	135.0	100.0	58.5	75.0	26.5	29.70
10AUG731	1	4.	53.	20.0	80.0	85.0	45.0	25.0	.02	295.0	243.8	.1	256.0	209.0	144.2	81.3	128.2	25.0	29.61
10AUG732	2	3.	32.	25.0	82.0	85.0	45.0	27.5	.03	294.8	253.5	.2	258.0	198.0	133.0	80.0	125.0	42.0	29.61
10AUG733	3	2.	55.	21.0	81.0	85.0	45.0	24.5	.03	290.0	250.0	.2	258.0	193.0	124.0	74.5	119.0	33.5	29.61
13AUG731	1	4.	54.	20.5	80.0	86.0	45.0	22.0	-.	20.0	20.0	.0	30.0	56.0	43.0	34.0	35.0	27.0	29.58
13AUG732	2	3.	33.	22.0	81.0	85.0	45.0	24.5	.02	21.5	21.5	.1	27.0	34.0	30.0	26.0	28.5	26.5	29.58
13AUG733	3	2.	55.	26.0	81.0	85.0	45.0	23.5	.02	20.5	20.5	.1	24.5	28.5	25.0	24.0	24.0	24.0	29.58
14AUG732	2	3.	34.	21.0	80.0	85.0	45.0	25.0	.02	290.0	246.0	.1	253.0	198.0	128.0	78.5	121.0	30.0	29.61
14AUG733	3	2.	56.	23.0	80.0	85.0	45.0	27.5	.04	295.0	261.0	.2	253.0	199.5	148.0	80.0	124.0	30.0	29.61
15AUG732	2	3.	35.	19.5	79.0	85.0	45.0	22.0	.02	180.0	162.0	.1	165.0	129.0	97.0	58.0	84.0	29.0	29.58
15AUG733	3	2.	56.	21.0	79.5	85.0	45.0	23.5	.03	179.0	164.0	.2	163.0	125.8	93.5	56.0	81.0	27.0	29.56
15AUG731	1	4.	53.	21.5	80.5	85.0	45.0	24.5	.01	179.0	160.5	.2	166.0	139.0	101.5	60.5	84.0	29.0	29.58
15AUG734	1	4.	54.	22.5	80.5	84.0	45.0	27.5	.02	298.0	249.0	.1	260.0	205.0	150.0	82.0	125.0	31.0	29.58
15AUG735	3	2.	55.	23.0	81.0	84.0	45.0	28.0	.04	298.0	264.0	.2	256.0	198.0	148.0	79.0	123.0	30.0	29.50
16AUG731	1	4.	50.	19.0	78.8	85.0	45.0	19.0	-.	19.0	-0.	-0.	28.0	58.5	52.0	37.3	40.2	-0.	29.60
16AUG733	3	2.	56.	19.0	78.0	85.0	45.0	19.0	-.	-0.	-0.	-0.	-0.	-0.	-0.	-0.	-0.	-0.	29.60
26AUG731	1	4.	49.	20.0	80.5	85.0	45.0	22.0	-.	20.0	20.0	.0	-0.	-0.	-0.	-0.	-0.	-0.	29.60
26AUG732	1	4.	48.	20.0	80.0	85.0	45.0	22.0	-.	-0.	-0.	-0.	-0.	-0.	-0.	-0.	-0.	-0.	29.60
28AUG731	1	4.	55.	18.5	79.0	84.0	44.0	20.5	-.	21.0	22.0	.0	-0.	-0.	-0.	-0.	-0.	-0.	29.59
28AUG732	1	4.	54.	21.0	90.0	84.0	44.0	23.0	-.	21.0	23.0	.0	-0.	-0.	-0.	-0.	-0.	-0.	29.59
6DEC731	1	4.	54.	16.5	79.0	85.0	44.0	17.5	-.	16.5	16.5	.0	-0.	59.5	45.0	32.0	-0.	-0.	29.90
7DEC731	1	4.	52.	16.0	78.5	84.5	44.0	16.5	-.	16.0	16.5	.0	-0.	58.5	44.5	31.5	-0.	-0.	30.40
7DEC732	2	3.	36.	16.0	79.0	85.5	44.0	16.5	.01	16.5	16.5	.1	-0.	46.0	37.0	27.5	-0.	-0.	30.40

TABLE B-2 (Continued). List of raw operating data

```
 8DEC733 3  2. 55. 16.8 78.0 84.5 44.0 16.8  .01  17.0  16.8   .1  -0.   25.0  22.0  19.0  -0.   -0.  30.08
10DEC731 1  4. 56. 12.5 76.5 85.0 44.0 16.0  .02 175.0 162.0   .1 173.0 164.0 118.0  74.0  -0.   -0.  29.80
10DEC732 2  3. 27. 16.5 77.5 85.0 44.0 17.0  .02 173.0 162.0   .1 157.0 151.0 110.0  68.5  -0.   -0.  29.80
14DEC731 1  4. 56. 16.0 77.5 85.0 44.0 20.0  .03 284.0 243.0   .1 268.0 229.0 167.0 100.0  -0.   -0.  20.77
14DEC732 2  3. 32. 17.0 78.5 85.0 44.0 21.0  .04 283.0 253.0   .2 263.0 222.0 162.0  98.5  -0.   -0.  28.77
14DEC733 3  2. 56. 17.0 78.0 85.0 45.0 21.0  .05 289.0 262.0   .2 266.0 222.0 163.0  98.0  -0.   -0.  28.77
17DEC733 3  2. 56. 16.5 78.5 85.0 45.0 18.5  .01 179.0 165.0   .2 164.0 147.0 107.0  66.5  -0.   -0.  28.75
17DEC732 2  3. 31. 18.0 78.5 86.5 45.5 20.0  .01 179.0 169.0   .1 167.0 149.0 107.0  66.5  -0.   -0.  28.75
 9JAN741 1  4. 49. 12.5 77.0 85.0 44.5 12.0 -.    12.0  12.0   .0  20.0  52.0  39.0  26.5  -0.   -0.  29.56
11JAN741 1  4. 53. 17.0 77.0 85.0 44.5 17.0  .01  15.5  10.0   .0  23.5  51.0  39.0  20.5  -0.   -0.  29.64
14JAN741 1  4. 55. 19.0 78.5 85.0 44.5 19.5 -.    19.0  19.0   .0  27.0  56.0  43.5  33.0  -0.   -0.  29.79
15JAN741 2  3. 36. 20.0 79.5 85.0 45.0 21.0  .01  20.0  20.5   .1  25.5  42.0  35.5  30.0  -0.   -0.  29.61
15JAN742 3  2. 55. 20.5 79.5 85.0 45.0 21.0  .02  21.0  21.0   .1  28.0  25.5  27.5  25.0  -0.   -0.  29.61
22JAN741 1  4. 54. 17.0 77.5 84.5 44.5 18.0  .01 174.0 164.0   .1 164.0 165.0 115.5  72.0   0.   -0.  30.06
22JAN742 2  3. 34. 18.0 78.5 84.5 44.5 20.0  .02 172.0 158.0   .1 159.0 140.0 102.0  61.0  -0.   -0.  30.06
22JAN743 3  2. 54. 19.0 78.5 85.0 44.5 22.0  .04 174.0 168.0   .2 160.0 142.0 100.0  67.0  -0.   -0.  30.06
23JAN743 3  2. 55. 17.0 78.5 86.0 44.5 20.0  .04 292.0 273.0   .2 263.0 227.0 160.0  98.0  -0.   -0.  29.91
23JAN742 2  3. 35. 19.0 79.5 86.0 44.5 24.0  .03 290.0 261.0   .1 261.0 229.0 158.0  90.5  -0.   -0.  29.91
23JAN741 1  4. 53. 21.0 79.5 86.0 44.5 25.0  .03 280.0 222.0   .1 256.0 271.0 159.0  93.0  -0.   -0.  29.91
24JAN741 1  4. 56. 16.0 79.0 85.5 44.5 16.0  .01  15.0  17.0   .0  -0.   -0.   -0.   -0.   -0.   -0.  29.82
24JAN742 2  3. 36. 16.0 78.5 86.0 45.0 17.5  .02  17.5  17.0   .1  -0.   -0.   -0.   -0.   -0.   -0.  29.82
24JAN743 3  2. 55. 19.0 78.5 86.0 45.0 20.0  .03  20.0  19.5   .1  -0.   -0.   -0.   -0.   -0.   -0.  29.82
25JAN741 1  4. 52. 16.0 76.5 86.0 44.5 17.0  .01 172.0 161.0   .1 174.0 182.0 127.0  76.0  -0.   -0.  29.75
25JAN742 2  3. 38. 17.0 77.0 85.0 44.5 18.0  .02 174.0 169.0   .1 172.0 169.0 119.0  71.0  -0.   -0.  29.75
25JAN743 3  2. 55. 17.5 77.0 85.0 44.5 19.0  .03 172.0 169.0   .2 162.0 148.0 105.0  64.0  -0.   -0.  29.75
25JAN744 3  2. 55. 17.5 77.5 85.5 44.5 20.0  .04 286.0 267.0   .2 270.0 237.0 164.0  95.0  -0.   -0.  29.75
25JAN745 2  3. 36. 18.0 77.5 85.5 45.0 21.0  .03 290.0 260.0   .1 270.0 247.0 173.0 100.0  -0.   -0.  29.75
25JAN746 1  4. 58. 18.0 78.5 85.5 45.0 21.5  .02 283.0 253.0   .1 280.0 261.0 181.0 105.0  -0.   -0.  29.75
26JAN741 1  4. 57. 16.5 76.0 85.0 44.5 16.5 -.    16.0  15.5   .0  -0.   -0.   -0.   -0.   -0.   -0.  29.79
27JAN741 1  4. 56. 18.0 76.0 85.0 47.0 18.0  .01  17.0  18.0   .0  -0.   -0.   -0.   -0.   -0.   -0.  29.93
27JAN742 2  3. 34. 18.5 76.5 85.0 47.0 18.5  .01  18.5  18.5 -0.   -0.   -0.   -0.   -0.   -0.   -0.  29.93
27JAN743 3  2. 54. 18.5 77.5 85.0 47.0 18.5 -.    -0.   -0.  -0.   -0.   -0.   -0.   -0.   -0.   -0.  29.93
```

APPENDIX C

Mass Spectrometer and CO Data

This appendix is a comprehensive compilation of all of the mass spectrometer and carbon monoxide data that were collected during the course of the study. The mass spectrometer data include the species: water, nitrogen, oxygen, carbon dioxide, and unburnt fuel. The data have been corrected to represent the actual mass fractions on a wet basis following the correction procedures outlined in section 3.3.1.

For purposes of analysis and visualization of the data, scatter diagrams were plotted at each axial sampling location for each of the experimental conditions. Samples of these diagrams are shown in Figs. C-1 and C-2. The representative data presented in chapter 4 were developed from these plots. Because of space limitations, all of these diagrams cannot be included. Instead, the data are listed in Tables C-1 to C-3.

The variables used in the tables are:

DAY - day of month for mass spectrometer data, all runs in December

HW - V_A/V_F; 1 = 45:1, 2 = 61:1, 3 = 75:1

X - axial location from injector tip, inches X 100

R - radial location in horizontal direction, inches

R/A - nondimensional radial location

H_2O, N_2, etc. - species mole fraction

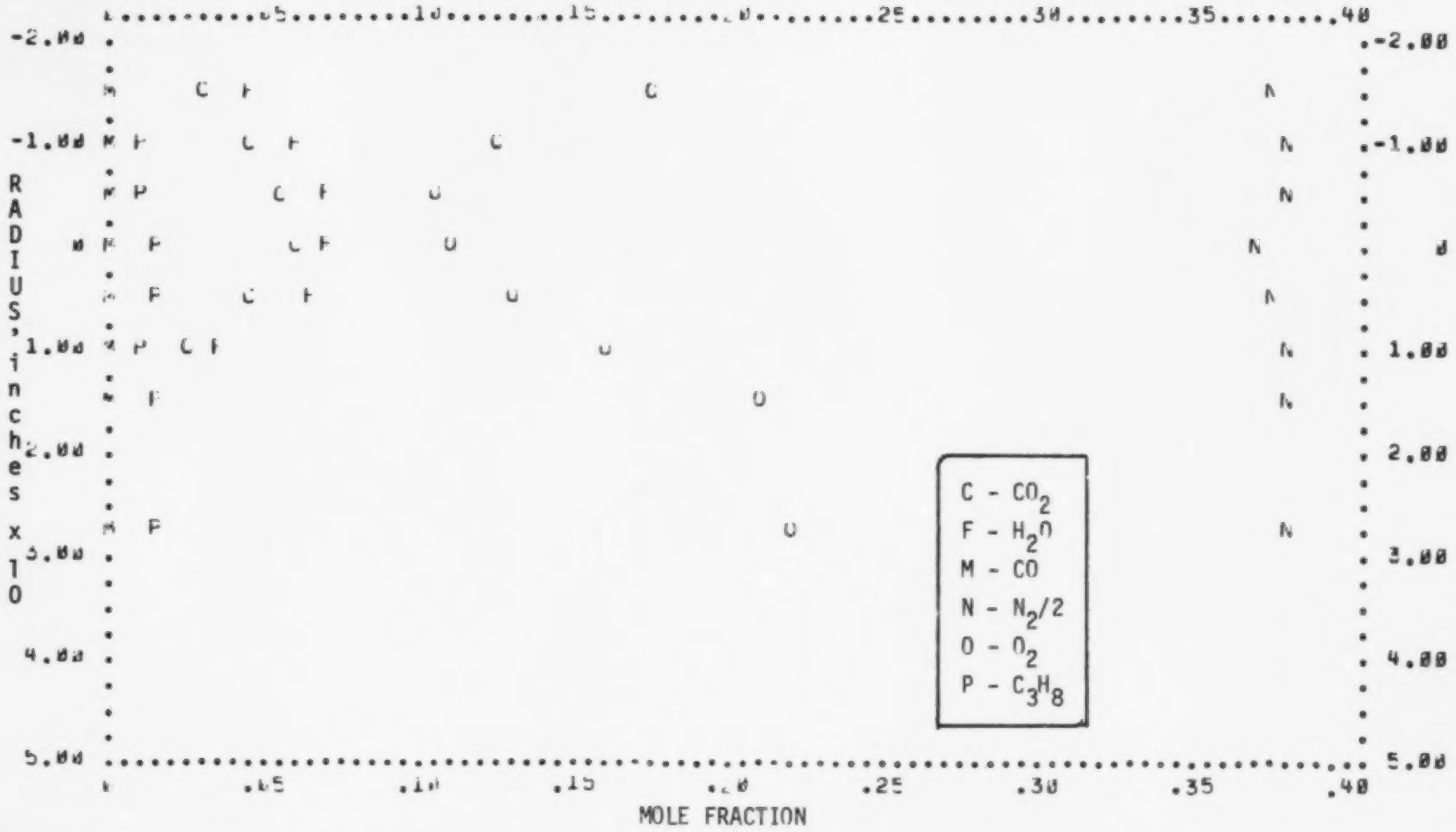

Figure C-1. Scatter diagram of mass spectrometer and CO data at V_A/V_F = 45 and 300°K initial reactant temperature, X/D = 21.33.

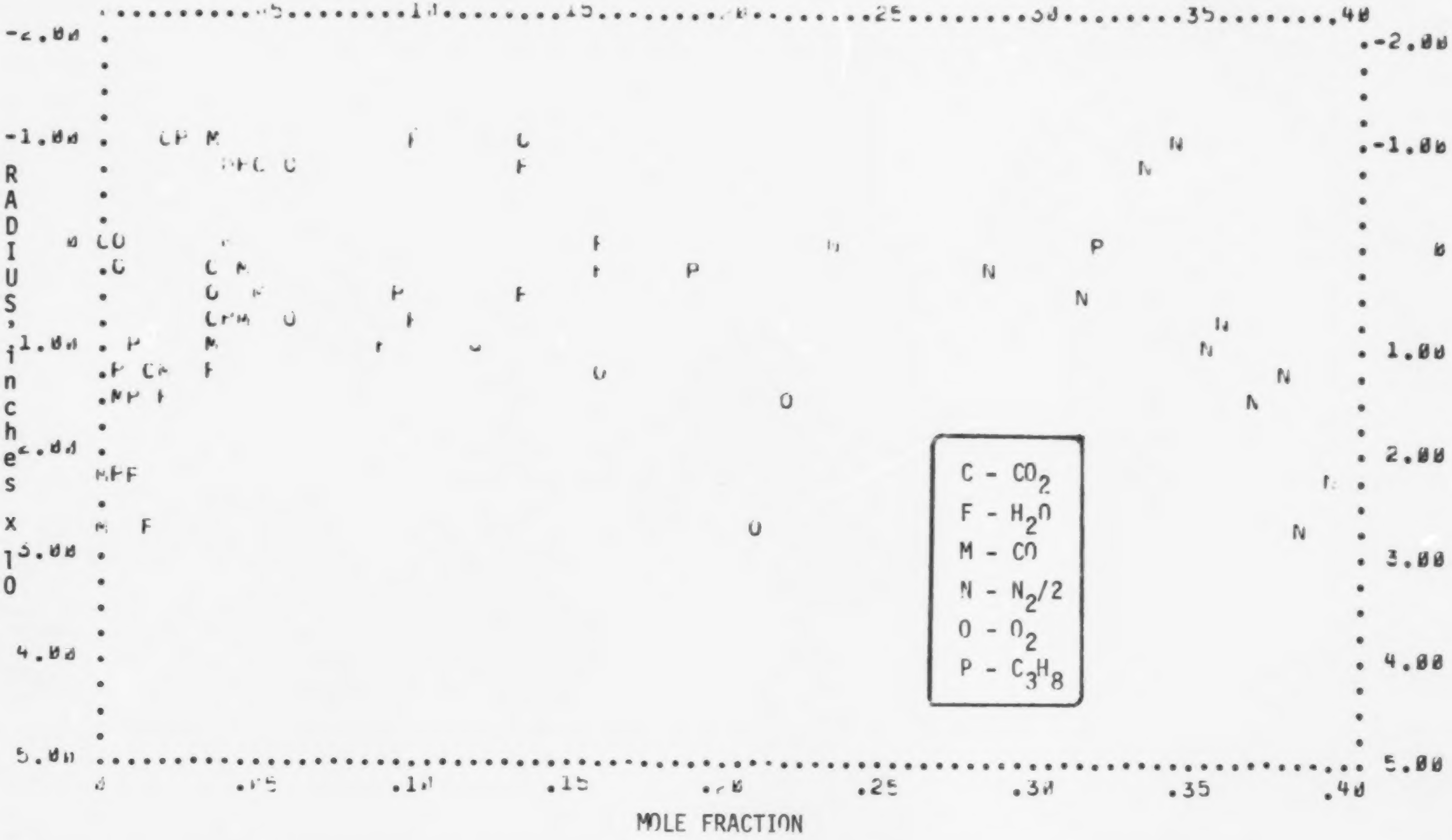

Figure C-2. Scatter diagram of mass spectrometer and CO data at V_A/V_F = 45 and 300°K initial reactant temperature, X/D = 1.33.

TABLE C-1. Mass spectrometer and CO data for 300°K initial reactant temperature.

```
IDV NU %    F        R-H     H2O     N2/2     O2      CO2     C3H8     CO
THE FOLLOWING DATA IS FOR CASE  6 1  AXIAL POSITION 800  X/I=-21.333
  6 1 800 -.5000-2.6[illegible] .04[illegible]  .3751  .1255  .0303 0.       .0000
  6 1 800 [illegible]  [illegible]  .0607  [illegible]  .1246  .0441  .0117   .0000
  6 1 800 [illegible]  [illegible]  .0636  [illegible]  .1346  .0568  .0124   .0000
  6 1 800 0.      0.       .0700  [illegible]  .1120  .0624  .01[illegible]   .0000
  6 1 800 .[illegible]000 [illegible]  .0626  [illegible]  .1289  .0361  .01[illegible]   .0000
  6 1 800 .2000 1.0[illegible]  .0[illegible]  .3019  .0622  .0244  .01[illegible]   .0000
  6 1 800 .[illegible]000 [illegible]  [illegible]  .3[illegible]  .[illegible]073 0.       .0125   .0000
  6 1 800 .[illegible]000 [illegible]  [illegible]  .381[illegible]  .[illegible]222 0.       .0152   .0000
THE FOLLOWING DATA IS FOR CASE  6 1  AXIAL POSITION 600  X/I=-16.000
  6 1 600 [illegible]  [illegible]  .0061  [illegible]  .1164  .0567  .0189   .0000
  6 1 600 [illegible]  [illegible]  .0086  [illegible]  .0756  .0609  .0179   .0001
  6 1 600 0.      0.       .0085  [illegible]  .0651  .0729  .0[illegible]   .0003
  6 1 600 .[illegible]000 [illegible]  .0[illegible]  [illegible]  .1003  .0585  .0172   .0003
  6 1 600 .[illegible]000 [illegible]  .0[illegible]  .3642  .1539  .0328  .0067   .0001
  6 1 600 .[illegible]000 1.0[illegible]  .0[illegible]  .3647  .2187  .0037  .0155   .0000
  6 1 600 .4000 2.[illegible]  .0065  .3815  .2150 0.       .0147   .0000
  6 1 600 .5000 2.[illegible]  .0057  .376[illegible]  .2327 0.       .0086   .0000
TOO FEW POINTS TO PLOT IN CASE  6 1  AXIAL POSITION 500  X/I=-13.333
  6 1 500 0.      0.       .1169  .3415  .1004  .1021  .0371   .0060
THE FOLLOWING DATA IS FOR CASE  6 1  AXIAL POSITION 400  X/I=-10.667
  6 1 400 [illegible]  [illegible]  [illegible]  [illegible]  .0676  .0916  .0055   .0010
  6 1 400 [illegible]  [illegible]  [illegible]  [illegible]  .[illegible]74  .1019  .0346   .0069
  6 1 400 0.      0.       [illegible]  [illegible]  .0[illegible]61  .1116  .00[illegible]   .0105
  6 1 400 0.      [illegible]  [illegible]  [illegible]  .0[illegible]5[illegible]  .1100  .0079   .0108
  6 1 400 [illegible]  [illegible]  [illegible]  [illegible]  .[illegible]544  .0865  .0095   .0060
  6 1 400 [illegible]  [illegible]  [illegible]  [illegible]  .[illegible]027  .0504  .0069   .0010
  6 1 400 [illegible]  [illegible]  [illegible]  [illegible]  .[illegible]008  .0211  .0065   .0001
  6 1 400 [illegible]  [illegible]  [illegible]  [illegible]  .[illegible]19   .0005  .0112   .0000
  6 1 400 .5000 2.[illegible]  [illegible]  .3019  .[illegible]102  .0010  .0095   .0000
TOO FEW POINTS TO PLOT IN CASE  6 1  AXIAL POSITION 300  X/I= 8.000
  6 1 300 0.      0.       [illegible]  .3790  .0083  .0536  .0291   .0351
THE FOLLOWING DATA IS FOR CASE  6 1  AXIAL POSITION 200  X/I= 5.333
  7 1 200 0.      0.       [illegible]  [illegible]  .[illegible]156  .0430  .0772   .0569

  7 1 200 .0500 [illegible]  .1[illegible]  .3569  .[illegible]033  .0540  .0310   .0566
  7 1 200 .[illegible]000 [illegible]  .09[illegible]  .3872  .1034  .0458 0.       .0587
  6 1 200 [illegible]  [illegible]  [illegible]  [illegible]  [illegible]75  .064[illegible]  .0125   .0391
  6 1 200 .[illegible]000 1.[illegible]  .1[illegible]  .351[illegible]  [illegible]  .0770  .0023   .0308
  7 1 200 .2500 [illegible]  [illegible]  [illegible]  [illegible]05  .04[illegible]  .0044   .0165
  6 1 200 .3000 [illegible]  [illegible]  [illegible]  [illegible]51  .0170  .0155   .0030
  6 1 200 .4000 2.[illegible]  [illegible]  .381[illegible]  [illegible]041 0.       .01[illegible]   .0001
  6 1 200 .5000 2.[illegible]  [illegible]  [illegible]  [illegible]55  .0002 0.       .0000
TOO FEW POINTS TO PLOT IN CASE  7 1  AXIAL POSITION 150  X/I= 4.000
  7 1 150 0.      0.       [illegible]  .3107  .[illegible]110  .0277  .1144   .0524
THE FOLLOWING DATA IS FOR CASE  7 1  AXIAL POSITION 100  X/I= 2.667
  7 1 100 0.      0.       .1820  .3205  .1084  .0242  .1242   .0538
  7 1 100 .0500 .[illegible]  .1655  .3323  .1044  .0251  .0862   .0538
  7 1 100 .1000 .5[illegible]  .1677  .3175  .1064  .0474  .1023   .0550
  6 1 100 .1000 .5[illegible]  .1632  .3337  .1176  .0308  .0646   .0561
  7 1 100 .1500 .8000  .1566  .3260  .0447  .0804  .0[illegible]5   .0413
  6 1 100 .1500 .8000  .1297  .3511  .0602  .0561  .0173   .0339
  6 1 100 .2000 1.0[illegible]  .0705  .371[illegible]  .1004  .0424  .01[illegible]6   .0288
  6 1 100 .2500 1.[illegible]  .0435  .3828  .1408  .0163  .0119   .0153
  6 1 100 .3000 1.6000  .0263  .3863  .1875  .0131 0.       .0024
  6 1 100 .4000 2.1[illegible]  .0006  .3849  .2149 0.       .0063   .0001
  6 1 100 .5000 2.6667  .0063  .3710  .2327 0.       .0108   .0000
  7 1 100 .6000 3.2000  .0557  .3637  .[illegible]63 0.       .0102   .0000
```

TABLE C-1 (Continued). Mass spectrometer and CO data for 300°K initial reactant temperature.

```
 TOO FEW POINTS TO PLOT IN CASE   7 1  AXIAL POSITION  75  X/D= 2.000
  7 1  75 0.      0.       .1467  .2996  .0077  .0009  .1980  .0469
 THE FOLLOWING DATA ARE FOR CASE  7 1  AXIAL POSITION  50  X/D= 1.333
  7 1  50 -.2000-1.0667  .1021  .3441  .1333  .0187  .0230  .0341
  7 1  50 -.1500 -.8000  .1357  .3332  .0610  .0477  .0463  .0423
  7 1  50 0.      0.     .1625  .2348  .0075 0.      .3158  .0402
  7 1  50  .0500  .2667  .1587  .2846  .0040  .0327  .1897  .0454
  7 1  50  .1000  .5333  .1341  .3148  .0373  .0525  .0942  .0520
  7 1  50  .1500  .8000  .1006  .3611  .0584  .0352  .0392  .0441
  7 1  50  .2000 1.0667  .0986  .3563  .1190  .0330  .0118  .0346
  7 1  50  .2500 1.3333  .0362  .3810  .1598  .0154  .0067  .0193
  7 1  50  .3000 1.6000  .0201  .3724  .2210  .0036  .0160  .0034
  7 1  50  .4000 2.1333  .0097  .3927  .1989 0.      .0055  .0001
  7 1  50  .5000 2.6667  .0155  .3853  .2118 0.      .0018  .0000
 THE FOLLOWING DATA ARE FOR CASE  7 2  AXIAL POSITION 800  X/D=21.333
  7 2 800 -.2000-1.0667  .0526  .3914  .1137  .0405  .0096  .0001
  7 2 800 -.1000 -.5333  .0471  .4028  .0956  .0461  .0067  .0001
  7 2 800 0.      0.     .0500  .3926  .1074  .0426  .0025  .0001
  7 2 800  .1000  .5333  .0483  .3823  .1493  .0374 0.      .0001
  7 2 800  .2000 1.0667  .0354  .3849  .1677  .0087  .0160  .0001
  7 2 800  .3000 1.6000  .0121  .3946  .1920  .0063 0.      .0001
  7 2 800  .4000 2.1333  .0042  .3916  .2125 0.     0.      .0000
 THE FOLLOWING DATA ARE FOR CASE  7 2  AXIAL POSITION 600  X/D=16.000
  7 2 600 -.2000-1.0667  .0743  .3819  .1051  .0406  .0157  .0001
  7 2 600 -.1000 -.5333  .0706  .3806  .0927  .0741  .0089  .0001
  7 2 600 0.      0.     .0653  .3816  .0958  .0630  .0122  .0001
  7 2 600  .1000  .5333  .0609  .3748  .1360  .0316  .0215  .0001
  7 2 600  .2000 1.0667  .0417  .3963  .1349  .0237  .0068  .0001
  7 2 600  .3000 1.6000  .0212  .3877  .1848  .0015  .0167  .0001
  7 2 600  .4000 2.1333 0.      .3948  .2062 0.      .0026  .0000
 TOO FEW POINTS TO PLOT IN CASE   7 2  AXIAL POSITION 500  X/D=13.333
  7 2 500 0.      0.     .0825  .3894  .0823  .0670  .0068  .0014
 THE FOLLOWING DATA ARE FOR CASE  7 2  AXIAL POSITION 400  X/D=10.667
  7 2 400 -.2000-1.0667  .0959  .3794  .0842  .0708 0.      .0008
  7 2 400 -.1000 -.5333  .1107  .3599  .0509  .0924  .0255  .0014
  7 2 400 0.      0.     .1173  .3689  .0563  .0775  .0167  .0029
  7 2 400  .1000  .5333  .0903  .3690  .0838  .0712  .0162  .0019
  7 2 400  .2000 1.0667  .0762  .3514  .1445  .0416  .0344  .0005
  7 2 400  .3000 1.6000  .0327  .3880  .1708  .0091  .0167  .0001
  7 2 400  .4000 2.1333 0.      .3926  .2004  .0021 0.      .0001
 THE FOLLOWING DATA ARE FOR CASE  7 2  AXIAL POSITION 300  X/D= 8.000
  7 2 300 0.      0.     .1234  .3673  .0275  .0857  .0178  .0105
  7 2 300  .1000  .5333  .1285  .3643  .0485  .0668  .0164  .0087
  7 2 300  .2000 1.0667  .1126  .3412  .1363  .0468  .0214  .0050
  7 2 300  .3000 1.6000  .0588  .3794  .1566  .0030  .0223  .0009
 TOO FEW POINTS TO PLOT IN CASE   7 2  AXIAL POSITION 250  X/D= 6.667
  7 2 250 0.      0.     .1405  .3666  .0037  .0613  .0220  .0307
 THE FOLLOWING DATA ARE FOR CASE  7 2  AXIAL POSITION 200  X/D= 5.333
  7 2 200 -.0500 -.2667  .1135  .3762  .0029  .0583  .0220  .0505
  7 2 200 0.      0.     .1360  .3571  .0026  .0353  .0580  .0536
  7 2 200  .0500  .2667  .1283  .3720  .0038  .0601  .0135  .0497
  7 2 200  .1000  .5333  .1127  .3819  .0079  .0628  .0061  .0461
  7 2 200  .1500  .8000  .1030  .3665  .0357  .0826  .0113  .0332
  7 2 200  .2000 1.0667  .0972  .3775  .0656  .0541  .0074  .0200
  7 2 200  .2500 1.3333  .0684  .3743  .1257  .0458 0.      .0112
  7 2 200  .3000 1.6000  .0388  .3765  .1847  .0200  .0030  .0020
  7 2 200  .4000 2.1333  .0096  .3865  .2115  .0052 0.      .0002
 TOO FEW POINTS TO PLOT IN CASE   7 2  AXIAL POSITION 150  X/D= 4.000
  7 2 150 0.      0.     .1433  .3405  .0043  .0421  .0697  .0591
```

TABLE C-1 (Continued). Mass spectrometer and CO data for 300°K initial reactant temperature.

```
THE FOLLOWING DATA ARE FOR CASE  8 3  AXIAL POSITION 100  X/D= 2.667
[illegible]
[illegible]
[illegible]
[illegible]
[illegible]
[illegible]
[illegible]
[illegible]
[illegible]
[illegible]
THE FOLLOWING DATA ARE FOR CASE  8 3  AXIAL POSITION  50  X/D= 1.333
[illegible]
[illegible]
[illegible]
[illegible]
[illegible]                                  .0272  .0365  .0519
[illegible]                                  .0047  .0184  .0180
[illegible]                                  .0193 0.      .0030
[illegible]                                  .0010 0.      .0005
TOO FEW POINTS TO PLOT IN CASE  8 3  AXIAL POSITION  20  X/D=  .533
[illegible]                                         .3771  .0547
THE FOLLOWING DATA ARE FOR CASE  8 3  AXIAL POSITION 800  X/D=21.333
  8 3 800 -.2000-1.0667  .0508  .3800  .1405  .0302  .0062  .0002
  8 3 800 -.1000  .5333  .0462  .3821  .1409  .0437  .0345  .0002
  8 3 800 0.      0.     .0460  .3737  .1553  .0401  .0104  .0002
  8 3 800  .1000  .5333  .0480  .3732  .1587  .0252  .0115  .0002
  8 3 800  .2000 1.0667  .0130  .3796  .2096  .0121  .0052  .0002
  8 3 800  .3000 1.6000 0.      .3782  .2328 0.      .0160  .0002
  8 3 800  .4000 2.1333 0.      .3727  .2329 0.      .0214  .0001
  8 3 800  .5000 2.6667  .0031  .3802  .2342 0.      .0018  .0000
  8 3 800  .7000 3.7333 0.      .3938  .2115 0.      .0067  .0000
THE FOLLOWING DATA ARE FOR CASE  8 3  AXIAL POSITION 600  X/D=16.000
  8 3 600 -.2000-1.0667  .0520  .3676  .1608  .0480  .0076  .0003
  8 3 600 -.1000 -.5333  .0395  .3849  .1359  .0547 0.      .0003
  8 3 600 0.      0.     .0616  .3874  .1118  .0515 0.      .0002
  8 3 600  .1000  .5333  .0731  .3637  .1520  .0348  .0120  .0002
  8 3 600  .2000 1.0667  .0403  .3702  .1966  .0144  .0080  .0005
  8 3 600  .3000 1.6000  .0209  .3773  .2065 0.      .0180  .0002
  8 3 600  .4000 2.1333  .0032  .3918  .2107  .0021 0.      .0001
TOO FEW POINTS TO PLOT IN CASE  8 3  AXIAL POSITION 500  X/D=13.333
  8 3 500 0.      0.     .0842  .3623  .1139  .0524  .0244  .0002
THE FOLLOWING DATA ARE FOR CASE  8 3  AXIAL POSITION 400  X/D=10.667
  8 3 400 -.2000-1.0667  .0756  .3807  .1009  .0588  .0075  .0003
  8 3 400 -.1000 -.5333  .0924  .3637  .0910  .0630  .0255  .0002
  8 3 400 0.      0.     .0809  .3665  .0964  .0591  .0231  .0002
  8 3 400  .1000  .5333  .0655  .3751  .1181  .0626  .0018  .0002
  8 3 400  .2000 1.0667  .0472  .3631  .1749  .0263  .0146  .0003
  8 3 400  .3000 1.6000  .0201  .3859  .1906  .0111 0.      .0003
  8 3 400  .4000 2.1333  .0184  .3842  .2011 0.      .0115  .0001
TOO FEW POINTS TO PLOT IN CASE  8 3  AXIAL POSITION 300  X/D= 8.000
  8 3 300 0.      0.     .1129  .3561  .0775  .0720  .0249  .0000
TOO FEW POINTS TO PLOT IN CASE  8 3  AXIAL POSITION 250  X/D= 6.667
  8 3 250 0.      0.     .0995  .3786  .0462  .0777  .0081  .0108
THE FOLLOWING DATA ARE FOR CASE  8 3  AXIAL POSITION 200  X/D= 5.333
```

TABLE C-1 (Continued). Mass spectrometer and CO data for 300°K initial reactant temperature.

```
   8 3 200 -.2000-1.0667  .1202  .3567  .0599  .0832  .0231  .0044
   8 3 200 -.1000 -.5333  .1380  .3550  .0406  .0930  .0078  .0102
   8 3 200 0.      0.     .1057  .3694  .0525  .0816  .0066  .0143
   8 3 200  .1000  .5333  .1081  .3639  .0751  .0685  .0095  .0105
   8 3 200  .2000 1.0667  .1004  .3618  .1141  .0471  .0145  .0044
   8 3 200  .3000 1.6000  .0353  .3820  .1816  .0189 0.      .0010
   8 3 200  .4000 2.1333  .0158  .3939  .1848 0.      .0112  .0003
   8 3 200  .7000 3.7333  .0077  .3741  .2350 0.      .0090  .0000
 TOO FEW POINTS TO PLOT IN CASE   8 3  AXIAL POSITION 150  X/D= 4.000
   8 3 150 0.      0.     .1157  .3625  .0178  .0850  .0200  .0363
 TOO FEW POINTS TO PLOT IN CASE   8 3  AXIAL POSITION 125  X/D= 3.333
   8 3 125 0.      0.     .1176  .3720  .0131  .0480  .0276  .0494
 THE FOLLOWING DATA ARE FOR CASE  8 3  AXIAL POSITION 100  X/D= 2.667
   8 3 100 -.2000-1.0667  .1173  .3613  .0580  .0504  .0230  .0282
   8 3 100 -.1000 -.5333  .1308  .3638  .0022  .0644  .0266  .0539
   8 3 100 -.0500 -.2667  .1774  .3344  .0026  .0584  .0385  .0539
   8 3 100 0.      0.     .1368  .3529  .0111  .0432  .0431  .0596
   8 3 100  .0500  .2667  .1709  .3553  .0031  .0465  .0141  .0543
   8 3 100  .1000  .5333  .1440  .3453  .0184  .0617  .0319  .0531
   8 3 100  .1500  .8000  .1214  .3454  .0473  .0730  .0256  .0413
   8 3 100  .2000 1.0667  .0998  .3775  .0667  .0418  .0074  .0288
   8 3 100  .2500 1.3333  .0861  .3834  .0847  .0325  .0129  .0164
   8 3 100  .3000 1.6000  .0508  .3872  .1406  .0151  .0105  .0046
   8 3 100  .3500 1.8667  .0258  .3895  .1790  .0126  .0070  .0020
   8 3 100  .4000 2.1333  .0026  .4529  .0665  .0247 0.      .0007
   8 3 100  .5000 2.6667  .0050  .3881  .2093 0.      .0090  .0002
 TOO FEW POINTS TO PLOT IN CASE   8 3  AXIAL POSITION  75  X/D= 2.000
   8 3  75 0.      0.     .1112  .3628  .0184  .0454  .0347  .0644
 THE FOLLOWING DATA ARE FOR CASE  8 3  AXIAL POSITION  50  X/D= 1.333
   8 3  50 -.1000 -.5333  .1303  .3179  .0540  .0445  .0773  .0574
   8 3  50 -.0500 -.2667  .1308  .3205  .0343  .0343  .0812  .0617
   8 3  50 0.      0.     .1265  .3201  .0363  .0298  .1001  .0664
   8 3  50  .0500  .2667  .1236  .3334  .0455  .0272  .0741  .0622
   8 3  50  .1000  .5333  .1590  .3076  .0390  .0380  .0929  .0555
   8 3  50  .1500  .8000  .1059  .3485  .0731  .0424  .0408  .0402
   8 3  50  .2000 1.0667  .0630  .3676  .1326  .0333  .0138  .0215
   8 3  50  .2500 1.3333  .0414  .3762  .1741  .0190  .0012  .0115
   8 3  50  .3000 1.6000  .0192  .3972  .1753  .0050  .0033  .0024
   8 3  50  .4000 2.1333  .0115  .3904  .2065 0.      .0065  .0004
 TOO FEW POINTS TO PLOT IN CASE   8 3  AXIAL POSITION  25  X/D=  .667
   8 3  25 0.      0.     .1583  .2565  .0605  .0326  .1973  .0379
```

TABLE C-2. Mass spectrometer and CO data for 440°K initial reactant temperature.

```
DAY HW X     R         R/A    H20     N2/2     O2     CO2     C3H8     CO
THE FOLLOWING DATA AFE FOR CASE 10 1  AXIAL POSITION 800  X/D=21.333
 10 1 800 -.2000-1.0667  .0269  .3759  .2028  .0140  .0040  .0000
 10 1 800 -.1000 -.5333  .0334  .3880  .1540  .0362 0.      .0000
 10 1 800 0.     0.      .0595  .3621  .1612  .0504  .0045  .0000
 10 1 800  .1000  .5333  .0494  .3828  .1333  .0466  .0045  .0000
 10 1 800  .2000 1.0667  .0540  .3718  .1440  .0503  .0079  .0000
 10 1 800  .3000 1.6000  .0428  .3832  .1642  .0162  .0100  .0000
 10 1 800  .4000 2.1333  .0237  .3690  .2209 0.      .0169  .0000
 10 1 800  .5000 2.6667  .0126  .3856  .2115 0.      .0045  .0000
 10 1 800  .6000 3.2000 0.      .3869  .2241 0.      .0018  .0000
THE FOLLOWING DATA AFE FOR CASE 10 1  AXIAL POSITION 600  X/D=16.000
 10 1 600 -.2000-1.0667  .0341  .3716  .1939  .0225  .0060  .0000
 10 1 600 -.1000 -.5333  .0369  .3923  .1211  .0399  .0172  .0000
 10 1 600 0.     0.      .0559  .3925  .0985  .0564  .0036  .0000
 10 1 600  .1000  .5333  .0099  .3577  .1171  .0666  .0105  .0000
 10 1 600  .2000 1.0667  .0603  .3770  .1232  .0596  .0026  .0000
 10 1 600  .3000 1.6000  .0512  .3695  .1708  .0313  .0073  .0000
 10 1 600  .4000 2.1333  .0241  .3798  .1944  .0068  .0145  .0000
 10 1 600  .5000 2.6667  .0194  .3725  .2252 0.      .0100  .0000
TOO FEW POINTS TO PLOT IN CASE  10 1  AXIAL POSITION 500  X/D=13.333
 10 1 500 0.     0.      .0815  .3819  .0800  .0687  .0055  .0009
THE FOLLOWING DATH AFE FOP CASE 10 1  AXIAL POSITION 400  X/D=10.667
 10 1 400 -.2000-1.0667  .0406  .3841  .1573  .0241  .0090  .0002
 10 1 400 -.1000 -.5333  .0899  .3572  .1254  .0544  .0155  .0007
 10 1 400 0.     0.      .0981  .3682  .0794  .0665  .0150  .0017
 10 1 400  .1000  .5333  .0988  .3722  .0620  .0777  .0156  .0017
 10 1 400  .2000 1.0667  .0981  .3653  .0889  .0642  .0179  .0006
 10 1 400  .3000 1.6000  .0640  .3712  .1364  .0531  .0036  .0001
 10 1 400  .4000 2.1333  .0530  .3757  .1656  .0163  .0134  .0000
TOO FEW POINTS TO PLOT IN CASE  10 1  AXIAL POSITION 350  X/D= 9.333
 10 1 350  .1000  .5333  .1051  .3664  .0459  .0871  .0160  .0125
TOO FEW POINTS TO PLOT IN CASE  10 1  AXIAL POSITION 300  X/D= 8.000
 10 1 300  .1000  .5333  .0964  .3866  .0297  .0660  .0070  .0271
TOO FEW POINTS TO PLOT IN CASE   0 1  AXIAL POSITION 250  X/D= 6.667

 10 1 250  .1000  .5333  .1422  .3595  .0024  .0733  .0240  .0386
THE FOLLOWING DATA AFE FOR CASE 10 1  AXIAL POSITION 200  X/D= 5.333
 10 1 200 -.0500 -.2667  .1080  .3723  .0176  .0694  .0092  .0508
 10 1 200 0.     0.      .1165  .3866  .0010  .0621 0.      .0468
 10 1 200  .0500  .2667  .1344  .3615  .0033  .0674  .0218  .0493
 10 1 200  .1000  .5333  .1585  .3623  .0026  .0552  .0060  .0505
 10 1 200  .1500  .8000  .1455  .3699  .0031  .0610  .0059  .0402
 10 1 200  .2000 1.0667  .1148  .3886  .0238  .0347  .0198  .0292
 10 1 200  .2500 1.3333  .1261  .3678  .0430  .0689  .0101  .0157
 10 1 200  .3000 1.6000  .0964  .3613  .1175  .0480  .0151  .0034
 10 1 200  .4000 2.1333  .0492  .3885  .1566  .0170 0.      .0002
 10 1 200  .5000 2.6667  .0263  .3697  .2259  .0009  .0070  .0000
TOO FEW POINTS TO PLOT IN CASE  10 1  AXIAL POSITION 150  X/D= 4.000
 10 1 150  .1000  .5333  .1426  .3614  .0048  .0305  .0424  .0566
THE FOLLOWING DATA AFE FOR CASE 10 1  AXIAL POSITION 100  X/D= 2.667
 10 1 100 -.1000 -.5333  .1292  .3296  .0566  .0435  .0415  .0697
 10 1 100 -.0500 -.2667  .1425  .3449  .0145  .0270  .0571  .0686
 10 1 100 0.     0.      .1817  .3287  .0064  .0099  .0786  .0655
 10 1 100  .0500  .2667  .1229  .3412  .0051  .0214  .0977  .0702
 10 1 100  .1000  .5333  .1215  .3527  .0051  .0327  .0646  .0703
 10 1 100  .1500  .8000  .1282  .3423  .0360  .0393  .0539  .0575
 10 1 100  .2000 1.0667  .1075  .3574  .0461  .0518  .0338  .0455
 10 1 100  .2500 1.3333  .0874  .3736  .0784  .0367  .0223  .0274
```

TABLE C-2 (Continued). Mass spectrometer and CO data for 440°K initial reactant temperature.

```
 10 1 100  .3000 1.6000  .0483  .3826  .1398  .0336  .0127  .0090
 10 1 100  .4000 2.1333  .0238  .3983  .1669  .0126 0.      .0007
 10 1 100  .5000 2.6667  .0105  .3740  .2332  .0070  .0006  .0001
TOO FEW POINTS TO PLOT IN CASE  10 1  AXIAL POSITION  75  X/D= 2.000
 10 1  75  .1000  .5333  .1518  .3322  .0076  .0082  .1049  .0628
THE FOLLOWING DATA ARE FOR CASE 10 1  AXIAL POSITION  50  X/D= 1.333
 10 1  50 -.1000 -.5333  .1379  .3261  .0931  .0185  .0383  .0595
 10 1  50 -.0500 -.2667  .1670  .3173  .0403  .0279  .0726  .0571
 10 1  50 0.     0.      .1199  .3189  .0134  .0241  .1445  .0598
 10 1  50  .0500  .2667  .1316  .2912  .0079  .0268  .1914  .0595
 10 1  50  .1000  .5333  .1382  .3037  .0164  .0351  .1429  .0595
 10 1  50  .1500  .8000  .1192  .3365  .0049  .0270  .1244  .0511
 10 1  50  .2000 1.0667  .1206  .3484  .0427  .0255  .0725  .0413
 10 1  50  .2500 1.3333  .1063  .3602  .0939  .0209  .0347  .0232
 10 1  50  .3000 1.6000  .1030  .3665  .1307  .0171  .0158  .0064
 10 1  50  .4000 2.1333  .0524  .3773  .1765 0.      .0159  .0003
 10 1  50  .5000 2.6667 0.      .3933  .2110  .0021 0.      .0000
TOO FEW POINTS TO PLOT IN CASE  10 1  AXIAL POSITION  25  X/D=  .667
 10 1  25  .1000  .5333  .0876  .2540  .0052  .0006  .3509  .0456
THE FOLLOWING DATA ARE FOR CASE 10 2  AXIAL POSITION 800  X/D=21.333
 10 2 800 -.2000-1.0667  .0255  .3939  .1768  .0047  .0048  .0000
 10 2 800 -.1000 -.5333  .0452  .3796  .1589  .0313  .0052  .0000
 10 2 800 0.     0.      .0567  .3858  .1260  .0450 0.      .0000
 10 2 800  .1000  .5333  .0533  .3783  .1273  .0491  .0131  .0000
 10 2 800  .2000 1.0667  .0429  .3809  .1497  .0232  .0220  .0000
 10 2 800  .3000 1.6000  .0360  .4022  .1403  .0191 0.      .0000
 10 2 800  .4000 2.1333  .0171  .3985  .1715  .0141 0.      .0000
 10 2 800  .5000 2.6667 0.      .4007  .1966 0.      .0020  .0000
THE FOLLOWING DATA ARE FOR CASE 10 2  AXIAL POSITION 600  X/D=16.000
 10 2 600 0.     0.      .0543  .3963  .1027  .0499 0.      .0000

 10 2 600  .1000  .5333  .0598  .3774  .1264  .0556  .0020  .0000
 10 2 600  .2000 1.0667  .0581  .3955  .1089  .0417 0.      .0000
 10 2 600  .3000 1.6000  .0343  .3893  .1600  .0126  .0141  .0000
 10 2 600  .4000 2.1333  .0191  .3888  .1943  .0063  .0018  .0000
TOO FEW POINTS TO PLOT IN CASE  10 2  AXIAL POSITION 500  X/D=13.333
 10 2 500  .1000  .5333  .0729  .3794  .0857  .0674  .0149  .0005
THE FOLLOWING DATA ARE FOR CASE 10 2  AXIAL POSITION 400  X/D=10.667
 10 2 400 0.     0.      .0743  .3910  .0595  .0739 0.      .0007
 10 2 400  .1000  .5333  .0806  .3832  .0737  .0750  .0040  .0010
 10 2 400  .2000 1.0667  .1009  .3435  .1196  .0674  .0249  .0004
 10 2 400  .3000 1.6000  .0451  .3751  .1639  .0329  .0073  .0001
 10 2 400  .4000 2.1333  .0181  .3977  .1727  .0057  .0075  .0001
TOO FEW POINTS TO PLOT IN CASE  10 2  AXIAL POSITION 300  X/D= 8.000
 10 2 300  .1000  .5333  .0861  .3916  .0428  .0737  .0139  .0072
TOO FEW POINTS TO PLOT IN CASE  10 2  AXIAL POSITION 250  X/D= 6.667
 10 2 250  .1000  .5333  .1077  .3794  .0119  .0945 0.      .0268
THE FOLLOWING DATA ARE FOR CASE 10 2  AXIAL POSITION 200  X/D= 5.333
 10 2 200 0.     0.      .1344  .3670  .0032  .0628  .0201  .0450
 10 2 200  .0500  .2667  .1246  .3575  .0027  .0884  .0186  .0508
 10 2 200  .1000  .5333  .1064  .3690  .0098  .0668  .0217  .0572
 10 2 200  .1500  .8000  .0694  .3881  .0228  .0839  .0034  .0437
 10 2 200  .2000 1.0667  .1735  .3398  .0258  .0789  .0170  .0248
 10 2 200  .2500 1.3333  .0717  .3910  .0564  .0737 0.      .0158
 10 2 200  .3000 1.6000  .0754  .3794  .1114  .0484  .0055  .0034
 10 2 200  .4000 2.1333  .0576  .3626  .2008  .0035  .0127  .0002
 10 2 200  .5000 2.6667 0.      .3964  .1966 0.      .0101  .0000
```

TABLE C-2 (Continued). Mass spectrometer and CO data for 440°K initial reactant temperature.

```
 THE FOLLOWING DATA ARE FOR CASE 10 2  AXIAL POSITION 100  X/D= 2.667
 17 2 100 0.     0.       .1143   .3626   .0033   .0213   .0566   .0788
 17 2 100  .0500  .2667   .1106   .3330   .0055   .0152   .1228   .0796
 10 2 100  .0500  .2667   .1166   .3482   .0057   .0312   .0707   .0791
 10 2 100  .1000  .5333   .1654   .3295   .0047   .0145   .0808   .0751
 10 2 100  .1500  .8000   .1147   .3634   .0039   .0427   .0459   .0655
 10 2 100  .2000 1.0667   .0776   .3861   .0224   .0350   .0389   .0535
 10 2 100  .2500 1.3333   .1403   .3405   .0790   .0371   .0320   .0301
 10 2 100  .3000 1.6000   .0613   .3812   .1351   .0250   .0044   .0113
 10 2 100  .4000 2.1333   .0181   .3857   .2022   .0007   .0070   .0011
 10 2 100  .5000 2.6667 0.        .3780   .2168 0.        .0272   .0002
 THE FOLLOWING DATA ARE FOR CASE 17 2  AXIAL POSITION  50  X/D= 1.333
 17 2  50 0.     0.       .0683   .3108   .0183   .0075   .2157   .0680
 17 2  50  .0500  .2667   .0740   .3149   .0200 0.        .2063   .0694
 17 2  50  .1000  .5333   .0883   .3226   .0136 0.        .1823   .0702
 17 2  50  .1500  .8000   .0924   .3282   .0217   .0246   .1528   .0517
 17 2  50  .2000 1.0667   .0651   .3336   .0658   .0590   .0899   .0523
 17 2  50  .2500 1.3333   .0445   .3904   .0902   .0244   .0317   .0277
 17 2  50  .3000 1.6000   .0504   .3808   .1577   .0158   .0141   .0010
 17 2  50  .4000 2.1333   .0142   .3801   .1981 0.        .0272   .0008
 TOO FEW POINTS TO PLOT IN CASE  17 2  AXIAL POSITION  25  X/D=  .667
 17 2  25  .0500  .2667   .0667   .2673   .0161 0.        .3450   .0373
 THE FOLLOWING DATA ARE FOR CASE 17 3  AXIAL POSITION 800  X/D=21.333
 17 3 800 -.2000-1.0667   .0367   .3697   .1984   .0208   .0042   .0001
 17 3 800 -.1000 -.5333   .0387   .3874   .1489   .0318   .0052   .0001
 17 3 800 0.     0.       .0472   .3840   .1509   .0314   .0021   .0001
 17 3 800  .1000  .5333   .0458   .3814   .1569   .0319   .0022   .0001

 17 3 800  .2000 1.0667   .0319   .3975   .1424   .0304 0.        .0001
 17 3 800  .3000 1.6000   .0190   .3827   .2027   .0085   .0039   .0001
 17 3 800  .4000 2.1333   .0124   .3795   .2164 0.        .0120   .0001
 17 3 800  .8000 4.2667   .0073   .3802   .2263 0.        .0057   .0000
 THE FOLLOWING DATA ARE FOR CASE 17 3  AXIAL POSITION 600  X/D=16.000
 17 3 600 -.2000-1.0667   .0367   .3866   .1657   .0207   .0031   .0001
 17 3 600 -.1000 -.5333   .0471   .3782   .1524   .0381   .0053   .0002
 17 3 600 0.     0.       .0691   .3628   .1592   .0378   .0079   .0001
 17 3 600  .1000  .5333   .0544   .3737   .1494   .0305   .0177   .0001
 17 3 600  .2000 1.0667   .0358   .3834   .1727   .0243 0.        .0001
 17 3 600  .3000 1.6000   .0160   .3064   .1990   .0096   .0021   .0002
 17 3 600  .4000 2.1333   .0104   .3862   .2073 0.        .0055   .0001
 17 3 600  .5000 2.6667   .0105   .3928   .2007 0.        .0027   .0001
 TOO FEW POINTS TO PLOT IN CASE  17 3  AXIAL POSITION 500  X/D=13.333
 17 3 500 0.     0.       .0609   .3751   .1253   .0455   .0173   .0001
 THE FOLLOWING DATA ARE FOR CASE 17 3  AXIAL POSITION 400  X/D=10.667
 17 3 400 -.2000-1.0667   .0484   .3747   .1684   .0335 0.        .0002
 17 3 400 -.1000 -.5333   .0737   .3619   .1421   .0499   .0100   .0002
 17 3 400 0.     0.       .0882   .3637   .1143   .0597   .0099   .0001
 17 3 400 0.     0.       .0680   .3719   .1114   .0668   .0095   .0001
 17 3 400  .1000  .5333   .0632   .3857   .1091   .0522   .0036   .0001
 17 3 400  .2000 1.0667   .0523   .3788   .1585   .0312 0.        .0002
 17 3 400  .3000 1.6000   .0245   .3773   .1981   .0145   .0080   .0002
 17 3 400  .4000 2.1333   .0154   .3755   .2225 0.        .0107   .0002
```

TABLE C-2 (Continued). **Mass spectrometer and CO data for 440°K initial reactant temperature.**

```
 TOO FEW POINTS TO PLOT IN CASE  17 3  AXIAL POSITION 300  X/D= 8.000
  17 3 300  .3000 1.6000  .0804  .3711  .1040  .0651  .0020  .0005
  17 3 300 0.     0.      .0739  .3809  .0941  .0678  .0021  .0006
 THE FOLLOWING DATA AFE FOR CASE 17 3  AXIAL POSITION 200  X/D= 5.333
  17 3 200 -.1000 -.5333  .0935  .3798  .0786  .0642  .0036  .0059

  17 3 200 0.     0.      .1021  .3610  .0750  .0907  .0099  .0064
  17 3 200 0.     0.      .1091  .3643  .0553  .0884  .0101  .0061
  17 3 200  .1000  .5333  .0939  .3781  .0628  .0796  .0067  .0059
  17 3 200  .2000 1.0667  .0992  .3518  .1349  .0457  .0161  .0026
  17 3 200  .3000 1.6000  .0560  .3705  .1799  .0227 0.      .0007
  17 3 200  .4000 2.1333  .0184  .3890  .1977 0.      .0053  .0002
 TOO FEW POINTS TO PLOT IN CASE  17 3  AXIAL POSITION 150  X/D= 4.000
  17 3 150 0.     0.      .0744  .3790  .0226  .0937 0.      .0509
 THE FOLLOWING DATA AFE FOR CASE 17 3  AXIAL POSITION 100  X/D= 2.667
  17 3 100 -.1000 -.5333  .0658  .3748  .0502  .0706  .0128  .0504
  17 3 100 -.0500 -.2667  .0639  .3830  .0316  .0765  .0157  .0459
  17 3 100 0.     0.      .0913  .3616  .0205  .0840  .0397  .0409
  17 3 100  .0500  .2667  .0621  .3867  .0248  .0807  .0127  .0460
  17 3 100  .1000  .5333  .0710  .3736  .0423  .0696  .0192  .0502
  17 3 100  .1500  .8000  .0620  .3849  .0557  .0645  .0054  .0422
  17 3 100  .2000 1.0667  .0751  .3612  .1066  .0486  .0140  .0330
  17 3 100  .2500 1.3333  .0478  .3680  .1515  .0322  .0129  .0190
  17 3 100  .3000 1.6000  .0651  .3550  .1977  .0110  .0158  .0077
  17 3 100  .4000 2.1333  .0589  .3661  .2008  .0018  .0056  .0014
  17 3 100  .5000 2.6667  .0512  .3638  .2137 0.      .0068  .0005
  17 3 100  .8000 4.2667  .0445  .3724  .2087 0.      .0019  .0000
 TOO FEW POINTS TO PLOT IN CASE  17 3  AXIAL POSITION  75  X/D= 2.000
  17 3  75 0.     0.      .0537  .3437  .1596  .0005  .0443  .0539
 THE FOLLOWING DATA AFE FOR CASE 17 3  AXIAL POSITION  50  X/D= 1.333
  17 3  50 -.1000 -.5333  .0672  .3529  .0787  .0248  .0510  .0718
  17 3  50 -.0500 -.2667  .0884  .3562  .0468  .0404  .0443  .0665
  17 3  50 0.     0.      .0858  .3611  .0332  .0278  .0676  .0631
  17 3  50  .0500  .2667  .0621  .3736  .0276  .0371  .0570  .0685
  17 3  50  .1000  .5333  .0812  .3658  .0413  .0334  .0412  .0707
  17 3  50  .1500  .8000  .0612  .3844  .0640  .0325  .0194  .0535
  17 3  50  .2000 1.0667  .0642  .3445  .1475  .0246  .0389  .0352
  17 3  50  .2500 1.3333  .0467  .3676  .1700  .0162  .0121  .0191
  17 3  50  .3000 1.6000  .0324  .3839  .1870  .0080  .0045  .0074
  17 3  50  .4000 2.1333  .0524  .3740  .1883 0.      .0110  .0014
  17 3  50  .5000 2.6667  .0524  .3651  .2031 0.      .0140  .0002
 TOO FEW POINTS TO PLOT IN CASE  17 3  AXIAL POSITION  25  X/D=  .667
  17 3  25 0.     0.      .0548  .3051  .1478 0.      .1207  .0662
```

TABLE C-3. Mass spectrometer and CO data for 550°K initial reactant temperature.

```
DAY HW X    R        R/A   H2O    N2/2    O2    CO2    C3H8    CO
THE FOLLOWING DATA ARE FOR CASE 14 1  AXIAL POSITION 800  X/D=21.333
 14 1 800 -.1000 -.5333  .0306  .3853  .1756  .0228 0.       .0000
 14 1 800-0.      0.     .0338  .3707  .1744  .0500 0.       .0000
 14 1 800  .1000  .5333  .0342  .3811  .1432  .0485  .0114  .0000
 14 1 800  .2000 1.0667  .0440  .3763  .1536  .0443  .0052  .0000
 14 1 800  .3000 1.6000  .0348  .3718  .1882  .0289  .0042  .0000
 14 1 800  .4000 2.1333  .0220  .3712  .2167  .0155  .0030  .0000
 14 1 800  .5000 2.6667  .0146  .3916  .1966  .0053 0.       .0000
THE FOLLOWING DATA ARE FOR CASE 14 1  AXIAL POSITION 600  X/D=16.000
 14 1 600 -.2000-1.0667  .0190  .3841  .2027  .0080  .0018  .0000
 14 1 600 -.1000 -.5333  .0225  .3888  .1662  .0330 0.       .0000
 14 1 600-0.      0.     .0400  .3862  .1429  .0418  .0023  .0000
 14 1 600  .1000  .5333  .0579  .3733  .1271  .0644  .0036  .0000
 14 1 600  .2000 1.0667  .0569  .3760  .1306  .0576  .0025  .0000
 14 1 600  .3000 1.6000  .0512  .3872  .1330  .0384  .0023  .0000
 14 1 600  .4000 2.1333  .0235  .3802  .1958  .0198  .0001  .0000
 14 1 600  .5000 2.6667  .0157  .3765  .2240  .0050  .0018  .0000
TOO FEW POINTS TO PLOT IN CASE  14 1  AXIAL POSITION 500  X/D=13.333
 14 1 500  .1000  .5333  .0880  .3519  .1194  .0645  .0239  .0005
THE FOLLOWING DATA ARE FOR CASE 14 1  AXIAL POSITION 400  X/D=10.667
 14 1 400 -.2000-1.0667  .0174  .3811  .2074  .0045  .0079  .0010
 14 1 400 -.1000 -.5333  .0456  .3810  .1612  .0296  .0011  .0010
 14 1 400 0.      0.     .0626  .3797  .0988  .0674  .0114  .0009
 14 1 400  .1000  .5333  .0876  .3802  .0693  .0739  .0086  .0010
 14 1 400  .2000 1.0667  .0901  .3687  .0899  .0823 0.       .0010
 14 1 400  .3000 1.6000  .0632  .3804  .1261  .0452  .0040  .0003
 14 1 400  .4000 2.1333  .0402  .3786  .1691  .0150  .0183  .0001
 14 1 400  .5000 2.6667  .0156  .3880  .2003 0.       .0077  .0000
TOO FEW POINTS TO PLOT IN CASE  14 1  AXIAL POSITION 300  X/D= 8.000
 14 1 300  .1000  .5333  .0790  .3859  .0394  .1093 0.       .0059
TOO FEW POINTS TO PLOT IN CASE  14 1  AXIAL POSITION 250  X/D= 6.667
 14 1 250  .1000  .5333  .0812  .3832  .0235  .0876  .0150  .0257
THE FOLLOWING DATA ARE FOR CASE 14 1  AXIAL POSITION 200  X/D= 5.333
 14 1 200 -.1000 -.5333  .0616  .3633  .0760  .0540  .0123  .0689
 14 1 200 0.      0.     .0721  .3939  .0096  .0771  .0116  .0412
 14 1 200  .0500  .2667  .1494  .3640  .0021  .0659  .0032  .0510
 14 1 200  .1000  .5333  .0645  .3750 0.      .0963  .0203  .0687
 14 1 200  .1500  .8000  .1530  .3611  .0012  .0707 0.       .0525
 14 1 200  .2000 1.0667  .0641  .3865  .0151  .0944  .0056  .0474
 14 1 200  .2500 1.3333  .0471  .3993  .0428  .0778 0.       .0333
 14 1 200  .3000 1.6000  .0593  .3659  .1262  .0425  .0285  .0113
 14 1 200  .3500 1.8667  .0530  .3659  .1741  .0285  .0120  .0060
 14 1 200  .4000 2.1333  .0547  .3725  .1771  .0055  .0172  .0010
 14 1 200  .5000 2.6667  .0523  .3733  .1908 0.       .0100  .0001
 14 1 200  .9000 4.8000  .0504  .3728  .1992 0.       .0045  .0000
TOO FEW POINTS TO PLOT IN CASE  14 1  AXIAL POSITION 150  X/D= 4.000
 14 1 150  .1000  .5333  .1870  .3478  .0033  .0240  .0270  .0626
THE FOLLOWING DATA ARE FOR CASE 14 1  AXIAL POSITION 100  X/D= 2.667
 14 1 100 0.      0.     .0956  .3667  .0209  .0410  .0423  .0664
 14 1 100  .0500  .2667  .1293  .3656  .0023  .0248  .0449  .0670
 14 1 100  .1000  .5333  .1350  .3571  .0030  .0161  .0606  .0706
 14 1 100  .1500  .8000  .0844  .3712  .0150  .0415  .0420  .0742
 14 1 100  .2000 1.0667  .0752  .3689  .0340  .0451  .0332  .0742
 14 1 100  .2500 1.3333  .1169  .3401  .0774  .0130  .0625  .0495
 14 1 100  .3000 1.6000  .0743  .3583  .1392  .0232  .0173  .0289
 14 1 100  .4000 2.1333  .0422  .3835  .1760  .0042  .0102  .0041
 14 1 100  .5000 2.6667  .0168  .3780  .2221 0.       .0045  .0003
```

TABLE C-3 (Continued). Mass spectrometer and CO data for 550°K initial reactant temperature.

```
 THE FOLLOWING DATA ARE FOR CASE 14 1  AXIAL POSITION  50  X/D= 1.333
  14 1  50 0.      0.       .1534  .3263  .0471  .0560  .0396  .0508
  14 1  50  .0500  .2667   .1082  .3462  .0159  .0060  .1146  .0624
  14 1  50  .1000  .5333   .0838  .3655  .0066  .0022  .1076  .0684
  14 1  50  .1500  .8000   .1596  .3245  .0081  .0258  .0943  .0628
  14 1  50  .2000 1.0667   .1230  .3381  .0338  .0356  .0656  .0655
  14 1  50  .2500 1.3333   .0915  .3603  .0641  .0282  .0478  .0472
  14 1  50  .3000 1.6000   .0576  .3799  .1087  .0275  .0174  .0283
  14 1  50  .4000 2.1333   .0269  .3695  .2102 0.       .0238  .0026
  14 1  50  .5000 2.6667   .0463  .3643  .2183 0.       .0063  .0001
 TOO FEW POINTS TO PLOT IN CASE  14 1  AXIAL POSITION  25  X/D=  .667
  14 1  25  .1000  .5333   .0956  .2739  .0151  .0005  .2862  .0543
 THE FOLLOWING DATA ARE FOR CASE 14 2  AXIAL POSITION 800  X/D=21.333
  14 2 800 -.1000 -.5333  .0290  .3748  .1932  .0058  .0221  .0000
  14 2 800 0.      0.      .0422  .3771  .1567  .0286  .0179  .0000
  14 2 800  .1000  .5333  .0451  .3787  .1539  .0232  .0200  .0000
  14 2 800  .2000 1.0667  .0482  .3712  .1710  .0368  .0011  .0000
  14 2 800  .3000 1.6000  .0276  .3793  .1786  .0065  .0282  .0000
  14 2 800  .4000 2.1333  .0125  .3885  .1974  .0007  .0119  .0000
 THE FOLLOWING DATA ARE FOR CASE 14 2  AXIAL POSITION 600  X/D=16.000
  14 2 600 -.1000 -.5333  .0382  .3847  .1676  .0204  .0049  .0000
  14 2 600 0.      0.      .0481  .3863  .1254  .0357  .0179  .0000
  14 2 600  .1000  .5333  .0518  .3894  .1181  .0356  .0155  .0000
  14 2 600  .2000 1.0667  .0536  .3559  .1691  .0331  .0319  .0000
  14 2 600  .3000 1.6000  .0292  .3862  .1707  .0170  .0104  .0000
  14 2 600  .4000 2.1333  .0223  .3049  .1950  .0125 0.      .0000
 TOO FEW POINTS TO PLOT IN CASE  14 2  AXIAL POSITION 500  X/D=13.333
  14 2 500  .1000  .5333  .0649  .3763  .1164  .0469  .0178  .0004
 THE FOLLOWING DATA ARE FOR CASE 14 2  AXIAL POSITION 400  X/D=10.667
  14 2 400 -.1000 -.5333  .0428  .3910  .1437  .0222  .0086  .0003
  14 2 400 0.      0.      .0647  .3771  .1192  .0420  .0197  .0005
  14 2 400  .1000  .5333  .0948  .3704  .0880  .0760 0.      .0009
  14 2 400  .2000 1.0667  .0916  .3697  .1034  .0431  .0221  .0005
  14 2 400  .3000 1.6000  .0628  .3698  .1468  .0151  .0350  .0001
  14 2 400  .4000 2.1333  .0314  .3626  .2145 0.      .0286  .0000
  14 2 400  .5000 2.6667  .0175  .3977  .1833 0.      .0036  .0000
 TOO FEW POINTS TO PLOT IN CASE  14 2  AXIAL POSITION 300  X/D= 8.000
  14 2 300  .1000  .5333  .0773  .3872  .0527  .0821  .0131  .0034
 THE FOLLOWING DATA ARE FOR CASE 14 2  AXIAL POSITION 200  X/D= 5.333
  14 2 200 0.      0.      .0789  .3740  .0319  .0698  .0214  .0496
  14 2 200  .1000  .5333  .0598  .3771  .0224  .0906  .0166  .0560
  14 2 200  .2000 1.0667  .0908  .3516  .0592  .0901  .0254  .0308
  14 2 200  .3000 1.6000  .0599  .3821  .1280  .0328  .0145  .0047
  14 2 200  .4000 2.1333  .0229  .4023  .1658  .0055  .0010  .0003
  14 2 200  .5000 2.6667  .0117  .3881  .2038  .0050  .0026  .0000
 TOO FEW POINTS TO PLOT IN CASE  14 2  AXIAL POSITION 150  X/D= 4.000
  14 2 150  .1000  .5333  .0929  .3719  .0011  .0788  .0258  .0571
 THE FOLLOWING DATA ARE FOR CASE 14 2  AXIAL POSITION 100  X/D= 2.667
  14 2 100 0.      0.      .1097  .3491  .0263  .0646  .0241  .0766
  14 2 100  .0500  .2667  .0960  .3672  .0107  .0445  .0356  .0785
  14 2 100  .1000  .5333  .1393  .3301  .0151  .0305  .0633  .0752
  14 2 100  .1500  .8000  .1172  .3633  .0290  .0488  .0251  .0530
  14 2 100  .2000 1.0667  .0727  .3829  .0514  .0473  .0292  .0331
  14 2 100  .2500 1.3333  .0756  .3695  .0996  .0437  .0166  .0250
  14 2 100  .3000 1.6000  .0749  .3570  .1552  .0241  .0135  .0178
  14 2 100  .4000 2.1333  .0733  .3524  .1928  .0010  .0276  .0026
  14 2 100  .5000 2.6667  .0649  .3568  .2084 0.      .0126  .0002
```

TABLE C-3 (Continued). Mass spectrometer and CO data for 550°K initial reactant temperature.

```
TOO FEW POINTS TO PLOT IN CASE  14 2  AXIAL POSITION  75  X/D= 2.000
 14 2  75  .1000  .5333  .1247  .3513  .0091  .0198  .0759  .0674
THE FOLLOWING DATA ARE FOR CASE 14 2  AXIAL POSITION  50  X/D= 1.333
 14 2  50 0.      0.     .0860  .3612  .0450  .0335  .0467  .0640
 14 2  50  .0500  .2667  .1020  .3187  .0332  .0079  .1516  .0673
 14 2  50  .1000  .5333  .0932  .3201  .0276  .0079  .1578  .0727
 14 2  50  .1500  .8000  .1523  .3465  .0197  .0195  .0642  .0509
 14 2  50  .2000 1.0667  .1300  .3638  .0473  .0097  .0514  .0335
 14 2  50  .2500 1.3333  .0862  .3699  .0886  .0218  .0367  .0265
 14 2  50  .3000 1.6000  .0564  .3803  .1325  .0094  .0210  .0197
 14 2  50  .3500 1.8667  .0336  .3746  .1752 0.      .0310  .0106
 14 2  50  .4000 2.1333  .0292  .3832  .1855  .0001  .0187  .0014
 14 2  50  .5000 2.6667  .0221  .3839  .1848 0.      .0249  .0001
TOO FEW POINTS TO PLOT IN CASE  14 2  AXIAL POSITION  25  X/D=  .667
 14 2  25  .1000  .5333  .1150  .2530  .0218 0.      .2992  .0575
THE FOLLOWING DATA ARE FOR CASE 14 3  AXIAL POSITION 800  X/D=21.333
 14 3 800 -.1000 -.5333  .0400  .3781  .1806  .0130  .0097  .0001
 14 3 800 0.     0.      .0394  .3659  .1798  .0263  .0221  .0000
 14 3 800  .1000  .5333  .0482  .3823  .1444  .0410  .0015  .0001
 14 3 800  .2000 1.0667  .0464  .3780  .1683  .0150  .0140  .0001
 14 3 800  .3000 1.6000  .0286  .3852  .1737  .0162  .0105  .0001
 14 3 800  .4000 2.1333  .0255  .3634  .2306  .0042  .0124  .0000
 14 3 800  .5000 2.6667  .0151  .3750  .2126 0.      .0219  .0000
THE FOLLOWING DATA ARE FOR CASE 14 3  AXIAL POSITION 600  X/D=16.000
 14 3 600 -.1000 -.5333  .0338  .3664  .1978  .0106  .0247  .0001
 14 3 600 0.     0.      .0499  .3910  .1294  .0268  .0115  .0000

 14 3 600  .1000  .5333  .0577  .3720  .1471  .0181  .0326  .0001
 14 3 600  .2000 1.0667  .0430  .3788  .1604  .0266  .0116  .0001
 14 3 600  .3000 1.6000  .0242  .3880  .1749  .0121  .0121  .0001
 14 3 600  .4000 2.1333  .0243  .3773  .2061  .0040  .0104  .0000
 14 3 600  .5000 2.6667  .0181  .3825  .2122  .0006  .0026  .0000
TOO FEW POINTS TO PLOT IN CASE  14 3  AXIAL POSITION 500  X/D=13.333
 14 3 500 0.     0.      .0558  .3823  .1371  .0261  .0161  .0001
THE FOLLOWING DATA ARE FOR CASE 14 3  AXIAL POSITION 400  X/D=10.667
 14 3 400 -.1000 -.5333  .0396  .3802  .1710  .0190  .0099  .0002
 14 3 400 0.     0.      .0628  .3767  .1291  .0444  .0099  .0002
 14 3 400  .1000  .5333  .0783  .3623  .1258  .0544  .0162  .0002
 14 3 400  .2000 1.0667  .0661  .3791  .1200  .0463  .0089  .0001
 14 3 400  .3000 1.6000  .0491  .3776  .1623  .0171  .0158  .0001
 14 3 400  .4000 2.1333  .0282  .3857  .1904  .0077  .0021  .0001
```

TABLE C-3 (Continued). Mass spectrometer and CO data for 550°K initial reactant temperature.

```
TOO FEW POINTS TO PLOT IN CASE  14 3  AXIAL POSITION 300  X/D= 8.000
 14 3 300  .1000  .5333  .0628  .3953  .0783  .0623  .0055  .0012
THE FOLLOWING DATA AFE FOR CASE 14 3  AXIAL POSITION 200  X/D= 5.333
 14 3 200 -.1000 -.5333  .0722  .3477  .1711  .0303  .0303  .0082
 14 3 200 0.     0.      .0754  .3776  .0714  .0808  .0073  .0093
 14 3 200  .1000  .5333  .0903  .3707  .0497  .0874  .0306  .0082
 14 3 200  .2000 1.0667  .0922  .3732  .0792  .0649  .0170  .0022
 14 3 200  .3000 1.6000  .0499  .3942  .1348  .0251  .0015  .0004
 14 3 200  .4000 2.1333  .0212  .3424  .2596  .0007  .0331  .0001
TOO FEW POINTS TO PLOT IN CASE  14 3  AXIAL POSITION 140  X/D= 3.733
 14 3 140  .1000  .5333  .0816  .3688  .0278  .0884  .0230  .0413
TOO FEW POINTS TO PLOT IN CASE  14 3  AXIAL POSITION 150  X/D= 4.000
 14 3 150 0.     0.      .0221  .3816  .1736  .0009  .0026  .0372
THE FOLLOWING DATA AFE FOR CASE 14 3  AXIAL POSITION 100  X/D= 2.667
 14 3 100 -.1000 -.5333  .0572  .3494  .1189  .0427  .0236  .0584
 14 3 100 -.0500 -.2667  .0546  .3708  .0638  .0533  .0057  .0605
 14 3 100 0.     0.      .0711  .3683  .0481  .0463  .0363  .0610
 14 3 100  .0500  .2667  .0867  .3829  .0143  .0500  .0241  .0584
 14 3 100  .1000  .5333  .1153  .3750  .0150  .0589  .0055  .0549
 14 3 100  .1500  .8000  .0744  .3737  .0398  .0569  .0402  .0407
 14 3 100  .2000 1.0667  .0686  .3859  .0684  .0457  .0213  .0236
 14 3 100  .2500 1.3333  .0645  .3849  .0937  .0443  .0132  .0140
 14 3 100  .3000 1.6000  .0638  .3843  .1386  .0231  .0055  .0046
 14 3 100  .3500 1.8667  .0615  .3745  .1608  .0070  .0211  .0030
 14 3 100  .4000 2.1333  .0573  .3589  .2035 0.      .0211  .0010
TOO FEW POINTS TO PLOT IN CASE  14 3  AXIAL POSITION  75  X/D= 2.000
 14 3  75  .1000  .5333  .1168  .3541  .0228  .0340  .0543  .0636
THE FOLLOWING DATA AFE FOR CASE 14 3  AXIAL POSITION  50  X/D= 1.333
 14 3  50 0.     0.      .0853  .3680  .0571  .0348  .0181  .0683
 14 3  50  .0500  .2667  .0766  .3635  .0474  .0358  .0393  .0734
 14 3  50  .1000  .5333  .0746  .3689  .0162  .0217  .0710  .0782
 14 3  50  .1500  .8000  .0593  .3874  .0352  .0219  .0482  .0602
 14 3  50  .2000 1.0667  .0654  .3796  .0672  .0359  .0409  .0308
 14 3  50  .2500 1.3333  .0646  .3645  .1247  .0144  .0491  .0178
 14 3  50  .3500 1.8667  .0390  .3908  .1630  .0141  .0021  .0030
 14 3  50  .3000 1.6000  .0495  .3718  .1715  .0137  .0211  .0046
 14 3  50  .4000 2.1333  .0280  .3799  .1944 0.      .0173  .0007
 14 3  50  .5000 2.6667  .0127  .3909  .1980 0.      .0073  .0001
TOO FEW POINTS TO PLOT IN CASE  14 3  AXIAL POSITION  25  X/D=  .667
 14 3  25  .1000  .5333  .0645  .3617  .0251  .0302  .0778  .0786
```

APPENDIX D

NO_x and Temperature Data

Selected results and comparisons of NO, NO_2, NO_x, and temperature for various operating conditions were presented in Chapter 4. This appendix presents the complete set of the NO_x and temperature data collected. Figures D-1 to D-3 present centerline distributions of total NO_x and temperature for the nine experimental conditions and Figs. D-4 through D-12 show the radial profiles for these same species. Figures D-13 to D-24 give the NO and NO_2 data for these same conditions. All of the data represent mean values as measured.

The legends used are consistent for all radial and all centerline profiles. For the centerline profiles:

○ - T = 300°K
□ - T = 450°K
△ - T = 550°K ;

while for the radial profiles:

◊ - X/D = 1.33
○ - X/D = 2.66
□ - X/D = 5.33
△ - X/D = 10.66
▽ - X/D = 16.00
◇ - X/D = 21.33 .

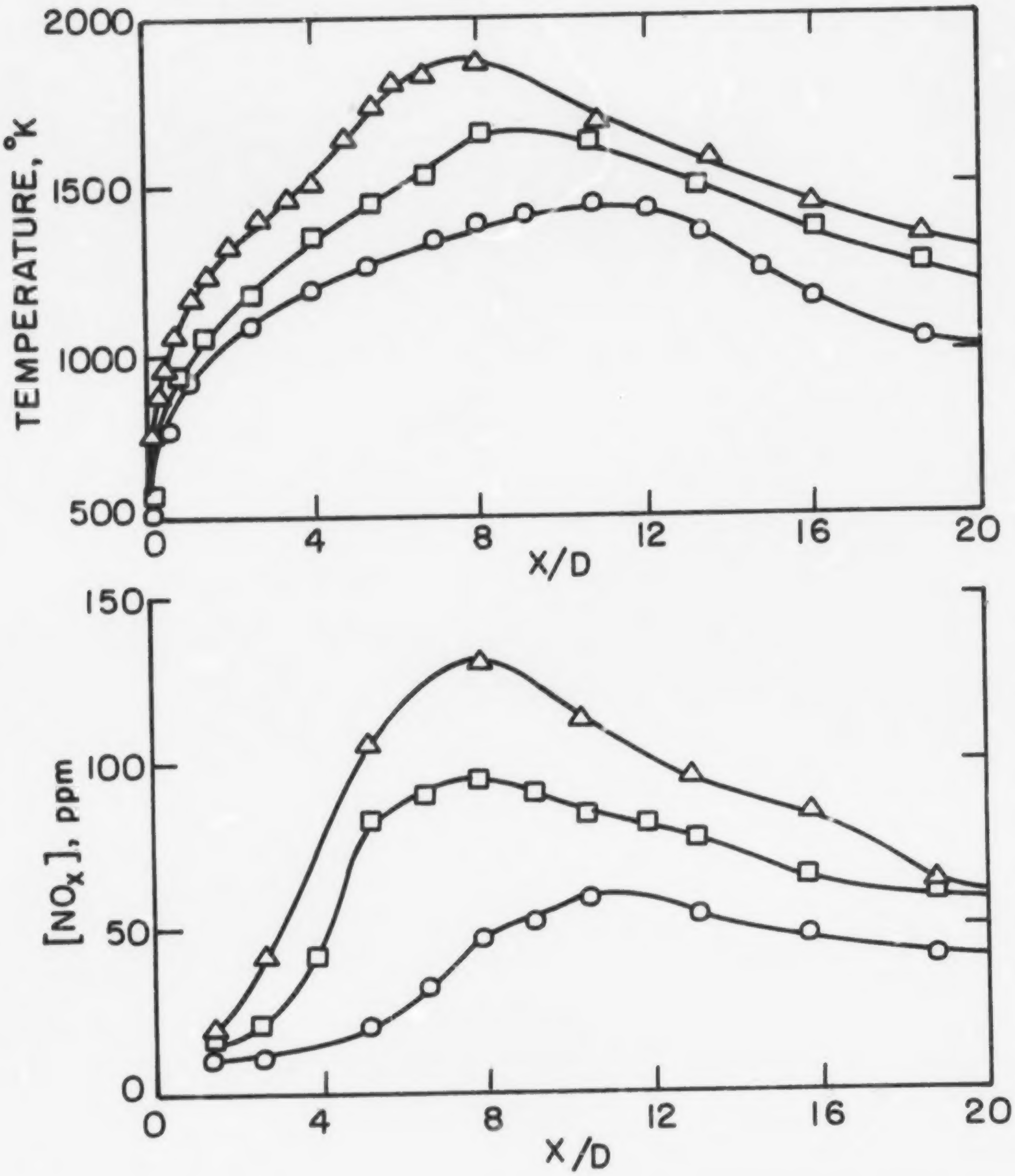

Figure D-1. Centerline distributions of temperature and oxides of nitrogen for different initial reactant temperatures at $V_A/V_F = 45$.

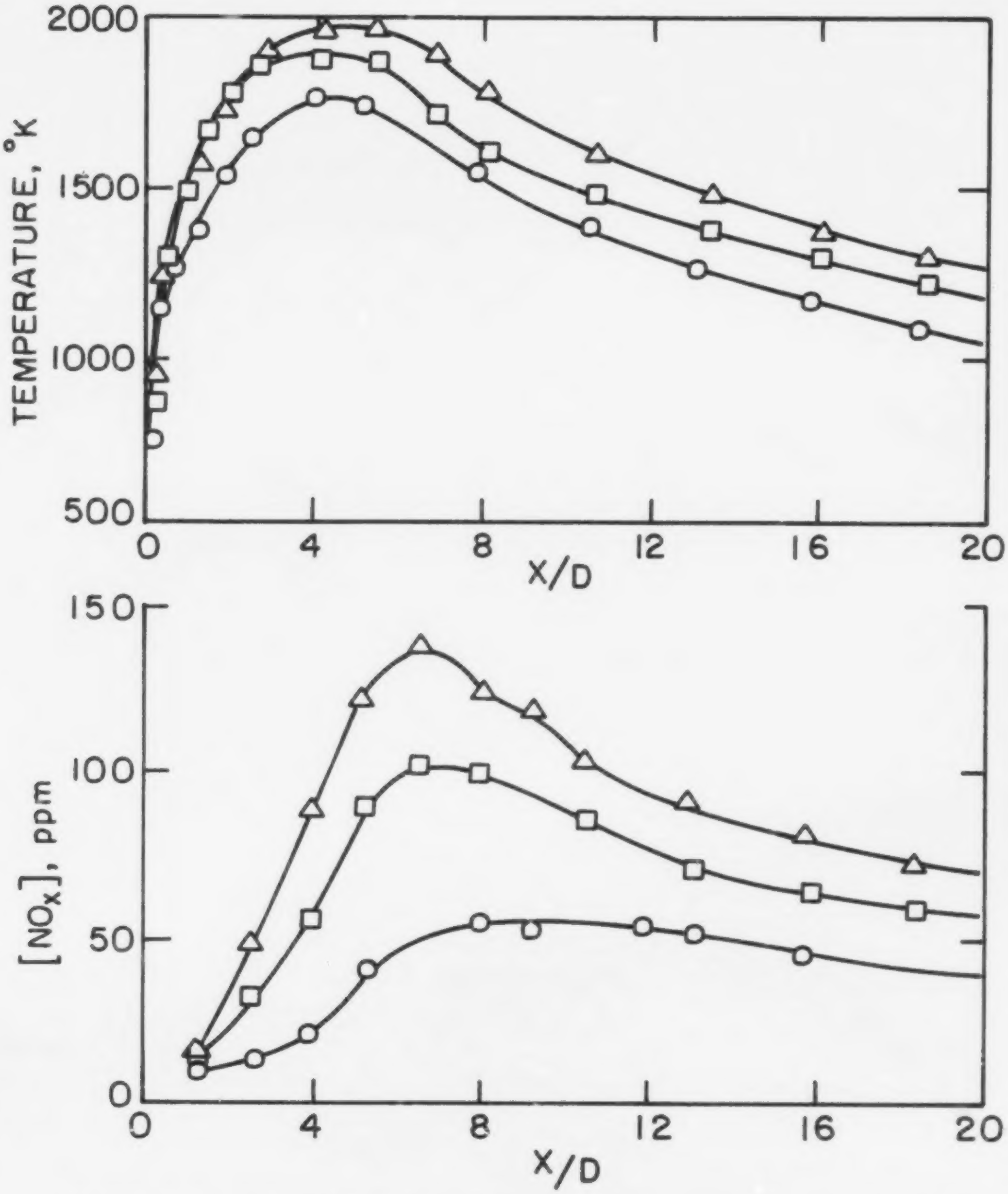

Figure D-2. Centerline distributions of temperature and oxides of nitrogen for different initial reactant temperatures at $V_A/V_F = 61$.

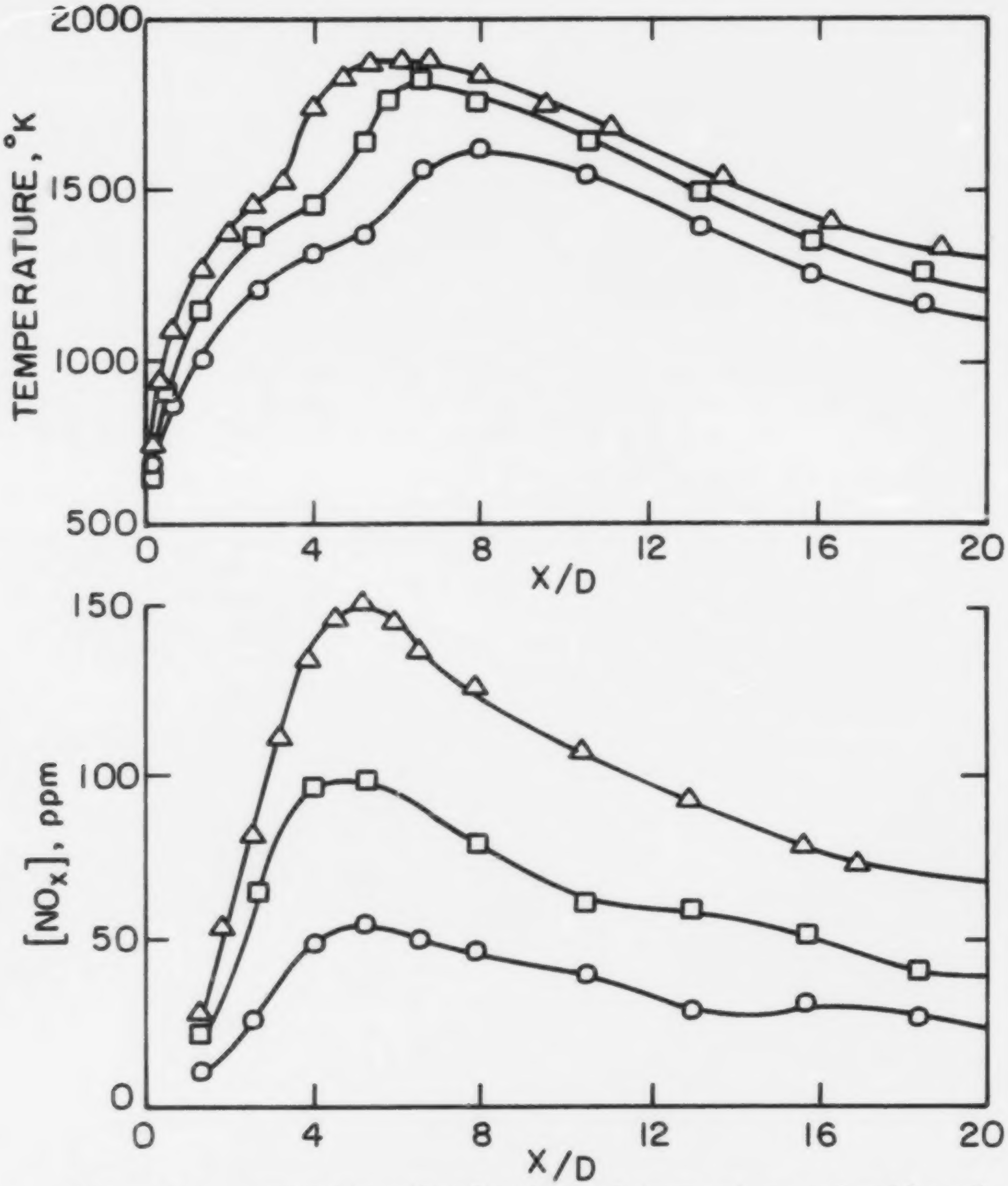

Figure D-3. Centerline distributions of temperature and oxides of nitrogen for different initial reactant temperatures at $V_A/V_F = 75$.

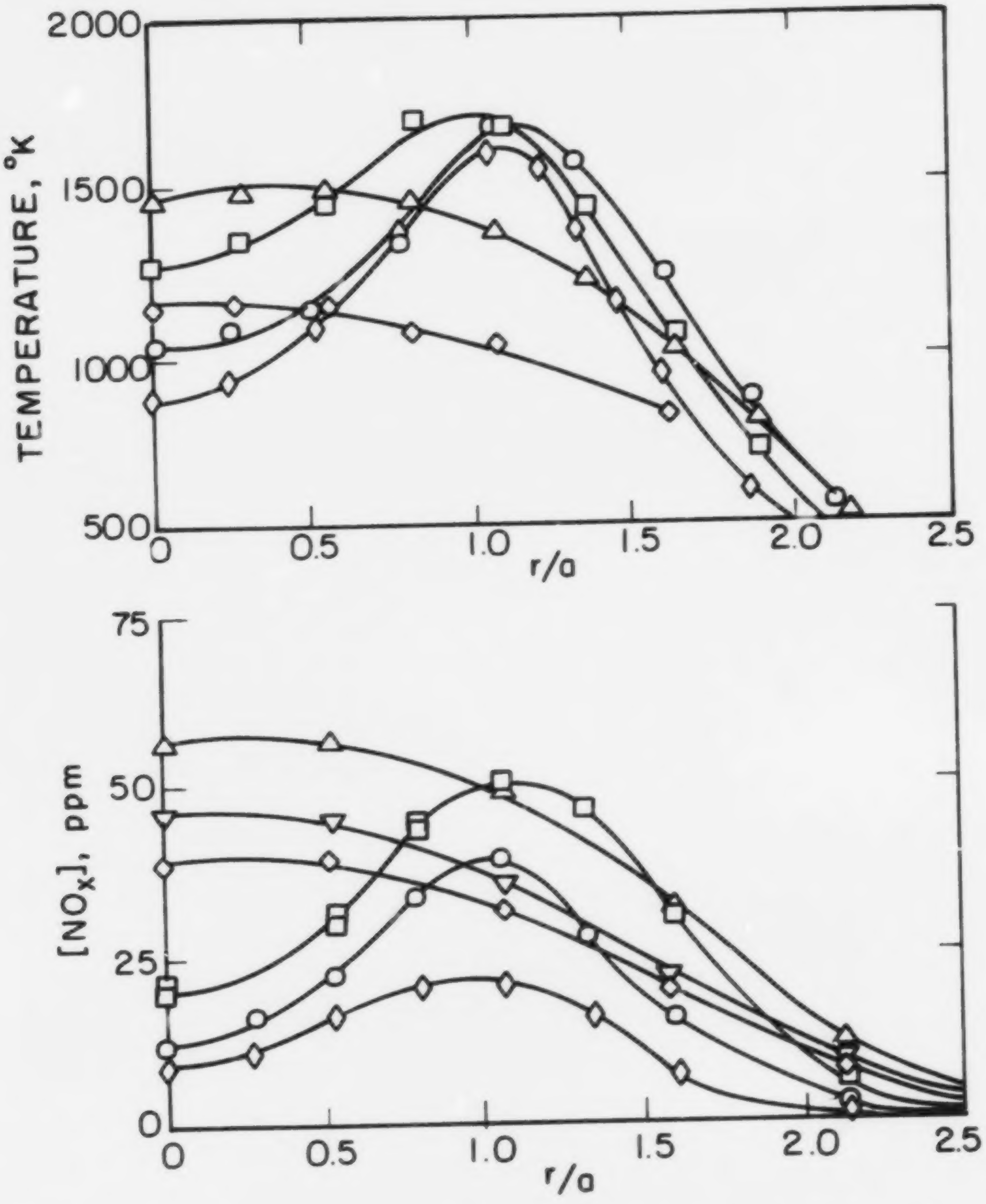

Figure D-4. Radial distributions of temperature and oxides of nitrogen at V_A/V_F = 45 and 300°K initial reactant temperature.

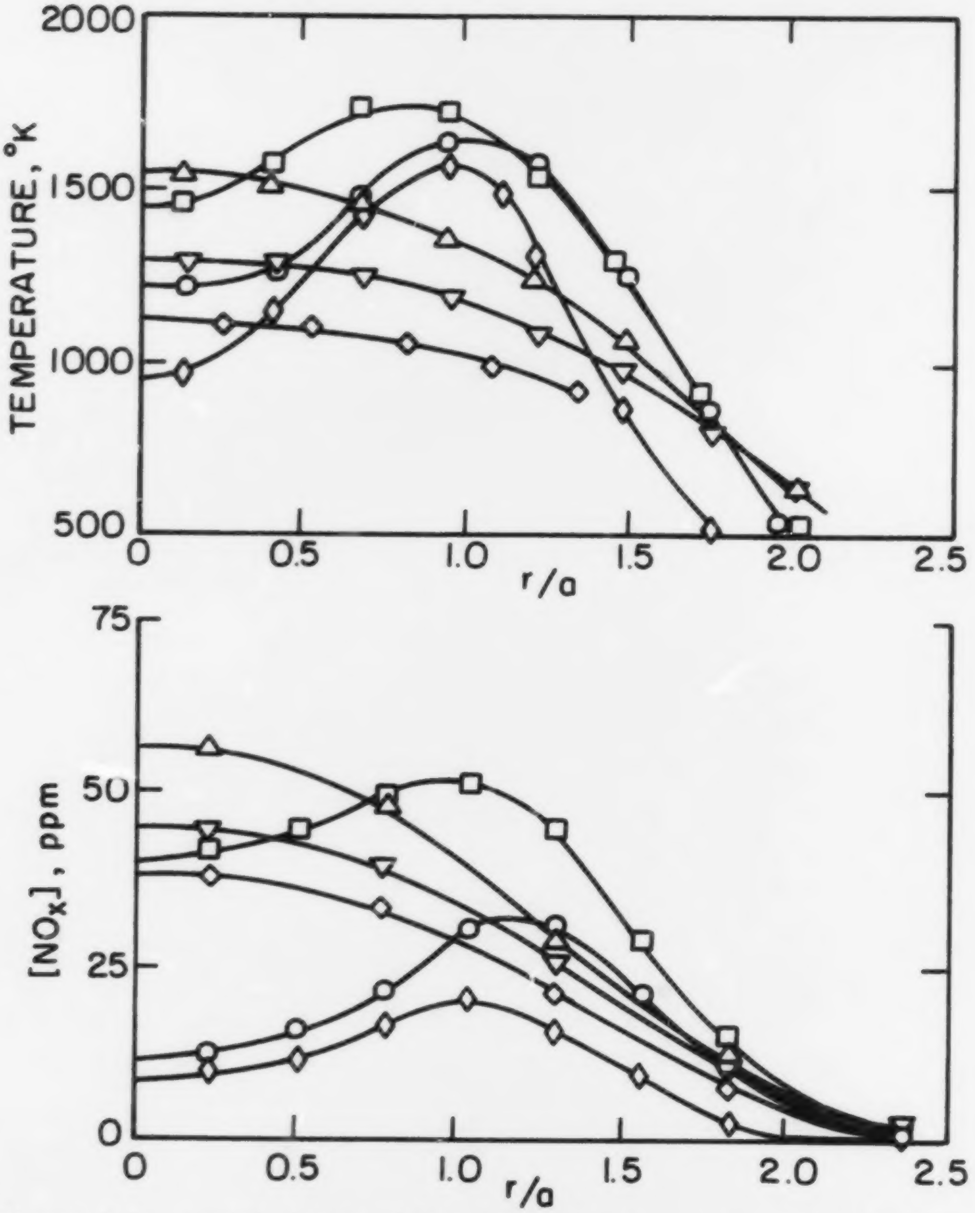

Figure D-5. Radial distributions of temperature and oxides of nitrogen at V_A/V_F = 61 and 300°K initial reactant temperature.

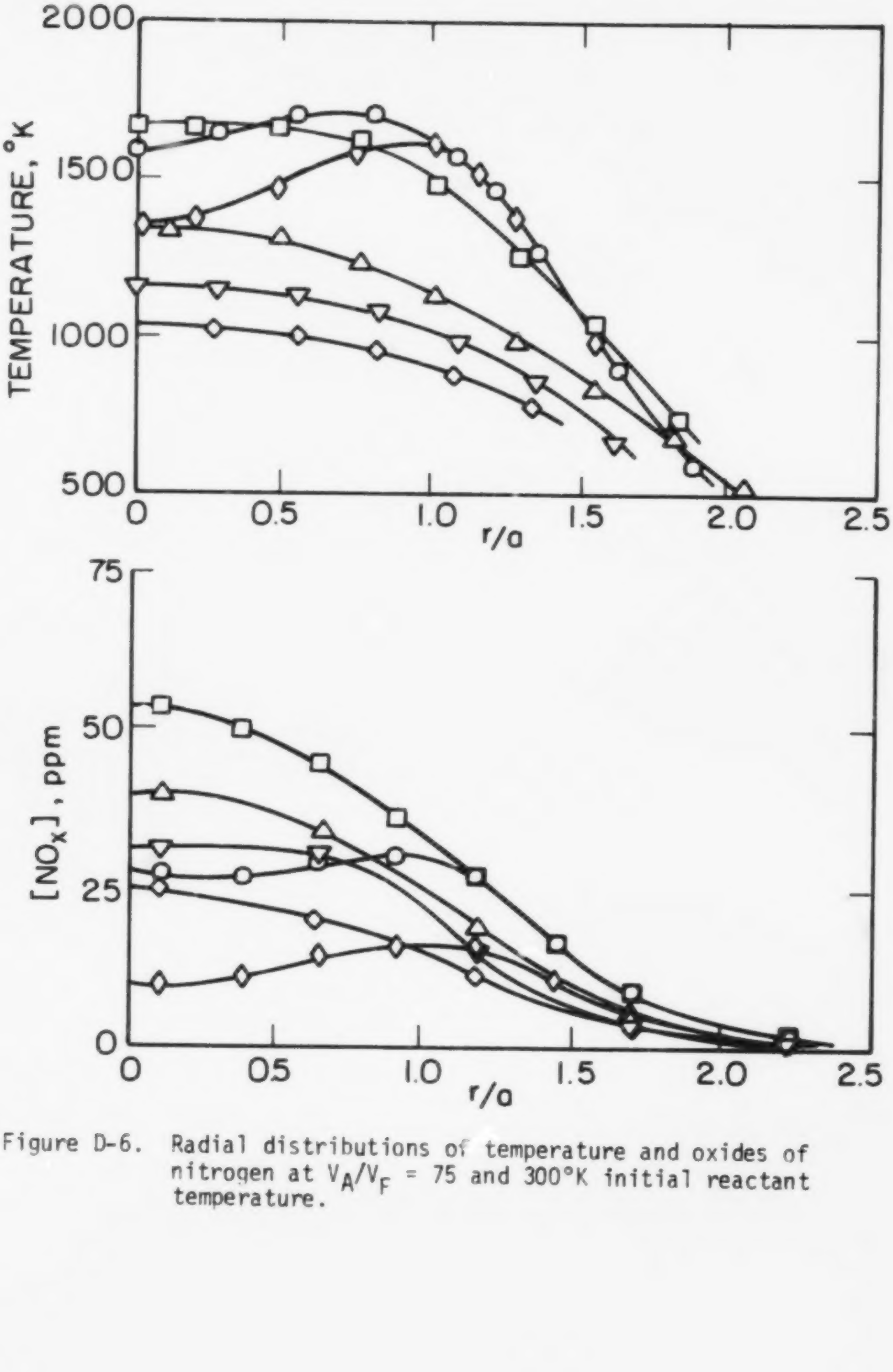

Figure D-6. Radial distributions of temperature and oxides of nitrogen at V_A/V_F = 75 and 300°K initial reactant temperature.

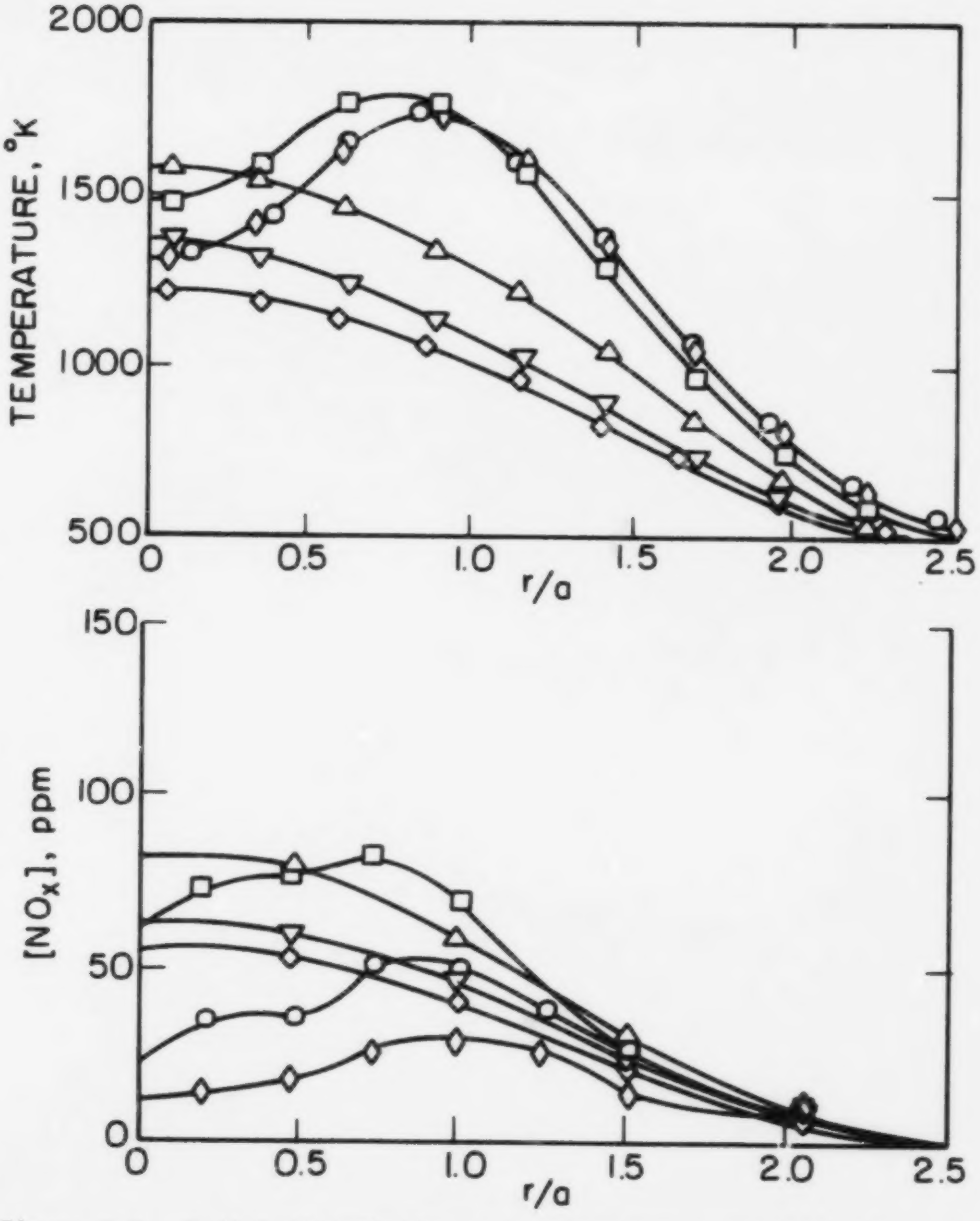

Figure D-7. Radial distributions of temperature and oxides of nitrogen at V_A/V_F = 45 and 440°K initial reactant temperature.

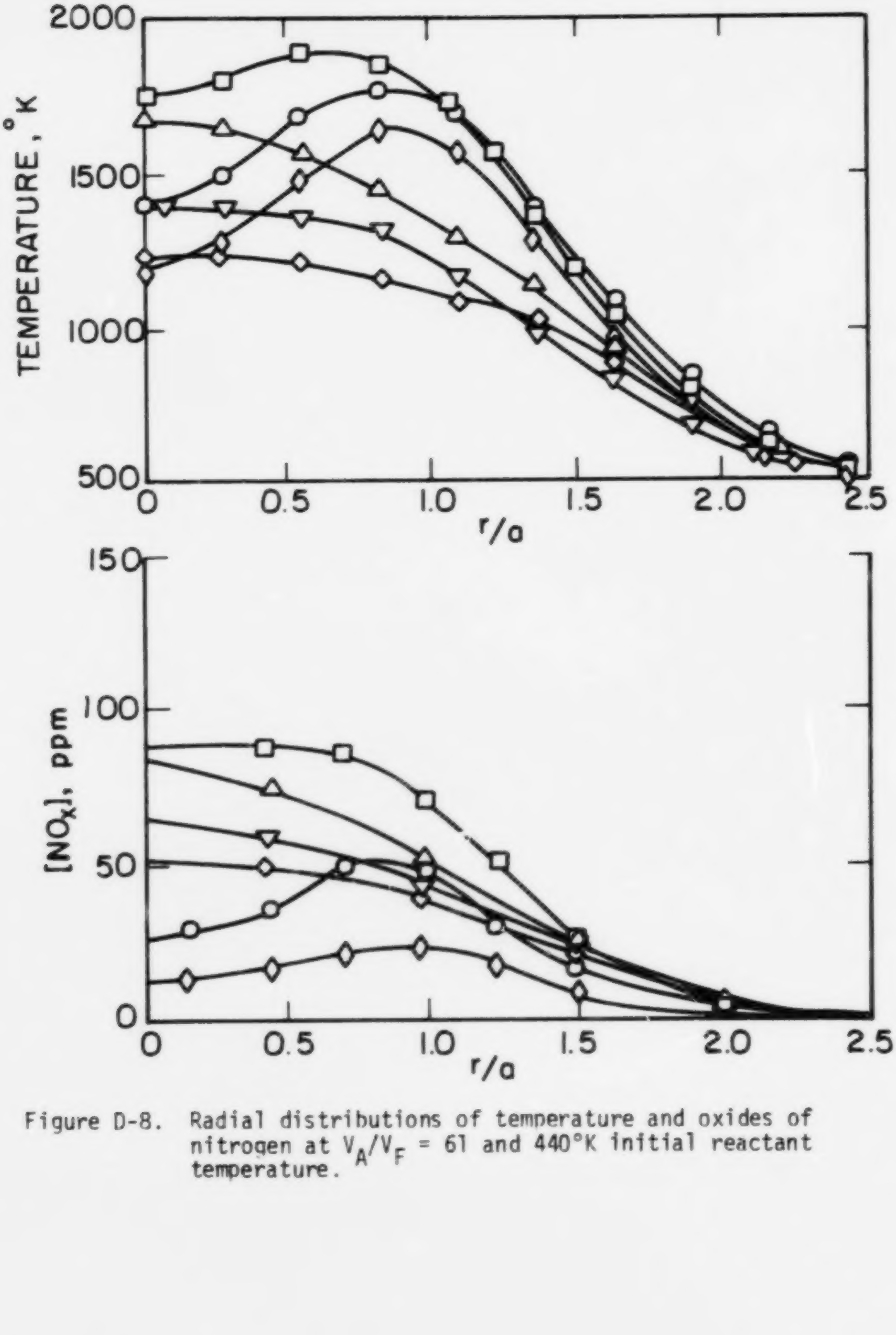

Figure D-8. Radial distributions of temperature and oxides of nitrogen at V_A/V_F = 61 and 440°K initial reactant temperature.

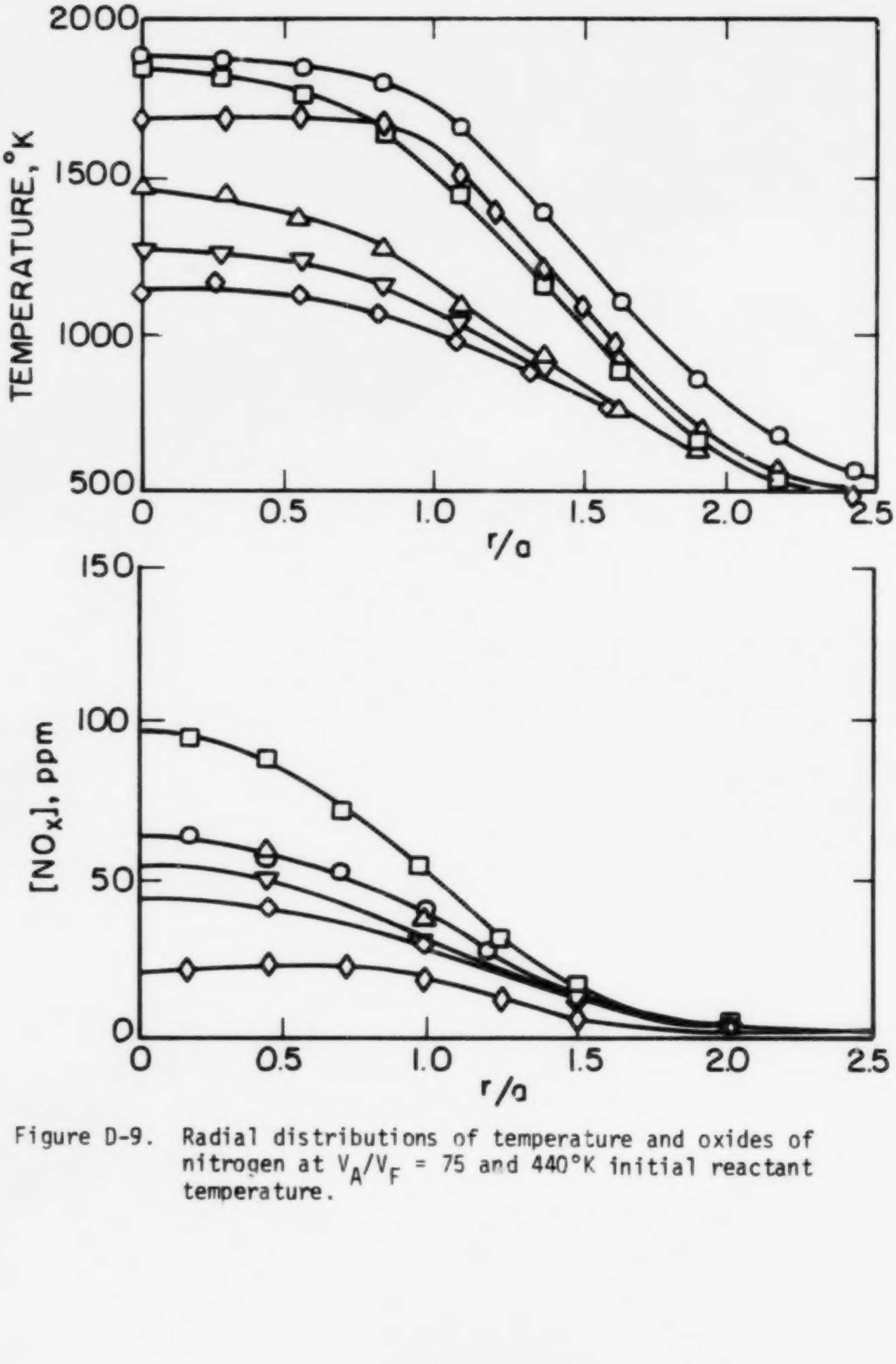

Figure D-9. Radial distributions of temperature and oxides of nitrogen at V_A/V_F = 75 and 440°K initial reactant temperature.

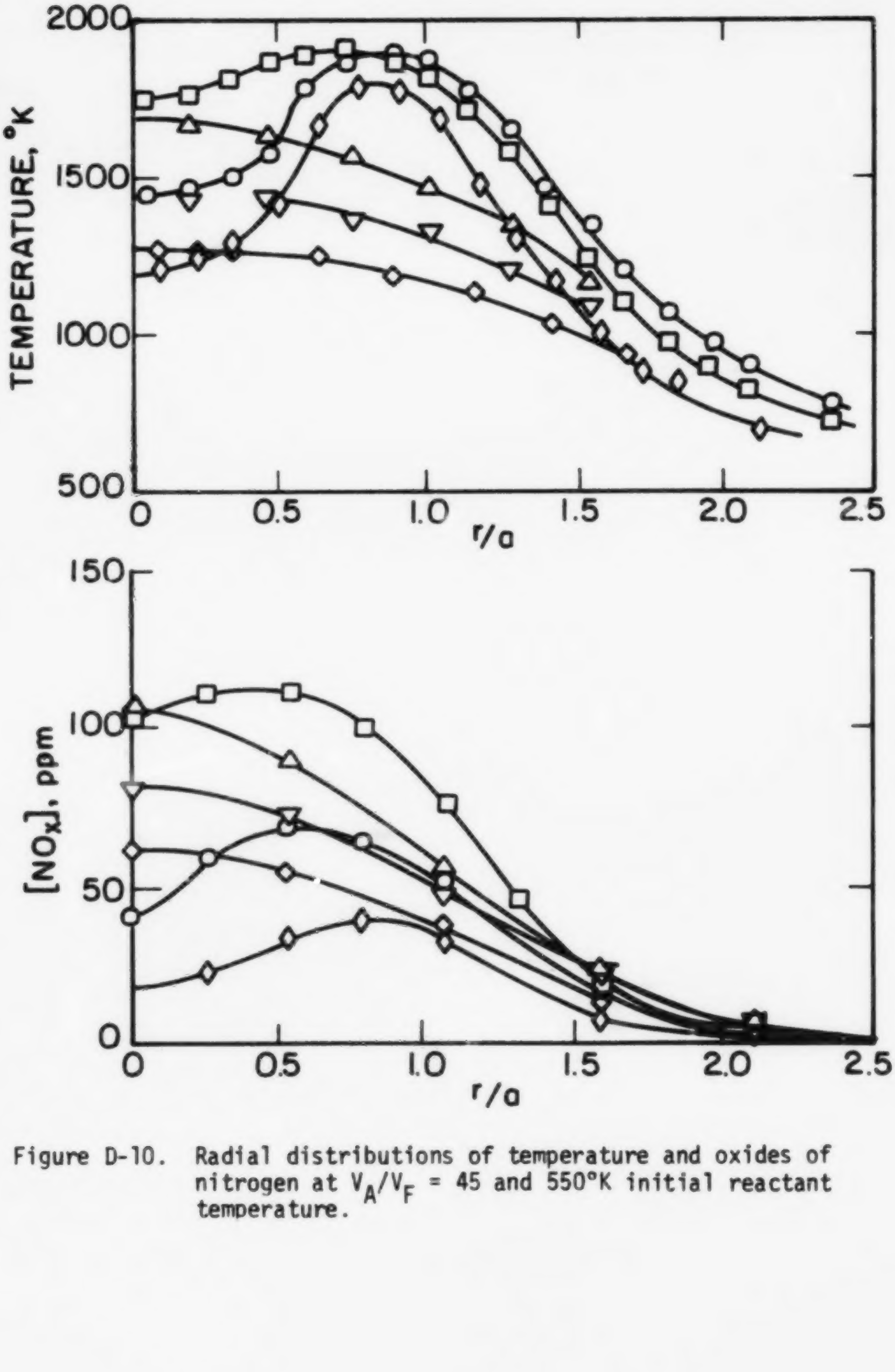

Figure D-10. Radial distributions of temperature and oxides of nitrogen at V_A/V_F = 45 and 550°K initial reactant temperature.

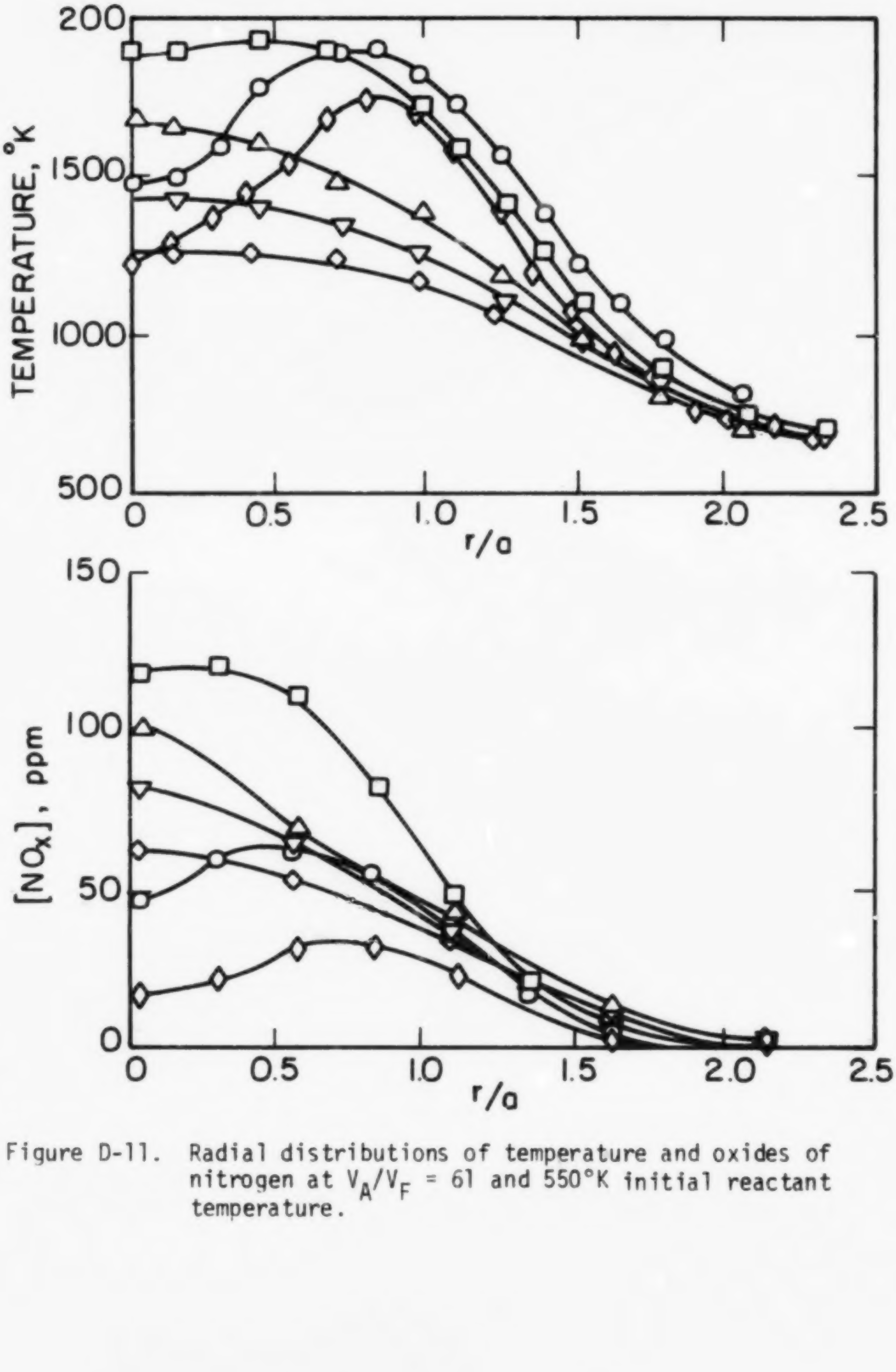

Figure D-11. Radial distributions of temperature and oxides of nitrogen at V_A/V_F = 61 and 550°K initial reactant temperature.

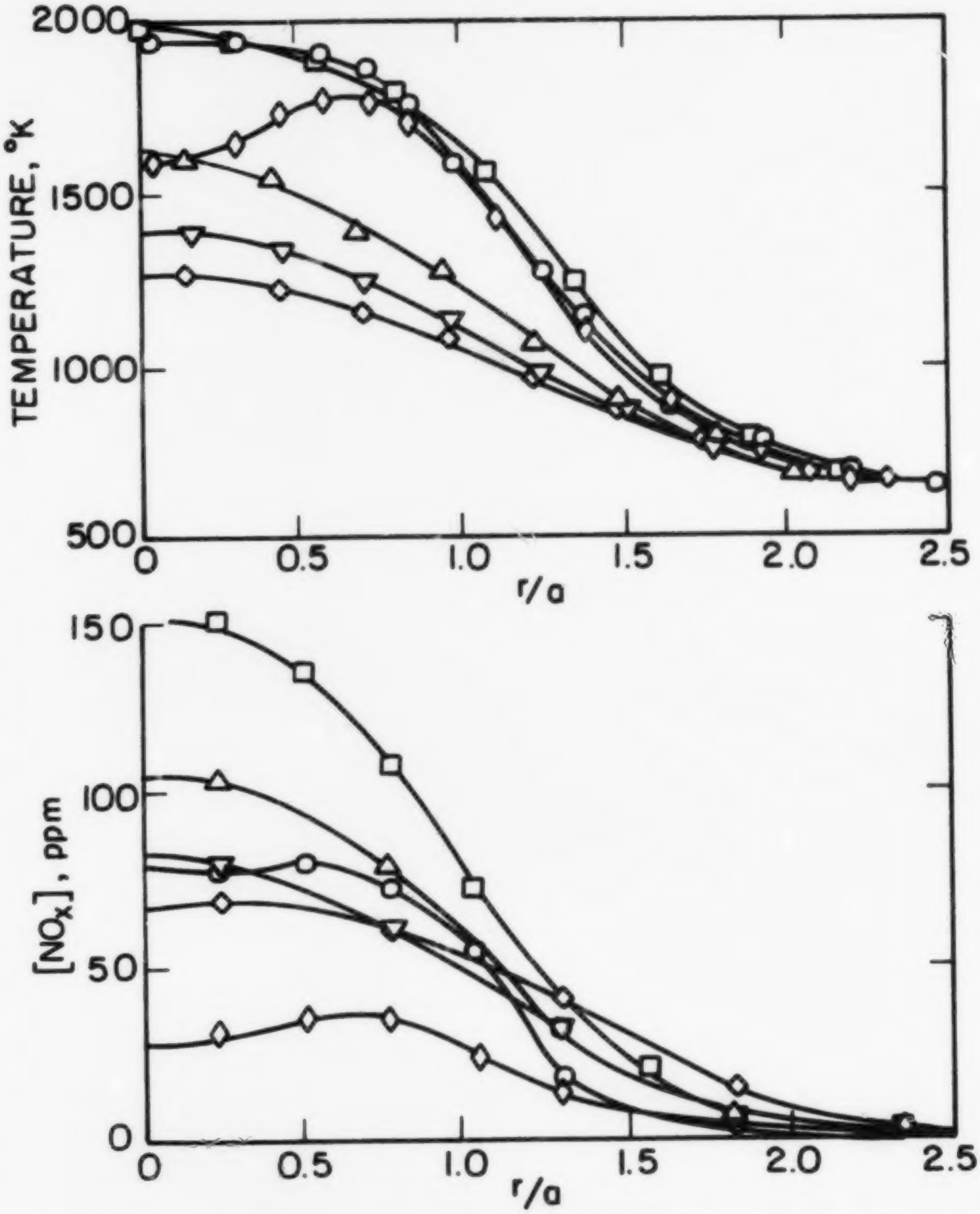

Figure D-12. Radial distributions of temperature and oxides of nitrogen at V_A/V_F = 75 and 550°K initial reactant temperature.

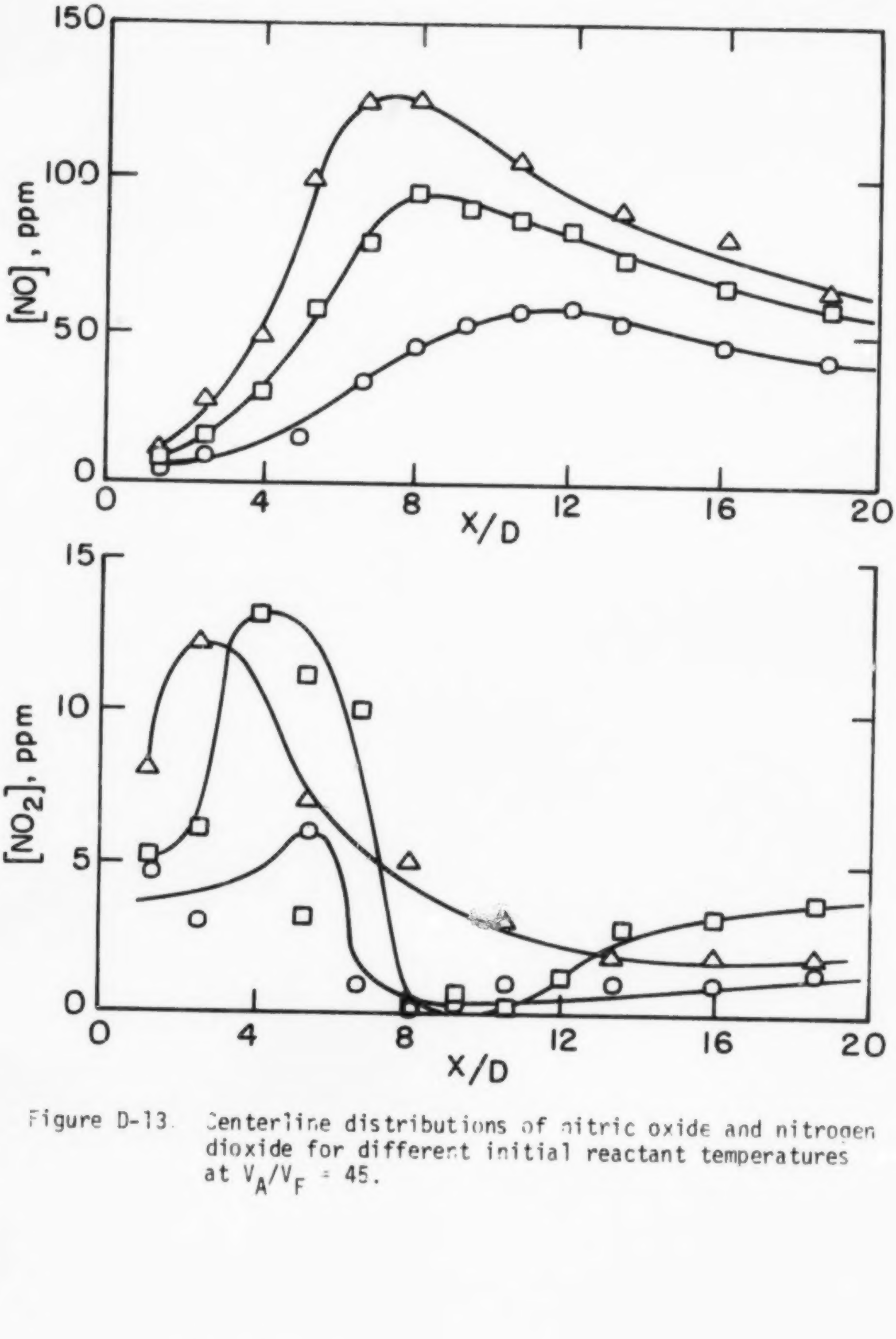

Figure D-13. Centerline distributions of nitric oxide and nitrogen dioxide for different initial reactant temperatures at $V_A/V_F = 45$.

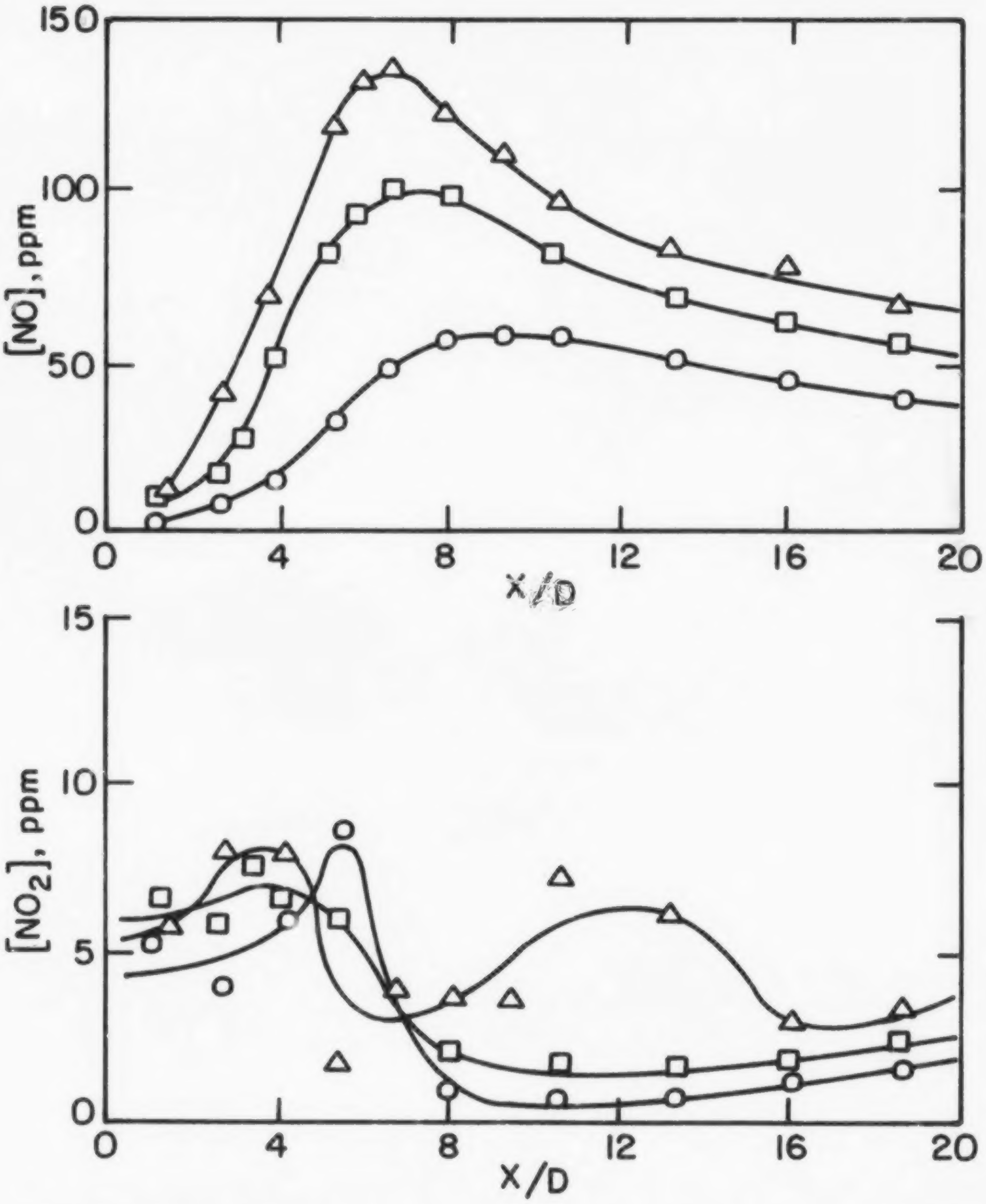

Figure D-14. Centerline distributions of nitric oxide and nitrogen dioxide for different initial reactant temperatures at $V_A/V_F = 61$.

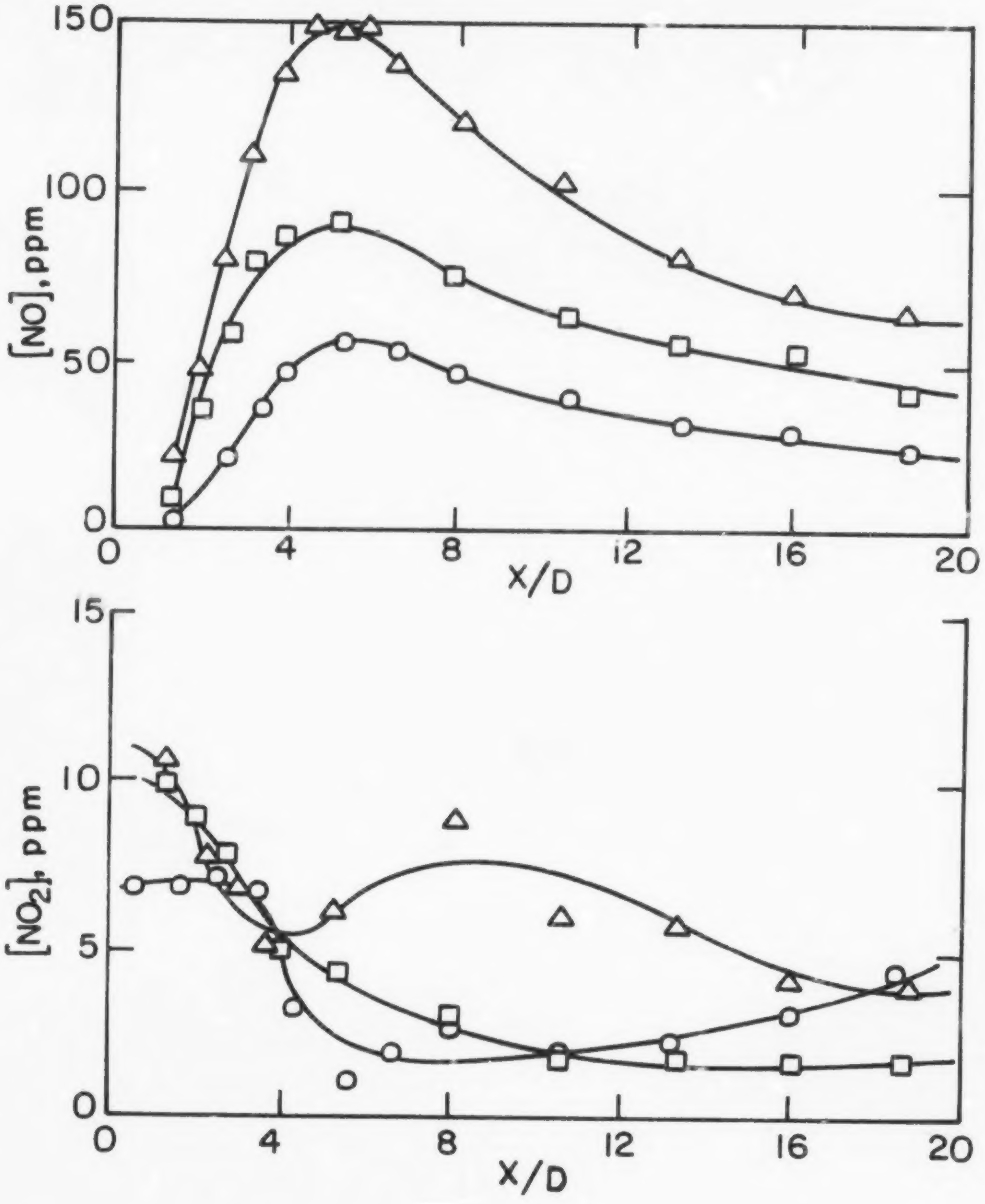

Figure D-15. Centerline distributions of nitric oxide and nitrogen dioxide for different initial reactant temperatures at V_A/V_F = 75.

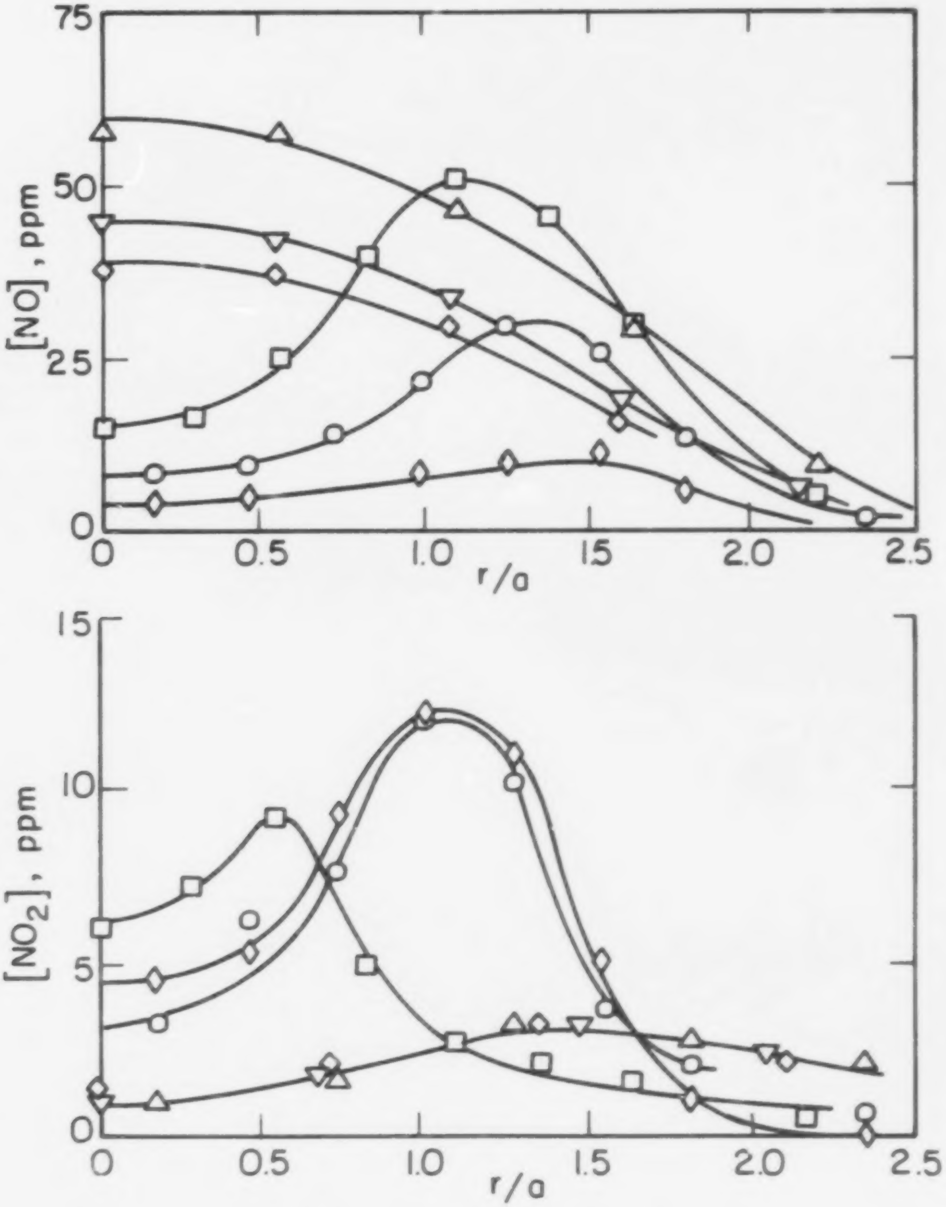

Figure D-16. Radial distributions of nitric oxide and nitrogen dioxide at V_A/V_F = 45 and 300°K initial reactant temperature.

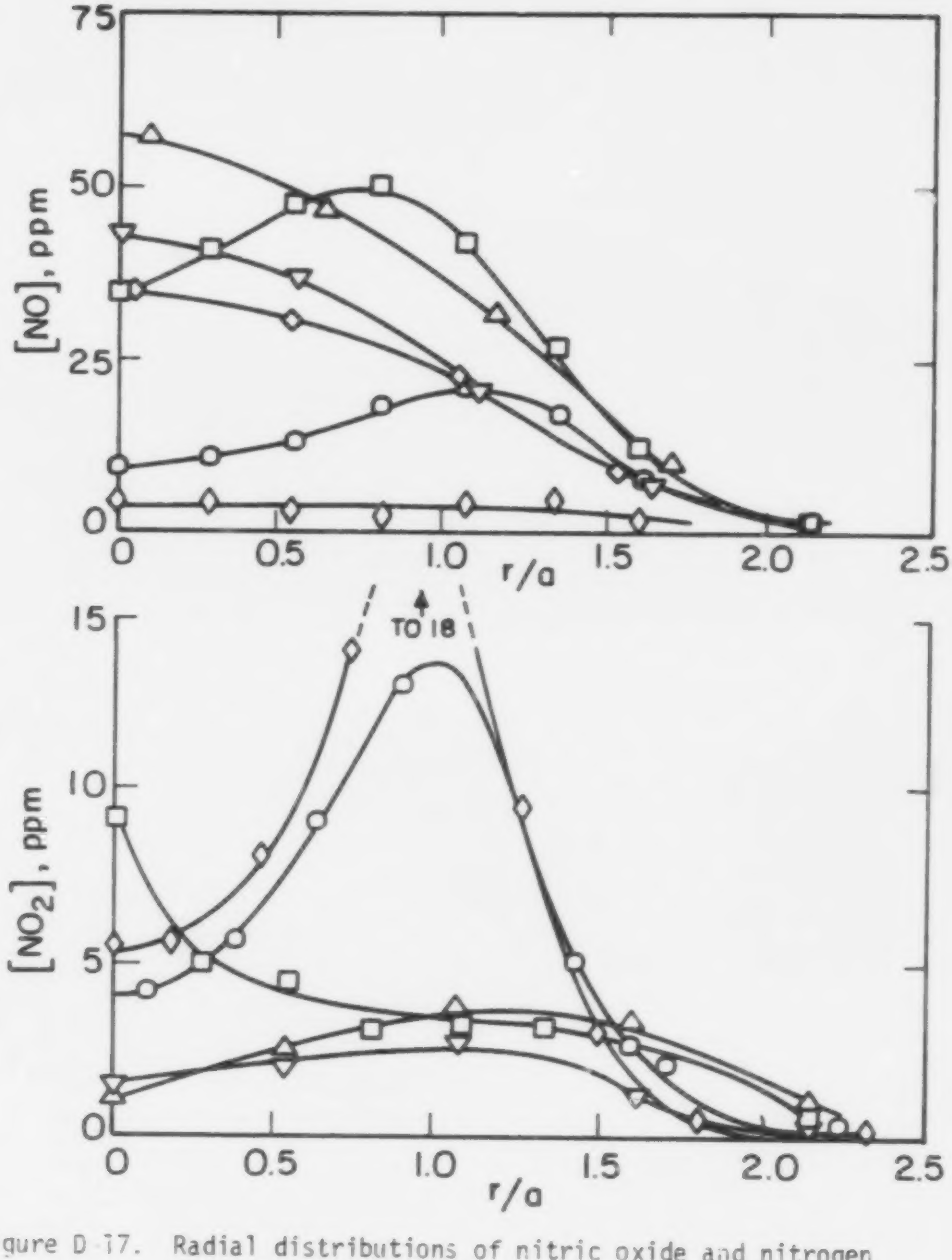

Figure D-17. Radial distributions of nitric oxide and nitrogen dioxide at V_A/V_F = 61 and 300°K initial reactant temperature.

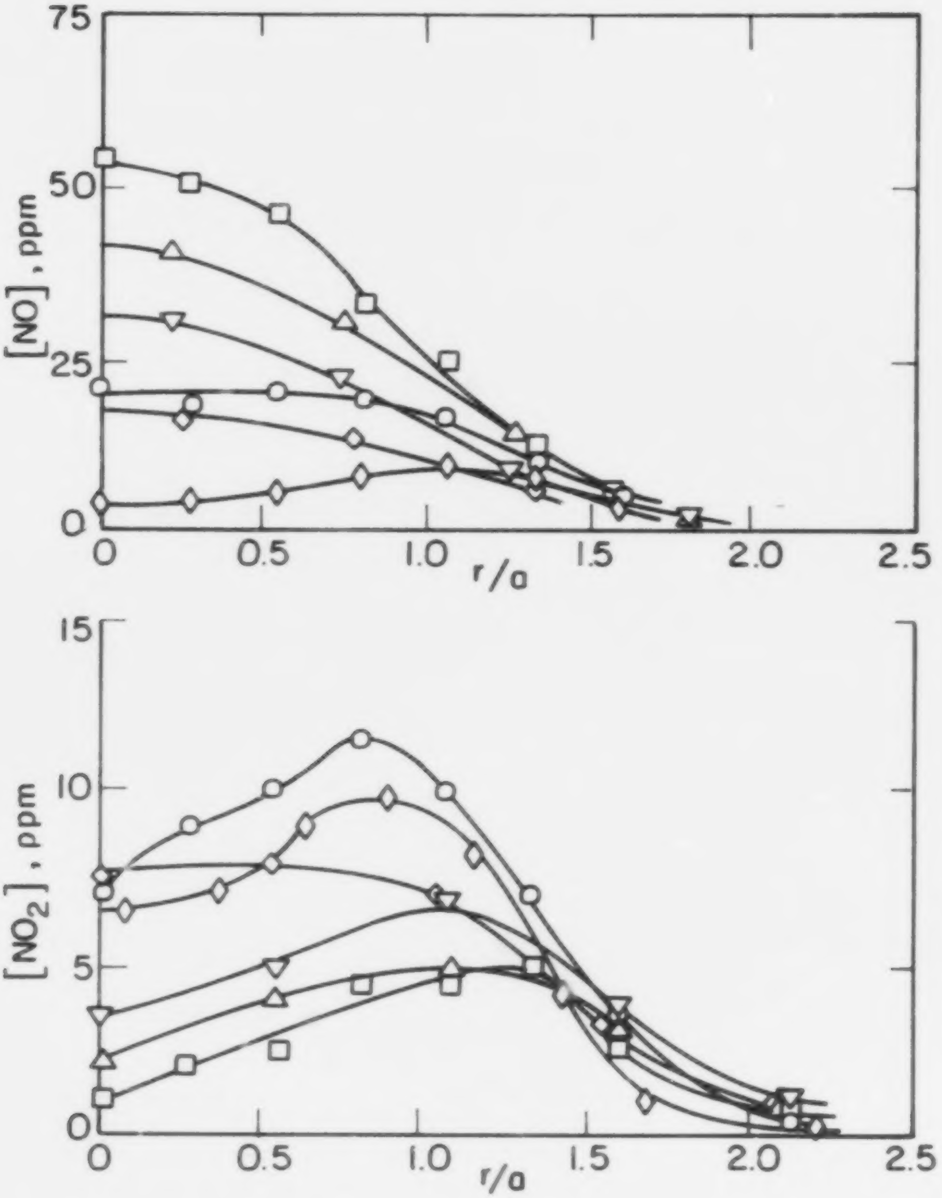

Figure D-18. Radial distributions of nitric oxide and nitrogen dioxide at V_A/V_F = 75 and 300°K initial reactant temperature.

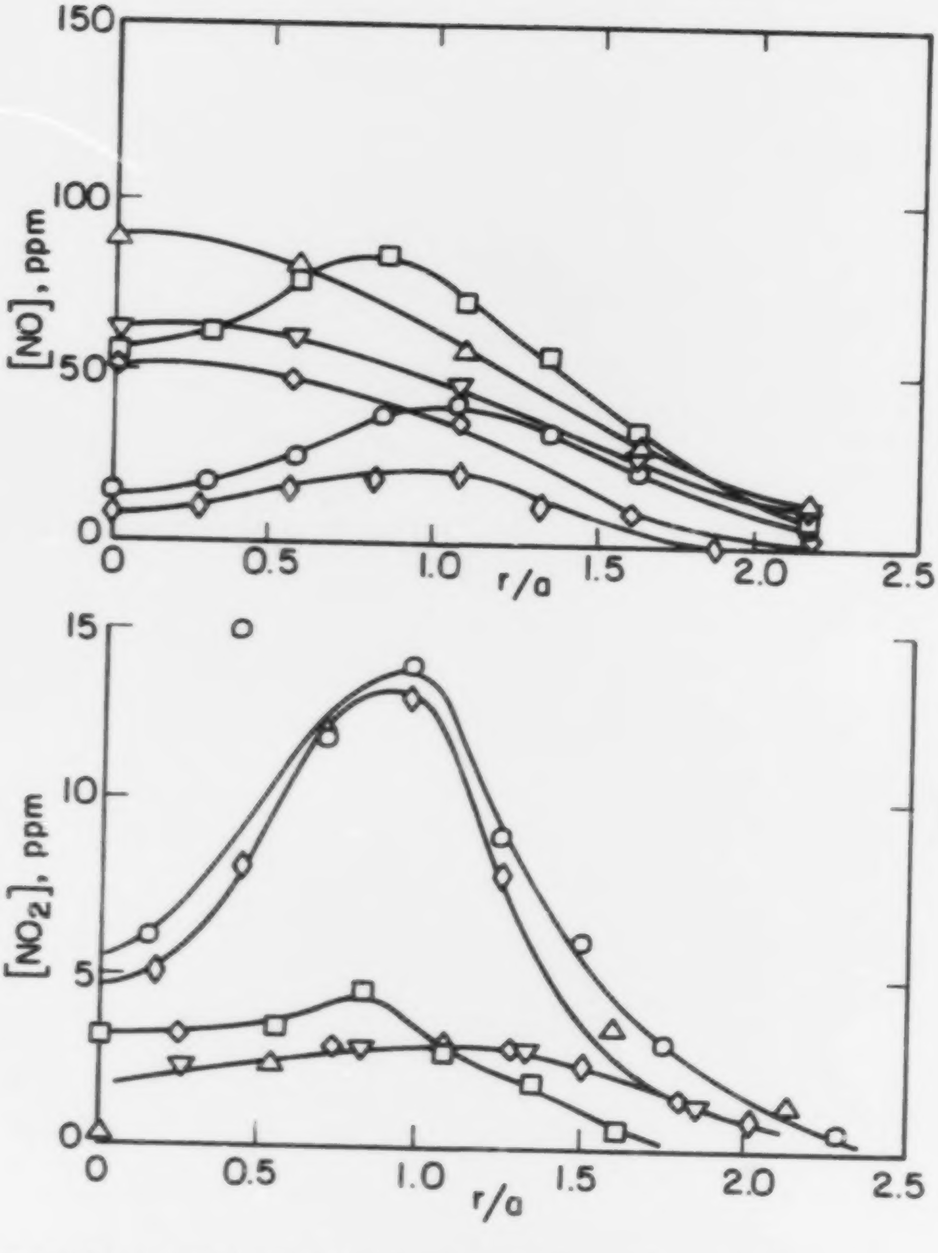

Figure D-19. Radial distributions of nitric oxide and nitrogen dioxide at V_A/V_F = 45 and 440°K initial reactant temperature.

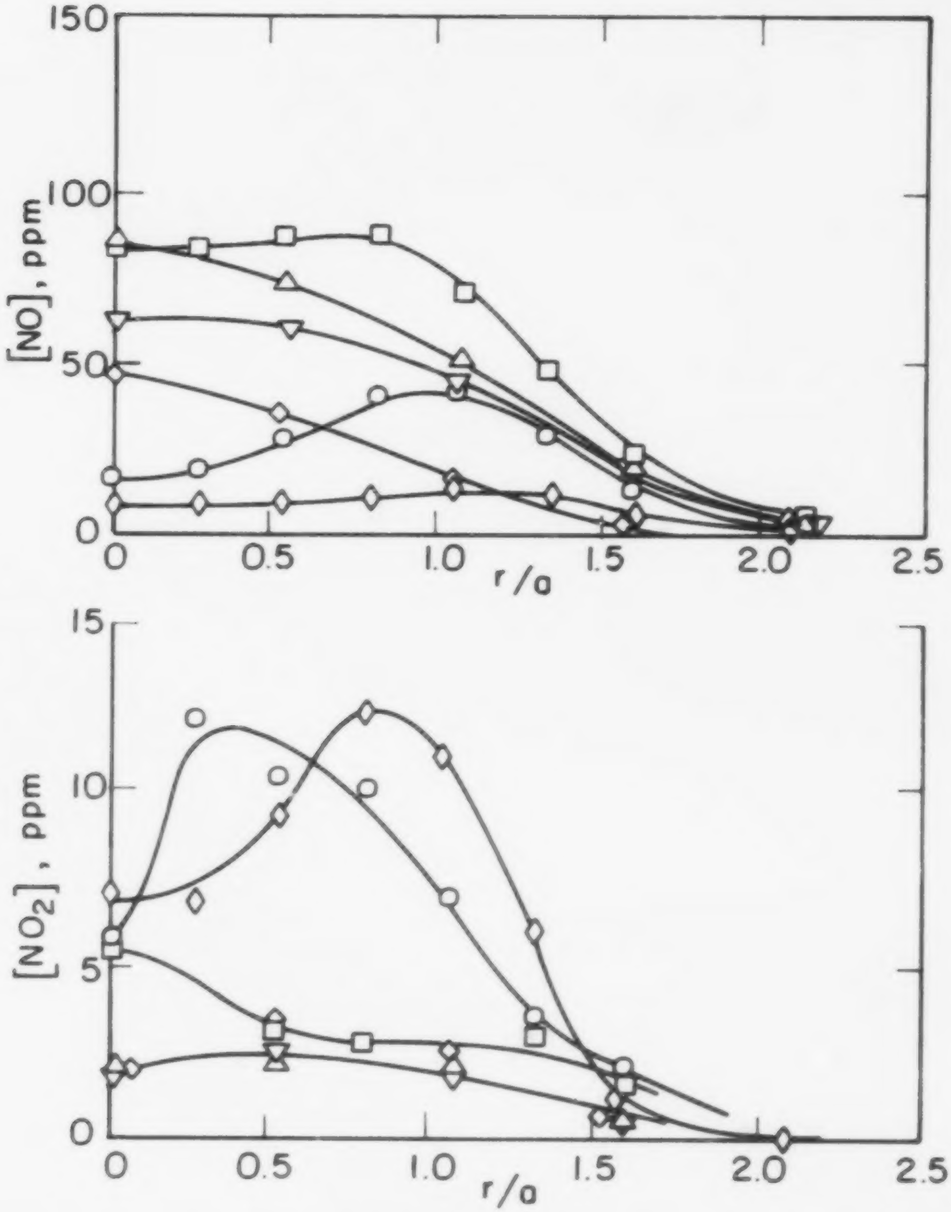

Figure D-20. Radial distributions of nitric oxide and nitrogen dioxide at V_A/V_F = 61 and 440°K initial reactant temperature.

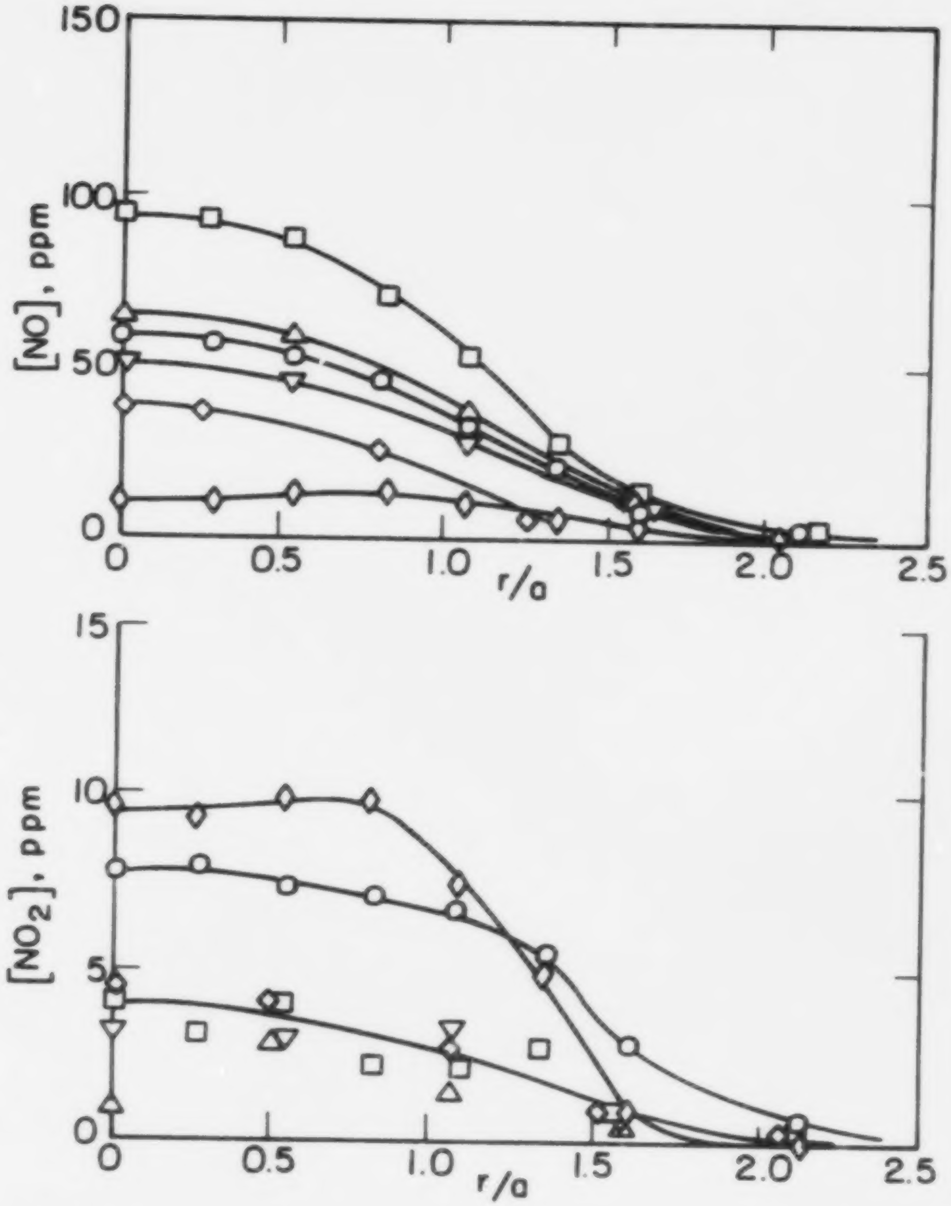

Figure D-21. Radial distributions of nitric oxide and nitrogen dioxide at V_A/V_F = 75 and 440°K initial reactant temperature.

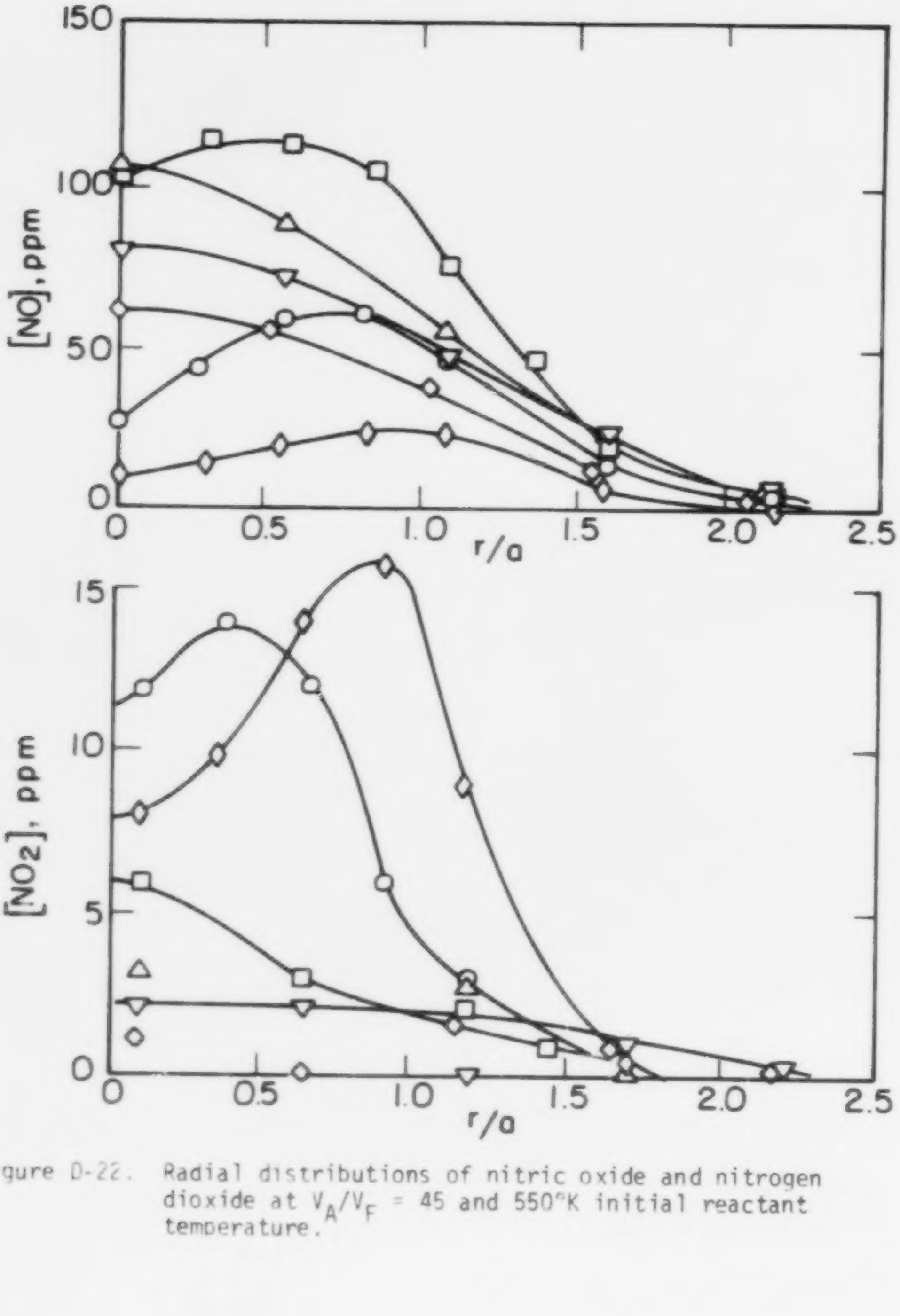

Figure D-22. Radial distributions of nitric oxide and nitrogen dioxide at V_A/V_F = 45 and 550°K initial reactant temperature.

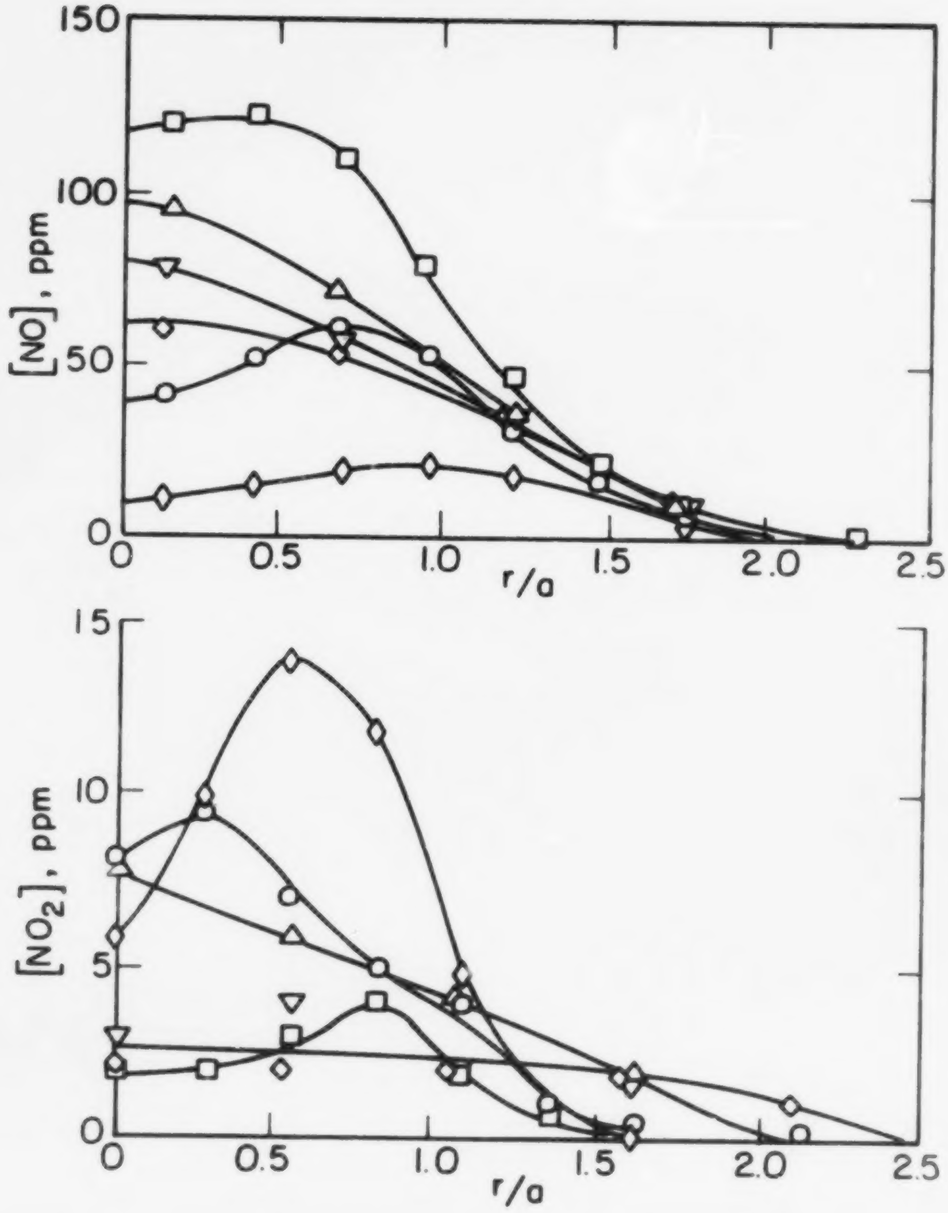

Figure D-23. Radial distributions of nitric oxide and nitrogen dioxide at V_A/V_F = 61 and 500°K initial reactant temperature.

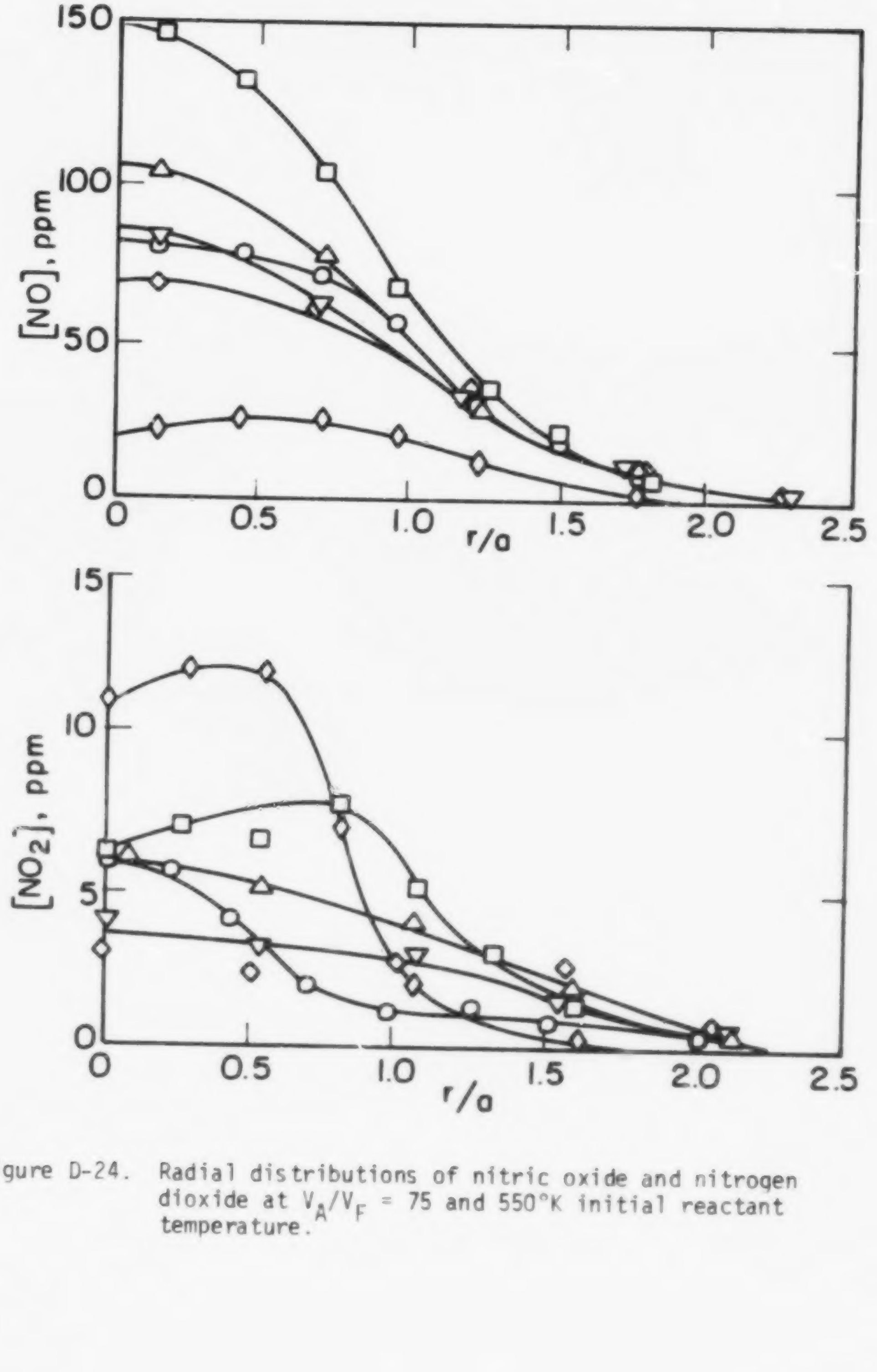

Figure D-24. Radial distributions of nitric oxide and nitrogen dioxide at V_A/V_F = 75 and 550°K initial reactant temperature.

APPENDIX E

Kinetic Calculations

E.1 Introduction

Detailed kinetic calculations were performed for idealized combustion and sampling conditions to establish the plausibility of the formation and existance of the measured NO_2. For these purposes, all of the calculations were performed using the Generalized Kinetic Analysis Program - GKAP developed by Nickerson and Frey (1971).

E.2 Reaction Scheme

The most general set of reactions that was used included:

*Principal Reactions exchanging NO and NO_2

$$NO + O + M = NO_2 + M \tag{E-1}$$

$$H + NO_2 = NO + OH \tag{E-2}$$

$$O + NO_2 = NO + O_2 \tag{E-3}$$

$$NO + HO_2 = NO_2 + OH \tag{E-4}$$

$$NO + O_3 = NO_2 + O_2 \tag{E-5}$$

*Possible NO_x sink reactions

$$NO_2 + OH + M = HNO_3 + M \tag{E-6}$$

$$NO + OH + M = HNO_2 + M \tag{E-7}$$

$$HNO_2 + O = NO_2 + OH \tag{E-8}$$

$$HNO_2 + OH = H_2O + NO_2 \tag{E-9}$$

*Ozone Reactions

$O + O_2 + M = O_3 + M$ (E-10)

$O + O_3 = O_2 + O_2$ (E-11)

$H + O_3 = OH + O_2$ (E-12)

*CO oxidation to CO_2

$CO + OH = CO_2 + H$ (E-13)

$CO + O + M = CO_2 + M$ (E-14)

$CO + HO_2 = CO_2 + OH$ (E-15)

*Reactions controlling H, O, and OH levels

$H + O_2 = OH + O$ (E-16)

$OH + OH = H_2O + O$ (E-17)

$O + H_2 = H + OH$ (E-18)

$H_2 + OH = H_2O + H$ (E-19)

$OH + OH = O_2 + H_2$ (E-20)

$H + H + M = H_2 + M$ (E-21)

$O + O + M = O_2 + M$ (E-22)

$H + OH + M = H_2O + M$ (E-23)

$O + H + M = OH + M$ (E-24)

*Reactions involving HOO and H_2O_2

$$\mathrm{H + O_2 + M = HO_2 + M} \qquad \text{(E-25)}$$

$$\mathrm{H + HO_2 = OH + OH} \qquad \text{(E-26)}$$

$$\mathrm{OH + HO_2 = H_2O + O_2} \qquad \text{(E-27)}$$

$$\mathrm{O + HO_2 = OH + O_2} \qquad \text{(E-28)}$$

$$\mathrm{H + HO_2 = H_2 + O_2} \qquad \text{(E-29)}$$

$$\mathrm{H + HO_2 = H_2O + O} \qquad \text{(E-30)}$$

$$\mathrm{OH + OH + M = H_2O_2 + M} \qquad \text{(E-31)}$$

$$\mathrm{HO_2 + HO_2 = H_2O_2 + O_2} \qquad \text{(E-32)}$$

$$\mathrm{H_2O_2 + OH = H_2O + HO_2} \qquad \text{(E-33)}$$

$$\mathrm{H + H_2O_2 = H_2 + HO_2} \qquad \text{(E-34)}$$

Calculations were performed including all of these groups of reactions as well as combinations of them in order to isolate the effect of particular mechanisms.

Rate data for these reactions were taken from the compilation of Cernansky (1974) and generally represent the most recent and best data for overall combustion and quench conditions.

E.3 Base Cases and Initial Conditions

Two sets of initial conditions were generally used for each trial, one fuel rich ($\phi = 1.4$) and one fuel lean ($\phi = 0.8$). These conditions were selected because they are matched in that they yield the same adiabatic flame temperature (≈ 2050°K) and also because they were conditions achievable in many laboratory combustion devices. The initial species concentrations for all calculations were chosen as the equilibrium species concentrations at the adiabatic flame temperature. The concentrations were determined using the NASA equilibrium program of Gordon and McBride (1971). Because of the known nonequilibrium behavior of NO_x, NO and NO_2 levels were held to levels more consistent with the experimental observations (~ 50 ppm). The initial conditions are shown in Table E-1.

E.4 Results

Initially, the hydroperoxy radical (HOO) reactions were superimposed on the equilibrium mixtures at flame temperatures to see if they could alter the NO/NO_2 kinetics. No significant effects were predicted.

Next, quenching of burning eddies was modeled, in the limit, as an instantaneous temperature change. In these runs NO_2 destruction was always predicted for fuel rich mixtures while NO_2 production was generally favored by fuel lean mixtures. These results are presented in Figs. E-1 through E-9. Figures E-1, E-2, and E-3 show the predicted radical relaxation curves for 1300°K, 900°K, and 500°K end temperatures when only the "usual" radicals (H, O, OH) are considered. Figures E-4, E-5, E-6 includes the effect of adding the hydroperoxy radical reactions and Figs. E-7, E-8, and E-9 also include the nitrous acid, nitric acid, and ozone reactions. For clarity, only the radicals and other species of interest are plotted. The plots may be summarized as follows. When only the "usual" reactions and radical species are considered, no appreciable conversion of NO is predicted down to a temperature of 500°K. If the hydroperoxy radical reactions are included, TABLE E-1. Initial Species Concentrations for Kinetic Calculations, 2050°K, 1 atm.

SPECIES	MOLE FRACTION	
	$\phi = 0.8$	$\phi = 1.4$
N_2	7.28 E-01	6.49 E-01
O_2	3.75 E-02	1.50 E-06
H_2O	1.25 E-01	1.46 E-01
CO_2	9.34 E-02	5.65 E-02
CO	9.20 E-04	9.02 E-02
H_2	2.60 E-04	4.94 E-02
H	4.00 E-05	5.10 E-04
O	1.80 E-04	1.20 E-06
OH	1.84 E-03	1.60 E-04
HOO	5.00 E-07	3.00 E-10
H_2O_2	5.00 E-08	3.00 E-11
N	1.50 E-09	1.50 E-09
O_3	5.00 E-10	-
HNO_2	-	-
HNO_3	-	-
NO	5.00 E-05	5.00 E-05
NO_2	-	-

substantial NO conversion is predicted in very short times, with more conversion as the final temperature is lowered. Including the nitrous acid, nitric acid, and ozone reactions accentuates this NO conversion at lower temperatures (although into species other than simply NO_2).

Some other rough preliminary calculations of the effect of the rapid aerodynamic quenching in the probe were also attempted. Again, the quenching process was modeled as an instantaneous cooling. As a limiting case, wall effects were ignored; this can be a source of considerable error, as wall quenching may be the dominant mechanism of radical removal in the small diameter sampling probe. Again, calculations predicted destruction of NO_2 for the fuel rich initial conditions irrespective of the mechanism chosen. For the fuel lean situation, on the other hand, the final NO_x distribution was a function of the mechanism, the initial NO and NO_2 concentrations, and the cooling rate. Figure E-10 shows the results for only the "usual" mechanism and Fig. E-11 presents results for the full mechanism, both with initial NO_2 concentrations. The full mechanism without NO_2 is shown in Fig. E-12. Results of an additional case where a linear cooling from 2000°K to 300°K is specified over 20 msec, including the hydroproxy-radical mechanism, is shown in Fig. E-13. As can be seen in the figures, NO_x reactions are predicted in the sampling probe. Care must be taken not to read too much into these results, as they are modeling a somewhat unrealistic situation and also much of the reaction rate data is subject to question. They do indicate, however, that additional work on modeling probe reactions is required.

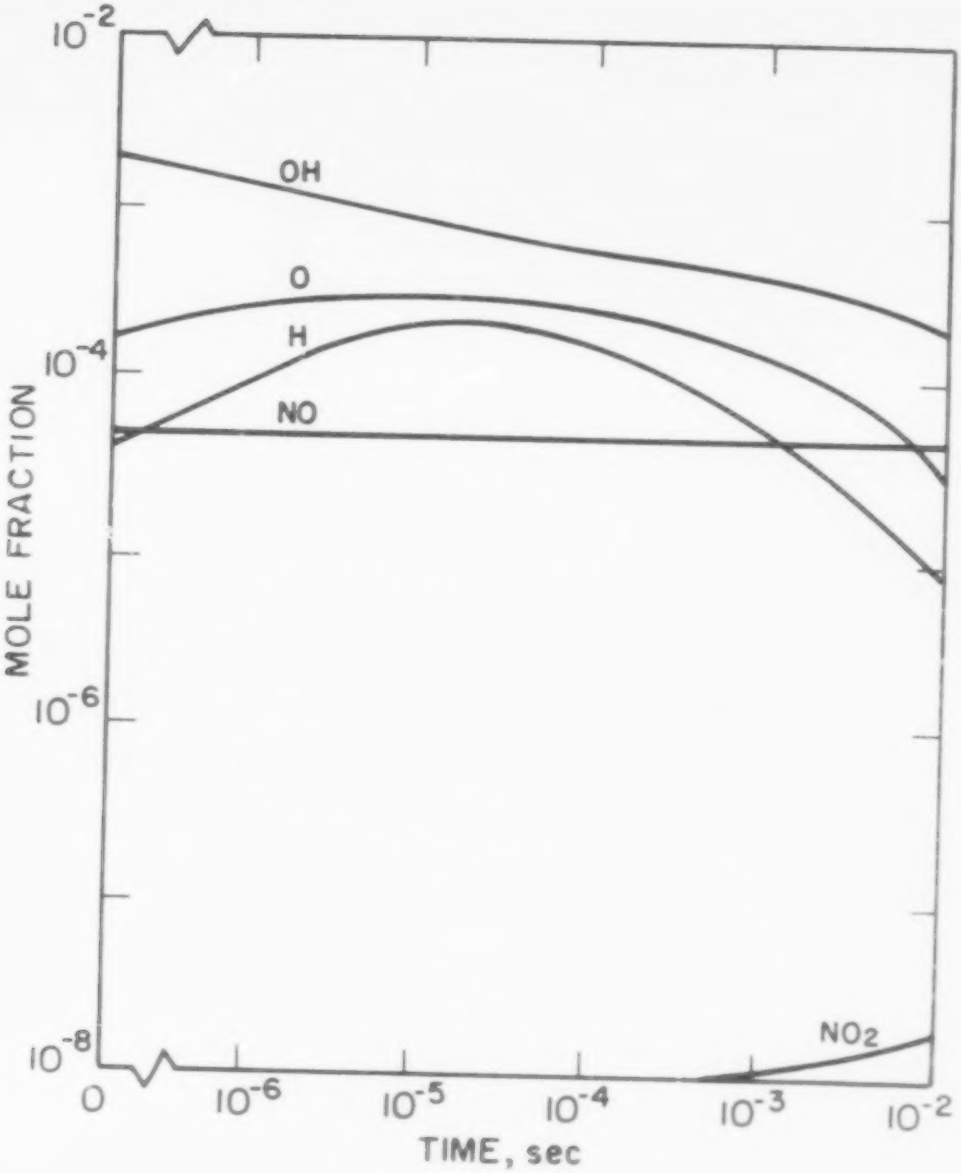

Figure E-1. Time history of selected species when equilibrium concentrations of radicals for ϕ = 0.8 at 2050°K and 50 ppm NO are instantaneously cooled to 1300°K.

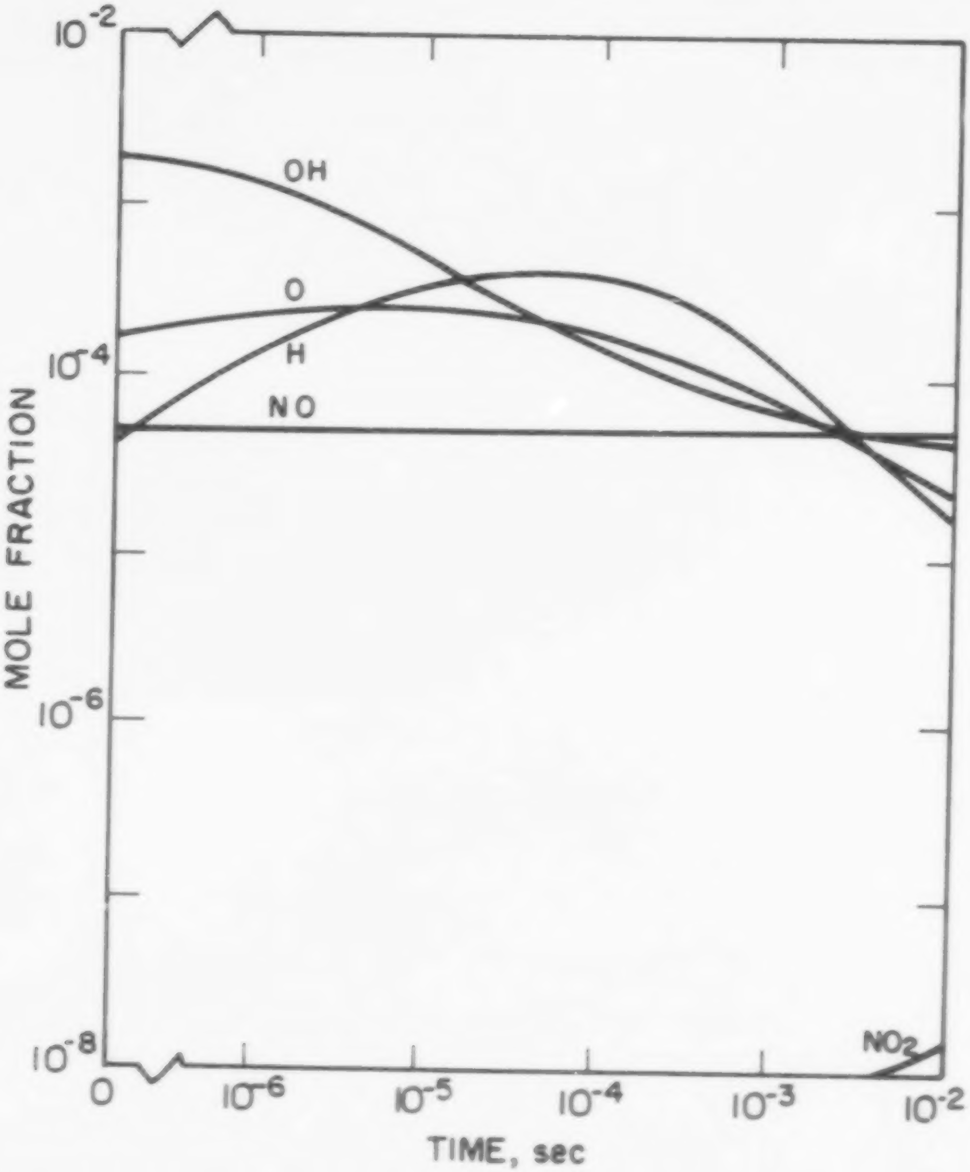

Figure E-2. Time history of selected species when equilibrium concentrations of radicals for $\phi = 0.8$ at 2050°K and 50 ppm NO are instantaneously cooled to 900°K.

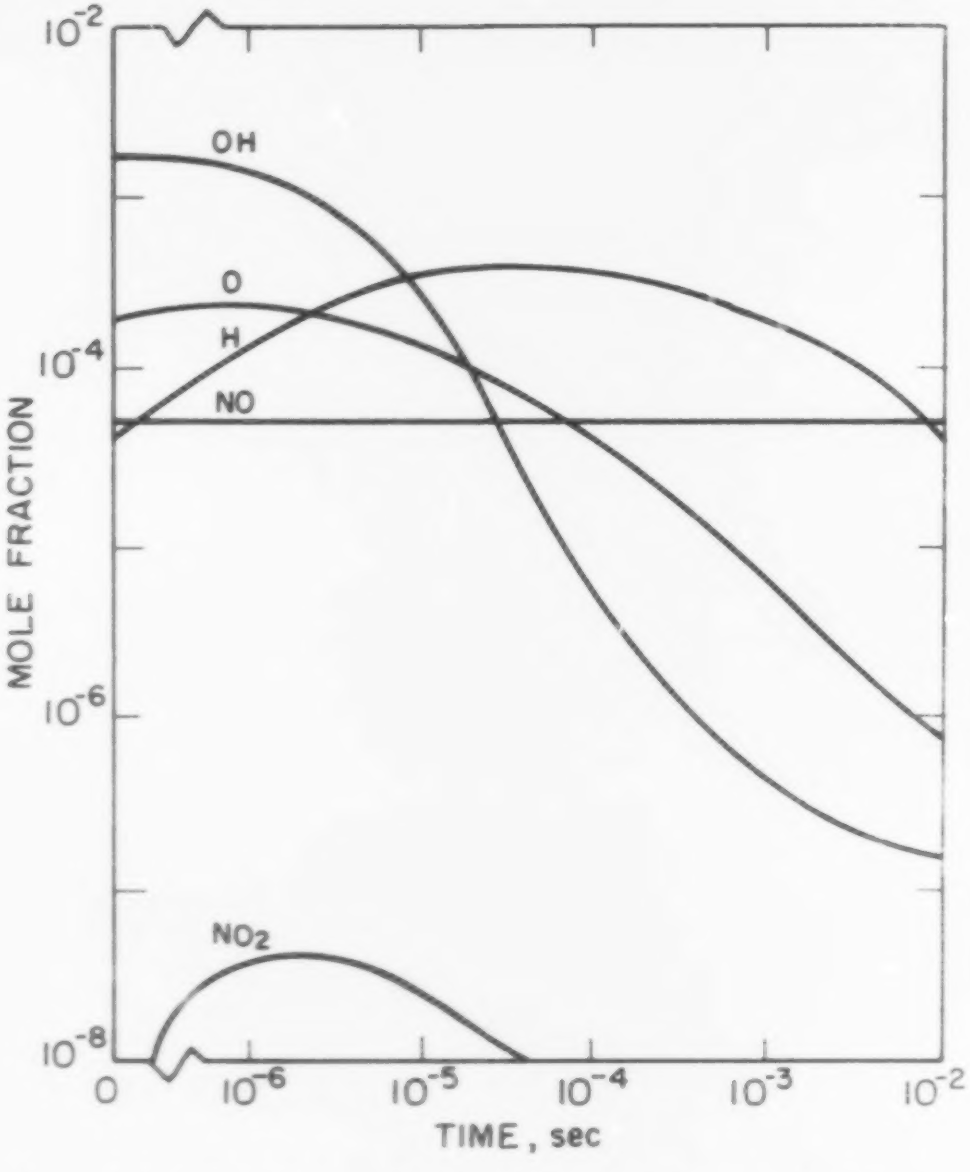

Figure E-3. Time history of selected species when equilibrium concentrations of radicals for $\phi = 0.8$ at 2050°K and 50 ppm NO are instantaneously cooled to 500°K.

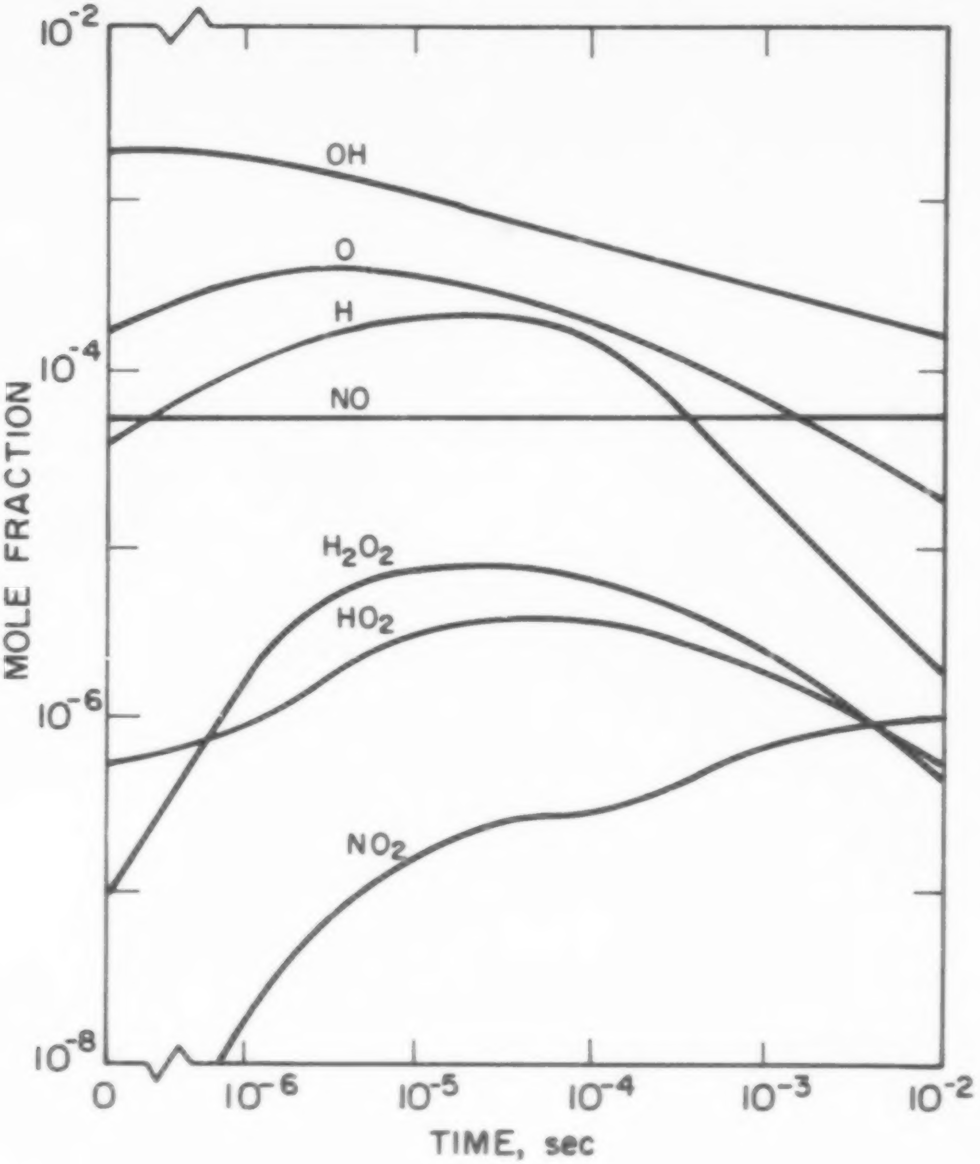

Figure E-4. Time history of selected species when equilibrium concentrations of radicals for ϕ = 0.8 at 2050°K and 50 ppm NO are instantaneously cooled to 1300°K, including HOO mechanism.

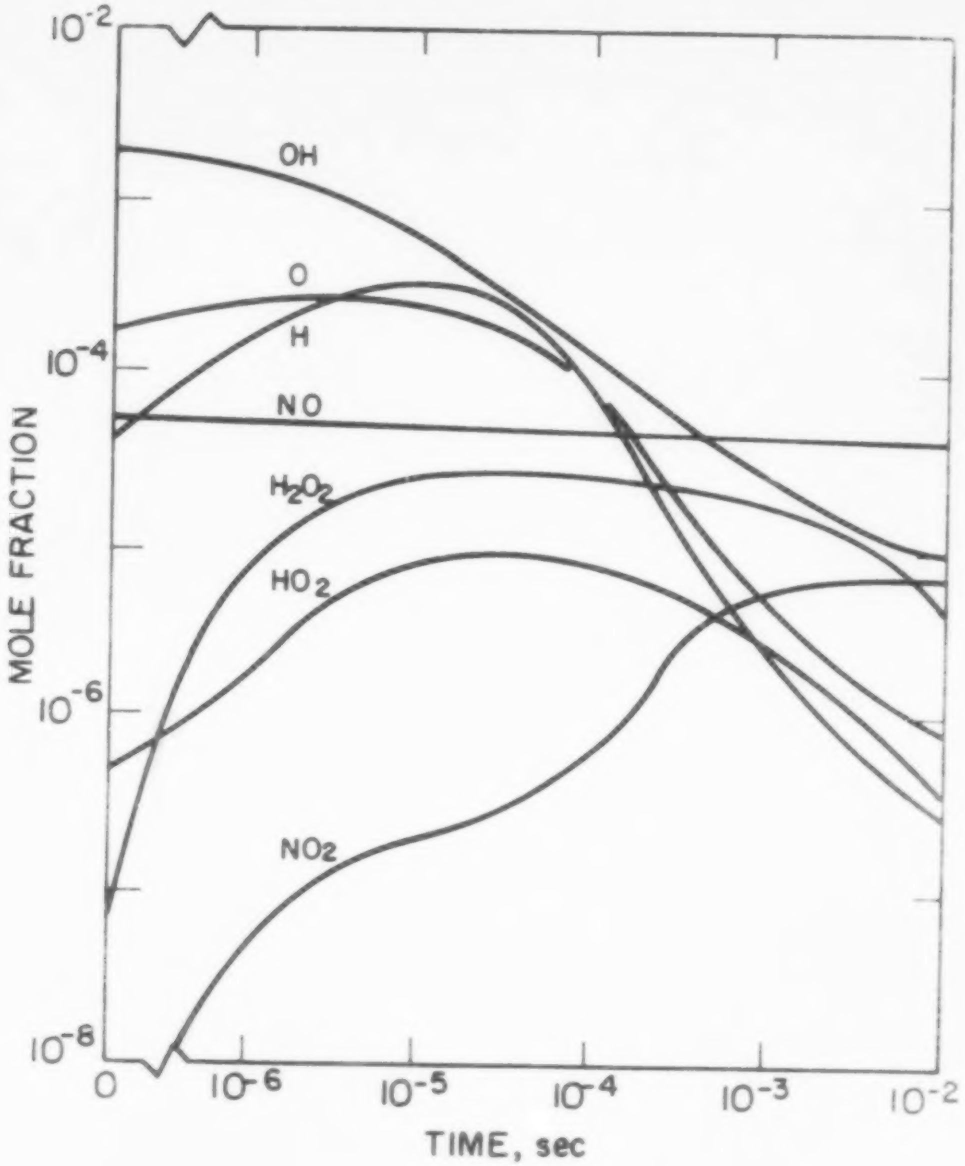

Figure E-5. Time history of selected species when equilibrium concentrations of radicals for $\phi = 0.8$ at 2050°K and 50 ppm NO are instantaneously cooled to 900°K, including HOO mechanism.

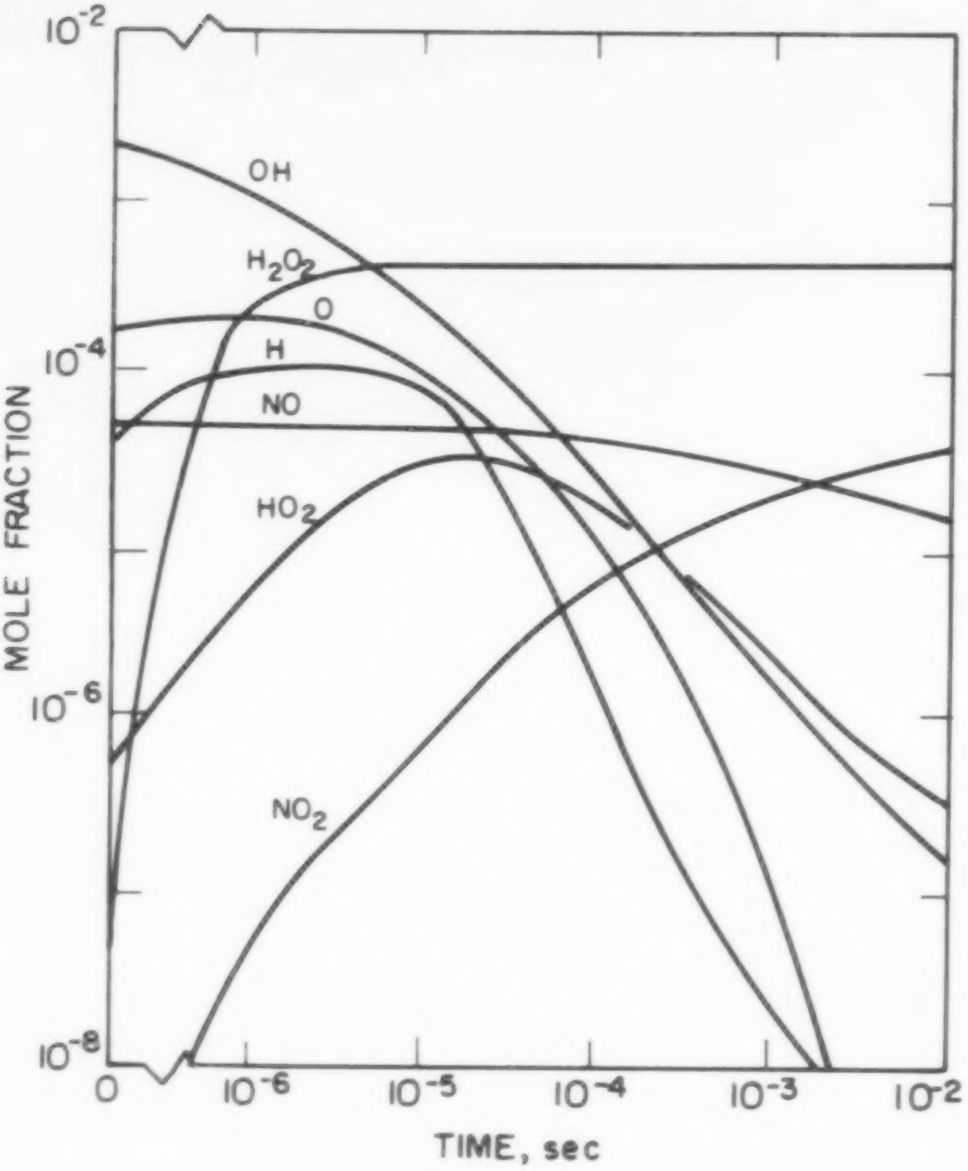

Figure E-6. Time history of selected species when equilibrium concentrations of radicals for $\phi = 0.8$ at 2050°K and 50 ppm NO are instantaneously cooled to 500°K, including HOO mechanism.

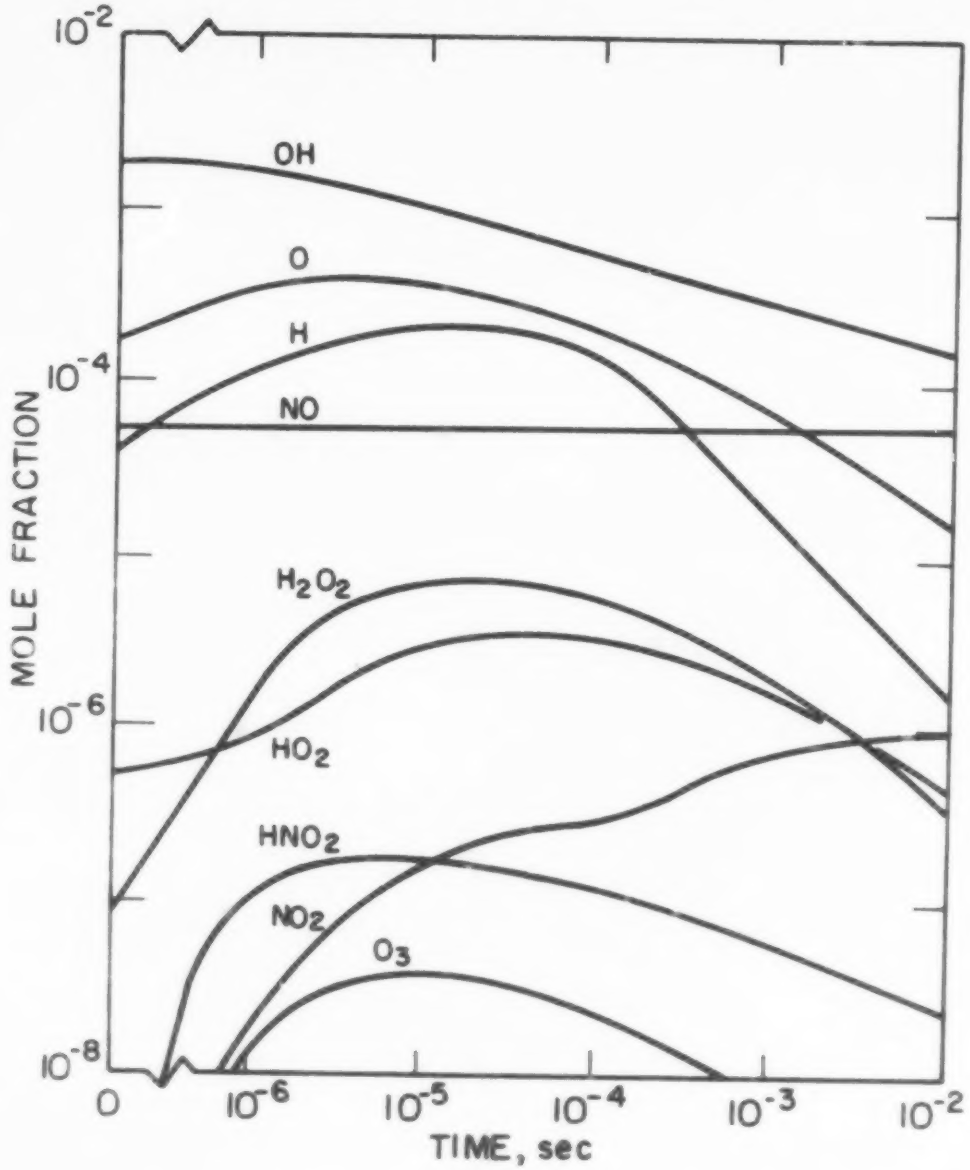

Figure E-7. Time history of selected species when equilibrium concentrations of radicals for $\phi = 0.8$ at 2050°K and 50 ppm NO are instantaneously cooled to 1300°K, including HOO, HNO_2, HNO_3, O_3 mechanisms.

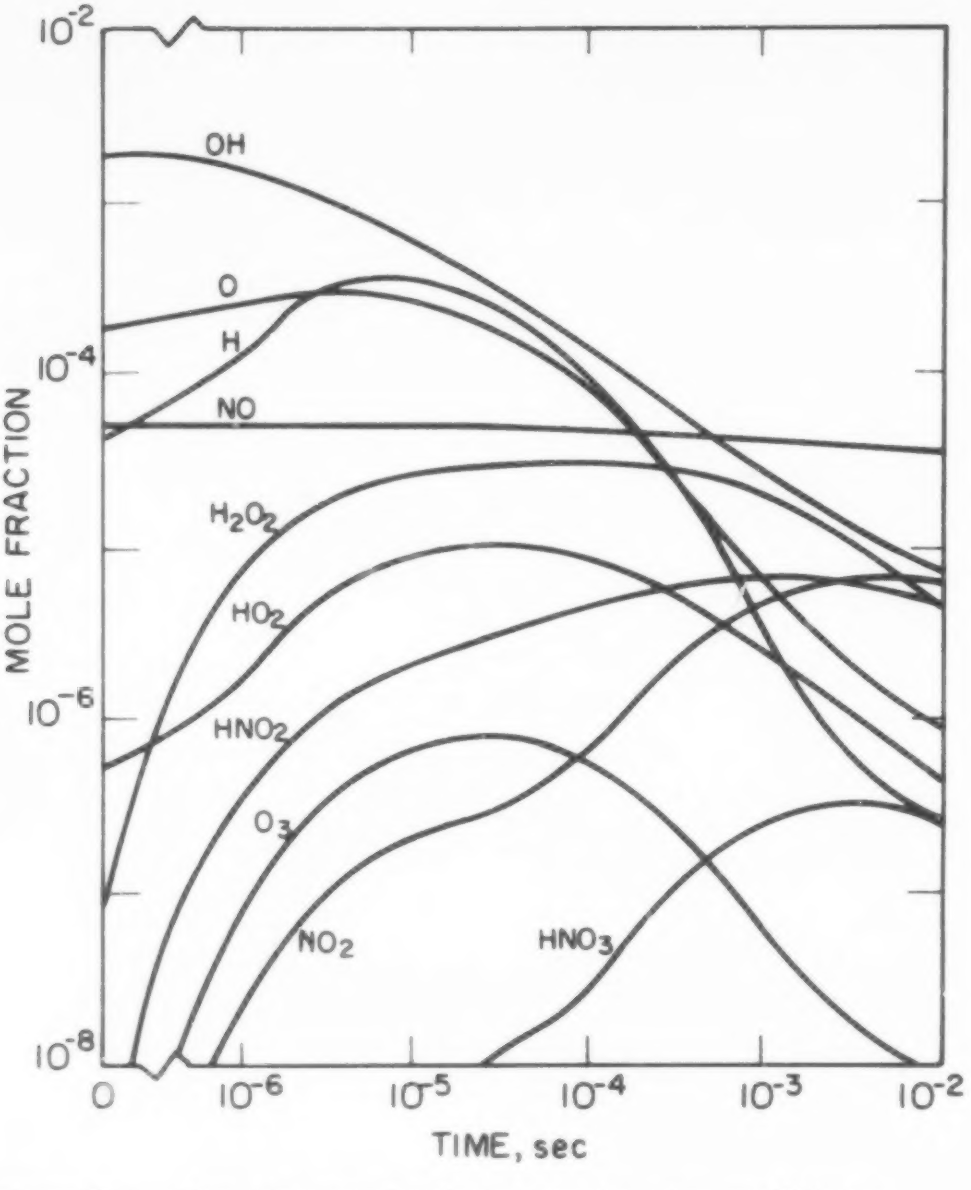

Figure E-8. Time history of selected species when equilibrium concentrations of radicals for $\phi = 0.8$ at 2050°K and 50 ppm NO are instantaneously cooled to 900°K, including HOO, HNO_2, HNO_3, O_3 mechanisms.

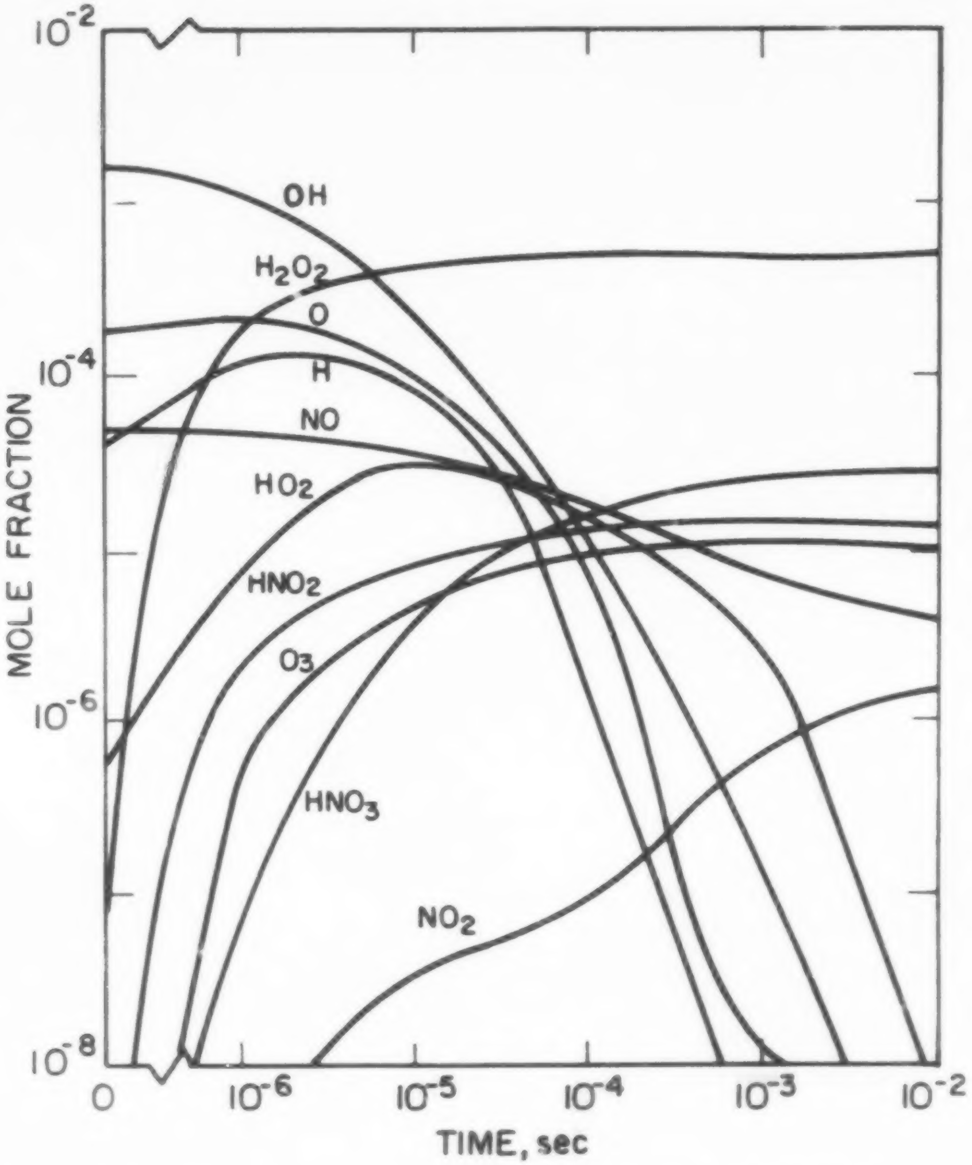

Figure E-9. Time history of selected species when equilibrium concentrations of radicals for ϕ = 0.8 at 2050°K and 50 ppm NO are instantaneously cooled to 500°K, including HOO, HNO_2, HNO_3, O_3 mechanisms.

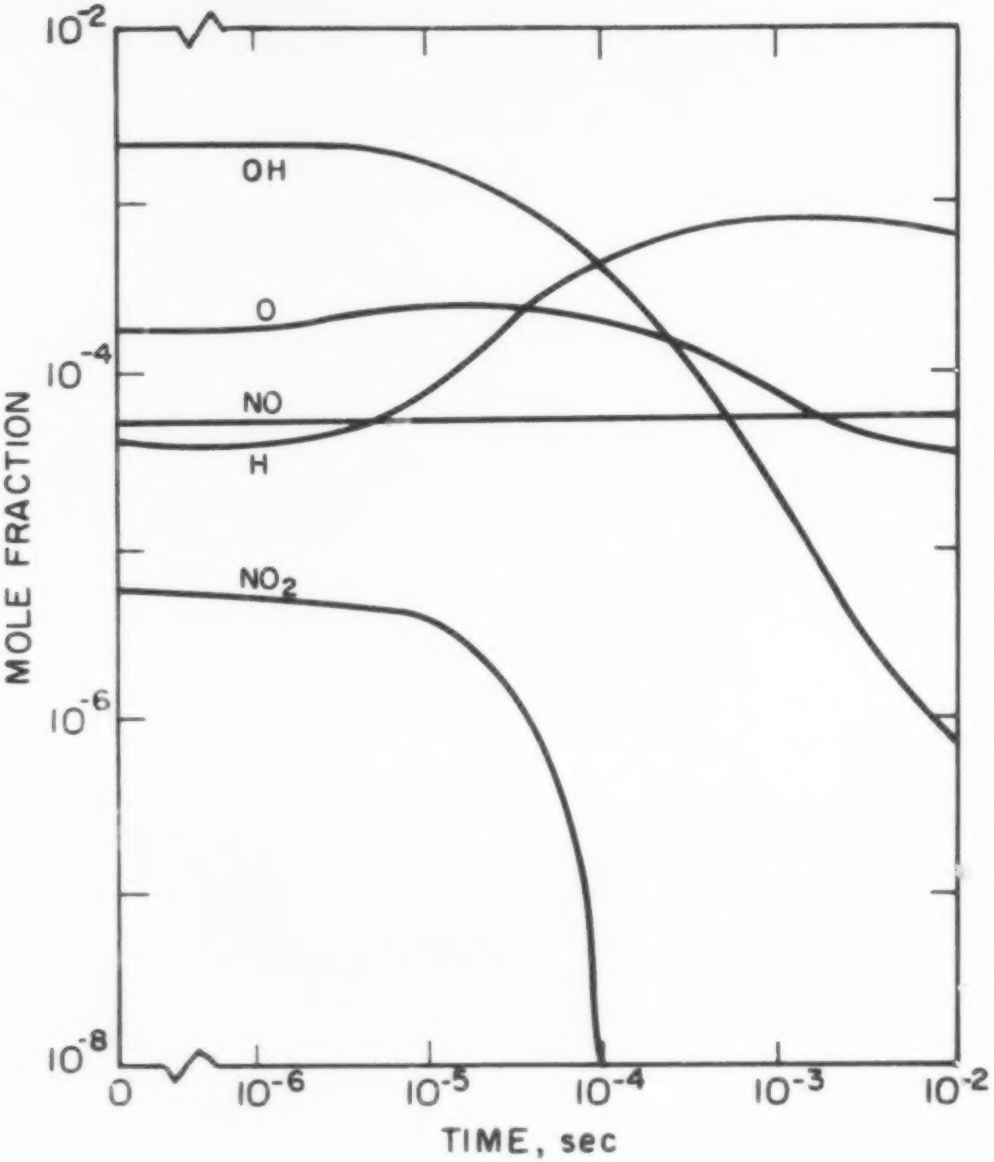

Figure E-10. Time history of selected species when equilibrium concentrations of radicals for $\phi = 0.8$ at 2050°K, 50 ppm NO and 6 ppm NO_2 are instantaneously cooled to 300°K, 80 torr.

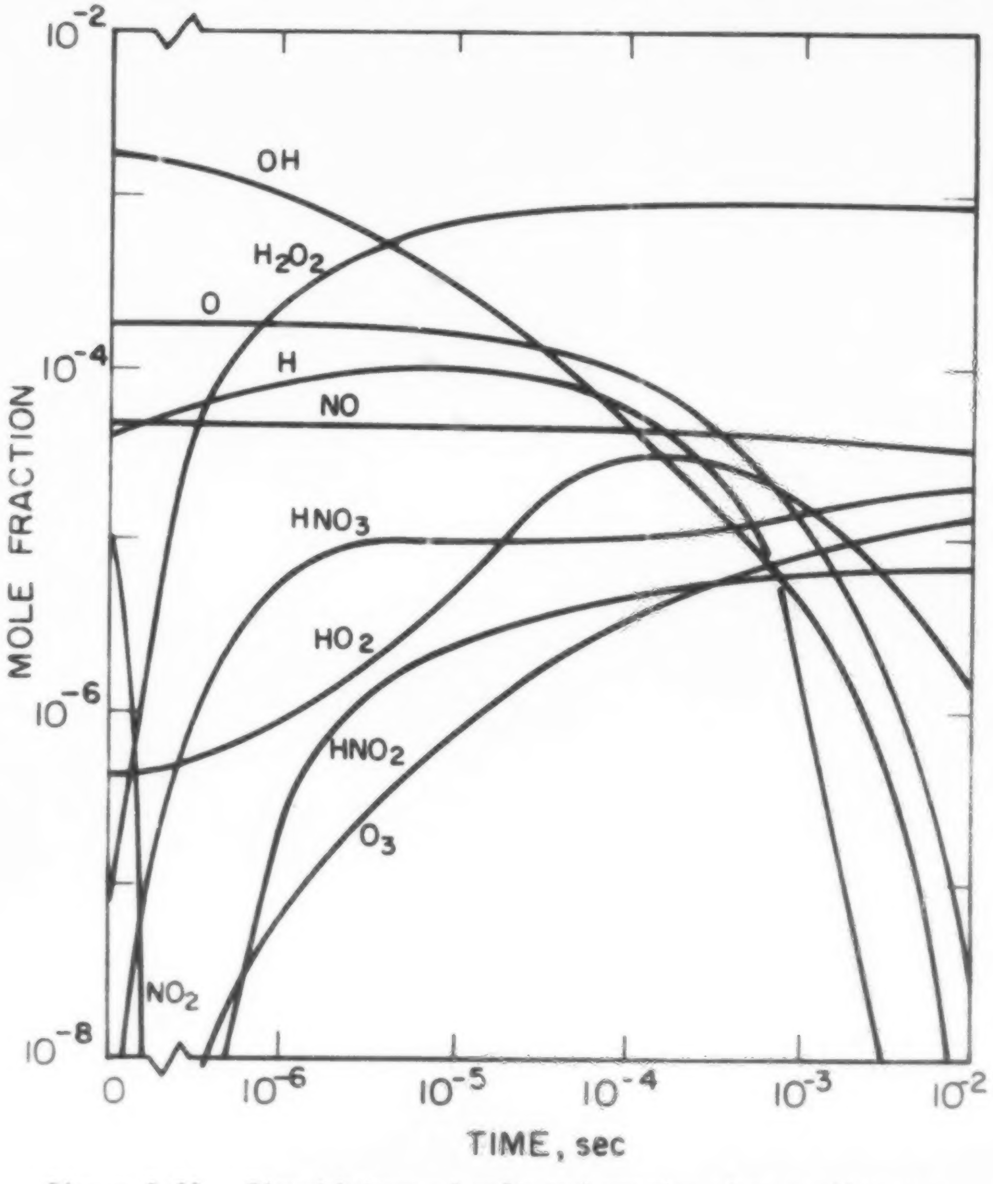

Figure E-11. Time history of selected species when equilibrium concentrations of radicals for $\phi = 0.8$ at 2050°K, 50 ppm NO and 10 ppm NO_2 are instantaneously cooled to 300°K, 80 torr including HOO, HNO_2, HNO_3, and O_3 mechanisms.

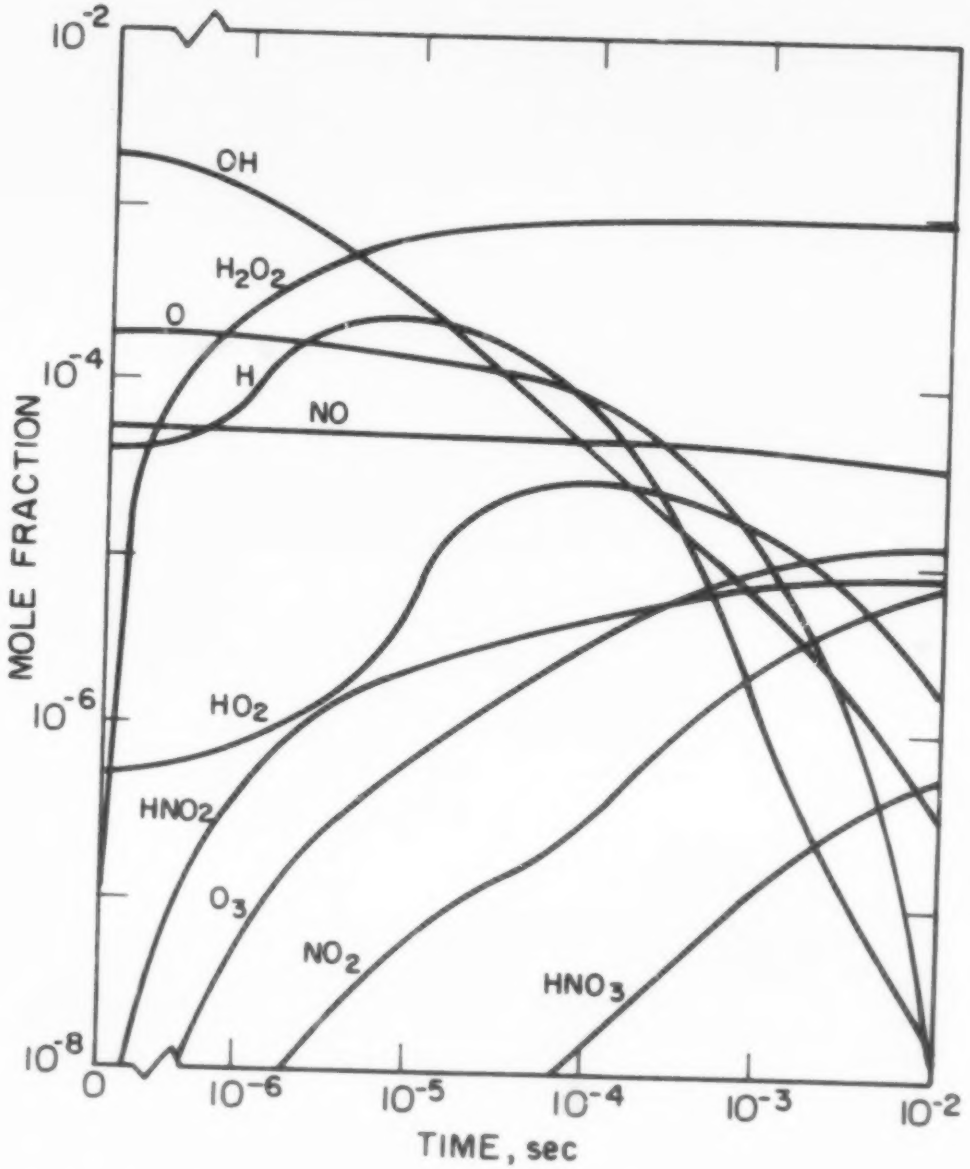

Figure E-12. Time history of selected species when equilibrium concentrations of radicals for φ = 0.8 at 2050°K, 50 ppm NO are instantaneously cooled to 300°K, 80 torr including HOO, HNO_2, HNO_3, and O_3 mechanisms.

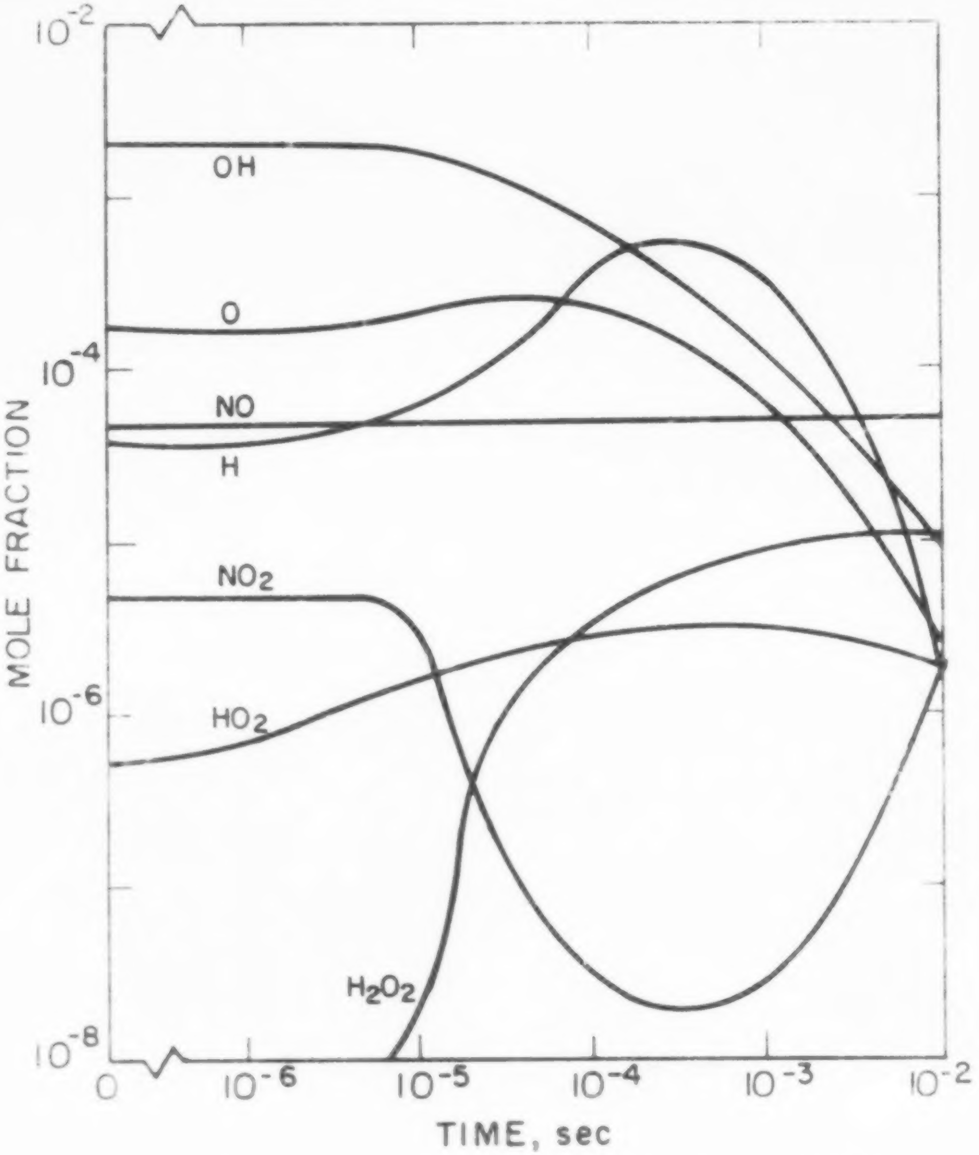

Figure E-13. Time history of selected species when equilibrium concentrations of radicals for $\phi = 0.8$ at 2050°K, 50 ppm NO and 6 ppm NO_2 are cooled linearly from 2000°K to 300°K in 20 msec, P = 80 torr.

APPENDIX F

Sampling Probes and Sampling Difficulties

F.1 Introduction

Several particular problems with sampling and analyzing for NO and NO_2 were discussed in Chapters 3, 4, 5 and Appendix E. This appendix attempts to treat sampling and analytical difficulties more comprehensively. In addition to mentioning and, where appropriate, elaborating upon the problems already treated in the text, several other problem areas are discussed.

There are three major areas of concern related to measuring gaseous species using physical sampling techniques: 1) obtaining a representative sample of the gases to be measured; 2) transporting the sample to the analytical equipment without altering its composition; and 3) accurately measuring the species of interest. Distinguishing among these three areas is not always easy because overlapping of effects is possible and often the same processes can be important in all three areas. For purposes of discussion in this appendix, the sampling and transfer problems are discussed together in section F.2 and the analysis problems are treated in section F.3.

F.2 Sampling for NO and NO_2

F.2.1 Sampling probes

As was indicated, the first problem in any physical sampling system is that of obtaining a representative sample. The problem to be treated here is that of not altering what is sampled by the probe rather than whether or not what is entering the probe is a good representation of the mean composition being sampled. (This latter problem is treated by Kent and Bilger (1973a, 1973b) and others.)

A number of choices must be made initially with regard to probe design: isokinetic or aerodynamic, cooled or uncooled, quartz or stainless steel or other material. No one type of probe is best for all sampling problems. In general, particulate studies require the use of isokinetic probes while for gas analysis aerodynamic type probes are usually used in order to quench the reactions and freeze the species in the sample. This is adequate for the major gaseous species, however as was discussed in Chapter 5 and Appendix E, rapid quenching can affect the NO/NO_2 distribution. Because of uncertainties in the mechanisms, rates of reactions, etc., the magnitude of this problem cannot be quantized and optimum probe designs cannot be accomplished at this time. Additional work is required in this area.

Once the sample is in the probe, several factors can affect the NO and NO_2. High temperature stainless steel is a known catalyst for the reduction of NO_2 to NO (Patterson *et al.*, 1970). Thus, uncooled stainless steel probes would not be expected to yield correct values for NO and NO_2 unless the walls are not heated above the catalytic ignition temperature (~500°K). Similar effects have been observed for uncooled quartz probes, and also at higher temperatures, formation of NO in uncooled quartz probes has been observed (Schefer, 1974).

Surface effects can also be significant in sampling probes. Tuttle et al. (1973) reported that aging of uncooled stainless steel probes was evident when sampling from fuel rich flames. Measurements using hydrogen fuel in the current combustion system resulted in aging of both quartz and stainless steel probes; NO and NO_2 both decreased with time. Problems with aging are particularly acute in fuel rich systems where the surfaces (or particulate coatings on the surfaces) are in a reduced state and tend to reduce NO and NO_2. No such aging has been noted in fuel lean systems.

It appears then that cooled aerodynamic probes offer the best chance for success when sampling for NO and NO_2. Potentially severe problems exist but these can be minimized or at least, in time, corrections can be developed.

F.2.2 Transfer System

Once the sample gases have been cooled and quench reactions stopped, homogeneous reactions should be unimportant in the transfer system. The normal time scale for such reactions are much longer than the usual sampling and transfer times. However, each sampling configuration should be evaluated independently to verify this conclusion.

Heterogeneous reactions, on the other hand, can be important. Surface effects in reducing atmospheres were mentioned above. The effects of carbon particulate were discussed in Chapter 4 and will not be repeated here. (Chang and Novakov (1974) and Tuttle et al. (1973) also discuss these and other soot reactions in some detail.) While the particulate reduces NO_2 to NO in the transfer line, the magnitude of its effect in the quench region is unknown. Also unknown is the extent to which the particulate interacts in reducing atmospheres. The work of Chang and Novakov (1974) indicates that these latter effects may be important. This entire area requires further work.

If water vapor is removed from the sample either in a water trap or by condensation in the system, it has been observed that NO_2 is removed from the system as well (Tuttle, et al., 1973). This represents a substantial source of error and water condensation should be avoided when making NO_2 measurements.

Reaction of NO and NO_2 with hydrocarbon species has also been reported (Tuttle, et al., 1973; Myerson, 1974). The reactions and rates for the most part are not well known; additional work is required in this area.

F.3 Analysis of NO and NO_2

There are several methods for measuring NO and NO_2 and the preferred techniques generally involve the chemiluminescent NO analyzer (Patterson, et al., 1970; Tuttle et al., 1973; Breitenbach and Shelef, 1973). NO_2 measurements require some form of thermal or catalytic converter to reduce the NO_2 to NO so that it can be measured. The usual materials are stainless steel or molybdenum. An acute problem with these converters is the aging or history of the converter. Stainless steel is particularly sensitive and requires a long conditioning period on oxygen rich samples in order to give accurate results. Also, stainless steel will not only reduce NO_2 to NO, but also NO to N_2 and O_2 under fuel rich conditions. This occurs when the converter is in a reduced state and requires only about 10-20 seconds to attain this state. Molybderum behaves similarly but is much less sensitive to conditioning. Once in an oxidized state, molybdenum convertors can function for minutes in a reducing atmsophere before starting to reduce NO. (These differences may be due to the fact that the stainless steel is primarily a thermal converter while the molybdenum is primarily a catalytic converter.) Accurate measurements of NO_2 can be made in fuel rich mixtures using a molybdenum converter if the converter is cycled with air or some other oxygen containing sample and the oxidized surface coating maintained.

The other major problem with NO and NO_2 measurements involves sample gas composition effects on the measured NO level. Interferences arise due to different third body efficiencies for quenching the electronically excited nitrogen dioxide, NO_2^*. This effect was discussed at length in Chapter 4.

F.4 Conclusion

Problems associated with sampling and analyzing for NO and NO_2 have been discussed. These include: reactions resulting from rapid quenching; heterogeneous reactions involving carbon particulate and condensed water; heterogeneous reactions on the walls of the system--particularly acute in fuel rich samples; and interferences in the analytical equipment. All of these areas require further work before the effects can be fully understood and corrections developed.

APPENDIX G

Computer Codes

G.1 Description of Programs

This appendix lists the nonstandard or modified computer codes used during the investigation. Sections G.2 and G.3 give the programs for listing and reducing the operating data from the experiments. The modified mass spectrometer data reduction program, MSDATA, is listed in section G.4 and the cracking patterns and calibration data that were used follows this listing. ADDCO, the program to correct the MSDATA output for CO and to correct CO for water vapor, is listed in section G.5. Plotting of this corrected mass spectrometer and CO data is accomplished using PLOT, section G.6; PLOT is based upon the University of California at Berkeley Graphic Display System. Finally, the modified version of GENMIX 4 which was used for the analytical modeling is presented in section G.7. GENMIX 4 consists of four routines: MAIN, AUX, STRIDE, and WF.

G.2 Operating Data Reduction

```
[illegible]

[illegible]
[illegible]
[illegible]
[illegible]
[illegible]
[illegible]
[illegible]
[illegible]
[illegible]
[illegible]
[illegible]
[illegible]
[illegible]
[illegible]
[illegible]
[illegible]
[illegible]
[illegible]
[illegible]
[illegible]
[illegible]
[illegible] CALCULATIONS
[illegible]
[illegible]
[illegible]
[illegible]
[illegible]
 20  READ [illegible] HEADING,SEC,T1,P1,F[illegible],FR,T12,P12,T13,T6,P6,T7,T8,
    1[illegible],T10,DP
 10  FORMAT[illegible]
     IF (T[illegible]) GO TO 30
     TBAR=(T13+T6)/2.
  30 [illegible] TBAR=30. C IF T13 AND T6 ARE NOT REPORTED
     IF (TBAR.GT.0.) GO TO 50
     TBAR=30.
  50 CONTINUE
C  AIR CALCULATIONS
     FINA=[illegible](DP*.4912)[illegible](T2+273.16)*FIID[illegible]
     WAIR=FINA*[illegible].0596*(TBAR+273.16)[illegible]*MWA
C  FREON[illegible] CALCULATION
     VOLF=[illegible]14.2056[illegible].0124456*[illegible]RF[illegible]0.0000009425*[illegible]RF[illegible]**2
C    CORRECT FOR DENSITY
     DF=SQRT(294.25*DP*.4912/((T12+273.16)*14.7))
     VOLFPF=VOLF*DF
     FMASSF=0.0000[illegible]*VOLFPF
     WFUEL=FMASSF*82.0596*(TBAR+273.16)[illegible]*MWF
C  RATIO FUEL AND AIR FLOWS
```

```
C GET AVERAGES OF THE [illegible] PARTITIONS
 [illegible] DO [illegible] I=1,9
      FINVBT(I)=FINVBT(I)/[illegible]
      VAIRT(I)=VAIRT(I)/[illegible]
      FMWSRT(I)=FMWSRT(I)/[illegible]
      VFUELS(I)=VFUELS(I)/[illegible]
      [illegible]
      [illegible]
      PRINT [illegible]
      FORMAT([illegible])
      DO [illegible] I=1,9
 [illegible] PRINT 60,NUM(I),I,FINVBT(I),VAIRT(I),FMWSRT(I),VFUELS(I),
     1[illegible]
 60   FORMAT([illegible])
      CALL EXIT
      END
```

G.3 Operating Data List

```
      PROGRAM TO LIST RAW OPERATING DATA

      [illegible]
      [illegible]
      [illegible]
      READ(10,CASE,HU,FMIN,SEC,T1,P1,FWREX,SS,T12,P13,T13,T6,F6,T7,T8,
     1T9,T10,T11,T16,BP
10    FORMAT(A8,I1,F1.0,F2.0,5F3.1,F3.2,2F4.1,F3.2,5F4.1,F3.1,F4.2)
      IF(T1.EQ.99.9) GO TU 20
      PRINT 3,CASE,HU,FMIN,SEC,T1,P1,FWREX,SS,T12,P13,T13,T6,F6,T7,T8,T9
     1,T10,T11,T16,BP
      FORMAT([illegible]
      [illegible]
      [illegible]
      [illegible]
      [illegible]
```

G.4 MSDATA

```
[illegible]

C     PROGRAM [illegible] DATA
      [illegible]
      [illegible]
      [illegible]
      [illegible]
     +[illegible]
      [illegible]
C     READ [illegible]
      [illegible]
   10 [illegible]
      READ [illegible]
  100 FORMAT[illegible]
      IF[illegible]
      [illegible]
      READ [illegible]
  110 FORMAT [illegible]
      [illegible]
   15 [illegible]
C     READ [illegible] TO CONTINUE
C      [illegible] IN THE CORRESPONDING
C       [illegible]
C     [illegible] DATA [illegible] CALIBRATION DATA
  [illegible] READ [illegible]
  [illegible] FORMAT [illegible]
      READ [illegible]
   16 CONTINUE
      READ [illegible],FDATA(12),FDATA(14),
     &FDATA[illegible],FDATA(18),FDATA[illegible],FDATA(26),
     &FDATA[illegible],FDATA(39),FDATA(40),
     &FDATA[illegible],FDATA[illegible],FDATA(44)
  125 FORMAT(I2,[illegible])
C     CHECK FOR END OF DATA, -1=NEW CALIB DATA, -2=NEW MASS NO, -3=EXIT
      IF(IA.EQ.-1) GO TO [illegible]
      IF(IA.EQ.-2) GO TO [illegible]
      IF(IA.EQ.-3) GO TO [illegible]
C     SET ZERO PEAKS [illegible] TO A SMALL VALUE TO AVOID SINGULARITY
      DO 850 I=1,50
      IF(FDATA(I).NE.0.) GO TO 850
      FDATA(I)=0.001
  850 CONTINUE
C     FIND NDATFK AND FILL MNODAT AND HT ARRAYS
      NDATFK=0
      DO 950 II=1,50
      IF(MNCK(II).EQ.0) GO TO 950
      NDATFK=NDATFK+1
      MNODAT(NDATFK)=II
      HT(NDATFK)=FDATA(II)
  950 CONTINUE
C     ARRANGE THE DATA INTO THE A(I,J) MATRIX
C     I = NO OF UNKNOWNS [illegible]
```

[illegible]

```
[illegible]
      CONTINUE
[illegible]
      CONTINUE
      IF(I.NE.1) GO TO 85
      TERM(1,I)=TERM(1,I)
      GO TO 90
   85 TERM(2,I) = TERM(2,I) + TERM(1,I)
   90 CONTINUE
      TERM=TERM(2,I)+TERM(1,I)
      IF(TERM.LE.0.) TERM=ABS(TERM)
  100 TERM(1,I)=SQRT(TERM)
      DO 110 I=1,NN
```

```
[illegible]
[illegible]
[illegible]
[illegible]
[illegible]
[illegible]
[illegible]
[illegible]
[illegible]
[illegible]

[illegible]

[illegible]
[illegible]
[illegible]
[illegible]
[illegible]
[illegible]
[illegible]
[illegible]
[illegible]
[illegible]
[illegible]
[illegible]
[illegible]
[illegible]
[illegible]
[illegible]
[illegible]
[illegible]
[illegible]
[illegible]
[illegible]
[illegible]
[illegible]
[illegible]
[illegible]
[illegible]
[illegible]
[illegible]
[illegible]
[illegible]
[illegible]
[illegible]
      RETURN
      STOP
      END
C     SMITHSONIAN ASTROPHYSICAL OBSERVATORY [illegible]
C     [illegible] LEAST SQUARES PROGRAM
[illegible]
[illegible]
[illegible]
```

```
      M=MM
      N=NN
      IP=IPP
      INVRSE=INVPS
C     AX=B NORMAL EQUATIONS.A IS RECTANGULAR MATRIX.WITH M ROWS.N COLUMNS
C     WX=W1 .NEW SET OF NORMAL EQUATIONS. W=TR(A)*A .W1= TR(A)*B..
C     TO FORM MATRIX  W .WITH N ROWS AND N COLUMNS. (TR= TRANSPOSE )
C  WT = -1. MEANS  NO WEIGHTS  IN PROG.   ASSIGN   WEIGHTS = 1.
C  INVRSE = 0. MEANS NO CALCULATIONS OF STD. ERRORS OF ( X )*********
C  INVRSE = 1. MEANS  STD. ERRORS ARE CALCULATED.
C  STDERR  = STANDARD ERRORS OF  UNKNOWNS ( X ) .
      KK=N+1
      IF(M-N) 80,83,81
   81 DO 5 J=1.N
      DO 5 JJ=1.N
      W(J.JJ) = 0.
      IF ( WT) 611.622.622
C   NO WEIGHTS CASE
 611  DO 51 I= 1.M
 51   W(J.JJ) = W(J.JJ) + A(I.J) * A(I.JJ)
      GO TO 5
C   WEIGHTS ARE PRESENT
 622  DO 52 I=1.M
 52   W(J.JJ) = W(J.JJ) + A(I.J) * A(I.JJ)  * WT(I)
 5    CONTINUE
C     TO FORM  MATRIX W1 . WHICH IS STORED IN N+1 TO N+P COLUMNS OF W.
C     W1 .WITH N ROWS AND IP COLUMNS.
      IF ( INVRSE ) 201.203.201
 203  KIP = IP
      GO TO 200
 201  KIP = 1
 200  DO 8 K = 1. KIP
      DO 7 J=1.N
      W(J.KK) = 0.
      IF ( WT) 612.623.623
 612  DO 511 I=1.M
 511  W(J.KK) = W(J.KK)+A(I.J)* B(I.K)
      GO TO 7
 623  DO 522 I= 1.M
 522  W(J.KK) = W(J.KK)+A(I.J)* B(I.K)  * WT(I)
 7    CONTINUE
 8    KK = KK + 1
      GO TO 106
   83 DO 12 I=1.N
      IF ( WT) 613.624.624
 613  DO 512 J=1.N
 512  W(I.J) = A(I.J)
      GO TO 12
 624  DO 523 J=1.N
 523  W(I.J) = A(I.J) * WT(I)
 12   CONTINUE
      KKK = N+IP
      J=1
      IF ( INVRSE ) 401.403.401
  403 KKK = KKK
      GO TO 400
  401 KKK = KI
  400 DO 13 II= II.KKK
      IF ( WT ) 614.625.625
  614 DO 513 I= 1.N
  513 W(I.JJ) = B(I.J)
      GO TO 13
  625 DO 524 I= 1.N
  524 W(I.JJ) = B(I.J) * WT(I)
   13 J=J+1
  106 IF ( INVRSE ) 71.72.71
   71 I2 = N + 2
      KIP = N + IP
      KK = N + 1
      DO 75 I=1.N
      DO 75 J = I2.KIP
      IF ( J - I - KK ) 73.74.73
   74 W(I.J) = 1.
      GO TO 75
   73 W(I.J) = 0.
   75 CONTINUE
   72 CALL TRIANG (W.N.IP. DET )
C     WHERE W IS THE MATRIX WITH N ROWS AND(N+IP)COLUMNS TO BE TRIANGULA
C     RIZED
C     TO TEST THE SINGULARITY OF MATRIX W.. U = IP(A(N) . N(M) . N).
      IF ( DET ) 82.80.82
   82 CONTINUE
      GO TO 103
   80 SUM = 1
      GO TO 104
  103 CALL  SOLVE  (W.N.IP.X)
C     WHERE W IS THE TRIANGULARIZED. X IS THE SOLUTION  MATRIX  WITH
C     N ROWS AND  IP  COLUMNS.
C     TO COMPUTE RESIDUAL MATRIX . U = A*X - B .U IS RESIDUAL MATRIX(M.P)
  105 DO 16 I=1.M
      DO 16 K=1.IP
      U(I.K) =0.
      DO 15 J=1.N
   15 U(I.K) = U(I.K) + A(I.J) * X(J.K )
 16   U(I.K) = B(I.K) - U(I.K)
      DO 18 K=1.IP
      SUM(K) = 0.
      DO 18 I=1.M
   18 SUM(K) =SUM(K) +(U(I.K))**2
      IF (M.EQ.N) GO TO 104
      IF ( INVRSE ) 722.104.722
 722  DO 723  I = 1.N
      DO  723 J= 2.IP
 723  X(I.J)=X(I.J)*(SUM(1)/FLOAT (M-N))
      DO 724 I = 1.N
      STDERR(I) = 0.
      II = I + 1
 724  STDERR(I) = SQRT ( X(I.II))
  104 RETURN
      END
CTRIANG  TO BE USED WITH SUBROUTINE GLSP
      SUBROUTINE TRIANG(A.M.N.DET )
C .                WHERE A IS THE MATRIX WITH M ROWS AND M+N COLUMNS TO
C                  BE TRIANGULARIZED.
      DIMENSION A(10.21)
      DET=1.
      MM1=M-1
      MPN=M+N
      DO 5 J=1.MM1
      MAXX = J
      VALUE = ABS  ( A(J.J))
      JP1=J+1
      DO 1 K=JP1.M
      IF ( VALUE - ABS (A(K.J)))  2.1.1
   2  VALUE = ABS (A(K.J))
      MAXX=K
   1  CONTINUE
      DO 3 L=J.MPN
      TEMP = A(MAXX.L)
      A(MAXX.L) = A(J.L)
   3  A(J.L) = TEMP
      IF ( MAXX-J) 7.6.7
   7  DET  = - DET
   6  DET = DET*A(J.J)
      ROW = A(J.J)
      DO 4 L=J.MPN
   4  A(J.L) = A(J.L)/ROW
      DO 5 K=JP1.M
      ROW = A(K.J)
      DO 5 L=J.MPN
   5  A(K.L) = A(K.L)-ROW*A(J.L)
      DET = DET*A(M.M)
      ROW = A(M.M)
      DO 9 L = M.MPN
   9  A(M.L) = A(M.L)/ROW
      RETURN
      END
CSOLVE   TO BE USED WITH SUBROUTINE GLSP
      SUBROUTINE SOLVE(A.M.N.X)
C                WHERE A IS THE TRIANGULARIZED MATRIX WITH M ROWS AND
C                M+N COLUMNS.
C                      X IS THE SOLUTION MATRIX WITH M ROWS AND N
C                COLUMNS.
      DIMENSION A(10.21).X(10.11)
      MM1=M-1
      DO 2 L=1.N
      MPL=M+L
      DO 2 K=1.MM1
      MMK=M-K
      MMKP1=MMK+1
      X(M.L)-A(M.MPL) A(M.M)
      SUM-0.
      DO 3 I-MMKP1.M
3     SUM-SUM+A(MMK.I)*X(I.L)
2     X(MMK.L)-A(MMK.MPL)-SUM
      RETURN
      END

H2O         18 3 .341
17 36.9 18 100. 16.182
N2          28 6 1.0
14 5.2  27 2.5  28 100. 29 0.7  16.06   32.03
O2          32 2.3817
1612.4  32100.
CO2         44 5 .511
124.53  141.93  1612.2  2861.4  44100.              59.166  40.223
C3H8        4415 93.
14.0396 15.0793 16.0524 26.084  27.4154 29.9808 231.00  38.055
41.145  42.0864 43.223  44.3298 32.0017
END     000000000
            11111       11    1            1
```

G.5 ADDCO

```
C
      PROGRAM ADDCO(INPUT.OUTPUT.PUNCH)
C
C  PROGRAM TO ADJUST MOLEFRACTIONS FOR CO AND H2O
      DIMENSION D(5).ID(5).IPCT(5)
      PRINT 3
 3    FORMAT(1H1)
  5   CONTINUE
      READ 10.TCASE.TAX.THORZ.TVERT.(D(I).IPCT(I).I=1.5).CO
 10   FORMAT(3A4.A1.5(F4.4.I2.1X).F5.5)
      IF(CO.EQ.0.99999) GO TO 35
      CO=CO/10.
      IF(CO.LE.0.009) GO TO 20
      B1=CO*(1.-((D(1)-CO*D(1))/(1.-D(1)*CO)))
      B2=1.-B1
      CO=B1
      DO 15 I=1.5
 15   D(I)=D(I)*B2
 20   ICO=CO*1000000
      DO 25 I=1.5
 25   ID(I)=D(I)*10000
      PUNCH 30.TCASE.TAX.THORZ.TVERT.(ID(I).IPLT(I).I=1.5).ICO
 30   FORMAT(   3A4.A1.5(I4.I2.1X).I5)
      PRINT 31.TCASE.TAX.THORZ.TVERT.(ID(I).IPCT(I).I=1.5).ICO
 31   FORMAT(1X.3A4.A1.5(I4.I2.1X).I5)
      GO TO 5
 35   CALL EXIT
      END
```

G.6 PLOT

```
      PROGRAM PLOT(INPUT.OUTPUT.TAPE99)

      DIMENSION SL(8).CON(16.6) .II(16).IP(16).P(16).III(16)
      DIMENSION P1(16)
      COMMON S(30)
      RADIUS=0.1875
      DIA=0.375
      S(1)=0.8
      S(2)=1.0
      S(3)=0.4
      S(4)=0.
      S(5)=-2.
      S(6)=5.
      S(7)=8.
      S(8)=4.666
      S(9)=8.
      S(10)=7.
      S(11)=1.
      S(12)=99.
      S(14)=1.
      S(15)=1.
      S(17)=.1
      S(18)=.111
      S(19)=0.
      S(20)=0.
      S(21)=1.
      S(28)=2.
      SL(1)=16.
      SL(2) = 22.
      SL(3) = 23.
      SL(4) = 13.
      SL(5) = 24.
      SL(6) = 21.
      J = 1
      JA = 1
      PRINT 1
 1    FORMAT(1H1)
      PRINT 2
 2    FORMAT(/.4  DAY HW X    R       R/A   H2O    N2/2    O2    CO2    C
     13H8    CO+./)
11    READ 10.II(J).III(J).IP(J).P(J).(CON(J.I).I=1.6)
 10   FORMAT(I2.I2.I4.F4.3.1X.F4.4.3X.F4.4.3X.F4.4.3X.F4.4.3X.F4.4.2X.
     1F6.6)
      IF(II(J).EQ.-1) GO TO 4
      P1(J)=P(J)
      P(J)=P(J)/RADIUS
      CON(J.2)=CON(J.2)/2.
      IF(J.EQ.1) GO TO 6
      IF(IP(J).NE.IP(J-1)) GO TO 14
6      J = J+1
      GO TO 11
   14 CONTINUE
```

```
      XDDIA=IP(J-1)/DIA/100.
      IF(J-1.GE.3) GO TO 15
      PRINT 21.II(J-1).III(J-1).IP(J-1).XDDIA
      JJ=J-1
      DO 24 K=1.JJ
   24 PRINT 23.II(K).III(K).IP(K).P1(K).P(K).(CON(K.I).I=1.6)
   21 FORMAT(/.*  TOO FEW POINTS TO PLOT IN CASE *.2I2.2X.*AXIAL POSITIO
     1N=*.I4.2X.*X/D=*.F6.3)
      GO TO 13
   15 CONTINUE
      S(13) = J-1
      S(24)=0.
      S(25)=0.
      S(26)=.111
      S(27)=0.
      CALL SAXLIT(S)
      CALL SAXLIR(S)
      CALL NODLIT(S)
      CALL NODLIB(S)
      CALL NODLIL(S)
      CALL NODLIR(S)
      CALL AXLILI(S)
      DO 16 I=1.6
   16 CALL PLT(CON(1.I).P(1).SL(I))
      PRINT 20.II(J-1).III(J-1).IP(J-1).XDDIA
   20 FORMAT(/2X.*THE FOLLOWING DATA IS FOR CASE * .2I2.*  AXIAL POSITIO
     1N=*.I4.2X.*X/D=*.F6.3)
      JJ=J-1
      DO 22 K=1.JJ
   22 PRINT 23.II(K).III(K).IP(K).P1(K).P(K).(CON(K.I).I=1.6)
   23 FORMAT(3X.2I2.I4.8F7.4)
      IF(JA.EQ.15) GO TO 4
      JA = JA+ 1
      CALL NXTFRM(S)
   13 II(1) = II(J)
      III(1)=III(J)
      IP(1) = IP(J)
      P(1) = P(J)
      P1(1)=P1(J)
      DO 3 I=1.6
    3 CON(1.I) = CON(J.I)
      J = 2
      GO TO 11
    4 CALL GDSEND(S)
      STOP
      END
      SUBROUTINE PLT(X.Y.SS)
      DIMENSION X(20).Y(20)
      COMMON S(30)
      S(16) = SS
      CALL PSLILI(X.Y.S)
      RETURN
      END
```

G.7 GEMINIX 4

G.7.1 MAIN

```
C
C**3.3.70********************** G E N M I X 4 ******************************
C**********  D.B.SPALDING. IMPERIAL COLLEGE. AUGUST. 1969  *************
C**********  GENMIX 4 VERSION OF THE PATANKAR-SPALDING PROGRAM  ********
C
C  PROGRAM MODIFIED FOR SWIRLING DUCT FLOW.  NICK CERNANSKY  JUNE 1974
C
C
      PROGRAM MAIN(INPUT.OUTPUT.TAPE5=INPUT.TAPE6=OUTPUT)
C
CHAPTER0000000000000000000  PRELIMINARIES  00000000000000000000000000
CHAPTER 0  **************  DIMENSIONS AND COMMON BLOCKS  **************
      DIMENSION RDR(43)
      COMMON/GENRAL/ AJE(5).AJI(5).CSALFA.DPDX(43).DX.EMU(43).F(5.43).
     1  FS(5.43).H.IFIN.INDE(5).INDI(5).ISTEP.ITEST.IUTRAP.KEX.KIN.KRAD.
     2  N.NEQ.NPH.NP1.NP2.NP3.OM(43).PEI.PR(5).PREF(5.43).PSIE.PSII.
     3  R(43).RHO(43).RME.RMI.RU(43).SD(5.43).SU(5.43).TAUE.TAUI.U(43).
     4  XD.XU.Y(43).YE.YI
      COMMON/GM4/ AK.ALMG.ARRCON.EWALL.IPRINT.FR.AFU.OXDFU.PREEXP.PRESS.
     1   UBAR.UFAC.TMIN.ELMXFC.ELFRFC
      COMMON/NOX/ TFAC.PREXNO.ARCONO
      COMMON/RAD/ IRAD.EMISSG.EMISSP.STPHBZ.TCUT.OXCUT
C  ------------------------------------------------------------------
CHAPTER1111111111111111  PARAMETERS AND CONTROL INDICES  111111111111
C    THE FOLLOWING VARIABLES ARE USED IN THE RADIATION MODEL IN AUX
      IRAD=0
      EMISSG=0.2
      EMISSP=0.8
      OXCUT=0.05
      STPHBZ=5.7*10.**-8.
      TCUT=1300.
C    TFAC.PREXNO.ARCONO ARE USED FOR NO KINETICS IN AUX
      ARCONO=68222.
      TFAC=1.0
      PREXNO=10.**15.563
C    ELMXFC AND ELFRFC ARE USED IN THE TURB MODEL IN AUX
      ELFRFC=0.012
      ELMXFC=0.2
      ITB=300
      IPRINT=0
      ITEST=0
      IUTRAP=2
      NSTA=10
C  ------------------------------------------------------------------
CHAPTER2222222222222222222222  GRID AND GEOMETRY  2222222222222222222
      DX= 1.0E-10
      DXU=DX
      FRA=0.02
      N=30
           NP1=N+1
           NP2=N+2
           NP3=N+3
           OM(1)=0.
           DM(NP3)=1.
C     DM(I)S NOW SET IN CHAPTER 5 TO GET SPECIAL GRID
           ISTEP=0
      LASTEP=700
           XU=0.
           IFIN=0
      XULAST=0.2
      ULIN=.01
C     R(1) ADJUSTMENT MADE JUST BEFORE CALL STRIDE(1)
           KRAD=1
           CSALFA=1.
      KIN=3
           KEX=1
C  -----------------------------------------------------------------------
CHAPTER3333333333333333333333333  DEPENDENT VARIABLES SELECTION  3333333
C       U(I)=VELOCITY
C     F(1.I)=STAGNATION ENTHALPY
C     F(2.I)=CONCENTRATION OF FUEL
C     F(3.I)=CONCENTRATION OF OXIDANT-OXDFU*F(2.I)=PHI
C     F(4.I)=SWIRL VELOCITY*RADIUS
C     F(5.I)=CONCENTRATION OF NO
C     FS(1.I)=CONCENTRATION OF OXIDANT
C     FS(2.I)=TEMPERATURE
C     FS(3.I)=CONCENTRATION OF PRODUCT
C     FS(4.I)= CENTRIFUGAL FORCE
C     PRES(I)= PRESSURE FIELD
      NEQ=6
           NPH=NEQ-1
C  -----------------------------------------------------------------------
CHAPTER4444444444444444444444444  MATERIAL CONSTANTS  4444444444444444
C                                                  S.I. UNITS
           GASCON=8300.
C   ASSUME  C=CFU*T-10.. ETC
C      SEE INITIAL PROFILES AND T CALCULATION FOR ADJUSTMENTS
      CFU=1000.
      COX=1000.
      CPR=1000.
      CMIX=1000.
      WFU=44.
      WOX=32.
      WPR=28.
      VISFU=    .000001
      VISOX=    .000001
      VISPR=.000001
C     ARRCON IS ACTIVATION ENERGY DIVIDED BY UNIVERSAL GAS CONSTANT
      ARRCON=10000.
      PREEXF=.02
      HFU=40000000.
      OXDFU=3.63
C    TMIN IS THE MINIMUM IGNITION TEMPERATURE
      TMIN=300.
      DO 40 J=1.NPH
      PR(J)=.7
      PREF(J.1)=.86
   40 A=.9
      AK=.435
      ALMG=.09
      FR=.033
      DFAC=.01
C  ---------------------------------------------------------------------
CHAPTER55555555555555555555555555555555  INITIAL CONDITIONS  555555555
      DIAM=0.375*0.0254
      RADIUS=0.1875*0.0254
      TWALL=299.
      TA=ITB
      TF=ITB
C    CHANGE BOTH U'S AND FLO'S WHEN VELOCITY RATIO CHANGES
C   FLO'S ARE FLOW RATES / (2.*PI)
C   VA/VF=45
      UA=2.54*TA/300.
      UF=0.0570*TF/300.
      FLOA=0.0011777
      FLOF=0.0000011777
C    PRESS IS THE INITIAL PRESSURE ON THE CENTERLINE
      PRESS=      100 000.
      IPDDS=0.
      KSII=0.
      R(1)=0.
      OMDIV=FLOF/(FLOF+FLOA)
C    SET UP SPECIAL GRID
C       NIT=NUMBER OF GRIDS IN FUEL TUBE
      NIT=10
      NITP2=NIT+2
      NITP3=NIT+3
      DO 10 I=2.NITP2
   10 OM(I)=OMDIV*FLOAT(I-2)/FLOAT(NIT)
      NNNIT=N-NIT
      DO 11 I=NITP3.NP2
   11 OM(I)=OMDIV+((1.-OMDIV)*FLOAT(I-NITP2)/FLOAT(NNNIT))**2.
C  INITIAL PROFILES ARE UNIFORM
          DO 50 I=1.NP3
          IF(OM(I).GT.OMDIV) GO TO 51
      U(I)=UF
          F(2.I)=1.
      F(1.I)=CFU*TF+.5*UF*UF*F(2.I)*HFU
      F(1.I)=F(1.I)+0.1*TF*TF
      F(3.I)=-OXDFU
      F(4.I)=0.
      F(5.I)=0.
          GO TO 50
 51   U(I)=UA
          F(2.I)=0.
          F(3.I)=.232
C  ASSUME R*V=R*UA*TAN(ANGLE)
C    S=.318.A=25.TAN=.466 . S=.248.A=20.TAN=.364 . S=30.A30%TAN=.577
C  SET F(4.I)=V HERE. MULTIPLY BY R AFTER STRIDE 1
```

```
      F(4.I)=0.466*UA
      F(5.I)=0.
      F(1.I)=(CPR*.768+COX*.232)*TA+.5*UA*UA
      F(1.I)=F(1.I)+0.1*TA*TA
   50       CONTINUE
            F(1.NP3)=(CPR*.768+COX*.232)*TWALL
      FEI=FLOF+FLOW
            PSIE=PSII+FEI
CHAPTER6666666666666666666666666666  THERMODYNAMIC PROPERTIES  666666
C  *********************  START OF MAIN LOOP  *********************
   60 CONTINUE
C  -------------------------------------------  TEST 1
      IF(ITEST.EQ.0) GO TO 1001
      TEST=1001.
      WRITE(6.107) TEST.R(1).PRESS.DX
      WRITE (6.101) (U(I).I=1.NP3)
      WRITE (6.101) (F(1.I).I=1.NP3)
      WRITE (6.101) (F(2.I).I=1.NP3)
      WRITE (6.101) (F(3.I).I=1.NP3)
      WRITE(6.101) (F(4.I).I=1.NP3)
 1001 CONTINUE
      DXUU=DXU
      DXU=DX
C    PRESSURE IS PRESSURE AT OUTER WALL
      PRESS=PRESS+DPDIX*DX
      PDGSCN=PRESS/GASCON
      DO 61 I=1.NP3
C     CORRECTION OF EFFECTS OF EXCESSIVE REACTION
      FS(1.I)=F(3.I)+OXDFU*F(2.I)
      IF(I.EQ.1.OR.I.EQ.NP3) GO TO 62
      IF(ISTEP.EQ.0) GO TO 62
      IF(SU(2.I)+SD(2.I)*F(2.I).LE.0.) GO TO 62
      IF(SU(2.I).EQ.0.) GO TO 63
C------------------------------------------------  FUEL-RICH REGION
      FS(1.I)=0.
      F(2.I)=-F(3.I)/OXDFU
      GO TO 62
C--------------------------------------------  OXIDANT-RICH REGION
   63 F(2.I)=0.
      FS(1.I)=F(3.I)
   62 CONTINUE
      FS(3.I)=1.-F(2.I)-FS(1.I)
      ENTH=F(1.I)-.5*U(I)*U(I)-HFU*F(2.I)
      FS(2.I)=0.5*(SQRT(100.*CMIX*CMIX+40.*ENTH)-10.*CMIX)
      IF(FS(2.I).LE.0.) FS(2.I)=TF
            RHOCON=PDGSCN/FS(2.I)
      VMIX=F(2.I)/WFU+FS(1.I)/WOX+FS(3.I)/WPR
   61       RHO(I)=RHOCON/VMIX
C  -------------------------------------------------  TEST 2
      IF(ITEST.EQ.0) GO TO 1002
      TEST=1002.
      WRITE(6.100) TEST
      WRITE(6.101) (FS(1.I).I=1.NP3)
      WRITE (6,101) (FS(2,I),I=1,NP3)
      WRITE (6,101) (FS(3,I),I=1,NP3)
      WRITE (6,101) (RHO(I),I=1,NP3)
 1002 CONTINUE
C-----------------------------------------------------------------------
C   STRIDE 1 STRIDE 1 STRIDE 1 STRIDE 1 STRIDE 1 STRIDE 1
C------------------------------------------------------------ADJUST R(1)
      IF(KIN.EQ.2.AND.KRAD.EQ.1) R(1)=SQRT(ABS(2.*PSI1/(RHO(1)*U(1))))
      CALL STRIDE(1)
C-----------------------------------------------------------------------
CHAPTER7777777777777777777777777777777777777  FORWARD STEP  7777777
C  CALCULATE Y OF R AND STORE IN F(4,I) THE FIRST TIME THROUGH
      IF(ISTEP.GT.0) GO TO 75
      DO 74 I=1,NP3
   74 F(4,I)=F(4,I)*R(I)
   75 CONTINUE
      D=ERRAY(NP3)
   71 IF(D .GT.0.) GO TO 72
      WRITE(6,700)
  700 FORMAT([illegible] IS ZERO OR NEGATIVE)
            IFIN=1
            GO TO 102
   72 IF([illegible]) GO TO 73
      [illegible]
      IF([illegible].NE.0.) GO TO [illegible]
      [illegible]
      [illegible]
   73 CONTINUE
      DO 76 I=1,NP3
   76 [illegible] RADIUS
C FURTHER ADJUSTMENTS TO DX ARE MADE IN CHAPTERS 8 AND 9
C-----------------------------------------------------------------------
CHAPTER8888888888888888888888888888  ADJUST LONGITUDINAL CONDITIONS  888888
C-------------------------------BOTH WALLS IMPERVIOUS.INNER WALLADIABATIC
      F(1,NP3)=CHI*TWALL+RFU*F(2,NP3)
      F(2,NP3)=TWALL
      F(4,1)=0.
      F(4,NP3)=0.
            IF(ISTEP.GT.0) GO TO 80
            TAUI=0.
            TAUE=0.
      U(1)=0.
            U(NP3)=0.
      EWALL=0.
      EMI=0.
      EME=0.
      DO 81 J=1,NFH
      INDI(J)=2
      INDE(J)=2
      AJI(J)=0.
   81 AJE(J)=0.
      INDI(4)=1
      INDE(4)=1
```

```
              ROUT=R(NP3)
              FLOTOT=PEI
              AD2PI=(ROUT*ROUT-R(1)*R(1))/2.
   80   CONTINUE
C-----  --------------------  PRELIMINARIES FOR PRESSURE GRADIENT
    86 UBAR=0.
       DO 83 I=2.NP1
   83         UBAR=UBAR+(U(I)+U(I+1))* (OM(I+1)-OM(I))
              UBAR=.5*UBAR
       AD2PI=ROUT**2*.5
       IF(KIN.EQ.1) AD2PI=AD2PI-R(1)**2*.5
              DYNHED=UBAR*FLOTOT/AD2PI
              REX=R(NP3)-ROUT
       REXD=REX/ROUT
       IF(XD.EQ.XULAST) GO TO 88
       IF(ABS(REXD).GT..01) DX=DX*.01/ABS(REXD)
       XD=XU+DX
C******************  SPECIFICATION OF VARIATION OF OUTER RADIUS
   88  ROUT=ROUT
C******************  PRESSURE GRADIENT
C     PRESSURE GRADIENT
C           IGNORE LATERAL PRESSURE GRADIENT
       DA=-.1*ROUT*(R(NP3)-ROUT)
       DPDDX=(DYNHED*DA/DX-TAUI*R(1)-TAUE*R(NP3))/AD2PI
    87 CONTINUE
       DO 108 I=1.NP3
       DPDX(I)=DPDDX
   108 CONTINUE
C  ----------------- --------------------------  TEST 3
       IF(ITEST.EQ.0) GO TO 1003
       TEST=1003.
       WRITE(6.100) TEST.UBAR.DYNHED.DX.DA.DPDDX.REXD.RMI.KIN.KEX.
      1                                                        ISTEP.IEND
       WRITE (6.101) (Y(I).I=1.NP3)
       WRITE (6.101) (R(I).I=1.NP3)
       WRITE(6.101) (RU(I).I=1.NP3)
  1003 CONTINUE
C  ------- ------------------------------------------------------------------
CHAPTER9999 9999999999999999  TRANSPORT AND ENTRAINMENT PROPERTIES  9999
C  LAMINAR VISCOSITY ACCORDING TO SQUARE-ROOT FORMULA
C                                WITH WEIGHTING ACCORDING TO MASS FRACTION
    90        DO 92 I=1.NP3
       ROOT=SQRT(FS(2.I))
       VFU=VISFU*ROOT
       VOX=VISOX*ROOT
       VPR=VISPR*RUOT
    92 EMU(I)=VFU*F(2.I)+VOX*FS(1.I)+VPR*FS(3.I)
C  ----------------------------------------------  TEST 4
       IF(ITEST.EQ.0) GO TO 1004
       TEST=1004.
       WRITE (6.100) TEST.RMI.RME.PEI
       WRITE (6.101) (EMU(I).I=1.NP3)
  1004 CONTINUE
```

```
      CALL AUX
C ------------------------------- ENTRAINMENT CONTROL --------------------
            IF(KIN.NE.2) GO TO 94
      RAT=ABS((U(3)-U(1))/(U(NP3)-U(1)+1.E-30))
      IF(RAT.LT.ULIM) EM U(2)=EM U(2)*RAT/ULIM
      RMI=-2.*EM U(2)
   94       CONTINUE
      IF(KEX.NE.2) GO TO 97
      RAT=ABS((U(NP1)-U(NP3))/(U(NP3)-U(1)+1.E-30))
      IF(RAT.LT.ULIM) EM U(NP1)=EM U(NP1)*RAT/ULIM
      RME=-2.*EM U(NP1)
   97 IF(XD.EQ.XULAST) GO TO 96
C     LIMIT ON INCREMENT IN PEI
      IF((RMI-RME)*DX.LT.PEI*.01) GO TO 96
      DX=.01*PEI/(RMI-RME)
      XD=XU+DX
   96 CONTINUE
C  STRIDE 2 STRIDE 2 STRIDE 2 STRIDE 2 STRIDE 2.......
   95 CALL STRIDE(2)
C ----------------------------------------------------------------------
CHAPTER 10 10 10 10 10 10 10 10 10 10 10 10 10 10 10   OUTPUT   10 10 10
            IF(ISTEP.GT.0) GO TO 106
            ANSTA=NSTA
CHAPTER 10A  ------------ ------------------------- HEADINGS
      REY=(FLOA+FLOF)*4./EMU(1)/R(NP3)
      EQRAT=FLOF*OXDEN/FLOA/.232
      AMACH=UBAR/SQRT(1.4*GASCON*TF/WFM)
      WRITE(6.1010) UA.UF.TA.TF.PRESS.PREEXP.REY.EQRAT.AMACH
 1010 FORMAT(1H1.2X.2HUA.9X.2HUF.9X.2HTA.5X.2HTF.9X.
     1 5HPRESS.6X.6HPREEXP.5X.3HREY.8X.5HEQRAT.6X.5HAMACH/1H .1P11E11.3)
  107 FORMAT(1H1.1P8E 11.3. 4I6)
  100 FORMAT(1H .1P8E 11.3. 4I6)
      WRITE(6.1011) (OM(I).I=1.NP3)
 1011 FORMAT(6H OM'S .1P11E11.3/(1H .4X.1P11E11.3))
  101       FORMAT(1H .5X.1P11E11.3)
      PRESS1=PRESS
  106       CONTINUE
C ----------------------------- ------------- TEST S.
      IF(ITEST.EQ.0) GO TO 1005
      TEST=1005.
      WRITE(6.100) TEST.RMI.RME.DX
 1005 CONTINUE
CHAPTER 10B --------------------------------------- TESTS FOR PRINTOUT
      IPRINT=0
      IF(ISTEP.EQ.0) GO TO 102
      IF(ITEST.EQ.1) GO TO 102
      IF(IFIN.EQ.1) GO TO 102
      IF(FLOAT(ISTEP/NSTA).EQ.FLOAT(ISTEP)/ANSTA) GO TO 102
      IPRINT=0
      GO TO 105
CHAPTER 10C --------------------------------------- STATION VARIABLES
  102 IPRINT=1
  103 IPRINT=IPRINT+1
```

```
      PRDRP=(PRESS1-PRESS)
      TAUED=TAUE/DYNHED
      FUFLUX=0.
      FIFLUX=0.
      F1BAR=0.
      DO 108 I=2.NP1
      OMDIF=.5*(OM(I+1)-OM(I))
      FUFLUX=FUFLUX+OMDIF*(F(2.I)+F(2.I+1))
      F1BAR=F1BAR+OMDIF*(F(1.I)+F(1.I+1))
  108 FIFLUX=FIFLUX+OMDIF*(F(3.I)+F(3.I+1))
      AJED=AJE(1)*.5*(R(1)+R(NP3))+Y(NP3)/PEI/
     1                        (F1BAR-F(1.NP3)-HFU*(FUFLUX-F(2,NF3)))
      FUFLUX=PEI*FUFLUX
      FIFLUX=PEI*(FIFLUX-.232)/PSII*.232
      XDD=XU/DIAM
      WRITE (6.1012)XU.PRDRP.TAUED.REXD.UBAR.FUFLUX.FIFLUX.AJED.
     1                 ISTEP.XDD
 1012 FORMAT(//.3X.2HXU.9X.5HPRDRP.6X.5HTAUED.6X.4HREXD.7X.4HUBAR.7X.
     1 6HFUFLUX.5X.6HFIFLUX.5X.4HAJED.7X.5HISTEP./1H .1P8E11.3.I6.
     2 /.3X.5HX/D= .1P8E11.3)
CHAPTER 10D  - -------------------------------------  PROFILE VARIABLES
C  ----------------------------------------------- TEST 6
      IF(ITEST.EQ.0) GO TO 1006
      TEST=1006.
      WRITE (6.100) TEST
 1006 CONTINUE
      IF(IPRINT.LT.2) GO TO 105
  104 CONTINUE
C  PROFILE VARIABLE HEADING
      WRITE(6.1096)
 1096 FORMAT(/.8X.*R/A'S*.6X.*R'S*.8X.*U'S*.8X.*F4'S*.7X.*FS2'S*.6X.
     1*F5'S*.7X.*F2'S*.7X.*FS1'S*./)
      WRITE(6.1097)(PIR(I).R(I).U(I).F(4.I).FS(2.I).F(5.I) .F(2.I).
     1      FS(1.I).              I=1.NP3)
 1097 FORMAT(6X.1P8E11.3/(6X.1P8E11.3))
  105        CONTINUE
C  ------------------------------------------------------------------------
CHAPTER 11 11 11 11 11 11 11 11 11 11 11 11 11   TERMINATION   11 11 11
  113        IF(IFIN.EQ.1) GO TO 110
      IF(ISTEP.LT.LASTEP.AND.XU.LT.XULAST) GO TO 112
      GO TO 110
C  ------------------------------------------------------------------------
C  STRIDE 3 STRIDE 3 STRIDE 3 STRIDE 3 STRIDE 3
  112 CALL STRIDE(3)
             GO TO 60
  110        CONTINUE
C  ------------------------------------------------------------------------
  120 CONTINUE
      STOP
      END
```

G.7.2 AUX

```
C
      SUBROUTINE AUX
C
C*****  AUX SUBROUTINE FOR GENMIX 4 VERSION OF PATANKAR-SPALDING PROGRAM
C*****  FOR BOUNDARY LAYERS
C**********  D.B.SPALDING. IMPERIAL COLLEGE. AUGUST. 1969
      DIMENSION YEDGE(6)
      COMMON/GENRAL/ AJE(5).AJI(5).CSALFA.DPDX(43).DX.EMU(43).F(5.43).
     1 FS(5.43).H.IFIN.INDE(5).INDI(5).ISTEP.ITEST.IUTPAR.KEX.KIN.KRAD.
     2 N.NEQ.NPH.NP1.NP2.NP3.OM(43).PEI.PR(5).PREF(5.43).PSIE.PSII.
     3 R(43).RHO(43).RME.RMI.RU(43).SD(5.43).SU(5.43).TAUE.TAUI.U(43).
     4 XD.XU.Y(43).YE.YI
      COMMON/GM4/ AK.ALMG.ARRCON.ENALL.IPRINT.FR.AFU.OXDFU.PREEXP.PRESS.
     1   UBAR.UFAC.THIN.ELMFC.ELFPFC
      COMMON/NOX/ TFAC.PYENO.ARCONO
      COMMON/RAD/ IRAD.EMISSG.EMISSP.STPHEZ.ICUT.OXCUT
C  SU(1.I) IS USED FOR VELOCITY GRADIENT
C  SU(2.I) INDICATES WHETHER DUDY EXCEEDS A MINIMUM VALUE
C  SU(3.I) IS USED FOR MIXING LENGTH
C  IIIIIIIIIIIIIIIIIIIIIIIIIIIIIIIIIIIIIIIIIIIIIIIIII  MIXING LENGTH
C **** WARNING **** CONSIDER IN EVERY NEW PROBLEM WHETHER UBAR-U(NP3)
C SHOULD NOT BE REPLACED BY ANOTHER REFERENCE VELOCITY. E.G. ABS(U(1)-U(NP3))
      DUDYMN=FR*(UBAR-U(NP3))/Y(NP3)
      DO 10 I=2.NP1
      SU(1.I)=(U(I+1)-U(I))/(Y(I+1)-Y(I))
      IF(R(1).EQ.0.) GO TO 5
      SU(2.I)=.5*(R(I+1)+R(I))*(F(4.I+1)/(R(I+1)*R(I+1))-F(4.I)/
     1 (R(I)*R(I)))/(Y(I+1)-Y(I))
      SU(1.I)=SQRT(SU(1.I)*SU(1.I)+SU(2.I)*SU(2.I))
    5 CONTINUE
      SU(2.I)=0.
   10 IF(ABS(SU(1.I)).GT.DUDYMN) SU(2.I)=1.
      IF(KIN.EQ.1) SU(2.2)=1.
      IF(KEX.EQ.1) SU(2.NP1)=1.
      SU(2.1)=0.
C ------------------------------------------- TEST 7
      IF(ITEST.EQ.0) GO TO 1007
      TEST=1007.
      WRITE(6.101) TEST.DUDYMN.FR.AK.ALMG.UBAR
      WRITE(6.101) (SU(1.I).I=1.NP3)
      WRITE(6.101) (SU(2.I).I=1.NP3)
 1007 CONTINUE
C ------------------------------------------------------
      K=1
      DO 13 L=1.6
   13 YEDGE(L)=Y(NP3)
      DO 11 I=2.NP1
      IF(SU(2.I).EQ.SU(2.I-1)) GO TO 11
      YEDGE(K)=Y(I)
      K=K+1
      IF(K.GT.6) GO TO 14
   11 CONTINUE
   14 EL12=(YEDGE(2)-YEDGE(1))*ALMG
```

Reproduced from
best available copy.

```
      EL34=(YEDGE(4)-YEDGE(3))*ALMG
      EL56=(YEDGE(6)-YEDGE(5))*ALMG
      IF(ITEST.EQ.0) GO TO 1008
      TEST=1008.
      WRITE(6,101) TEST,EL12,EL34,EL56,(YEDGE(I),I=1,6)
 1008 CONTINUE
      DO 12 I=2,NP1
      S U(3,I)=0.
      IF(Y(I).GE.YEDGE(1)) S U(3,I)=EL12
      IF(Y(I).GE.YEDGE(2)) S U(3,I)=0.
      IF(Y(I).GE.YEDGE(3)) S U(3,I)=EL34
      IF(Y(I).GE.YEDGE(4)) S U(3,I)=0.
      IF(Y(I).GE.YEDGE(5)) S U(3,I)=EL56
C     UPPER LIMIT TO MIXING LENGTH
      IF(S U(1,I).EQ.0.) GO TO 15
      IF(R(I).EQ.0) GO TO 15
      ELMAX=ELMFC*(U(I)+F(4,I)/R(I))/ABS(S U(1,I))
      IF(S U(3,I).GT.ELMAX) S U(3,I)=ELMAX
   15 CONTINUE
      IF(KIN.EQ.1.AND.S U(3,I).GT.AK*.5*(Y(I)+Y(I+1)))
     1                    S U(3,I)=AK*.5*(Y(I)+Y(I+1))
   12 IF(KEX.EQ.1.AND.S U(3,I).GT.AK*(Y(NP3)-.5*(Y(I)+Y(I+1))))
     1          S U(3,I)=AK*(Y(NP3)-.5*(Y(I)+Y(I+1)))
C     ALLOW FOR FREE STREAM TURBULENCE
      ELFREE=ELFREE*Y(NP3)
      DO 9 I=2,NP1
    9 S U(3,I)=S U(3,I)+ELFREE
C  -------- ------ ------------------------- TEST 9
      IF(ITEST.EQ.0) GO TO 1009
      TEST=1009.
      WRITE(6,101) TEST
      WRITE(6,101) (S U(3,I),I=1,NP3)
 1009 CONTINUE
C------------------------------    LAMINAR VISCOSITIES FOR CELL BOUNDARIES  --
      DO 23 I=2,NP1
   23 EMU(I)=.5*(EMU(I)+EMU(I+1))
C  --- ------- ----------------------------- ---------  TURBULENT CONTRIBUTION
      DO 20 I=2,NP1
      DUDYL=ABS(S U(1,I)*S U(3,I))
      UDMIN=UFAC*.5*(U(I)+U(I+1))
      IF(R(I).EQ.0) GO TO 19
      UDMIN=UDMIN+UFAC*.5*(F(4,I)/R(I)+F(4,I+1)/R(I+1))
   19 CONTINUE
      IF(DUDYL.LT.UDMIN) DUDYL=UDMIN
      RHM=.5*(RHO(I)+RHO(I+1))
      EMUT=RHM*S U(3,I)*DUDYL
C  ---------- ---- ------- -------------------  LAMINAR CONTRIBUTION
      IF(KIN.EQ.2.AND.I.LT.5) GO TO 21
      IF(KEX.EQ.2.AND.I.GT.N-2) GO TO 21
      IF(EMUT.GT.EMU(I)*50.) GO TO 21
      IF(EMUT.GT.EMU(I)*10.) GO TO 22
      EMU(I)=EMU(I)+EMUT+EMUT*.008/EMU(I)
      GO TO 20
 22 EMU(I)=1.5*EMUT-0.5*EMU(I)
    GO TO 20
 21 EMU(I)=EMU(I)[illegible]
 20 CONTINUE
C                                         TEST 10
    IF([illegible].EQ.0) GO TO 1011
    TE[illegible]
    WRITE(6,10[illegible]
    WRITE[illegible]
    WRITE(6,101)[illegible]I=1,NI)
1011 CONTINUE
C                      [illegible] OF EMU WERE[illegible]          ---- ----
    DO 25 J=2,NJ
    [illegible]
    IF([illegible].EQ.0) GO TO 25
    DO 26 I=2,NI
 26 EMU(I,J)=EMU(I,J)[illegible]
 25 CONTINUE
C                               [illegible]                   ------
    IF([illegible].EQ.0) GO TO 1011
    DO 27 J=1,NJ
    DO 27 I=1,NI
 27 P(I,J)=[illegible]
 28 CONTINUE
 101 FORMAT([illegible]
1011 CONTINUE
C   [illegible]                                  SOURCES
C   [illegible] FOR [illegible] IN THE [illegible] OF THE
C   GRID [illegible] SEE EQ 6.4-1
C                      [illegible]                   ----   ---
C            [illegible]
C            [illegible]
    DO 30 I=2,NI
 30 S D(1,I)=[illegible]
    DO 31 I=2,NI
 31 S D(1,I)=EMU(I)*(S D(1,I+1)-S D(1,I))
         S D(1,[illegible]
         S D(1,NI)[illegible]
    [illegible]
    DO 32 I=2,NI
 32 SU(1,I)=(S D(1,I)-S D(1,I-1))*RT
    DO 33 I=2,NI
 33 SP(1,I)=0
C   CORRECTION FOR RADIATION
    IF(IRAD.EQ.0) GO TO 31
    DO 34 I=2,NI
    IF(F(2,I).LE.TOUT) GO TO 34
    T4=F(2,I)**4.
    EMISS=EMISSG
    IF(F(1,I).LE.0.CUT) EMISS=EMISSG+EMISSP
    RADRAT=EMISS*STHAR2*T4*.5*[illegible]-Y(I-1))
    SU(1,I)=SU(1,I)-RADRAT
 34 CONTINUE
```

```
C ----------------------------------- FUEL --------------------------------
      [illegible]
      DO 40 I=2,NP2
      IF(F(2,I).LT.TMIN) GO TO 41
      F2=F(2,I)
      F3=F(3,I)
      FS1=FS(1,I)
      FS2=FS(2,I)
      IF(I.NE.2) GO TO 42
      F2=F2+.25*(F(2,3)-F2)
      F3=F3+.25*(F(3,3)-F3)
      FS1=FS1+.25*(FS(1,3)-FS1)
      FS2=FS2+.25*(FS(2,3)-FS2)
   42 IF(I.NE.NP2) GO TO 43
      F2=F2+.25*(F(2,NP1)-F2)
      F3=F3+.25*(F(3,NP1)-F3)
      FS1=FS1+.25*(FS(1,NP1)-FS1)
      FS2=FS2+.25*(FS(2,NP1)-FS2)
   43 IF(F2.LT..0001.OR.FS1.LT..0001) GO TO 41
      FUBRNT=.5*(ABS(F3)-F3)/OXDFU
      EXPO=EXP(-[illegible]/FS2)
      SD(2,I)=-T1*FS1*EXPO*R(I)*(Y(I+1)-Y(I-1))*F2/(F2-FUBRNT)
      SD(3,I)=FUBRNT*SD(2,I)
      GO TO 40
   41 SD(2,I)=0.
      SD(3,I)=0.
   40 CONTINUE
C                        ---- OX-FU OXDFU ----------------------------- ---
      DO 50 I=2,NP2
      SD(3,I)=0.
   50 SD(5,I)=0.
C------ ------P+V---------------------
      DO 51 I=2,NP2
      SD(4,I)=0.
   51 SD(4,I)=0.
C                         --- NO   -----------------------------------------
      DO 60 I=2,NP2
      F5=F(5,I)
      FS1=FS(1,I)
      FS2=FS(2,I)
      FS3=FS(3,I)
      IF(I.NE.2) GO TO 62
      F5=F5+.25*(F(5,3)-F5)
      FS1=FS1+.25*(FS(1,3)-FS1)
      FS2=FS2+.25*(FS(2,3)-FS2)
      FS3=FS3+.25*(FS(3,3)-FS3)
   62 IF(I.NE.NP2) GO TO 63
      F5=F5+.25*(F(5,NP1)-F5)
      FS1=FS1+.25*(FS(1,NP1)-FS1)
      FS2=FS2+.25*(FS(2,NP1)-FS2)
      FS3=FS3+.25*(FS(3,NP1)-FS3)
   63 IF(FS2.LT.1500) GO TO 61
      EXPO=EXP(-APCONO/FS2)
      IF(FS2.LE.0.) GO TO 61
      SU(5,I)=TFAC*(PREXNO+EXPO*SQRT(FS1)+FS3/FS2)*.5*(Y(I+1)-Y(I-1))
     1          *R(I)
      SD(5,I)=0.
      GO TO 60
   61 SU(5,I)=0.
      SD(5,I)=0.
   60 CONTINUE
      RETURN
      END
```

G.7.3 STRIDE

```
      SUBROUTINE STRIDE(ISW)
C
C     STRIDE SUBROUTINE FOR GENMIX4 VERSION OF PATANKAR-SPALDING PROGRAM
C.2.70)****  D.B SPALDING. IMPERIAL COLLEGE. AUGUST 1969  ************
      DIMENSION A(5.43).AU(43).B(5.43).BU(43).C(5.43).CU(43).FDIFE(5).
     1  FDIFI(5).GE(5).GI(5).HDF(5)
      COMMON GENRAL. AJE(5).AJI(5).CSALFA.DPDX(43).DX.EMU(43).F(5.43).
     1  FS(5.43).H.IFIN.INDE(5).INDI(5).ISTEP.ITEST.IUTRAF.KEX.KIN.KRAD.
     2  N.NEQ.NPH.NP1.NP2.NP3.OM(43).PEI.PR(5).PREF(5.43).PSIE.PSII.
     3  R(43).RHO(43).RME.RMI.RU(43).SD(5.43).SU(5.43).TAUE.TAUI.U(43).
     4  XD.XU.Y(43).YE.YI
C
      GO TO (1000.2000.3000). ISW
C
C************************************** S T R I D E 1 ****************
 1000 IF(ISTEP.GT.0) GO TO 1100
      OM(1)=0.
      OM(2)=0.
      OM(NP2)=1.
      OM(NP3)=1.
      DUI=.5*OM(3)
      DOE=.5*(1.-OM(NP1))
      UPI=1.
      EPI=1.
      R(1)=0.
      IF(KRAD.EQ.1) GO TO 1100
      DO 1001 I=1.NP3
 1001 R(I)=1.
      R25=1.
      RN15=1.
      IF(ITEST.EQ.0) GO TO 9018
      WRITE(6.9010) (R(I).I=1.NP3).R25.RN15
 9010 FORMAT(1H .1P11F11.3)
 9018 CONTINUE
C---                              CALCULATION OF RHO*U 'S  ---------------
 1100 DO 1101 I=1.NP3
      IF(RHO(I).GT.0.) GO TO 1101
      WRITE(6.1108) RHO(I).I.RHO(I)
 1108 FORMAT(25H NEGATIVE OR ZERO RHO(I)=.1PE11.3.6H AT I=.I3.6X.
     1 21HSET TO ABS OF RHO(I)=.E11.3)
      RHO(I)=ABS(RHO(I))
 1101 RU(I)=RHO(I)*U(I)
      RU3=RU(3)
      RUN1=RU(NP1)
      DO 1102 I=2.NP1
      RU(I)=.5*(RU(I)+RU(I+1))
 1102  CONTINUE
      IF(ITEST.EQ.0) GO TO 9019
      WRITE(6.9010) (RU(I).I=1.NP3).RUN1.RU3.PEI
 9019 CONTINUE
C-------------------------  CALCULATION OF Y 'S AND R 'S  -----------
C  ---------------------------------------  Y'S FOR PLANE GEOMETRY
```

```
      YI=PEI*OM1/(BP1*RU(2))
      Y(3)=YI+PEI*OM(3)/(RU(2)*RU3)
      Y(2)=2.*YI-Y(3)
      DO 1103 I=4,NP1
 1103 Y(I)=Y(I-1)+PEI*(OM(I)-OM(I-1))/RU(I-1)
      YN15=Y(NP1)+PEI*(1.-OM(NP1))/(RU(NP1)*RUN1)
      YE=PEI*OME/(BPE*RU(NP1))
      Y(NP3)=YN15+YE
      Y(NP2)=2.*YN15-Y(NP1)
      IF(KRAD.EQ.0) RETURN
C ------ -------------          Y'S AND R'S FOR AXISYMMETRICAL GEOMETRY
      IF(CSALFA.EQ.0.) GO TO 1110
C ---- ------------------------ ----------  CSALFA NE ZERO
      COSD2=.5*CSALFA
      IF(R(1).NE.0.) GO TO 1105
C------------------------------------------------  R(1)=0.
      DO 1106 I=2,NP3
      Y(I)=SQRT(ABS(Y(I)/COSD2))
 1106 R(I)=Y(I)*CSALFA
      YI=SQRT(ABS(YI/COSD2))
      YN15=SQRT(ABS(YN15/COSD2))
      GO TO 1107
C ------------------------------  -------------  R(1) NE 0.
 1105 RID2=.5*R(1)
      RID2SQ=RID2*RID2
      DO 1104 I=2,NP3
      Y(I)=Y(I)/(RID2+SQRT(ABS(RID2SQ+COSD2*Y(I))))
 1104 R(I)=R(1)+Y(I)*CSALFA
      YI=YI/(RID2+SQRT(ABS(RID2SQ+COSD2*YI)))
      YN15=YN15/(RID2+SQRT(ABS(RID2SQ+COSD2*YN15)))
 1107 R25=R(1)+YI*CSALFA
      RN15=R(1)+YN15*CSALFA
      YE=Y(NP3)-YN15
      RETURN
C ---------------------------- --------- ----  CSALFA EQ ZERO
 1110 DO 1111 I=2,NP3
      Y(I)=Y(I)/R(1)
 1111 R(I)=R(1)
      YI=YI/R(1)
      YN15=YN15/R(1)
      R25=R(1)
      RN15=R(1)
      YE=Y(NP3)-YN15
      RETURN
C*************************************** S T R I D E 2 *************
C ------ ---------- --- ---------   PRELIMINARIES FOR COEFFICIENTS
 2000 PX=PEI/DX
            G=RMI-RME
            PD8=.125*PX
      PD4=.25*PX
            PG=PX*G
      PGD8=.125*PG
      PGD4=PGD8+PGD8
      [illegible]
                                     ---------- GRID POINT 2
                                     ---- THUI, DPI, TI
      [illegible]
      [illegible]*RU(1)*RU(2)
      [illegible]*RU(2))*3.*R25
      [illegible](1)+RU(2)))/6.*(R(1)+R25)*RU(2)
                          ---------- BOUNDARY COEFFICIENTS FOR VELOCITY
      [illegible]
      [illegible]R(1)+R25)*Y)
      [illegible]
                          ---------- BOUNDARY COEFFICIENTS FOR R'S
      [illegible]
      [illegible].TIF,GT(J))
      IF(IOE(J).EQ.2) GO TO 2303
      [illegible]*(J,3))-FDIF(J))
      [illegible]
                          ------------------ COEFFICIENTS
      ADF=TTFF(J)-THLF-TIF*PGOMP+.5*SD(J,2)
      [illegible].5*(R(2)+R(3))-R(3))**2.
     1 [illegible]*(R(2)+R(3)))**2.-PGOMP+.5*SD(J,2)
      DDF=2.*(TIF+FID)
      TF=ADF+DDF+F[illegible]-2.*SD(J,2)
      IF(J.EQ.4.AND.R(1).EQ.0.) DF=TTFF(J) +TIF+THLP+3.*PCOMP
     1 -1.5*SD(J,2)
      IF(J.EQ.4.AND.R(1).NE.0.) DF=TTFF(J)*(.5*(R(2)+R(3))-R(1))**2.
     1 +TIF+THLP+3.*PGOMP-1.5*SD(J,2)
      T=TIF+FDIF(J)
      GO TO 2305
C     NOTE   FLUX OF R*V NECER SPECIFIED AT INNER BOUNDRY
 2303 ADF=TTFF(J)-THLF-PGOMP+.5*SD(J,2)
```

```
      BDF=0.
      DF=ADF+RX*BOMP-2.*SD(J.2)+RMI*2.
      T=RMI*F(J.1)+AJI(J)*R(1)
 2305 TT=3.*F(J.2)-F(J.3)
      CDF=P4OMP*TT+2.*(T+SD(J.2))
      A(J.2)=ADF/DF
      B(J.2)=BDF/DF
 2300 C(J.2)=CDF/DF
C -------------------------------------------- GRID POINT NP2
C------------------------------------------- TAUE. BPE. TNP3
 2304 IF(KEX.NE.1) GO TO 2003
      CALL WF(0.NP3.NP2.NP1.BPE.TNP3.TAUE)
      GO TO 2310
 2003 TNP3=0.
      IF(KRAD.EQ.0) BPE=.33333+.66667*PU(NP3)/PU(NP1)
      IF(KRAD.EQ.1) BPE=(R(NP3)*(5.*PU(NP3)+PU(NP1))+3.*RN15*
     1             (PU(NP3)+PU(NP1)))/6./(R(NP3)+RN15)/PU(NP1)
C ---------------------- BOUNDARY COEFFICIENTS FOR VELOCITY
 2310 BOMM=OM(NP2)-OM(NP1)
      HLM=RMID2-GD4*(OM(NP1)+OM(NP2))
      AHLM=ABS(HLM)
      THLM=HLM+HLM
      TM=EM/U(NP1)
      TTM=TM+AHLM+ABS(TM-AHLM)
      PGOMM=PGD4*BOMM
      P4OMM=PD4*BOMM
      AD=2.*(TNP3-RME)
      BD=TTM+THLM-TNP3-PGOMM
      CD=P4OMM*(3.*U(NP2)-U(NP1))-DPDX(NP2)*(RN15+R(NP3))*YE
      DU=AD+BD+RX*BOMM
      AU(NP2)=AD/DU
      BU(NP2)=BD/DU
      CU(NP2)=CD/DU
      IF(NEQ.EQ.1) RETURN
C ---------------------- BOUNDARY COEFFICIENTS FOR F'S
      DO 2320 J=1.NPH
      TMF=TM/PREF(J.NP1)
      TTMF=TMF+AHLM+ABS(TMF-AHLM)
      IF(KEX.NE.1) GO TO 2311
      CALL WF(J.NP3.NP2.NP1.FDIFE(J).TNP3F.GE(J))
      IF(INDE(J).EQ.2) GO TO 2313
      AJE(J)=GE(J)*(.5*(F(J.NP2)+F(J.NP1))+FDIFE(J)-F(J.NP3))
      GO TO 2312
 2311 TNP3F=0.
      FDIFE(J)=0.
C ------------------------------------------- COEFFICIENTS
 2312 ADF=2.*(TNP3F-RME)
      BDF=TTMF+THLM-TNP3F-PGOMM+.5*SD(J.NP2)
      IF(J.EQ.4) BDF=TTMF*(.5*(R(NP2)+R(NP1))/R(NP1))**2.+THLM-TNP3F*
     1  (R(NP3)/(.5*(R(NP2)+R(NP1))))**2. -PGOMM+.5*SD(J.NP2)
      DF=ADF+BDF+RX*BOMM-2.*SD(J.NP2)
      IF(J.EQ.4) DF=TTMF*(.5*(R(NP2)+R(NP1))/R(NP3))**2. +TNP3F -THLM
     1  +3.*PGOMM -1.5*SD(J.NP2)
```

```
      [illegible] DNP2F(PI)ICE(J)
      GO TO 2715
C(U) OF RAY NEVER SPECIFIER AT OUTER BOUNDRY
 2715 [illegible]=0.
      DD=TTMF*(DHLH+PGOMM+.5*SD(J,NP2)
      [illegible] .5*SD(J,NP2)-[illegible]*2.
      [illegible] R(NP3)
      [illegible] (J,NP1)
      [illegible] *SD(J,NP2))
      [illegible]
      [illegible]
      [illegible]
      [illegible]
C************************************************  S T R I D E S  ***************
      DO 3005 I=2,NR1
            [illegible]
            [illegible]
            [illegible]
            [illegible]
      [illegible]
            [illegible]
        [illegible]
      [illegible]
      [illegible]
            [illegible]
      [illegible]
            [illegible]
      [illegible]
            [illegible]
      [illegible]
      [illegible]
      [illegible]
       [illegible]+1)+DOMM*U(I-1))-
     1      [illegible]+(V(I+1)-V(I-1))
            [illegible]
            [illegible]
            [illegible]
            [illegible]
C     ----------------------------------------------  START OF J LOOP
            IF(NVC.EQ.1) GO TO 3005
            DO 3004 J=1,NPD
      [illegible]
      [illegible]
      [illegible]
      [illegible]
      IF(J.EQ.4) DD=TTPF(J)*(.5*(R(I)+R(I+1))/R(I+1))**2.-THLP-PGONP
      BD=TTMF*THLM+PGOMM
      IF(J.EQ.4.AND.R(I-1).NE.0.) BD=TTMF*(.5*(R(I)/R(I-1)+1.))**2.
     1 *THLM-PGOMM
      CD=PD*(BOMT3*F(J,I)+BOMP*F(J,I+1)+BOMM*F(J,I-1))
      ED=PD*2.*SD(J,I)
      DE=AD+BD+PROM-2.*SD(J,I)
      IF(J.EQ.4) DF=TTPF(J)*(.5*(R(I)+R(I+1))/R(I))**2.
     1 *TIS*(.5*(R(I)+R(I-1))/R(I))**2. +THLP -THLH +PGBOM -2.*SD(J.I)
            A(J.I)=AU/DF
            B(J.I)=BU/DF
 3004       C(J.I)=CU/DF
 3005 CONTINUE
      IF(ITEST.EQ.0) GO TO 9013
      WRITE(6.9001) (AU(I).I=2.NP2)
      WRITE(6.9002) (BU(I).I=2.NP2)
      WRITE(6.9003) (CU(I).I=2.NP2)
 9001 FORMAT(7H AU(I) .1P11E11.3)
 9002 FORMAT(7H BU(I) .1P11E11.3)
 9003 FORMAT(7H CU(I) .1P11E11.3)
      IF(NEQ.EQ.1) GO TO 9013
      DO 9000 J=1.NPH
      WRITE(6.9004) (A(J.I).I=2.NP2)
      WRITE(6.9005) (B(J.I).I=2.NP2)
 9000 WRITE(6.9006) (C(J.I).I=2.NP2)
 9004 FORMAT(8H A(J.I) .1P11E11.3)
 9005 FORMAT(8H B(J.I) .1P11E11.3)
 9006 FORMAT(8H C(J.I) .1P11E11.3)
 9013 CONTINUE
C----------------------------------------------------------------------
      IF(KIN.EQ.2.AND.RU(1).NE.0.) U(1)=U(1)-DPDX(1)*DX/RU(1)
      IF(KEX.EQ.2.AND.RU(NP3).NE.0.) U(NP3)=U(NP3)-DPDX(NP3)*DX/RU(NP3)
C---------------------------    SOLVE FOR DOWNSTREAM U 'S  ------------
 3046 BU(2)=BU(2)*U(1)+CU(2)
      DO 3048 I=3.NP2
      T=1./(1.-BU(I)*AU(I-1))
      AU(I)=AU(I)*T
 3048 BU(I)=(BU(I)*BU(I-1)+CU(I))*T
      DO 3050 IDASH=2.NP2
      I=N+4-IDASH
      U(I)=AU(I)*U(I+1)+BU(I)
C   TEST FOR NEGATIVE VELOCITY
C   IF U IS NEGETIVE NEAR OUTER WALL. SET U TO ZERO
C     IUTRAP=0 NO ACTION.  =1 SET U'S TO ZERO.  =2 PRINT AND STOP
      IF(IUTRAP.EQ.0) GO TO 3050
      IF(I.EQ.2.OR.I.EQ.NP2.OR.U(I).GE.0.) GO TO 3050
      IF(IUTRAP.EQ.1) GO TO 3051
      IFIN=1
      ITEST=1
      WRITE(6.3120)
 3120 FORMAT(1H .33HAT LEAST ONE VELOCITY IS NEGATIVE)
      RETURN
 3051 U(I)=1.E-30
 3050 CONTINUE
      IF(KIN.EQ.3)U(1)=.5*(U(2)+U(3))
      IF(KEX.EQ.3)U(NP3)=.5*(U(NP1)+U(NP2))
   72 IF(NEQ.EQ.1) GO TO 3060
      DO 3720 J=1.NPH
C-----------------------------  SOLVE FOR DOWNSTREAM F 'S  -----------
      B(J.2)=B(J.2)*F(J.1)+C(J.2)
      DO 3140 I=3.NP2
      T=1.-B(J.I)*A(J.I-1)
      A(J.I)=A(J.I)/T
 3140 B(J.I)=(B(J.I)+B(J.I-1)+C(J.I))/T
      DO 3150 IDASH=2.NP2
      I=N+4-IDASH
 3150 F(J.I)=A(J.I)*F(J.I+1)+B(J.I)
C----------------------------------- ADJUST F(J.1) AND F(J.NP3)  -------------
      GO TO (3210.3220.3230).KIN
 3210 IF(INDI(J).EQ.2) F(J.1)=FDIFI(J)+.5*(F(J.2)+F(J.3))+AJI(J)/GI(J)
      GO TO 3220
 3230 F(J.1)=.5*(F(J.2)+F(J.3))
 3220 GO TO (3310.3320.3330).KEX
 3310 IF(INDE(J).EQ.2) F(J.NP3)=FDIFE(J)+.5*(F(J.NP2)+
     1                               F(J.NP1))-AJE(J)/GE(J)
      GO TO 3320
 3330 F(J.NP3)=.5*(F(J.NP1)+F(J.NP2))
 3320 CONTINUE
 3060 XU=XD
      PSII=PSII-RMI*DX
      PSIE=PSIE-RME*DX
      PEI=PSIE-PSII
      ISTEP=ISTEP+1
      RETURN
      END
```

G.7.4 WF

```
C
      SUBROUTINE WF(J.I1.I2.I3.OUT1.OUT2.OUT3)
C
C****** WF SUBROUTINE FOR GENMIX 4 VERSION OF PATANKAR-SPALDING PROGRAM
C 3.2.70 ********* D.B.SPALDING. IMPERIAL COLLEGE. AUGUST 1969
      COMMON/GENRAL/ AJE(5).AJI(5).CSALFA.DPDX(43).DX.EMU(43).F(5.43).
     1 FS(5.43).H.IFIN.INDE(5).INDI(5).ISTEP.ITEST.IUTRAP.KEX.KIN.KRAD.
     2 N.NEQ.NPH.NP1.NP2.NP3.OM(43).PEI.PR(5).PREF(5.43).PSIE.PSII.
     3 R(43).RHO(43).RME.RMI.RU(43).SD(5.43).SU(5.43).TAUE.TAUI.U(43).
     4 XD.XU.Y(43).YE.YI
      COMMON/GEN/ AK.ALMG.APPCON.EWALL.IPRINT.FR.NFU.OXDFU.FREEXP.PRESS.
     1  UBAR.UFAC.TMIN.FUNCFC.ELFPFC
C EFFECTS OF PRESSURE GRADIENT. MASS TRANSFER AND
C     RADIUS VARIATION ARE NEGLECTED
C     FOR VELOCITY:      OUT1=DP.     OUT2=T.  OUT3=TAU
C     FOR F'S.           OUT1=FIDIF. OUT2=T.  OUT3=G
C
      DATA SHALF/.01/
      I25=I3-1/I1
      JDASH=J+1
      GO TO (100.200.200.200.200.200). JDASH
C------------------------------------------------------ VELOCITY
  100 UREF=.5*(U(I2)+U(I3))
      RHOREF=.5*RHO(I1)+.25*(RHO(I2)+RHO(I3))
      PREF=.5*(R(I2)+R(I3))
      VREF=EMU(I1)
      YREF=YI+(YE-YI)*OM(I1)
      RE=UREF*RHOREF*YREF/VREF
      PROREF=PREF*RU(I25)
      IF(RE.LT.120.) GO TO 110
C--------------------------------------------------------- LOG LAW
      ER=RE*EWALL
      NIT=0
  101 SHALFI=SHALF
      SHALF=AK/ALOG(ER*SHALF)
      IF(ABS(SHALF      -SHALFI).LT..0001.OR.NIT.GT.10) GO TO 102
      NIT=NIT+1
      GO TO 101
  102 S=SHALF**2
      OUT1=AK/(AK+SHALF)
      EMU(I25)=.25*RHOREF*PREF*ABS(U(I3)-U(I2))*(AK/OUT1)**2
      GO TO 103
C-------------------------------------------------- LAMINAR FLOW
  110 S=1./RE
      OUT1=.5
      EMU(I25)=VREF*PREF/ABS(Y(I3)-Y(I2))
  103 OUT2=S*PROREF
      OUT3=OUT2*UREF/R(I1)
      RETURN
C---------------------- STAGNATION ENTHALPY. FUEL . OX-FU/OXDFU
  200 IF(RE.LT.120.) GO TO 210
      PRRAT=PR(J)/PREF(J.I25)
      PJAY      =9.*(PRRAT-1.)/PRRAT**.25
      S=S/PREF(J.I25)/(1.+PJAY*SHALF)
      OUT1=0.
      IF(J.EQ.1) OUT1=(H-1.)*.5*UREF**2
      OUT2=S*PRUREF
      OUT3=OUT2/R(I1)
      RETURN
  210 S=S/PR(J)
      OUT1=0.
      IF(J.EQ.1) OUT1=(PR(J)-1.)*.5*UREF**2
      OUT2=S*PRUREF
      OUT3=OUT2/R(I1)
      RETURN
      END
```

The following is a list of publications dealing with engine combustion prepared under direct or partial support from NSF/RANN Grant No. NSF-GI-44379, "Engine combustion with excess air." Copies may be obtained by writing to the author or Professor R.F. Sawyer, Principal Investigator, at the following address:

Department of Mechanical Engineering
University of California
Berkeley, California 94720

ECG-01 N.P. Cernansky, "Formation of NO and NO_2 in a Turbulent Propane/Air Diffusion Flame," University of California, College of Engineering Report No. UCB-ME-74-5, November 1974.

ECG-02 N.P. Cernansky and R.F. Sawyer, "NO and NO_2 Formation in a Turbulent Hydrocarbon/Air Diffusion Flame," *Fifteenth Symposium (International) on Combustion*, 1039-1050, The Combustion Institute, Pittsburgh, 1975.

ECG-03 G.L. Yoder and P.J. Pagni, "Automotive Emissions from Fuel Sulfur," *Chemosphere 2*, 63-64, 1975.

ECG-04 J.E. Cichanowicz and R.F. Sawyer, "Extension of the Lean Operating Limit of a Rotary Combustion Engine by Hydrogen-Enriched Fuel," University of California, College of Engineering Report No. UCB-ME-75-9, September 1975.

ECG-05 P.J. Pagni and W.V. Krill, "Particulate Emissions from Spark Ignition Engines," University of California, College of Engineering Report No. UCB-ME-75-8, August 1975.

ECG-06 A.B. Harker, P.J. Pagni, T. Novakov, and L. Hughes, "Manganese Emissions from Combustors," College of Engineering Report No. UCB-ME-75-7, August 1975.

ECG-07 K. Wolfe and M.C. Branch, "Emissions and Fuel Economy of a Stratified Charge Engine Operating on a Gasoline/Methanol Blend," Western States Section, The Combustion Institute, Paper No. 75-9, October 1975.